



Catalysis Reviews

Science and Engineering

ISSN: (Print) (Online) Journal homepage: www.tandfonline.com/journals/lctr20

Upgrading biomass to high-added value chemicals: synthesis of monoterpenes-based compounds using catalytic green chemical pathways

Julián E. Sánchez-Velandia, Luis A. Gallego-Villada, Päivi Mäki-Arvela, Alexander Sidorenko & Dmitry Yu. Murzin

To cite this article: Julián E. Sánchez-Velandia, Luis A. Gallego-Villada, Päivi Mäki-Arvela, Alexander Sidorenko & Dmitry Yu. Murzin (08 Apr 2024): Upgrading biomass to high-added value chemicals: synthesis of monoterpenes-based compounds using catalytic green chemical pathways, *Catalysis Reviews*, DOI: [10.1080/01614940.2024.2329553](https://doi.org/10.1080/01614940.2024.2329553)

To link to this article: <https://doi.org/10.1080/01614940.2024.2329553>



© 2024 The Author(s). Published with license by Taylor & Francis Group, LLC.



Published online: 08 Apr 2024.



Submit your article to this journal [↗](#)



Article views: 750








View related articles [↗](#)



View Crossmark data [↗](#)

Upgrading biomass to high-added value chemicals: synthesis of monoterpenes-based compounds using catalytic green chemical pathways

Julián E. Sánchez-Velandia ^a, Luis A. Gallego-Villada ^{b,c}, Päivi Mäki-Arvela ^c, Alexander Sidorenko ^d, and Dmitry Yu. Murzin ^c

^aSustainable and Supramolecular Research Group, Universidad Jaume Castelló de la Plana, España; ^bEnvironmental Catalysis Research Group, Chemical Engineering Faculty, Universidad de Antioquia, Medellín, Colombia; ^cLaboratory of Industrial Chemistry, Process Chemistry Centre, Åbo Akademi University, Turku, Turku Finland; ^dLaboratory of Wood-Chemical products and technologies, institute of Chemistry of New Materials of NAS of Belarus, Belarus

ABSTRACT

Monoterpenes derived from various biomass constitute an important platform for synthesizing fragrances, intermediates, and pharmaceuticals. In this review, the most recent and relevant transformations of terpenes are discussed with the primary focus on heterogeneous catalysis emphasizing green chemistry and green chemical engineering aspects. This review aims to outline significant recent advancements in the transformations of terpenes of particular importance for academic and industrial research. This is accomplished by highlighting the most pivotal reactions, including oxidation, epoxidation, hydroformylation, CO₂ cycloaddition, isomerization, condensation, and one-pot synthesis (such as tandem and telescopic reactions), using heterogeneous catalytic routes that have been published in the literature in the last decade. The review provides insights on the catalyst design for the transformations mentioned above tailoring selectivity and highlights the structure–activity relationship.

ARTICLE HISTORY

Received 30 November 2023
Revised 4 March 2024
Accepted 7 March 2024

KEYWORDS

Monoterpenes;
heterogeneous catalysts;
green chemistry; One-pot
synthesis

1. Introduction

Fine chemistry represents one of the most important industries that involve the production of molecules used as precursors of fragrances, pharmaceutical products, drugs, and related compounds. Generally, fine chemicals are produced in limited quantities (10000 metric t y⁻¹), their costs are high (8 € kg⁻¹) in comparison with other chemicals, and moreover, they are highly pure substances (>99% and <10 ppm metal residues and ee>98% in pharmaceuticals). Additionally, exhibit a relatively high E-factor ((kg waste) (kg product)⁻¹) with

CONTACT Dmitry Yu. Murzin  dmurzin@abo.fi  Sustainable and Supramolecular Research Group, Universidad Jaume I, Av. Vicent Sos Baynot, s/n, 12006 Castelló de la Plana, España; Julián E. Sánchez-Velandia  velandia@uji.es  Sustainable and Supramolecular Research Group, Universidad Jaume I, Castelló de la Plana, España.

Table 1. Production volume and E-factor of different industries [1].

<i>Industry segment</i>	<i>Production volume (t y⁻¹)</i>	<i>E-factor value*</i>
<i>Oil refining</i>	10 ⁶ – 10 ⁸	< 0.1
<i>Bulk chemicals</i>	10 ⁴ – 10 ⁶	< 1-5
<i>Fine chemicals</i>	10 ² – 10 ⁴	5-50
<i>Pharmaceuticals</i>	10 – 10 ³	25-100

*E-factor value is defined as the ratio between kg of waste products to kg of the desired substance. A higher E-factor is associated with more waste and additionally, a larger negative environmental impact, while a lower E-factor corresponds to lower amounts of waste. In the calculation of the E-factor, water is excluded.

large amounts of unwanted products (Table 1) [2,3]. On the other hand, fine chemicals can be synthesized using flexible and multipurpose batch processes in relatively small amounts and with high-quality and purity products [4,5]. Fragrances, personal care, household products, or their precursors are fine chemicals products which can be composed of natural organic substances or their derivatives such as monoterpenes, carboxylic acids, esters, ketones, and complex mixtures of these molecules [6].

Essential oils (EOs) are products obtained from a natural raw material of plant origin, using dry or steam distillation or mechanical processes from the epicarp of citrus fruits [7,8]. EOs are composed of lipophilic and highly volatile secondary plant metabolites, reaching a mass 300 g/mol. In general, the main components of essential oils are formed by monoterpenes and sesquiterpenes; one of the examples is the turpentine oil which is mainly comprised of monoterpenes, such as α - and β -pinene [7]. Terpenes are hydrocarbons produced from a combination of several isoprene units (C₅H₈)_n. The classification of terpenes is given by the number of isoprene units: monoterpenes ($n=2$), sesquiterpenes ($n=3$), diterpenes ($n=4$), sesterpenoids ($n=5$), triterpenoids ($n=6$), carotenoids ($n=8$) and resinoids ($n>8$) [9,10].

Table 2 shows the monetary transactions related to imports and exports of the category of essential oils, as presented by the Trade Map tool [11], developed by the International Trade Center (INTRACEN). This category includes i) concretes and absolutes, ii) resinoids, iii) extracted oleoresins, iv) concentrates of essential oils in fats, fixed oils, waxes, or similar substances obtained by enfleurage or maceration, v) terpenic by-products of the deterpenation of essential oils, vi) aqueous distillates, and vii) aqueous solutions of essential oils. World imports and exports have varied between 5.2 and 6.1 billion US dollars, representing approximately 0.022 to 0.025% of the US gross domestic product in 2022 [12]. Furthermore, Figure 1 illustrates the top importers and exporters of

Table 2. World imports and exports (values in US Dollars thousand) of essential oils (Trade Map – Product: 3301 Essential oils, whether or not terpeneless [11]).

<i>Year</i>	<i>2018</i>	<i>2019</i>	<i>2020</i>	<i>2021</i>	<i>2022</i>
<i>Imports</i>	6,100,596	5,770,483	5,267,908	5,702,287	5,391,299
<i>Exports</i>	5,944,571	5,627,479	5,320,372	6,047,482	5,235,281

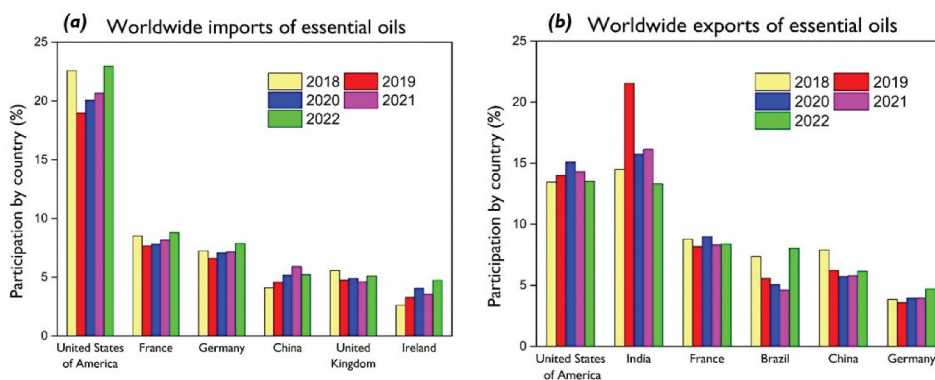


Figure 1. Imports (a) and exports (b) of the last five years of essential oils (Trade Map – Product: 3301 Essential oils, whether or not terpeneless [11]).

essential oils worldwide for the past 5 years, respectively. The United States stands out as the leading importer, accounting for around 23% in 2022, but also as the leading exporter in 2022 with 13.5%, followed by India with 13.3% [11].

Monoterpenes are, interestingly, organic, and biomolecules derived from the isoprene unit and obtained by the plant's metabolic processes. They are cheap and abundantly available. Because of their odor and taste, monoterpenes are useful in cosmetic materials, food additives, and attractant drugs, among others. Oxygenated monoterpenes (monoterpenoids) are distributed in higher plants, algae, fungi, and even some insects [13]. Currently, isoprene monoterpenes represent a significant percentage of biomass and they are also included as volatile organic compounds (VOCs) in which more than 55000 different isoprenoids are well known [14]. There are a lot of classifications of monoterpenes which include the type of structure and its disposition in the geometrical space. For example, monoterpenes can be classified into three groups: lineal, monocyclic terpenes, and bicyclic monoterpenes (with strained structures).

Catalytic conversion of monoterpenes and different derivatives is still a way to synthesize different medicines [15,16], cosmetics [17], fragrances [18], etc. Furthermore, polysulfides derived from renewable natural product-based monomers such as terpenes, terpenoids and essential oils [19] can be used in many fields such as infrared imaging [20], energy storage [21,22], heavy metal adsorbents [23,24], oil adsorbents [25,26], fertilizers [27] and antibacterial agents [28,29].

Among a lot of applications of monoterpenes in the field of medicine, it has been reported that different essential oils of aromatic plants exhibit anti-inflammatory action, for example, limonene and 1,8-cineole [30]. Several reviews about the analgesic and anti-inflammatory activity of monoterpenes have been published [30,31], which provided detailed information about acyclic monoterpenes (linalool, linalyl acetate, myrcene, neral, geranial,

citronellal, citronellol), monocyclic monoterpenes (menthol, pulegone, R-(+)-limonene, α -phellandrene, thymoquinone, thymol, thymol acetate, carvacrol, *p*-cymene, carvone, carvone, hydroxydihydrocarvone, α -terpineol), and bicyclic monoterpenes (1,8-cineol, α -pinene, β -pinene, fenchone, rotundifolone, limonene oxide, carvone epoxide, pulegoneoxide). On the other hand, the cardiovascular effects of 16 monoterpenes (carvacrol, citronellol, *p*-cymene, 1,8-cineole, linalool, menthol, myrtenal, myrtenol, α -pinene, rotundifolone, sobrerol, thymol, limonene, α -terpinen-4-ol, α -terpineol, and perillyl alcohol) have been reported, observing vasorelaxation as the main effect, which decreased the heart rate and blood pressure, showing applicability of monoterpenes for prevention or treatment of cardiovascular diseases [32].

The objective of this review is to outline significant recent advancements in the transformation of terpenes, which hold particular importance in both industry and academia. This will be accomplished by highlighting the most pivotal reactions, including oxidation, epoxidation, hydroformylation, cycloaddition of CO₂, isomerization, condensation, and one-pot synthesis (such as tandem and telescopic reactions), using heterogeneous catalytic routes that have been published in the last decade.

2. Isomerization of monoterpenes

2.1. Some general aspects

Non-Timber Forest Products (NTFPs) are biological resources derived from the coniferous forests, mainly from the *Pinus* genus [33]. The primary source of these products is raw resin, extracted from live pine trees. This resin is thick, sticky, and milky in appearance, often containing forest remnants like insects and bark [33,34]. Historically, this resin has held significant economic value and finds application in various industries including wax, paint, soap, adhesive, and pharmaceutical production [35–37]. The extraction process yields two major products: rosin and turpentine; steam distillation is the common method employed, resulting in a gaseous phase (turpentine) and a solid residue (rosin) [38]. Conceptually, this process involves placing a large quantity of resin inside the reactor, with steam being fed into the reactor through cylindrical coils surrounding it [39]. As a result of the steam distillation process, the lower boiling fraction present in the resin escapes the reactor and condenses to form turpentine, leaving behind rosin as a residue. On average, a pine tree can yield around 2.75 kg of resin containing roughly 20% turpentine and 65% rosin. However, the composition and properties of pine resin can vary due to several factors such as nature of pine species, climate, geographic location, and soil conditions [39]. In the same way, the mass yield of the resin obtained from a pine tree can vary depending on these factors, but in general terms, a single *Pinus caribaea* tree can yield about

around 2 tons of resin per hectare [40,41]. Turpentine oil is a colorless liquid of low viscosity that is mainly composed of α - and β -pinene monoterpenes, which have been widely used as a raw material for hydration of α -pinene using several types of catalysts [42–46]. However, a very common transformation route of turpentine is the isomerization of the monoterpenes contained in it such as α - and β -pinene (Figure 2), resulting in the formation of other monoterpenes that can be extracted in low amounts from essential oils such as limonene, camphene, terpinene, terpinolene, and β -phellandrene. Controlling the strength and type of the acid sites, selectivity toward a specific target can be obtained; while Brønsted acid sites are beneficial for the formation of monocyclic compounds, the Lewis acid sites favor the synthesis of bicyclic monoterpenes [47,48]. All these compounds have significant applications in fine chemistry. Furthermore, limonene is the major constituent of several essential citrus fruits (91–96%) such as limes, lemons, mandarins, grapefruits, and oranges [49,50], and can be oxidized yielding ketones, epoxides, and diepoxides; moreover, it can also be isomerized into such products as *p*-cymene, terpinene, terpinolene, among others. On the other hand, camphene is a widespread natural product found in *Liquidamar* species, *Chrysanthebmmum*, *Zingiber officinale*, and *Rosmarinus offinialis* [13]. Camphene can be used as a pyrogen for the production of nano/macroporous polycaprolactone for injectable cell delivery [51], and as starting material for the production of isborneol derivatives [52,53]. Borneol and isborneol

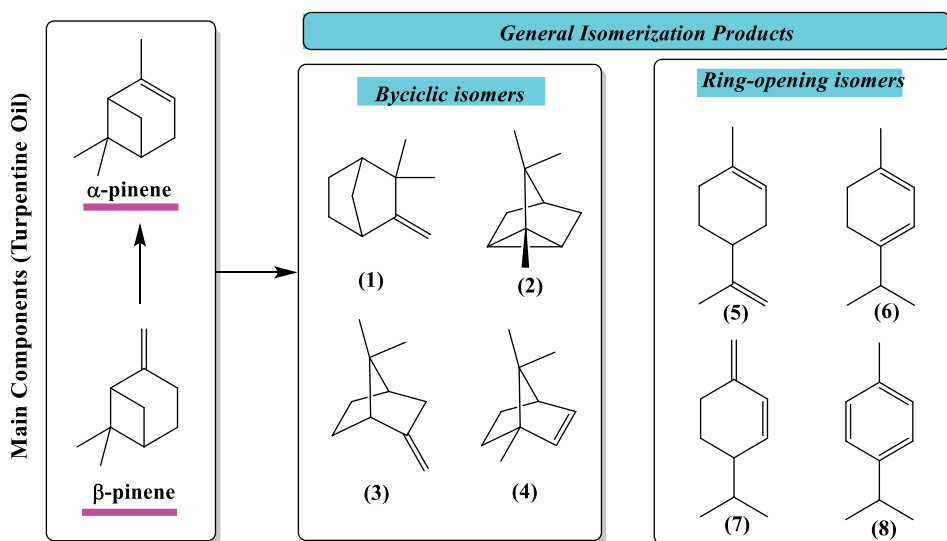


Figure 2. Main isomerization products of α -pinene and β -pinene: (1) camphene, (2) tricyclene (3) α -fenchene (4) bornylene (5) limonene (6) terpinene (7) β -phellandrene (8) *p*-cymene. **p*-cymene is obtained as a secondary product for the aromatization (or dehydrogenation) of limonene-derivatives not corresponding to isomers of α - or β -pinene.

derivatives have been found as promising compounds demonstrating antiviral activity against the influenza virus A/Puerto Rico/8/34 (H1N1) [54] and larvicidal activity against *Aedes aegypti* [55].

2.2. Relevant heterogeneous catalysts

Recently, a mild alkali-treated 13X zeolite [56] has been reported as an active catalyst for the isomerization of α -pinene toward limonene (Table 3, entry 1) with a yield of 59.1% at 150°C and 3 h in a solvent-free system, highlighting this system as a promising environmentally friendly route for α -pinene valorization. The study also emphasized that superior catalytic performance in limonene production was linked to a higher density of medium-strong acid sites, larger surface area of micropores, and an optimal Brønsted/Lewis acidity ratio ranging from 0.06 to 0.2. Activation of TiO₂ using various acids (formic, nitric, phosphoric, sulfuric, and acetic acids) has been investigated to evaluate their catalytic potential in the isomerization of α -pinene [57]. The experimental procedure involved an initial treatment with 30% NaOH solution at 110°C for 12 h, followed by thorough washing with deionized water until reaching a neutral pH. Subsequently, the resulting wet cake was dissolved in water, and the pH was adjusted to 2 through addition of the corresponding acid under stirring for 3 h. The highest yields of camphene were achieved using acetic (Table 3, entry 2) and nitric acids (Table 3, entry 3) as surface modifiers. These two modifications led to camphene yields of approximately 48.0% and 37.5%, respectively, after the reaction time of 1.5 h under reflux conditions in a solvent-free system. In both cases, limonene was also produced as the second major isomerization product, with selectivity falling within the range of 15–20%. Notably, acetic acid-activated TiO₂ exhibited a remarkable increase in the total surface area compared to commercial TiO₂ ($108 \text{ m}^2 \text{ g}^{-1} > 9 \text{ m}^2 \text{ g}^{-1}$), correlating well with enhanced reaction rates and maximum selectivity toward camphene. In addition, this catalyst was successfully reused eight times in the isomerization of α -pinene with a slight decrease in the selectivity toward camphene and no significant losses of conversion.

Preparation of porous carbon materials [58] was investigated for their potential as heterogeneous catalysts in α -pinene isomerization, utilizing three types of waste biomass: orange peels, coffee grounds, and sunflower seed husks. This method proved to be both cost-effective and environmentally friendly, resulting in minimal generation of chemical waste. The activation process involved the use of KOH, followed by carbonization at 800°C under nitrogen atmosphere. Although the activated carbon prepared from coffee grounds (Table 3, entry 4) exhibited the highest activity, it demonstrated limited selectivity for a specific product, namely 34% toward camphene and 38% toward limonene, even at a very high temperature (160°C). However, the material with the highest activity correlated well with the largest surface area

(1566 m² g⁻¹), total pore volume (0.694 cm³ g⁻¹), and the acid-site concentration (0.50 mmol g⁻¹), indicating a direct relationship between α -pinene conversion and those physicochemical properties. Acidity as a fundamental and critical factor can drive selectivity of pinenes isomerization because of the carbocation rearrangement. **Figure 3** shows the proposal reaction pathway in which the intermediate pinyl carbocation is generated when the acid site (Lewis or Brønsted) is coordinated with the double bond. As well known, tertiary carbocations are generally stable; however, for the mentioned case, the angles of the internal cyclobutene make the pinyl cation less stable promoting rearrangement into sabinyl cation after a 2,6 closure and 6,7 hydride shifts, with sabinene as the main product. For the second case, a C-C shift is preferred leading to camphene. Finally, elimination of the steric strain of the pinyl cation with a C-C shift can produce α -terpinyl cation which after elimination gives limonene and terpinolene as the main products.

Hierarchical zeolites represent some of the most promising acidic catalytic materials. These materials consist of a crystalline network that possesses not only uniform micropores but also secondary meso- or macro-porosity. This unique structure enables efficient conversion of bulky organic molecules [67–69]. Numerous synthetic methodologies have been reported in the literature for the creation of these materials, involving the use of amphiphilic organosilanes [70], cationic polymers [71], hard templates [72], and multi-quaternary ammonium surfactants [73]. Catalysts based on hierarchical mordenite [59,60] have demonstrated high activity for α -pinene conversion in a solvent-free system, achieving values above 94% (**Table 3, entries 5 and 6**). However,

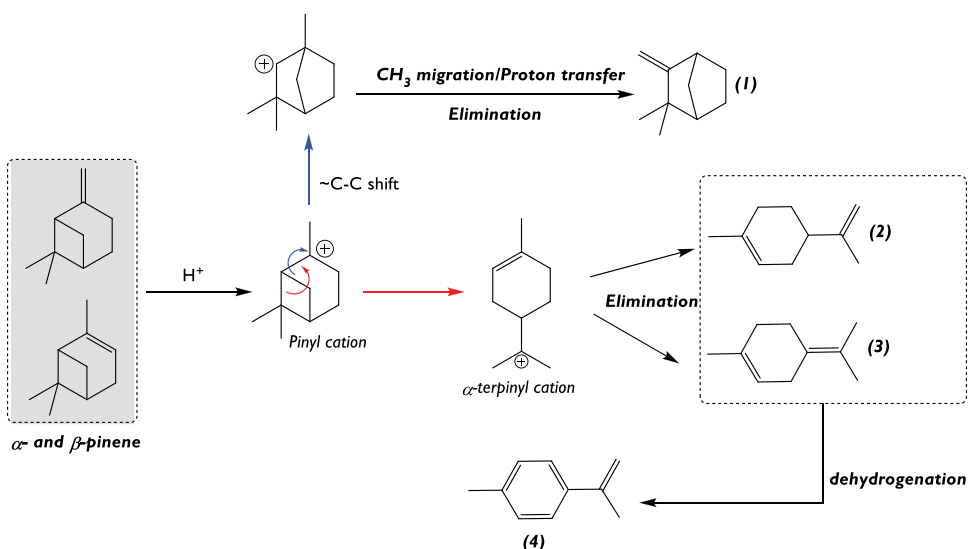


Figure 3. Proposal reaction pathway for the products obtained from the isomerization of pinenes. (1) Camphene (2) Limonene (3) Terpinolene (4) a-p-dimethylstyrene.

Table 3. Some relevant heterogeneous catalysts for the isomerization of the main monoterpenes.

Entry	Catalyst	Monoterpene	Solvent	Reaction conditions	X (%)	S (%)	Ref
1	Mild alkali-treated 13X	α -Pinene	Solvent-free	30 g of substrate, 1.5 g of catalyst, 150°C, 3 h.	100	59.1 limonene	[56]
2	Acetic acid activated TiO ₂	α -Pinene	Solvent-free	100 mL of substrate, 0.6% of catalyst loading, 90 min, reflux condition.	71.78	66.81 camphene 6.19 tricyclene 1.91 carene 15.17 limonene 1.23 terpinene 7.34 terpinolene 1.35 others	[57]
3	Nitric acid activated TiO ₂				58.36	64.27 camphene 18.5 limonene 5.86 tricyclene 1.2 carene 1.69 terpinene 6.87 terpinolene 1.61 others	
4	Activated carbon	α -Pinene	Solvent-free	3 g of substrate, 5 wt. % of catalyst, 160°C, 400 rpm, 3 h	84	34 camphene 38 limonene	[58]
5	Hierarchical mordenite	α -Pinene	Solvent-free	3 mL of substrate, 0.15 g of catalyst, 140°C, 40 min	94.7	33.1 camphene 30.0 limonene 12 α -terpinene 6 γ -terpinene 12 terpinolene 4 <i>p</i> -cymene	[59]
6	H-Mordenite	α -Pinene	Solvent-free	20 mL of substrate, 1 g of catalyst, 130°C, 4 h	98.5	NR	[60]
7	Hierarchical zeolite mazzite	α -Pinene	Solvent-free	3 mL of substrate, 5 mg of zeolite, 120°C, 3 h	44	39.6 camphene 38.4 limonene 1 β -pinene 3 α -terpinene 9 terpinolene	[61]
8	NT-TiO ₂ -wc	α -Pinene	Cyclohexane	0.25 mmol of substrate, 50 mg of catalyst, 3 mL of solvent, 90°C, 1 h, 450 rpm	90	77 camphene 11 limonene 12 others	[62]
		β -Pinene			99	69 camphene 18 limonene 2 α -pinene 11 others	
		Limonene			99	40 terpinene 40 <i>p</i> -cymene 2 menthene 15 phellandrene 3 others	
9	USY	Camphene			20	99 tricyclene	
		α -Pinene			> 99	14 camphene 7 limonene 2 β -pinene 22 terpinolene 5 <i>p</i> -cymene 15 β -phellandrene 35 others	
		β -Pinene			> 99	5 camphene 12 limonene 17 α -pinene 10 terpinolene 10 <i>p</i> -cymene 11 β -phellandrene 35 others	

(Continued)

Table 3. (Continued).

Entry	Catalyst	Monoterpene	Solvent	Reaction conditions	X (%)	S (%)	Ref
10	Supramolecular 2-NBSA@MMF	Limonene	Solvent-free	1 mol% of catalyst, 25°C, 51 h	45	91 terpinolene	[63]
11	HSIW/Q-10	Limonene	Solvent-free	Inert atmosphere (pyrolysis conditions), 250°C	24	31.6 <i>p</i> -cymene 7.9 γ -terpinene 5.3 α -phellandrene 10.5 terpinolene 13.2 menthenes 31.6 C ₊₁₀	[64]
12	Pd(OAc) ₂	Limonene	Anhydrous DMF	10 mol% of catalyst, 120°C, 3 h, 4 equiv. CuCl ₂ , 9 equiv. 2,6-lutidine, argon atmosphere	39	100 DMS	[65]
13	Ti ₃ C ₂ Mxene	α -pinene	HF as etching agent	1 g of substrate, 0.05 g of catalyst, 160°C, 500 rpm, 6 h	75	65 camphene 23 α -terpinene	[66]

wc: Without calcination. **C₊₁₀:** compounds with a carbon number larger than 10. **NR:** Not-reported. **DMS:** *p*, α -dimethylstyrene.

these systems require temperatures exceeding 130°C. Additionally, these materials exhibit limited selectivity toward specific products, with camphene (33.1%) and limonene (30%) being the primary products. Although the BET surface area (437 m² g⁻¹) and the total pore volume (0.16 cm³ g⁻¹) of this material are notably lower than those of activated carbon, its higher α -pinene conversion suggests that its activity stems from the superior acidity of zeolites

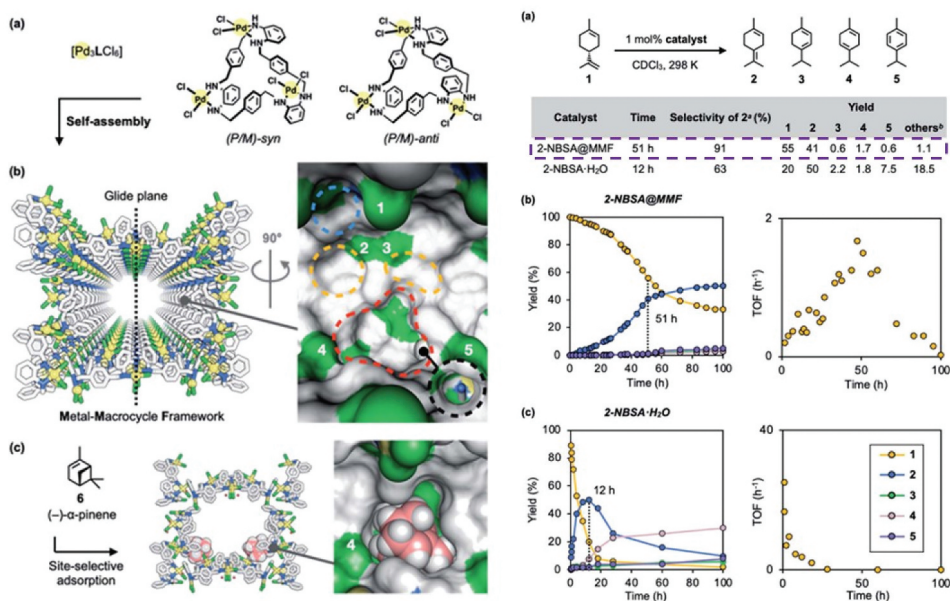


Figure 4. A) General scheme for the synthesis of Metal-Macrocycle Framework. B) catalytic application in the limonene isomerization into terpinolene. Reproduced with permission from ref [63].

compared to carbon. A mazzite-type zeolite with mesopores [61] (Table 3, entry 7) has also been evaluated in a solvent-free conditions at a similar temperature (120°C). However, the conversion does not exceed 44% even after 3 h of the reaction. Furthermore, this zeolite does not exhibit a clear preference for any specific product, rendering it unsuitable for efficient production of camphene or limonene. This limitation arises from significant challenges in separating these target products from the reaction mixture, primarily due to the formation of a mixture of three isomers at low conversion.

Hydrogen titanate was prepared using a hydrothermal treatment at 110°C for 24 h on a suspension of TiO₂ nano-powder and a 10 M NaOH solution [62]. This was followed by filtration and washing with deionized water until reaching a neutral pH. The resulting material was then dispersed in a 0.1 M nitric acid solution followed by stirring for 24 h, and subsequent washing until a neutral pH was achieved. Finally, the material was dried at 110°C for 6 h. This material was tested in pinenes, limonene and camphene isomerization (Table 3, entry 8) at 90°C for 1 h. Notably different from previous reports, this process required the use of cyclohexane as a solvent. Remarkably, such treatment gave one of the most active and selective catalysts, yielding approximately 69.3% and 68.3% of camphene from α-pinene and β-pinene, respectively. Additionally, limonene was identified as the primary secondary product. Although this material exhibited a low surface area (394 m² g⁻¹), its acidity was significantly enhanced due to the hydrothermal synthesis methodology and the subsequent nitric acid washing. In comparison, hierarchical zeolite-type Y (Table 3, entry 9) was also tested under the same reaction conditions as the titanates [62]. While it displayed high activity, as evidenced by substantial pinenes conversion, it did not demonstrate a preference for any specified product. This lack of selectivity represents a significant drawback of these materials for this application.

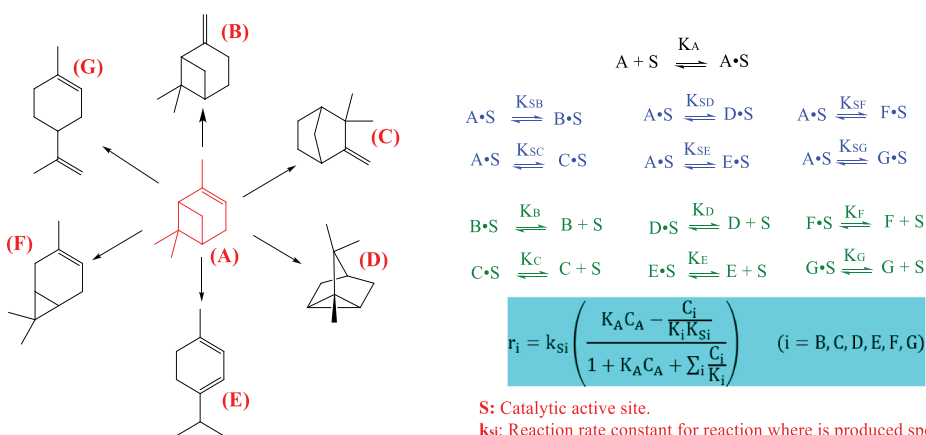


Figure 5. Kinetic scheme for the isomerization of α-pinene over a heterogeneous catalyst.

Terpinolene, a cyclic monoterpene, is a common constituent of certain commercial cannabis chemovars [51,74] and is a distinguishing feature of “sativa” strains [75]. This compound has demonstrated the ability to inhibit LDL oxidation, which holds significance in the treatment of atherosclerosis and coronary artery disease [76]. Additionally, it has been reported to possess antifungal and larvicidal properties [77]. Terpinolene has been identified as the primary isomerization product resulting from the conversion of limonene, accomplished by utilizing a porous metal-macrocycle framework (MMF) as a heterogeneous catalyst (Table 3, entry 10) [63]. This framework was created by immersing MMF crystals in an acetonitrile solution of 2-nitrobenzenesulfonic acid (2-NBSA·H₂O) for 1 day. This material, in a free-solvent system, exhibited a high selectivity toward terpinolene (91%) although at a relatively low limonene conversion of 45% after 51 h of reaction at 25°C (Figure 4). Preferred terpinolene formation was associated with the Brønsted acid sites supported in the pores of the MMF with high symmetry as was shown by molecular dynamic calculations (Figure 4). On the other hand, heterogeneity of this material was confirmed using ¹H NMR analysis of a CDCl₃ solution containing dissolved 2-NBSA·H₂O or a solution heterogeneously containing the catalyst (2-NBSA@MMF). Incorporation of 2-NBSA was confirmed by single-crystal X-ray diffraction, which showed that it was site-selectively adsorbed to the bottom pockets of the MMF with 37% occupancy, accompanied by two water molecules.

Heteropolyacids (HPAs) function as promising catalysts due to their cost-effectiveness, ease of handling, and reducing toxicity in comparison to corrosive and toxic liquid catalysts like HCl, HF, and H₂SO₄ [64]. Their inherent acidity and redox properties have led to their extensive use across various applications [78–81]. However, their practical utility is hampered by their very low surface area (<10 m²/g) and thermal stability [82]. To overcome these limitations, HPAs can be anchored to micro or mesoporous supports. In that way, different heteropolyacids (H₃PW₁₂O₄₀, H₃PMo₁₂O₄₀, H₄SiW₁₂O₄₀, and H₄PMo₁₁VO₄₀) have been supported on Q-10 (amorphous commercial silica), SBA-15, MCM-41, and KIT-6. These catalytic systems were evaluated in the limonene isomerization under highly elevated reaction temperatures (250°C) under inert N₂ atmosphere [64]. The outcomes of this study revealed that silicon-supported HPAs demonstrated a more pronounced activity for converting limonene to *p*-cymene than those with phosphorus. Of particular significance is the remarkable efficacy exhibited by H₄SiW₁₂O₄₀ supported on Q-10 (Table 3, entry 11), which attains limonene conversion of 24%. Nonetheless, selectivity toward *p*-cymene remains relatively subdued at 31.6%. An augmented Lewis/Brønsted acidic ratio coupled with lower BET surface area can potentially yield higher *p*-cymene amounts. Notably, the physical properties of this material encompass a surface area of 274 m² g⁻¹, a pore volume of 1.21 cm³ g⁻¹, and pore dimensions within the range of 13-

15.4 nm. On the other hand, nanoparticles of phosphotungstic acid-impregnated niobium-coated superparamagnetic iron oxide have been assessed as a heterogeneous catalyst in the isomerization of turpentine oil, which serves as a source of pinenes. This catalyst yielded approximately 50% of camphene and limonene, with polymeric byproducts accounting for 18% to 28% of the total products [83].

Although *p*-cymene ($C_{10}H_{14}$) is known as the main dehydrogenation product of pinenes and limonene [84], *p*, α -dimethylstyrene (DMS, $C_{10}H_{12}$) has been synthesized using several palladium catalysts, with copper chloride as an oxidant [65]. This system required the use of a sterically hindered base such as 2,6-di-*tert*-butylpyridine and 2,6-lutidine. The highest yield (30%) was reached under the reaction conditions presented in Table 3, entry 12. DMS is used in alcoholic beverages and soft confection at 5 ppm, in bakery and frozen confection at 2.5 ppm, and in desserts and nonalcoholic beverages at 1 ppm [85]. Additionally, DMS is reported to occur in citrus fruits, curry (*Bergera koenigii* L.), eucalyptus oil (*Eucalyptus globulus* Labill), mace (*Myristica fragrans* Houttuyn), mastic (*Pistacia lentiscus*), nutmeg (*Myristica fragrans* Houttuyn), pistachio oil (*Pistacia vera*), *Pistacia atlantica*, *Salvia* species, and turpentine oil [86]. 2D materials like MXenes ($M_{n+1}X_nT_x$), where M is an early transition metal, X is carbon and/or nitrogen, $n=1,2,3$, and T_x is a surface functional group (-F, =O, -OH) have been synthesized via acidic etching aluminum from MAX phase (Ti_3C_2 -Al- Ti_3C_2 -Al- Ti_3C_2), and tested in the isomerization of α -pinene (Table 3, entry 13), yielding 49% of camphene and 17% of α -terpinene.

A kinetic study for the isomerization of α -pinene (A) to different isomers, such as β -pinene (B), camphene (C), tricyclene (D), terpinene (E), 3-carene (F), and limonene (G), over a heterogeneous catalyst [57], can be illustrated by Figure 5, assuming the surface reactions as the rate-limiting steps. The reaction rate constants (k_{si}), and equilibrium adsorption (K_A), desorption (K_i), and reaction (K_{si}) constants can be estimated by optimization of the sum of squared errors between experimental and fitted data [87,88].

3. Oxidation and epoxidation

3.1. Why oxidation and epoxidation are important as chemical organic transformation?

Among transformations of monoterpenes, oxidation reactions of terpenes have been widely studied focusing on two routes: the first one related to the typical oxidation by radical pathways and using oxidizing agents, and the second associated with the epoxidation of the C=C bond to achieve the corresponding cyclic ether. Selective oxidation of monoterpenes under mild conditions is currently of great interest because of the valuable intermediates

used for the synthesis of fine chemicals. In the case of monoterpenes, biodevised biomass, recent development of epoxidation routes has featured several catalysts (homogeneous, heterogeneous, and enzymatic) to be highly selective at the laboratory scale; however, many of them cannot be scaled up or used in a continuous mode. Then, the practical implementation is still unexplored. In fact, the synthesis of biomass-derived epoxides is tremendously important in the modern era as they lead to a series of important chemicals, which can be used for the production of polymers, fragrances, formulations in manufacture, pharmaceuticals, cosmetics, etc.

3.2. Reactivity of some monoterpenes in oxidation and epoxidation

Figure 6 shows the main oxidized and epoxidation products obtained from the most abundant and commercially available monoterpenes: Limonene, α -pinene, and β -pinene. Conventionally, limonene (in their two stereochemical configurations *R*-(+) and *S*-(-)) is extracted from the peels of citric fruits such as lemon and orange. In the case of lemon, the peel contains a sole isomer, *S*-(-)-limonene, while for orange the main stereoisomer corresponds to *R*-(+)-limonene. Both contain two C=C bonds which are susceptible to oxidation and epoxidation. Interestingly, location of both alkene bonds drastically affects selectivity of the final product. Several factors such as the type of catalyst, reaction conditions, the oxidizing agent, and location of the C=C are the most reported factors to drive the selectivity to desired target. Because of the presence of an external C=C bond for limonene and with the use of thermal initiators, biodegradable polymers can be achieved. In many of these cases, the formation of oligomers (up to 40 of polymerization degree) has been reported [89]. Epoxidation of limonene is an interesting chemical route to obtain derived biomass substances for applications in fine chemistry, synthesis of intermediates used in disease treatments, building blocks in the polymeric industry, etc. The oxygen-rich epoxides are susceptible to replacing many common monomers such as bisphenol A, and they can also be used for the fabrication of new biodegradable materials [90]. In addition, epoxides can react together with other substrates to produce polyesters, polycarbonates, and copolymers with vinyl and non-vinyl monomeric units.

Limonene contains two C=C bonds susceptible to epoxidation: one of them is localized in the *endo* location while the other is in the *exo* position. From the chemical point of view, the *endo* C=C is epoxidized faster than *exo* C=C because of its reactivity. More rigid double bonds tend to be more reactive because of the strain. Then, the strainer is the most reactive in epoxidation. Several factors influence epoxidation selectivity and yield, namely, reaction conditions (temperature, pressure, additive) and the oxidizing agent nature. However, the reactivity of the olefin together with the type of catalyst and the

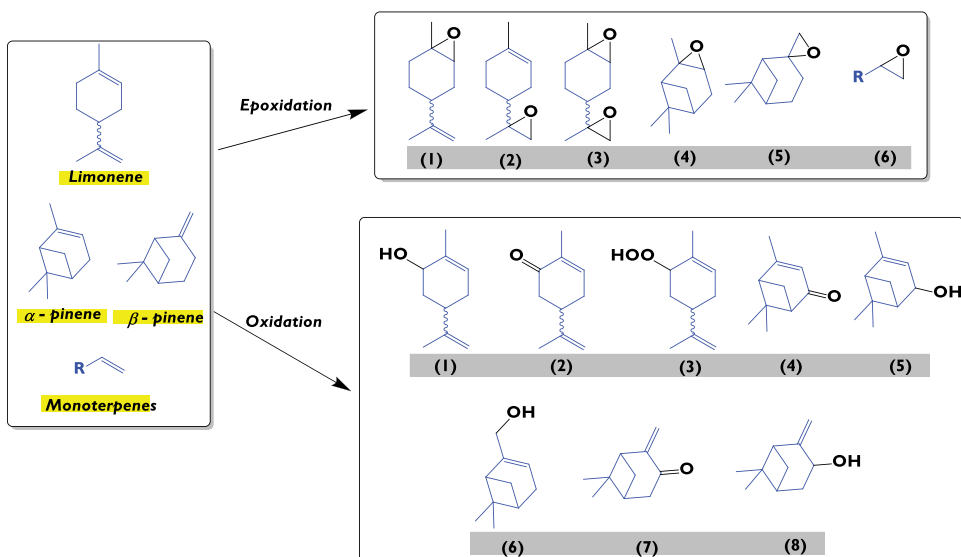


Figure 6. The most relevant oxidized and epoxidized products from commercial monoterpenes: **Epoxidation:** (1) 1,2-limonene-epoxide, (2) 8,9-epoxy-limonene, (3) limonene diepoxide, (4) α -pinene epoxide, (5) β -pinene epoxide, (6) other monoterpenes epoxides. **Oxidation:** (1) carveol, (2) carvone, (3) limonene-2-hydroperoxide, (4) verbenone, (5) verbenol, (6) myrtenol, (7) pinocampnone, (8) pinocarveol. *limonene-1,2-diol and 4-terpineol can be also obtained but after opening of limonene-1,2-epoxide by water.

oxidizing agent could be determined as the most critical factors in driving selectivity toward the epoxide product.

3.3. Recent literature involving heterogeneous catalysts

Several olefins including monoterpenes and monoterpenoids were converted into epoxides by using a one-pot procedure dissolving the olefin into DMSO (anhydrous grade) and adding NBS to the reaction mixture [91]. However, this strategy requires adding DBU at the final step, otherwise it would not work. By using this procedure, the yields of the desired epoxides with camphene and α -terpineol as the starting materials were up to 76% in both cases. Other monoterpenoids were also used to achieve the epoxides giving up to 88% yield of carvenone. With limonene, the yield of limonene epoxide did not exceed 69%. Interestingly, it appears that sterically hindered alcohols are oxidized more rapidly and give better results than less hindered substrates. This fact could be attributed to various factors: I) capacity of the oxidizing agent to produce radicals which then attack the C=C, II) steric hindrance, and III) reactivity of the alkene.

On the other hand, microporous zeolites have also been reported for the synthesis of epoxides starting from monoterpenes such as α -pinene, β -pinene, and limonene. For example, with the composite ZSM-5@Co-MOF (Table 4,

entry 1) and using a green oxidizing agent (air), selectivity to the cyclic ether was up to 96.2% in the case of α -pinene. Because of the presence of bicyclic structure, both α - and β -pinene are more reactive in comparison with limonene which did not exhibit a similar structure. Then, in these cases, reactivity will depend on the type of monoterpene structure and ability of the catalyst for the adsorption and activation of the oxidizing agent. Well-known methodology for the homogeneous synthesis of epoxides starting from hydrogen peroxide and acetonitrile has been used for several decades which is comparable with those reported for the composite of zeolite-MOF. The use of air as the oxidizing agent drastically decreases the E-factor, improving the green metrics and making it more sustainable. Comparatively, a complex based on Co achieved promising results with selectivity up to 99% to limonene epoxide albeit at mediocre conversion (less than 10%). Again, α -pinene as starting monoterpene achieved almost complete conversion and total selectivity to α -pinene epoxide. The same order of reactivity as for the composite was obtained. The use of this kind of complex catalyst makes the process difficult to reuse and scale up.

In the same way, the 5-(2-pyridyl) tetrazole complex of molybdenum (VI) (**Table 4, entry 3**) was tested as an active catalyst for the synthesis of limonene epoxide in different stereochemical configurations and using TBHP as an oxidizing agent. Relative low selectivity to the desired epoxide was achieved, which is related to ability of TBHP to form radicals and generate polymerization reactions of C=C in limonene. It is well known that many of these reactions (polymerization or oligomerization) depend on the initiator, solvation, and the intermediate carbocation. Control of epoxidation over oligomerization (or polymerization) is associated with the amount of the oxidizing agent, temperature, and the type of solvent. For radical polymerization, the use of nonpolar solvents (such as benzene and toluene) generates a co-lateral chain transfer reaction which affects the overall kinetics.

Among complexes covalently attached to heterogeneous supports, β -tetrabrominated meso-tetraphenylporphyrinatomanganese(III) acetate [MnTPPBr₄(OAc)] (MnPor) [95] was anchored onto a magnetite imidazole-modified graphene oxide nanosheet (Fe₃O₄.GO.Im) (**Table 4, entry 4**). The catalyst was successfully applied for epoxidation of different alkenes using hydrogen peroxide (UHP) and acetic acid (HOAc) as oxidant activators under mild conditions. Olefins were oxidized efficiently to their corresponding epoxide with 63–100% selectivity in the presence of Fe₃O₄.GO.Im@MnPor. Moreover, a remarkable turnover frequency (93 h⁻¹) was achieved for the oxidation of α -pinene. The graphene oxide-bound Mn-porphyrin was recovered from the reaction mixture by magnetic decantation and reused several times. Similarly, tungsten complexes were used as active catalysts for oxidation of commercial and naturally available limonene (including other natural-based compounds) (**Table 4, entry 5**). The molybdenum (II) catalyst

precursors are very active, reaching 100% of conversion and 98% of selectivity to the epoxide. However, their heterogenization seems to be beneficial with to improve the sustainability. In general, W complexes exhibit better activity than Mo complexes, however when supported on MCM-41, activity decreased substantially. This could be related to poor anchoring, dispersion, and size of the crystallite. The authors [96] performed DFT (Density Functional Theory) calculations to elucidate the reaction mechanism and the difference between the W and Mo centers. Surprisingly, in the catalytic cycle, tungsten complexes and iodide ligands can be oxidized from M(II) to M(VI) more readily than molybdenum complexes, even though the energies of the relevant species involved in the cycle are very comparable across all complexes. Furthermore, it appears that iodide complexes were more easily oxidized by ROOH, but the catalytic reaction was less favored than for bromides. In general, tungsten complexes serve as effective catalysts; however, their performance was not improved when supported on MCM-41. Due to the challenging synthesis process compared to molybdenum analogues, such complexes are not promising. On the other hand, certain molybdenum heterogeneous catalysts show activity, higher than the complexes and offer the advantages typical of heterogeneous catalysts.

In comparison with the previous reports [92–96], a series of composite materials composed of WO_x and SiO_2 (Table 4, entry 6) were synthesized by using a novel, template-free sol-gel method [97]. The effectiveness of the synthesis method lies in its custom-designed reactor, which enables interactions of the reactants exclusively in the presence of scCO_2 (supercritical carbon dioxide). Various synthetic parameters were carefully examined to optimize the performance of the resulting materials as heterogeneous catalysts in epoxidation reactions using H_2O_2 as an environmentally friendly oxidant.

On the other hand, modification of zeolite Y with a complex of the type $[\text{VO}(\text{Sal}_2\text{bz})_2]$ [98] was successfully applied as a heterogeneous catalyst for the synthesis of allylic products from the two renewable molecules such as limonene and α -pinene. Relatively mild conditions (Table 4, entry 7) have allowed to achieve conversion close to 99% and selectivity up to 70% to the desired products. Decrease of the steric hindrance increases the formation of the olefinic product at the expense of formation of allylic oxidation products. Formation of a specific product (epoxide vs allylic or diols) can be explained from coordination of the C=C bond (electron rich) to the oxo vanadium active specie (Figure 7).

On the other hand, two double-layer hydroxides ZnAl-LDH and MgAl-LDH were functionalized with *bis*(4-HOOC-phenyl)-acenaphthenequinonediimine) (H_2BIAN) [99] (Table 4, entry 8), and then tested for the selective synthesis of epoxides starting from limonene. The rational design of this catalyst was based on the idea that -based ligands exhibit high activity in the metal transition chemistry. In this way, the material was

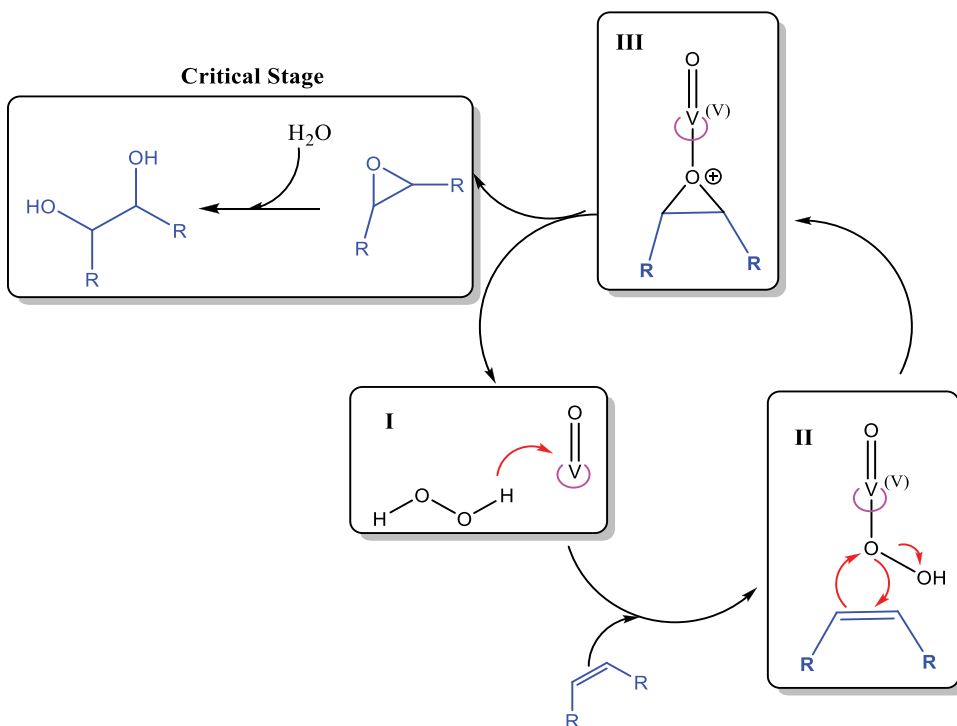


Figure 7. Proposed reaction mechanism for epoxidation and ring-opening of some epoxides. Steps: (I) Activation of hydrogen peroxide by coordination of the oxo-vanadium unit (II) back donation of the oxygen to the olefin (III) formation of the oxirane ring.

evaluated as a possible catalyst for the transformation of limonene with TBHP as the oxidizing agent. In comparison with the previously discussed reports [92–98], the temperature was as high as 110°C in toluene as a solvent. From the green chemistry point of view, the use of toluene as the solvent is deemed undesirable due to its toxicity and potential negative effects. ZnAl-LDH-BIAN- MgI_2 was the most active catalyst resulting in 94% of conversion with almost 97% selectivity to the epoxide [99]. Stereoselectivity was also assessed for R-(+)-limonene-1,2-epoxide which was found to be crucial to achieve one diastereomer over another other and comparing homogeneous and heterogeneous catalysts. Homogeneous catalysts clearly favor the *trans* diastereomer contrary to heterogeneous counterparts. Three catalysts did not show any preference, producing both diastereomers in approximately equal amounts (around 50/50 ratio). However, the ZnAl-LDH-BIAN- MoBr_2 catalyst displays an intermediate behavior, favoring the *trans* diastereomer with a ratio of 28-to-72.

Materials containing special textural properties, e.g. silica, zeolites, etc. can be of interest for the selective synthesis of organic reactions because of their ability to distribute active sites in confined spaces. In many cases, they can be highly dispersed increasing catalytic activity. A particular example of these

Table 4. Heterogeneous catalyst for the oxidation/epoxidation of monoterpenes.

Entry	Catalyst	Substrate	Reaction conditions	Oxidizing agent	X (%)	S ^b (%)	Ref
1	ZSM-5@Co-MOF	α -pinene	10 mg ZSM-5@Co-MOF-150 catalyst, 3 mmol olefin, 5 h	Air	98.2	96.2	[92]
		β -pinene			72.6	78.3	
		Limonene			48.1	98.0	
2	[Co(NH ₃) ₆]Cl ₃	α -pinene	5 mg of catalyst, 3 mol of pinene, 10 g of solvent, 90°C, 0.3 mmol of TBHP, 5 h, flow rate of air 40 mL min ⁻¹ .	Air	98	99	[93]
		β -pinene			43	55	
		Limonene			9	>99	
3	5-(2-pyridyl) tetrazole complex of molybdenum (VI)	Limonene	TFT, 70°C, ratio Mo: monoterpene: TBHP: 1:100:210, 24 h.	TBHP	>99	51 to monoepoxidesaa	[94]
4	Fe ₃ O ₄ .O. Im@MnPor	α -pinene	Molar ratios catalyst: substrate: UHP: HOAc of 1:100:200:300 in CH ₂ Cl ₄ , 1 h, room temperature.	UHP with acetic acid (HOAc)	93	95 to epoxide 95% exo-epoxide and 5% endo-epoxide	[95]
		Limonene			67		
5	MCM-MoI ₂	S-Limonene	2 eq. of oxidant, 3 mL of dichloromethane, and 175 mg of catalyst at 328 K and 24 h.	TBHP	100	98	[96]
6	WO ₃ -SiO ₂	Limonene	1 eq. of oxidant and 20 mg catalyst in 1-4-dioxane +isopropanol, at 80°C for 4 h.	H ₂ O ₂	54	53 epoxide 33 glycol 9 allylic products	[97]
7	[VO(<i>sal</i> ₂ <i>bz</i>) ₂]-Y	Limonene	2 eq. of oxidant, 15 mf of catalyst, 3 mL acetonitrile as solvent, at 80°C for 24 h.	H ₂ O ₂	90	39 glycol 49 allylic products	[98]
		α -pinene			100	70 allylic products	
8	ZnAl-LDH-BIAN-MoI ₂	Limonene	2 eq. of oxidant, toluene as solvent, at 110°C for 24 h	TBHP	94.0	97.0 epoxides	[99]
	ZnAl-LDH-BIAN-MoBr ₂				80.0	89.0 epoxides	
	MgAl-LDH-BIAN-MoI ₂				64.0	93.0 epoxides	
	MgAl-LDH-BIAN-MoBr ₂				79.0	93.0 epoxides	
9	Co/SBA-16	Limonene	3.6 mmol of substrate, 170 mg of catalyst, 10 mL min ⁻¹ of O ₂ , 12 mmol isobutyraldehyde, and 10 mL of ethyl acetate, at 301 K for 200 min.	O ₂	99 (Co/Si = 1.1%)	44 epoxide 41 diepoxide	[100]
					99 (Co/Si = 8.8%)	41 epoxide 25 diepoxide	
10	W/SiO ₂	Limonene	1 mmol of substrate, 2 mmol of oxidant, 5 mL of acetonitrile, 10 mg of catalyst, at 90°C for 6 h.	H ₂ O ₂	68	53% 1,2-epoxide 11% 8,9-epoxide	[101]
11	[VO(L).H ₂ O]-Y	α -Pinene	10 mmol substrate, 20 mmol of oxidant, 70 mg of catalyst, 2 mL of acetonitrile, at 75°C for 24 h.	H ₂ O ₂	85.4	46.5 verbenone 7.7 verbenol 44 nol 44.2 α -campholenic aldehyde 1.5 epoxide	[102]
		Limonene			87.4	40.6 carvone 32.0 carveol 9.1 glycol 6.5 1,2-epoxide 11.8 4-terpineol	

(Continued)

Table 4. (Continued).

12	ZnCo-MOF	α -Pinene	3 mmol of substrate, 40 mL min ⁻¹ of oxidant, 30 mg of catalyst, 10 g of DMF as solvent, at 90°C for 5 h.	Air	95.5	96.7 epoxide	[103]
		β -Pinene			70.8	62.5 epoxide	
		Limonene			42.4	80.3 epoxide	
13	Pd/HPA-300/ SBA-15	β -Pinene	1 mmol of substrate, 6.8 mmol of oxidant, 15 mg of catalyst, 1 mL of acetone as solvent, 50°C, 18 h, 450 rpm.	H ₂ O ₂	99	63 <i>trans</i> - pinocarveol 12	[104]
	Pd(0.5)/HPA/ SBA-15				90	pinocamphone 16 myrtenol 67 <i>trans</i> - pinocarveol 13 pinocamphone 15 myrtenol	
14	Co(II) complex	α -Pinene	20 g of α -pinene, 100 mg of catalyst, volumetric flow ratio 5:5 for mixture: CO ₂ , 160 atm, at 260°C in a tubular reactor of 7 cm ³ .	Atmospheric O ₂	59.8	21.1 camphene 3.0 tricyclene 5.5 α -fenchene 4.0 verbenone 6.2 β -pinene 19.4 limonene 5.7 <i>p</i> -cymene 4.2 bornyl acetate 4.2 α -fenchyl acetate	[105]
15	MgO	Limonene	0.1 mmol substrate, mass ratios for substrate/MgO/H ₂ O/acetone/acetonitrile:H ₂ O ₂ of 1:1.20:30.3:19.7:15.7:1.20, 50°C, 1000 rpm	Peroxy cetimidic acid ^a	80(0.5 h)	100 epoxides (1,2 + 8,9)	[106]
					100 (2 h)	96 diepoxide	

*Reported as the isolated yield. **Molar ratio of diepoxide/monoepoxides was 0.3. *BIAN*: bis(4-HOOC-phenyl)-acenaphthenequinonediimine. *LDH*: Layered double hydroxide. *Bipy*: 2,2'-bipyridine-4,4'-dicarboxylate. ^aIn-Situ production from H₂O₂ with acetonitrile. ^bThe epoxidized double bond is at the 1,2 position unless otherwise indicated.

kind of materials is Co/SBA-16 (Table 4, entry 9) in which Co can be located inside of the pores of the well-defined structure of SBA-16. Interestingly, the catalyst was used as heterogeneous material for aerobic Mukaiyama epoxidation of limonene in the presence of isobutyraldehyde, under mild conditions (28°C, ethyl acetate as the solvent, 200 min). Synthesis of these catalysts by adjusting the pH was performed with the aim to obtain isolated tetrahedrally coordinated Co²⁺ ions in the support which could act as the active species. The reported methodology affords materials with larger pore volumes and with larger pore sizes making them very attractive for the diffusion of relatively large molecules such as limonene. In general, these new materials displayed high reactivity for epoxidation of limonene yielding different epoxides in both the *endo* and *exo* positions. In addition, the authors [100] suggested that Co³⁺OO⁻ peroxy intermediate could be critical for the formation of the epoxides which was rigorously analyzed by kinetic analysis.

In a similar way, tungstenocene (IV) dichloride (Table 4, entry 10) was deposited and grafted on an amorphous silica using two approaches: liquid-

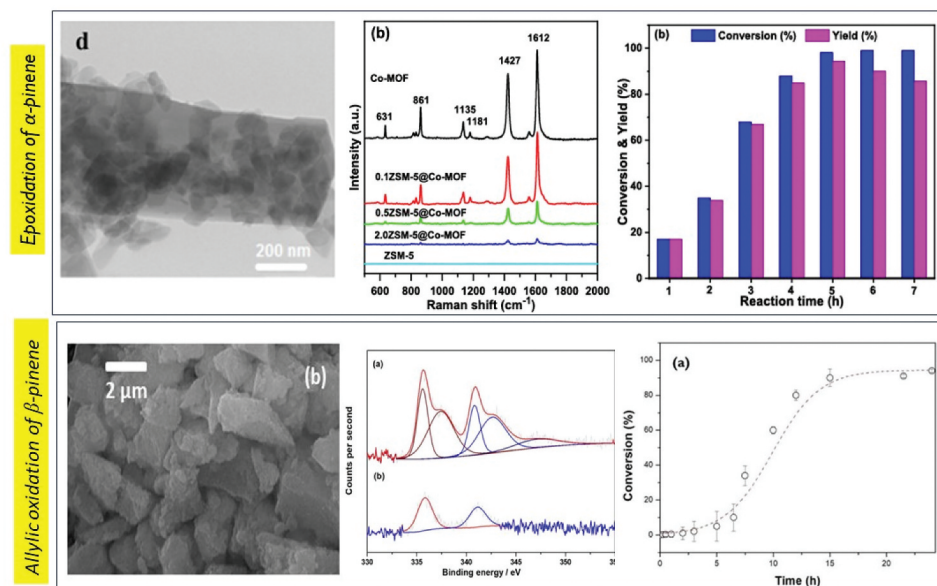


Figure 8. Some selected characterization and catalytic activity of materials active in oxidation or epoxidation of terpenes: a) epoxidation of α -pinene with ZSM-5@Co-MOF b) allylic oxidation of β -pinene with Pd/HPA/SBA-15. Images reproduced with permission of ref [92] (a) and [104] (b).

phase and dry impregnation. The results suggest that W-containing systems were active in the epoxidation of limonene when hydrogen peroxide was used as an oxidizing agent. Only WO_3 displayed mediocre activity because of the amount of tungsten in the bulk of pure tungsten oxide samples. In fact, selectivity to epoxide was good (for both 1,2- and 8,9- C=C bonds) while formation of carveol (and their isomers) was low. As no menthenediols were formed as side products, it is possible to suggest that with this catalyst oxidation via the homolytic pathway did not play a role. In comparison, when TBHP was used as the oxidant agent, limonene indeed underwent oxidation with a very large number of minor side-products which are related with the radical species generated by TBHP decomposition [107].

In comparison with the previous catalytic system, transition metals containing complexes with Schiff-base ligands (Table 4, entry 11) were entrapped and deposited in the cages of zeolite-Y and then were tested in the catalytic oxidation of limonene and α -pinene. Zeolite-Y [102] has gained attention because of their properties such as a high surface area, large pore volume as well as the typical channels and cavities which made it possible for entrapment of large size complexes [108,109]. Nevertheless, the post-activation of the complex for further uses is still a challenge. Because of the organic counterpart, typical calcination of these kind of materials is not possible. On the other hand, several steps required for the covalent anchoring of the complex to the zeolite, make this alternative not too simple. With respect to catalytic activity, the

material was successfully applied as an active catalyst for oxidation of both α -pinene and limonene monoterpenes and using hydrogen peroxide as a green oxidizing agent. The ratio monoterpene to the oxidizing agent was 1:2. Oxidation was performed at relatively mild conditions (75°C, 24 h and acetonitrile as a solvent). Interestingly, after such a long time, the conversion was not complete, achieving values up to close to 90% and with mediocre selectivity to verbenone (46.5%) in the case of α -pinene and carvone (40.6%) for limonene. Interestingly for oxidation of α -pinene, campholenic aldehyde was obtained almost in the same amounts as verbenone. It is well known that campholenic aldehyde (campholenal) is one of the main products of α -pinene epoxide isomerization with Lewis acidic sites. This suggests that a large amount of this epoxide is converted totally to campholenic aldehyde in the presence of Lewis acid sites. On the other hand, oxidation of limonene also gave limonene-1,2-diol (glycol) and 4-terpineol as the main subproducts, which also suggest that an intermediate epoxide is obtained thereafter being consumed by reacting with water. Diols can be obtained in a one-pot two steps in which the first step is formation of the epoxide and then, the ring-opening using water as the nucleophile. The stereochemistry of these diols remained unexplored.

ZnCo-MOF catalyst (Table 4, entry 12) was tested as an efficient material for the air epoxidation of monoterpenes (including also other cycloalkenes) [103]. Activation of oxygen is as well a very difficult process requiring energy or at least a sacrificial reducing agent and initiator to obtain the singlet-state atomic oxygen. The use of the sacrificial agent has been reported to have a negative effect on the epoxidation because of the large quantity of low-value secondary products. Metal organic frameworks, which are porous, crystalline materials, with a high surface area and adjustable structure, were successfully modified with Zn and Co by using the dry-gel method. Synthesis of the material was performed in only one vessel containing the desired amounts of the ligand (dicarboxylic acid), precursors of Zn and Co, HF and water. Exceptionally, synthesis of MOF does not require high temperature and pressure and usually the synthetic protocols are reproducible. A typical crystal structure and functional groups were identified by TEM and Raman spectroscopy (Figure 8). Growing crystalline MOFs together with Zn and Co avoids the use of a co-reductant and a sacrificial agent in the epoxidation of olefines. Almost complete conversion with 96.7% selectivity to α -pinene epoxide was achieved after 5 h of reaction time (Figure 8) [103]. Detected by-products such as campholenic aldehyde illustrate the nature of the Lewis acid sites in the catalyst.

The last example, i.e. combination of metal/acid sites for selective epoxidation, demonstrates that the nature of the metal center, together with the distribution of acid/basic sites can promote epoxidation rather than isomerization and allylic oxidation. Sometimes, the solvent also plays a critical role

together with the oxidizing agent. Then, a combination of these all factors can drive the reaction to the desired epoxide/oxidized product. Considering these facts, recently a Pd supported on a modified heteropolyacid-silica (HPA/SBA-15, **Table 4, entry 13**) [104] was reported to be active in the allylic oxidation of β -pinene into *trans*-pinocarveol as the main product and myrtenol/pinocamphone as the byproducts. Multifunctional heterogeneous materials containing both a metal and an acid function were prepared by using wetness impregnation, showing typical laminar geometry together with Pd²⁺ as the oxidation state (**Figure 8**). In this case, the material containing Pd with a heteropolyacid supported on SBA-15 (Pd/HPA-300/SBA-15) was one of the best materials to give *trans*-pinocarveol with the yield of 65% (total conversion of β -pinene). Independent on the Pd loading (0.5 wt% or 1.0 wt%) and calcination temperature (heteropolyacid over SBA-15), selectivity to the desired *trans*-pinocarveol was not affected. At the same time, the calcination temperature influenced conversion, Pd dispersion, acidity, and the surface area. It appears that when the support was changed to amorphous silica, the selectivity changed drastically. Then, distribution, dispersion and location of the metal and acid functions drive selectivity to the desired product. The catalyst was successfully reused, and the process was scaled up to 10 mL with no negative implication for selectivity or conversion.

CoBr₂ complex with 2,6-lutidine [Co(2,6-Me₂C₅H₃N)₂Br₂] (**Table 4, entry 14**) was prepared and tested for the oxidation of α -pinene in a flow reactor using a supercritical solvent (mixture of CO₂ and ethyl acetate) [105]. The range of temperature and pressure varied between 190-230°C and 110-125 atm, giving with these conditions' isomerization products with partial racemization. Oxidized products such as verbenone and pinocamphone were also obtained with high enantioselectivity in which selectivity seems to be lower (<20%). The authors suggest the presence of campholenic aldehyde, which is formed by the ring-opening of α -pinene epoxide. Formation of acetoxyated products was also observed (up to 6%). The studied reaction conditions with the Co-complex seem not to be favorable either for oxidation or epoxidation.

Recently, commercial MgO (**Table 4, entry 15**) has been reported as a versatile catalyst for the selective synthesis of limonene epoxides and diepoxide, depending on the reaction conditions [106]. The epoxidation catalytic route was carried out with H₂O₂ in a Payne system, which used acetonitrile as an oxidant activator, and water and acetone as solvents. The highest yields for limonene epoxide (80%) and diepoxide (96%) were achieved after 30 min and 2 h, respectively, at a low temperature (50°C). The catalyst exhibited a composition of 82.6 wt.% of the periclase phase (mineral form of MgO) and 17.4% of the brucite phase (mineral form of Mg(OH)₂). After the reaction, a slight phase transition was observed from periclase to brucite, explained by the hydration under the reaction conditions, which had a negative effect on the selectivity to diepoxide after three reuses (a decrease from 97% to 76%). In

general, the authors [106] reported that diepoxide is favored with high concentrations of MgO and H₂O₂, high temperatures, and long reaction times, while epoxide is favored mainly with low temperatures and short reaction times. A successful kinetic modeling was reported for the first time for the epoxidation of R-(+)-limonene using a Payne reaction system, with a set of three reactions describing the formation of intermediate oxidant, the H₂O₂ decomposition, and the epoxidation reaction of limonene with intermediate.

4. Isomerization of monoterpene epoxides

4.1. Reactivity of monoterpene epoxides and main factors that affect them

Isomerization of monoterpene epoxides refers to the rearrangement of the epoxy group within a monoterpene molecule, resulting in the formation of different isomers with altered chemical structures and properties. During isomerization of monoterpene epoxides, the epoxy group undergoes intramolecular rearrangement, leading to high-added value chemicals of interest in the field of natural product chemistry and has implications in various industries, such as fragrance, flavor, and pharmaceuticals. Because epoxides are highly strained (strain energy, SE, of 27.9 kcal mol⁻¹) due to the bond angle distortion [36], they react with nucleophiles and electrophiles that rearrange their structure into thermodynamically stable substances such as aldehyde, alcohols, and ketones, among other compounds. In the case of monoterpene epoxides such as α - and β -pinene epoxides (Figure 9) can rearrange using an acidic or basic medium onto oxygenated compounds. These epoxides are constituted by three organic cycles: cyclohexane, cyclobutene, and epoxy-cyclopropane. For α -pinene epoxide, the epoxy group is in the endo-position being for β pinene epoxide in the *exo*-position, which is the cause of their different reactivity. α -Pinene epoxide acquires more stress in comparison to β -pinene epoxide (see Figure 9). It is attributed to lower β -pinene epoxide torsional strain in comparison with α -pinene epoxide and for this reason, its arrangement energy is higher [36].

Both epoxides are usually starting materials for the synthesis of chemicals of interest in the fragrance industry. For example, from α -pinene epoxide, it is possible to achieve campholenic aldehyde, *trans*-carveol, *trans*-sobrrol, pino-carveol, and pinocamphone, among others. Campholenic aldehyde and *trans*-carveol are the main products when the epoxide is in contact with an acidic catalyst. Selectivity is dependent on the specific reaction conditions and also on the type of catalyst. In general, the most important factors that drive selectivity to a specific target starting from these epoxides are the type of acid sites (Brønsted, Lewis or their ratio) and the solvent (polar or nonpolar, e.g.: toluene, DMSO, DMF, etc.). Figure 9 shows the most relevant products obtained from isomerization of both epoxides.

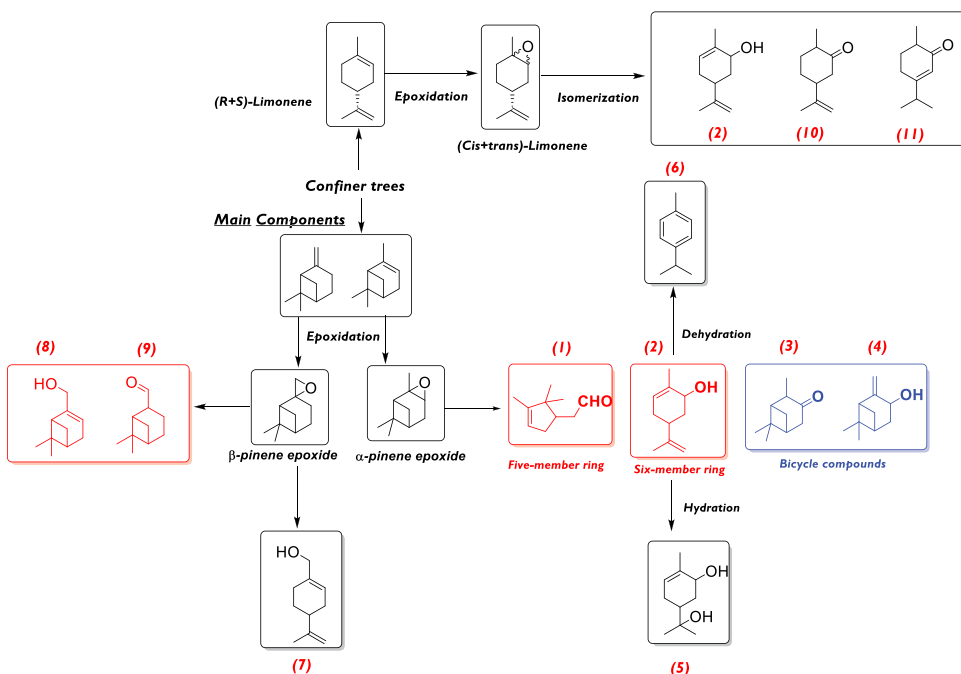


Figure 9. The most relevant isomerization products from α -, β -pinene and limonene epoxides by using acidic heterogeneous and homogeneous catalysts. 1=Campholenic aldehyde, 2=Carveol, 3=Pinocamphone, 4=Pinocarveol, 5=*trans*-sobrerol, 6=*p*-cymene, 7=Perillyl alcohol, 8=myrtenol, 9=Myrtanal, 10= Dihydrocarvone, 11= Carvenone.

Isomerization of α -pinene epoxide, one of the most studied monoterpene epoxides, can give two main products: campholenic aldehyde and *trans*-carveol with *trans*-sobrerol, pinocamphone, pinocarveol and *p*-cymene as the secondary products. Campholenic aldehyde can be selectively obtained using a Lewis acid catalyst and nonpolar solvents such as toluene. Ring-opening of the epoxide was described by coordination to the Lewis acid site and then rearrangement of the internal cyclobutene finally giving the desired isomerization products. Interestingly, the C-C shift to give a secondary carbocation in the second step can be carried out because of the internal tension of cyclobutene. This kind of bicyclic compound tends to relax their internal stress to give more favorable energetic products. The most relevant references for the synthesis of both industrially important commodities such as *trans*-carveol and campholenic aldehyde are mentioned in Table 5.

4.2. Analysis of the most relevant heterogeneous catalysts for synthesis of aldehydes and alcohols from monoterpenes epoxides

A selective catalyst based on zirconium phosphate was used as an inexpensive, efficient, and cost-effective material for synthesis of *trans*-carveol from α -

pinene epoxide. *Trans*-carveol has been widely reported as a precursor for the synthesis of fragrances, shampoo, toilet soaps and non-cosmetics products. It is the main constituent of spearmint essential oil. In addition, carveol as a phytochemical together with other monoterpenes was demonstrated to be active in the cloned $\alpha 7$ subunit of the human nicotinic acetylcholine receptor [126].

It is well known that Zr-phosphate catalysts comprising the Zr-framework together with the covalently anchored Zr-P can be effective for the ring-opening of epoxides (Table 5, **entry 1**). The acidic nature of the catalyst can be controlled by tuning Zr to P ratios. In [110], the authors claimed that exceptional activity is attributed to broad functionality of the phosphate groups which give the Brønsted acidic nature of this together with DMA as a solvent provided the best results reported up to now for the synthesis of the six-member ring product (*trans*-carveol). A similar yield of carveol (73%) has been reported using task-specific ionic liquids (TSILs) which act as both eco-friendly catalysts and reusable solvents in numerous industrial reaction [127]. The authors successfully correlated the reaction behavior with physical properties, such as conductivity, density, molecular volume, standard entropy, and lattice energy. In addition, the designed process complies with the green metrics criteria having 100% of atom economy and E-factor of 1 [127].

Fe supported catalysts [111,112] were reported to be selective in isomerization of α and β -pinene epoxides and also in the rearrangement of limonene epoxide with solvent polarity playing a critical role (Table 5, **entries 2-4**). As mentioned previously, this is a very sensitive reaction that can give a variety of aldehydes, alcohols, alkenes, etc. Then, controlling the type and strength of the acid sites as well as the solvent type can change the distribution of products. In the case of Fe/MCM-41, a decrease in selectivity to campholenic aldehyde was observed when the solvent was changed from toluene to *tert*-butanol, while selectivity to *trans*-carveol was apparently increased. The same trend was observed with Fe/SBA-15; however, the effect was more prominent. At total conversion of pinene oxide, selectivity decreased from 64% (for toluene) to 48% when *tert*-butanol was used as the solvent. When the authors [111] compared the same support with another metal (Cu), lower yields (in terms of conversion and selectivity) to the desired aldehyde and alcohol were achieved. For example, in the case of Cu/MCM-41, the maximum conversion was 20% while selectivity to campholenic aldehyde was 82%. An increase of conversion (46%) resulted in lower selectivity to the aldehyde (71%). The ability of Cu to coordinate *tert*-butanol is an explanation offered at such reaction conditions. The total Lewis acidity of Cu materials in comparison with Fe counterparts is the reason Cu being more selective to campholenic aldehyde. In the same way, thermodynamics of the isomerization of both epoxides at the reported reaction conditions showed that all the isomers (campholenic aldehyde, *trans*-carveol, isopinocampone, fencholenic

aldehyde from α -pinene oxide and myrtanal, myrtenol and perillyl alcohol from β -pinene oxide) are thermodynamically favorable, with campholenic aldehyde and myrtanal being preferential from thermodynamic viewpoint. The solvent effect was found not to be critical in thermodynamics [128].

The same Fe catalysts were also active in the isomerization of limonene and β -pinene epoxides (Table 5, *entries 3-4*) [111,112]; however, in the first case, poor activity and selectivity were obtained. Changing polarity of the solvent (from toluene to acetonitrile) induces a slight increase of conversion, however, selectivity to isomers was in all the cases lower than 50%. Competition between isomerization and hydrolysis is expected to be one of the most important factors to control. Remaining water (in the solvent, catalyst, or the additive) can produce limonene-1,2-diol rather than typical isomers (dihydrocarvone, *trans*-carveol, etc). Although the undesired diol finds applications in fine chemistry, formation of the isomers is more attractive because of their annual costs and direct implications in factory processes. On the other hand, isomerization of β -pinene epoxide which typically produces myrtanal, myrtenol and perillyl alcohol as the major products, was also tested with Fe catalysts showing that in all the cases and changing the polarity of the solvent, the major product is myrtanal [115]. However, modification of catalyst as well as the solvent can give perillyl alcohol as the main target; some examples are described in *Entries 6-7* (Table 5). In the case of zeolite-beta [114], the use of DMSO as a polar basic solvent improves selectivity to perillyl alcohol over myrtanal and myrtenol while for Ti- and Mo-based silica materials (MCM-41 and SBA-15) [115] the same main target was obtained but with a nonpolar solvent. It is well known that, generally, perillyl alcohol is favored with a polar basic solvent, whereas myrtanal is obtained with nonpolar ones. This exceptional case in which Ti or Mo materials were selective to perillyl alcohol using *n*-hexane as a nonpolar solvent is due to I) the typical texture and distribution of the active sites and II) the stabilization of the transition state. Myrtanal requires less steps from the opening of β -pinene epoxide, and the energetic barrier of the two transition states (TS) can be unfavored because of solvation and its interaction with TS. For perillyl alcohol, more steps are necessary in addition to a conformation change in which a Csp³ rotates to favor a hydrogen transfer [117].

In the same way, MoO₃ modified beta zeolite was also tested for the selective ring-opening of α -pinene epoxide at relatively mild conditions (Table 5, *entry 8*). In this case, the authors reported that effect of different solvents (cyclohexane, toluene, nitromethane, propan-1-ol, dichlorobenzene, cyclohexanone, cyclohexanol, ethyl acetate and N,N'-dimethylformamide) slightly influenced selectivity to campholenic aldehyde and *trans*-carveol. The highest selectivity (44.9%) to the aldehyde was achieved when nitromethane was used as a nonpolar solvent while N,N'-dimethylformamide (polar basic) favored *trans*-carveol. In the latter case, conversion was only 27%. As mentioned

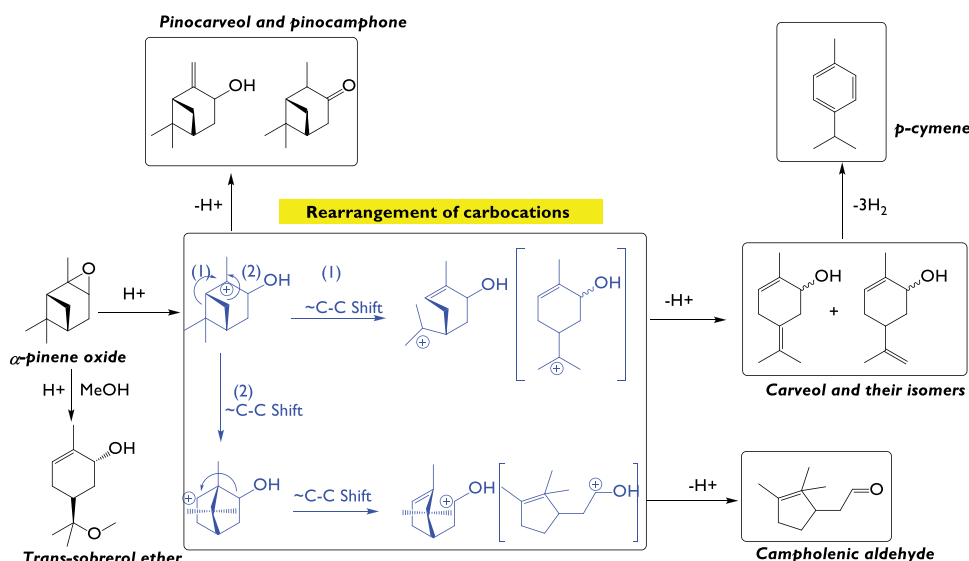


Figure 10. Schematic representation of the main reaction pathways in isomerization of α -pinene epoxide into various products. 1=Campholenic aldehyde, 2=carveol and their isomers, 3=*p*-cymene, 4=pinocarveol, 5=pinocamphone, 6=trans-sobrerol ether.

previously, the synergy between acidity (strength and type) and the solvent type can favor the formation of a specific product in isomerization of α -pinene epoxide. The use of alcohols of a low molecular weight can induce the formation of high-molecular weight substances which result from the nucleophilic attack of the alcohol to the epoxide. A typical example is methanolysis of α -pinene epoxide in an acid medium which can yield sobrerol ethers [129]. The proposed reaction pathways are depicted in Figure 10. As the first step, α -pinene oxide is coordinated to the acid site (Brønsted or Lewis which will change the strength of the non-covalent bond) leading to an intermediate carbocation. Then, different rearrangement of the carbocation to have a more thermodynamically favorable cation occurs. At this point, simple proton elimination can give pinocarveol and pinocamphone, while the C-C shift in the two routes can eliminate the strain of the internal cyclobutene generating two different carbocations. Thereafter, carveol and its isomers and campholenic aldehyde are formed as more favorable products. Kinetics (which could be affected by temperature, the type of the solvent and the catalyst) is crucial to obtain a specific target. Thermodynamics is also crucial in this reaction but less critical with respect to kinetics.

With the aim of investigating the oxidation state in Fe/MCM-41, different precursor salts were tested and then compared with the heterogeneous catalysts (Table 5, entry 9). For this, iron nitrate, chloride, sulfate, and iron oxide were tested at the same reaction conditions and the results suggest a crucial effect on the role of the oxidation state of both Fe^{3+} and Fe^{2+} . Although the

Table 5. Some heterogeneous catalysts for isomerization of monoterpene epoxides.

Entry	Catalyst	Monoterpene epoxide	Reaction conditions	X (%)	S (%)	Ref
1	ZrP ^a (0.6 M)	α -Pinene epoxide	3.28 mmol substrate, 50 mg catalyst, 2 mL N, N Dimethylacetamide, 160°C, 5 h.	45	72 TC 21 CA 7 Others	[110]
	ZrP ^a (1.2 M)			60	71 TC 20 CA 9 Others	
	ZrP ^a (2.4 M)			100	73 TC 19 CA 8 Others	
2	Fe/MCM-41 (1.7 wt%)	α -Pinene epoxide	0.25 mmol substrate, 1 mL solvent, 10 mg catalyst, 70°C, 2.5 h, 750 rpm	100 (Toluene)	66 CA	[111]
				100 (Ethyl acetate)	34 Others 58 CA	
	100 (<i>tert</i> -Butanol)			42 Others 53 CA		
	20 (Toluene)			47 Others 82 CA		
	Cu/MCM-41 (1.3 wt%)			18 Others 80 CA		
				5 (Ethyl acetate)	20 Others	
Fe/SBA-15 (3.9 wt%)	0 (<i>tert</i> -Butanol)	-				
	100 (Toluene)	64 CA 36 Others				
	100 (Ethyl acetate)	58 CA 42 Others				
Cu/SBA-15 (1.2 wt%)	98 (<i>tert</i> -Butanol)	48 CA 52 Others				
	46 (Toluene)	71 CA				
	5 (Ethyl acetate)	29 Others 79 CA				
	1 (<i>tert</i> -Butanol)	21 Others 72 CA				
3	Fe/SBA-15 (3.9 wt%)	Limonene epoxide	0.25 mmol substrate, 1 mL solvent, 10 mg catalyst, 70°C, 1 h, 750 rpm	21 (Toluene)	15 LD 3 CC 35 TC 42 DHCV 5 Others	[111]
				15 (Ethyl acetate)	6 LD 35 CC 15 TC 44 DHCV	
				5 (Acetonitrile)	50 LD 50 DHCV	
				17 (Acetone)	84 LD 16 CC	
				5 (THF)	48 DHCV 52 Others	
				8 (1,4-Dioxane)	74 LD 26 Others	
				5 (<i>tert</i> -Butanol)	71 LD 13 DHCV	
				12 (Cyclohexane)	16 Others 86 LD 7 TC	
				10 (Hexane)	7 DHCV 86 LD 7 CC 3 TC	
					2 DHCV 2 Others	

(Continued)

Table 5. (Continued).

4	Fe/MCM-41	β -pinene epoxide	0.25 mmol substrate, 1 mL solvent, 26% of catalyst, 70°C, 1 h, 750 rpm	18 (Hexane)	34 PA 63 Myrtanal 3 Myrtenol	[112]					
				23 (Acetonitrile)	8 PA 90 Myrtanal 2 Myrtenol						
				14 (tert-Butanol)	14 PA 81 Myrtanal 5 Myrtenol						
				27 (Hexane)	26 PA 68 Myrtanal 6 Myrtenol						
				20 (Acetonitrile)	13 PA 82 Myrtanal 5 Myrtenol						
	Fe/SBA-15				7 (tert-Butanol)	6 PA 87 Myrtanal 7 Myrtenol					
					92	45 TC 27 CA					
					100	36 PA 19 Myrtanal 10 Myrtenol 9 nol 9 p-Menth-1-en-7,8-diol					
					70	45 PA 9 Myrtanal 46 Others					
					> 99	45 PA 20 Myrtanal 35 Others					
5	MZ-5 (1.5)	α -Pinene epoxide ^b	2 mmol substrate, 100 mL of N, N-dimethylacetamide (solvent), 75 mg catalyst, 140°C, 3 h.	92	45 TC 27 CA	[113]					
				6	Zeolite beta 25		β -pinene epoxide	0.8 mL substrate, 25 wt % based on the weight of substrate, volume ratio substrate: DMSO = 1:5, demineralized water (molar ratio substrate: H ₂ O = 1:8), 70°C, 2 h.	100	36 PA 19 Myrtanal 10 Myrtenol 9 nol 9 p-Menth-1-en-7,8-diol	[114]
				7	SBA-15		β -pinene epoxide	0.25 mmol substrate, 0.5 mL hexane, 10 mg catalyst, 80°C, 1 h.	70	45 PA 9 Myrtanal 46 Others	
					Ti/SBA-15				> 99	45 PA 20 Myrtanal 35 Others	
					Mo/SBA-15				> 99	63 PA 37 Others	
					MCM-41				50	34 PA 20 Myrtanal 7 Myrtenol 39 nol 39 Others	
					Ti/MCM-41				60	47 PA 2 Myrtanal 51 Others	
					Mo/MCM-41				98	20 PA 2 Myrtanal 5 Myrtenol 73 nol 73 Others	
					SiO ₂				14	5 PA 95 Others	
					Ti/SiO ₂				64	15 PA 55 Myrtanal 4 Myrtenol 26 nol 26 Others	

(Continued)

Table 5. (Continued).

	Mo/SiO ₂			> 99	32 PA 12 Myrtanal 2 Myrtenol 54 nol 54 Others	
8	MoO ₃ -Modified Beta zeolite	α -Pinene epoxide	1.25 g substrate, 6 mL solvent, 125 mg catalyst, 70°C, 3 h.	99 (Cyclohexane)	34.6 CA 17.4 TC 13.9 PMD	[116]
				100 (Toluene)	34.2 CA 14.8 TC 14.0 PMD	
				86 (Nitromethane)	44.9 CA 10.7 TC 12.3 PMD	
				100 (Propan-1-ol)	3.3 CA 6.4 TC 2.7 PMD	
				100 (Dichlorobenzene)	42.1 CA 13.3 TC 13.1 PMD	
				100 (Cyclohexanone)	37.4 CA 15.0 TC 16.6 PMD	
				100 (Cyclohexanol)	24.1 CA 21.1 TC 5.1 PMD	
				97 (Ethyl acetate)	37.1 CA 15.8 TC 13.9 PMD	
				27 (N, N'- Dimethylformamide)	26.5 CA 43.8 TC 14.0 PMD	
9	Fe/MCM-41	α -Pinene epoxide	0.25 mmol substrate, 1 mL toluene, 15 mg catalyst, 70°C, 750 rpm, 2.5 h.	> 99	65 CA 14 Carveol 5 FA 16 Others	[117]
	Fe(NO ₃) ₃ ·9H ₂ O			97	59 CA 10 Carveol 6 FA 28 Others	
	FeCl ₃ ·4H ₂ O			99	61 CA 9 Carveol 3 FA 27 Others	
	FeSO ₄ ·7H ₂ O			7	40 CA 45 Carveol 5 FA 10 Others	
10	Fe ₂ O ₃ Cs _{2.5} H _{0.5} PW ₁₂ O ₄₀	α -Pinene epoxide	0.75 mmol substrate, 7.50 μ mol catalyst, 5 mL of reaction volume with acetone as solvent.	0 100 (5 min, 25°C)	- 17 CA 22 TC 9 TS 45 Pinol	[118]
				100 (180 min, 25°C)	19 CA 5 TC 70 Pinol	
				100 (5 min, 40°C)	17 CA 11 TS 62 Pinol	
				100 (120 min, 40°C)	17 CA 75 Pinol	

(Continued)

Table 5. (Continued).

11	SiO ₂ ^c	α-Pinene epoxide	0.25 mmol substrate, 2 mL dichloroethane, 5 mg catalyst, 30°C, 30 min.	3	50 CA 6 FA 10 TC 6 TS 28 Others	[119]
	Al-SiO ₂ ^c (12 wt %)			80	72 CA 2 FA 15 TC 8 TS 3 Others	
12	Ti/MCM-22	α-Pinene epoxide	Toluene, 70°C	100	96 CA 1 TC 1 FA 1 PC	[120]
13	C _{52.5} H _{0.5} PW ₁₂ O ₄₀	Limonene epoxide	1.5 mmol substrate, 5 mg Catalyst, 10 mL total volume with dichloromethane as solvent, 25°C, 240 min	100	69 DHCV 20 MICC 8 LD	[121]
14	HPW/SiO ₂	Limonene epoxide	0.45 mmol substrate, 14.29 mg catalyst μmol ⁻¹ HPW, 25°C, 15 min, 3 mL of total volume with dimethyl carbonate as solvent	100	84 DHCV 8 MICC 7 LD	[122]
15	Phosphonate/Carbon	α-Pinene epoxide	3.28 mmol substrate, 50 mg catalyst, 2 mL DMF, 140°C, 1 h	100	67 TC 22 CA 9 TPC	[123]
16	Ionic liquid-supported indenyl-molybdenum(II)-bipyridine complexes	α-Pinene epoxide	0.9 M initial substrate concentration, 0.044M Mo, [Ch][NTf ₂] as solvent, 35°C, 1 min.	100	79 CA 6 TCV	[124]
17	TECHNOSA-H2 mordenite	α-Pinene epoxide	25°C, 10 min	100	57 CA	[125]

^aValues in parenthesis refer to the concentration of H₃PO₄ employed in the synthesis of the catalyst. ^bSelectivities at 70% conversion. ^cValues in parenthesis refer to the aluminum loading. **ZrP**: Zirconium phosphate. **CA**: Campholenic aldehyde. **CC**: *cis*-Carveol. **TC**: *trans*-Carveol. **LD**: Limonene diol. **DHCV**: Dihydrocarvone. **PA**: Perillyl alcohol. **MZ**: Hierarchical beta zeolites, where the value in parenthesis denotes the Brønsted-to-Lewis acid site ratio. **CB-1**: Conventional beta zeolite. **PMD**: *p*-methadien-2-ol. **FA**: Fencholenic aldehyde. **TS**: *trans*-sobrerol. **MICC**: 1-methyl-3-isopropenyl-cyclopentyl-1-carboxaldehyde. **PC**: pinocampnone. **TPC**: *trans*-pinocarveol.

amount of Fe active sites was not the same, the excess (almost 7-10-fold with respect to iron in Fe/MCM-41) showed that, apparently, the most active site was Fe³⁺ rather than Fe²⁺. Only 7% of conversion was achieved when FeSO₄·7H₂O was used as the catalyst, Fe₂O₃ was completely inactive. In fact, it was evident that the nature and the oxidation state of the metal site play an important role in determining the conversion and selectivity of α-pinene epoxide isomerization. This fact could be explained by the acidic nature of Fe³⁺ with respect to Fe²⁺: In the first case, more available free d-orbital is present, enhancing Lewis acidity.

On the other hand, heteropolytungstate based on Cs [118] was selectively tested in biomass-derived α -pinene epoxide yielding mainly *trans*-carveol, *trans*-sobrerol and pinol in 60–80%, exceeding the yields reported previously for the synthesis of pinol (Table 5, entry 10). For this case, different reaction conditions were tested (mainly time, temperature, and polarity of the solvent) highlighting that relatively short reaction times (<180 min) and low temperature enhance formation of pinol over campholenic aldehyde and *trans*-sobrerol. Further optimization of the reaction temperature and catalyst loading enabled the pinol yield up to 80% while the combined selectivity with campholenic aldehyde was *ca.* 95%. In addition, low temperatures are favorable for the intermediate carbocation to form *trans*-carveol. Interestingly, decreasing the amount of residual water during the reaction (when acetone solutions were used) favors the intramolecular cyclization for the intermediate carbocation giving pinol as the main product.

On the other hand, a series of silicas modified chemically with Al were tested in the isomerization α -pinene oxide pointing out in the effect of Al amount (Table 5, entry 11) [119]. Particularly, the silica modification was performed by using a one-pot two-step synthesis in which the first step was activation of silica while in the second step, TEA (tetraethyl aluminum) was added with subsequent drying and calcination [119]. The best result was achieved for Al-SiO₂ containing 12 wt% of Al with 80% of conversion and 72% selectivity to campholenic aldehyde. In comparison with previously discussed literature, the relatively mild conditions used in this work (only 30°C and 30 min) enhanced formation of the desired aldehyde. However, under these conditions, the catalysts could not be reused. The expected activity was attributed mainly to the oligomeric species of Al₂O₃ present in the catalyst and to an increase in the textural properties. Among many heterogeneous catalysts reported for selective synthesis of campholenic aldehyde starting from α -pinene oxide, Ti-MCM-22 (Table 5, entry 12) [120] has been the most effective catalyst yielding up to 96% of the aldehyde with 4% of other isomers. Excellent performance of this catalyst was associated with the presence of isolated tetrahedrally coordinated Ti, which acts as a Lewis acid without undesired Brønsted acidity, together with the typical MWW shape which can favor the transition state for aldehyde formation. Finally, phosphotungstate-based catalyst (Cs_{2.5}H_{0.5}PW₁₂O₄₀ and HPW/SiO₂) was reported for isomerization of limonene epoxide yielding mainly dihydrocarvone as the major product (Table 5 entry 13–14). Exceptional acidity together with utilization of the green solvent (in case of HPA/SiO₂) can lead to a feasible method for synthesis of such isomer.

Recently [123], the reusable biomass-derived phosphonate carbon was used for the synthesis of *trans*-carveol from α -pinene oxide at relatively mild conditions indicating the role of the amounts and distribution of the phosphonate groups in the selective synthesis of this alcohol (Table 5 entry 15). The

use of DMF as a polar basic solvent confirms the hypothesis previously that such solvents favor formation of the alcohol over aldehydes (campholenic and fencholenic aldehydes). Although the process is in line with the typical green processes, the remaining issue is the removal of DMF from the reaction mixture.

Ionic liquid supported indenyl-molybdenum (II) bipyridine complexes as an organometallic and robust catalyst was used for the selective synthesis of campholenic aldehyde starting from α -pinene epoxide (Table 5 entry 16) [124]. Interestingly, only 1 min is enough for obtaining 94% of the desired aldehyde, which is comparable with Fe/MCM-41 (Table 5 entry 2). The authors [124] claimed that a change of the ligand during synthesis of the complexes can alter Lewis acidity of the metal center. For the mentioned complex, introduction of electron-donating or electron withdrawing groups can modify the overall reactivity of the catalysts, decreasing the electronic density and changing the catalytic activity and robustness of the material.

Finally, the mordenite-based natural zeolite (TECHNOSA-H₂) [125] coming from volcanic islands in Greek Islands (Table 5 entry 17) achieved up to 57% of selectivity to campholenic aldehyde at total conversion with only 10 min of the reaction. Although the authors did not measure acidity of the material by using TPD of ammonia or FTIR of pyridine, the authors suggested, for this case, that active sites on the mordenite-based catalyst are mostly Brønsted one because of selectivity. Despite these results, the catalyst was not tested in this reaction in additional cycles.

5. Synthesis of cyclic carbonates based on monoterpenes epoxides

5.1. General aspects

The current efforts for valorization of CO₂ have grown in the last years because of the increasing emission of greenhouse gases causing several climate changes. Then, new alternatives for decreasing the emissions and a rational use of CO₂ are a current approach that has been implemented to obtain high-added value chemicals in the context of green and sustainable chemistry. Among several strategies for using CO₂ is the synthesis of cyclic carbonates starting from epoxides and CO₂. In 2021, the production of cyclic carbonates was estimated to be in the order of 100 kton/y. These kinds of compounds find applications as a monomer in the preparation of polymers (e.g.: replacement of non-isocyanate polymers), components in batteries, green solvents, etc. [130]. Among many advantages, this reaction demonstrates 100% economy efficiency and can be performed at solventless conditions being thermodynamically favorable [131]. The main factors that affect the reaction are the type of catalyst used, reactivity of the epoxides, and the reaction conditions. Although different epoxides coming from hydrocarbons have been used for this

transformation (epichlorohydrin [132], styrene oxide [133], cyclohexene oxide, etc.), reactivity of monoterpene epoxides as a starting epoxide has been almost unexplored. The synthesis of cyclic carbonates starting from terpene scaffolds can result in 100% bio-based derived compounds with a high potential [134]. There are a few reports in which these epoxides (especially limonene epoxide) have been used to synthesize cyclic carbonates with CO_2 as a reactant [135,136]. Another strategy for synthesis of cyclic carbonate is the ring-opening of the epoxide giving the diol and then the ring closure with the use of a base and dimethyl carbonate as the CO_2 source [137].

The use of heterogeneous catalysts for the synthesis of cyclic carbonate follows a reaction mechanism illustrated in Figure 11. The control of water as well as the type and the amount of acid sites, mainly Lewis and the base are the

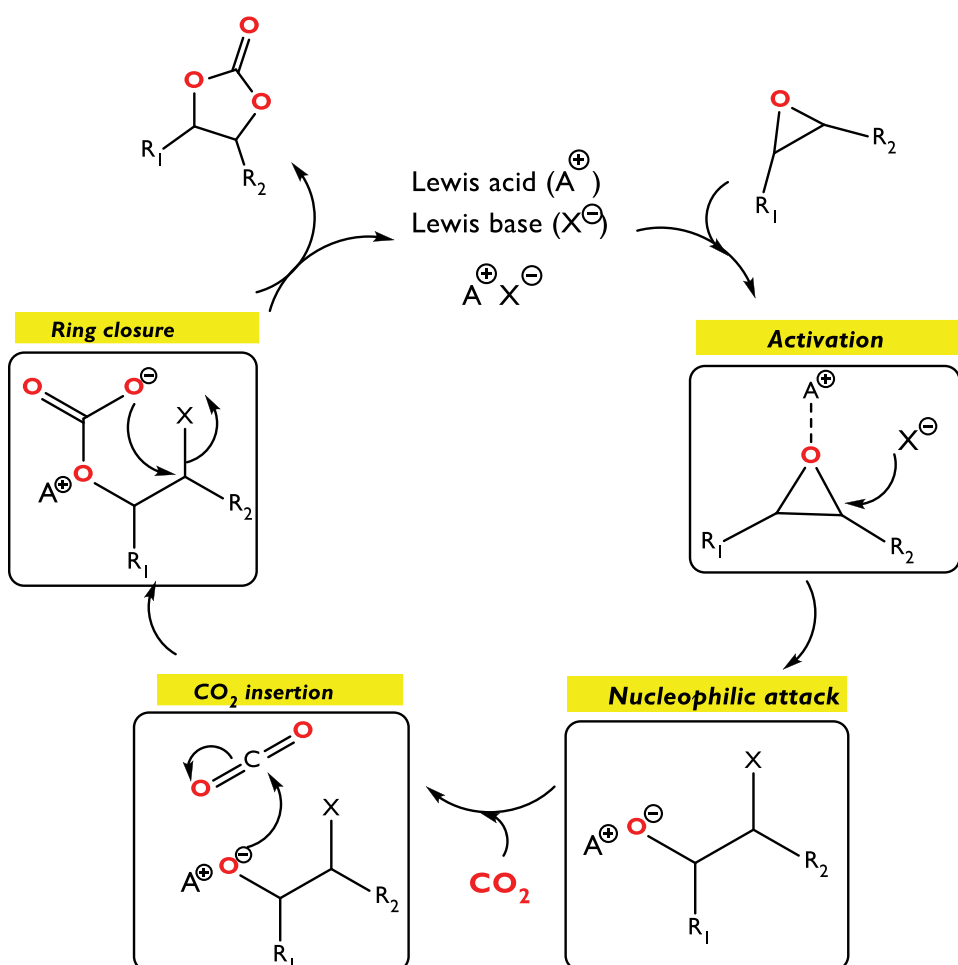


Figure 11. Proposed reaction pathway for catalytic cycloaddition of CO_2 to epoxides by using a bifunctional catalyst (Lewis acid and base).

most critical factors to achieve the desired target avoiding isomerization and condensation products (e.g.: hydrolysis). The reaction pathway starts from the coordination of the epoxide to the Lewis acid site, then activating the epoxide to further nucleophilic attack by a Lewis base, which leads to opening of the epoxide. The intermediate alkoxylate is then closed by an intermolecular reaction with CO₂. The design of a catalyst for this reaction would require a bifunctional character comprising a Lewis acid site (e.g.: by using metals) and the Lewis's base species, which are typically halides. Secondary reactions such as hydrolysis and isomerization could be present, but they can be avoided by drying the catalyst, decreasing the strength of acidity, and using a base (typically TBABr – tetrabutylammonium bromide-) while performing the reaction.

5.2. Current research and advances in synthesis of cyclic carbonates from monoterpene epoxides

There are a few reports in which the formation of cyclic carbonates has been explored by using monoterpene epoxides as the starting material. In general, synthesis of these kinds of compounds is of interest because of their versatility which aims to build more complex compounds such as monomers that can be used to replace the typical fossil-based polymers, e.g. polyurethanes. Figure 12 shows a general scheme invoking synthesis of cyclic carbonates starting from monoterpene scaffolds.

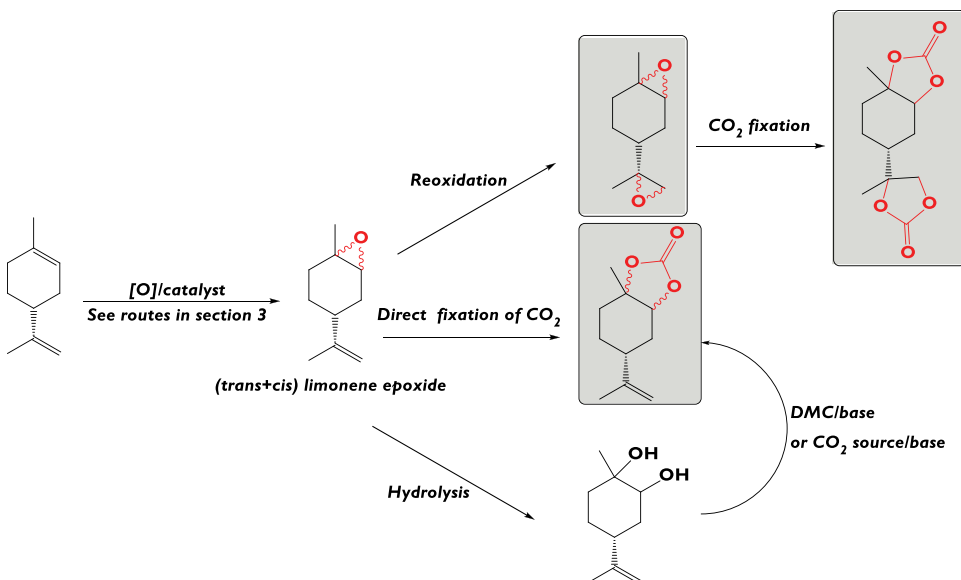


Figure 12. A general scheme of the synthesis of cyclic carbonates starting from monoterpenes scaffolds as well as CO₂ sources.

Limonene dicarbonate (starting from limonene diepoxide) was synthesized as a new monomer for the synthesis of a polymer based on non-isocyanate and polyurethanes [138]. In this study, TBABr was used as a homogeneous catalyst along with heterogeneous silica supported 4-pyrrolidinopyridinium iodide (SiO₂-I) in the synthesis of this carbonate. Tetrabutyl ammonium bromide has been reported as a selective catalyst for the synthesis of cyclic carbonates [139] starting from biomass-derived epoxides however its poor recyclability made this catalyst poorly attractive for further industrial applications. The maximum conversion achieved with the SiO₂-I system was 80% at 30 bar and 140°C. The required time for this step was 2 h. In comparison, the homogeneous TBABr catalyst was capable of converting all the epoxide into the limonene carbonate within only 50 min and the same reaction conditions. Monitoring of the reaction was successfully carried out using IR spectroscopy (namely a band close to 1800 cm⁻¹ in all the carbonates) and confirming the structure of the final product with ¹H-NMR.

Interestingly, the flow synthesis concept was applied for synthesis of limonene carbonate by using supercritical carbon dioxide (*T*_c: 31.0°C, *p*_c: 7.38 MPa) [140]. At such pressures and temperatures, carbon dioxide can act both as a reactant and as a solvent. High solubility of supercritical carbon dioxide in ionic liquids makes them promising candidates as the reaction media for catalytic and sustainable processes. Similarly [141], as in the previous case, tetrabutylammonium iodide (TBABI) was adsorbed on mesoporous silica to further obtain a supported ionic liquid phase (SILP). Under the best conditions, the maximum yield of the desired limonene carbonate was up to 17% without leaching. In the case of limonene diepoxide as the starting material, the maximum yield (in flow operation) of 16% was obtained; however, some traces related with the catalyst leaching were observed.

Coupling terpene oxides and CO₂ were performed using an amino-(trisphenolate) ligands (namely, tris(3,5-dichloro-2-hydroxybenzyl)amine and tris(3,5-ditertbutyl-2-hydroxybenzyl)amine) [134]. In this case, bis-(triphenylphosphine)iminium chloride was used as a co-catalyst. After 66 h of the reaction under 10 bar of pressure, the maximum yield obtained (via ¹H NMR) was 57% starting from *trans*-limonene epoxide. In the same way, for limonene diepoxide the maximum yield was up to 74% while for carvone epoxide it was 45%. The use of pure *cis* isomer only led to 4% yield of its respective carbonate. As expected, the retention of the configuration in the final cyclic carbonate is mainly associated with the double inversion pathway. Although relevant results were achieved, the catalyst was not reused at all, being not in line with principles of green and sustainable chemistry. Similarly, a homogeneous catalyst based on scorpionate-based helical organoaluminums was successfully used for the synthesis of limonene carbonate giving 79% conversion (70°C, 10 bar CO₂, 1 mol% catalyst, 66 h) [142]. The experiment

was only performed with *trans*-limonene epoxide achieving a mixture of diastereomers during formation of the cyclic carbonate.

Alkali and alkali earth metal salts in combination with polyethers as heterogeneous materials were applied as selective catalysts for the synthesis of limonene carbonate in which the *trans*- configuration was predominant [143]. Thus, poly (ethylene glycol) (PEG) dimethyl ethers were acceptable polymers for performing complexing agents with CaI_2 which also showed the best performance along with other tested salts (LiI, NaI, KI, RbI, CsI, MgI_2 , SrI_2 and BaI_2). Relatively mild tested conditions (90°C , 48 h, 50 bar) allowed to achieve only 18% yield with 10 mol% of CaI_2 supported on PEG. The catalytic systems were shown to be robust and could be used several times (up to 7) without a significant decrease in the catalytic activity when 2-(tert-butoxymethyl)oxirane was used as the reagent.

A series of ammonium, phosphonium, imidazolium and diazabicycloundecium tungstate and peroxotungstate ionic liquids were successfully synthesized and applied to the cycloaddition of CO_2 to limonene epoxide [144]. Synthesis of the material was performed by metathesis with Ag_2WO_4 . Furthermore, fixation of CO_2 to limonene epoxide render to achieve up to 43% of conversion with poor selectivity of only 33% to the desired carbonate (4 mmol of substrate, 50 bar of CO_2 , 90°C , 18 h, 0.12 mmol of catalyst). Although different epoxides (butyl glycidyl ether, hexene oxide, cyclohexene oxide) were evaluated with acceptable conversions and selectivity, the catalyst was not reusable.

6. Acetoxylation

6.1. General considerations for acetoxylation of terpenes

Acetoxylation of monoterpenes gives products with a special interest in the field of fine chemistry, including pharmaceuticals, perfumes, agrochemicals, and as intermediates in the synthesis of more complex molecules or as building blocks. These kinds of reactions involve the addition of an acetyl group ($-\text{COCH}_3$) to the $\text{C}=\text{C}$ bond of the monoterpene. The process usually requires the use of acetic anhydride and acid-based catalysts. The resulting product can have improved solubility, stability, and biological acidity in comparison with the starting product. Acetoxylation can occur in the hydroxyl group of the monoterpenoid. This reaction can be carried out under relatively mild reaction conditions and typically results in a high yield of the desired product. Overall, acetoxylation of monoterpenes is a very useful strategy for modifying the properties of these natural compounds making it possible to have applications in pharmaceuticals, cosmetics, and other industries. Figure 13 shows the most common acetoxylation products obtained from typical raw materials: α -pinene, β -pinene and limonene.

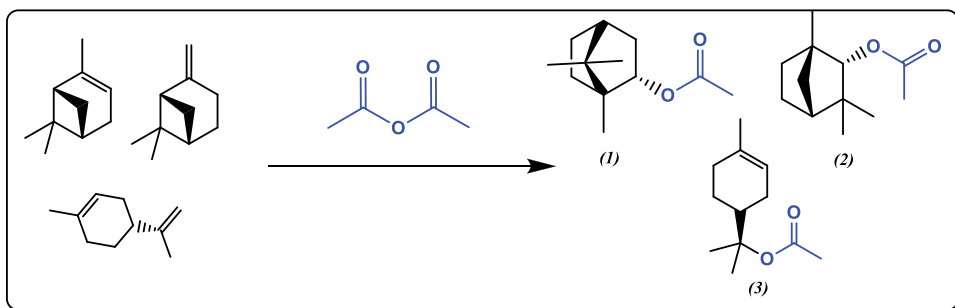


Figure 13. The most common acetylated products from typical monoterpenes (α -pinene, β -pinene and limonene) and acetic anhydride. 1=Bornyl acetate 2=Fenchyl acetate 3=Terpinyl acetate.

6.2. Designing a specific catalyst for acetoxylation of terpenes

Design of a heterogeneous catalyst that drives selectivity to the acetoxyated product requires an acidic function together with well-distributed active sites. There are few catalysts that have been reported for this specific application. Typically, a complex mixture of acetoxyated products together with isomers of the monoterpenes is obtained. For example, in one of the cases, Amberlyst-36 (Table 6, entry 1) [145] was tested as an active catalyst for synthesis of bornyl acetate starting from α -pinene (crude turpentine) using acetic acid as the acetoxyated agent. Although complete conversion of pinene was obtained the overall selectivity did not exceed 40% to bornyl acetate. Amberlyst-36 is a macroreticular resin in a bed form with sulfonic acid groups. The concentration of the acid sites is typically 1.95 eq/L [150] which made the material a strong acidic cation exchange. Isomerization of α -pinene took place under the reported reaction conditions [145]. Kinetic study of these reactions indicates that the reaction rate is slow in the temperature range 45 – 90°C; however, it was observed that acetoxylation requires a higher activation energy (94 kJ/mol) in comparison with the isomerization reaction (70 kJ/mol). Both reactions are kinetically driven, and an excess of the acid sites can promote isomerization rather than the desired acetoxylation.

In the second example (Table 6, entry 2), α -pinene was used as the starting monoterpene with the same acetylated group as in the previous case [145]. SBA-15 modified with MPTMS to introduce sulfonic acid groups was used as the active catalyst [146]. Modification of SBA-15 with such kind of sulfonic groups resulted in high activity exceeding than the commercial acidic resins (see Figure 14). Conversion was limited (80%), with a poor selectivity to the acetoxyated product (18% to α -terpinyl acetate). Terpinyl acetate is found in pine oil, cardamom oil and other essential oils and it is widely used as an aromatic compound [151]. Despite low catalytic activity, conversion of the monoterpene increased when increased the surface area and the pore volume of the catalyst, suggesting better accessibility of α -pinene to the active sites. In

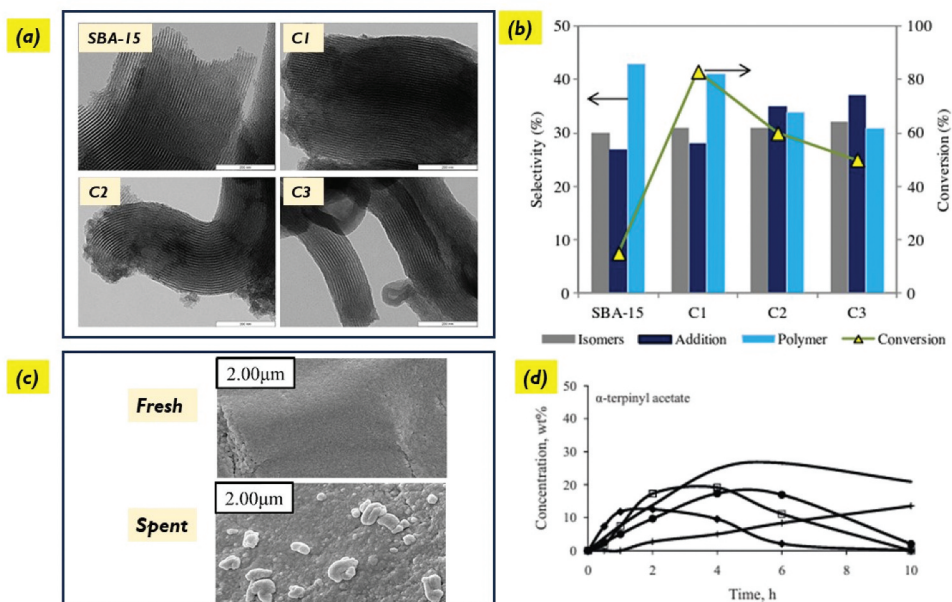


Figure 14. **A)** TEM images for neat SBA-15 and modified with sulfonic groups **b)** Catalytic activity of SBA-15 in the synthesis of terpinyl acetate **c)** SEM images of Amberlyst-70 before and after reaction **d)** Concentration curves as a function of time and using different reaction conditions. Images reproduced with permission of ref [146] (a and b) and ref [147] (c and d).

the same way, modification of SBA-15 by the sulfonic groups promotes conversion to the desired products. Changing the amount of catalyst increased the selectivity to the overall acetoxylation products (up to 30% to bornyl acetate + α -terpinyl acetate); however, the conversion decreased to 50–60%. It appears that strong acid sites promote isomerization and polymerization rather than acetoxylation. Then, application of materials with medium or even low acid sites could be enough for synthesis of acetated derived terpenes.

In the same way as for Amberlyst-36, a polymeric resin (Amberlyst 70), containing less acid sites (>0.9 eq/L) [152] but designed for high temperatures, was used as an active heterogeneous material for the synthesis of acetals starting from α -pinene (Table 6, entry 3). Amberlyst-70 is a low degree cross-linked chlorinated and sulfonated styrene-divinyl benzene resin. The same acetoxylation agent was used under two different reaction conditions. Using water as the co-solvent, a sum of both acetates (fenchyl acetate and bornyl acetate) was almost 48% while when nonpolar toluene was used as the co-solvent, selectivity decreased substantially to ca. 36% to all the acetates. An increase of temperature as well as hydrogen atmosphere increased formation of by-products, (products formation were formed under oxygen atmosphere) However, after several experimental runs the catalyst displayed dramatic catalyst morphology changes suggesting a loss of catalytic activity (starting from 95% to 60% of conversion of α -pinene).

Table 6. Heterogeneous catalysts for acetoxylation of some terpenes.

Entry	Catalyst	Terpenoid	Acetoxylation agents	Reaction conditions	X (%)	S (%)	Ref
1	Amberlyst 36	α -Pinene (turpentine oil)	Acetic acid	0.05 g mL ⁻¹ catalyst concentration, molar ratio of 1:1 for α -pinene: acetic acid, at 90°C for 8 h.	100	40 bornyl acetate	[145]
2	SBA-15 with MPTMS	α -Pinene	Acetic acid	6.3 mmol of α -pinene, 30 mL of acetic acid, 120 mg of catalyst, at 60°C for 30 h.	83	41 polymer 18 α -terpinyl acetate 5 bornyl acetate 12 camphene 14 limonene 5 terpinolene	[146]
3	Amberlyst 70	α -Pinene	Acetic acid	5.5 g of α -pinene, 120 mL of acetic acid, 100 mg of catalyst, 5 wt % of co-solvent, 20 bar O ₂ , at 100°C for 10 h.	99.2 (Water as co-solvent) 95.7 (Toluene as co-solvent)	42.5 limonene 1.1 γ -terpinene 7.0 fenchyl acetate 39.9 bornyl acetate 35.3 limonene 15.7 γ -terpinene 7.0 fenchyl acetate 28.1 bornyl acetate 0.3 α -terpinyl acetate	[147,148]
4	Ion-exchanged beta zeolite	Limonene	Acetic acid	2 mL of substrate, 10 mL of acetic acid, 0.1 g of catalyst, at 50°C for 24 h.	23	42 α -terpinyl acetate 16 terpinolene 14 α -terpinene 10 α -terpineol 6 γ -terpinene 3 α -phellendrene 3 <i>p</i> -cymene	[149]
		α -Pinene			93	27 limonene 14 bornyl acetate 13 camphene 8 <i>p</i> -cymene 8 terpinolene 7 α -terpinene 4 γ -terpinene 2 α -phellendrene 2 α -terpineol 2 α -terpinyl acetate	

*Reported as the isolated yield.

Another possibility to obtain acetals is starting from limonene which requires two steps: hydration and bioconversion in which limonene is converted into terpineol and then transformed into the desired acetal (Table 6, entry 4). For this case, a cation-exchanged zeolite beta was evaluated in the reaction using two monoterpenes (α -pinene and limonene) showing better performance in comparison with the conventional acidic catalysts such as sulfuric acid and Amberlyst-15 (comparable with Amberlyst-36 and Amberlyst-70). In the case of α -pinene, the distribution of products showed that more isomerization products were formed rather than the typical addition products. Although several metal-modified zeolites (Cu, Co, Zn, Ce, Ni, Fe, Mn, La, Sr, Li, Ag) were synthesized and tested in the reaction, the acetate products did not exceed 32% at total conversion of pinene. Overall, the authors [149] confirmed that hydration, isomerization and acetoxylation are governed by the Brønsted acid behavior of the catalysts. In the case of limonene, terpinyl acetate and terpineol were obtained as the main products. Usually, in the presence of strong acid catalysts, limonene can be arranged into oligomerization products, however this was not the case. Subsequently, only isomerization took place together with formation of hydration/acetoxylation products.

Alternatively, acetoxylation limonene derivatives were formed using a system containing Pd (II) acetate and benzoquinone with a mixture of DMSO/acetic acid as the solvent enabling acetoxylation of the exocyclic double bond [153]. Remarkable selectivity (up to 88% to terpinyl acetate) can be obtained via this way. The role of benzoquinone is just to drive reoxidation of the catalyst, while iron(II) phthalocyanine as co-catalyst which acted as the electron transfer mediator. Maximum conversion (91%) with selectivity up to 86% toward terpinyl acetate can be achieved. While no data on catalyst recycling are available in [153], the catalytic system is promising in comparison with the previously discussed heterogeneous materials. This type of systems could be further considered to increase both the conversion and selectivity in the acetoxylation of limonene.

7. Hydrogenation

7.1. General consideration for hydrogenation of terpenes

Typically, fine chemicals are produced using homogeneous catalysts, for example, menthol is synthesized via the Takasago process utilizing ZnBr_2 , H_2SO_4 and noble metal-based organometallic, homogeneous catalysts [154]. These processes are not environmentally benign, and metal complex catalysts are especially expensive and difficult to recover and reuse. Furthermore, fine chemical processes are often carried out in a batch mode, which limits their production capacity. The aim especially in academia is to develop inexpensive, easy to recover and recyclable heterogeneous catalysts and to enhance

productivity via implementing continuous operation. Supported metal catalysts have been widely explored and discussed in the literature for the synthesis of hydrogenated compounds. In the current review, some recent results of hydrogenation of biobased terpenes to valuable products are summarized. In addition to supported metal catalysts for hydrogenation with dihydrogen also results from the Meerwein-Ponndorf-Verley reduction of citral using 2-propanol as a hydrogen donor are discussed [155].

Hydrogenation of myrcene, farnesene, and squalene has yielded valuable saturated derivatives such as 2,6-dimethyloctane, farnesane, and squalane, respectively. Myrcene and farnesene are industrially available terpenes that can be obtained from fermentation of biomass-derived sugars like sugar cane or through biosynthesis [156,157]. These compounds are suitable as raw materials for synthesizing sustainable fine chemicals [158]. On the other hand, squalene is a polyunsaturated linear triterpene found in sources such as shark liver oil (which is not commonly used due to ethical concerns) or olive oil [159]. Hydrogenation of these terpenes has been performed using 3D-printed catalysts based on palladium in continuous flow reactors [158,160]. This process is conducted under moderate reaction conditions (25 bar and 200°C) and results in high purity of the target products (>74%), depending on the residence time in the flow reactor.

Other renewable molecules interesting to be used as intermediates and for pharmaceutical products are α -pinene, which can be produced from turpentine [161]. Citral is present in essential oil [162] and limonene, which in addition to natural resources, can be produced via hydropyrolysis of rubber gloves to produce limonene, which thereafter will be hydrogenated to cycloalkanes, suitable as fuel [163,164]. *Cis*-pinane, a valuable product from selective α -pinene hydrogenation exhibits biological inhibitory properties [165], while menthol produced from citral, finds applications in cosmetic, pharmaceutical, and fragrance industries [162]. A derivative of pinane, pinane hydroperoxide is used as an intermediate in the synthesis of perfumes and as an initiator in the radical polymerization of olefines such as styrene-butadiene synthetic rubber [166]. Citral hydrogenation to unsaturated alcohols, nerol and geraniol, has been investigated for decades. Unsaturated alcohols are used for synthesis of fine chemicals and special property polymers or as fuel additives [167]. Geraniol is one of the common products from hydrogenation of citral but also it can be extracted from the essential oils of different aromatic plants such as *Cinnamomum tenuipilum* Kosterm., *Valeriana officinalis* subsp. *collina* (Wallr.) Nyman, and *Phyla scaberrima* (Juss. ex Pers.) Moldenke [168]. Geraniol is a primary, acyclic, doubly unsaturated terpene alcohol with a characteristic flowery, rose-like odor, which possesses numerous beneficial medicinal properties like anti-inflammatory, antioxidant, antitumor, antimicrobial, hepatoprotective, cardioprotective, and neuroprotective ones [169,170].

7.2. Overview of the most recent literature on hydrogenation of terpenes

For terpenes hydrogenation, the following model compounds were recently used α -pinene [163,164,171], limonene [162,172], and citral [155,161,165,167,173,174]. For these reactions, both noble [161,172,173] and transition metals [155,163–165,167,171–173] were applied as catalysts. In α -pinene hydrogenation, high conversions and high selectivities to *cis*-pinane have been obtained both in the presence [163,171] and absence of solvents [164]. The main challenge in the selective α -pinene hydrogenation is that inexpensive transition metal catalysts, such as Ni-based catalysts, exhibit typically low activity due to its poor thermal stability and easy agglomeration of nickel particles [163]. Especially high nickel dispersion is desirable. Very good performance was, however, observed with an amorphous Ni-B alloy supported on mesoporous KIT-6 [163]. An important parameter in using this catalyst was the mass ratio between Ni²⁺ to KIT-6 with the optimum ratio of 1.3 giving the highest selectivity to *cis*-pinane, ca 97% in turpentine oil hydrogenation at 120°C in ethanol under 4 MPa (Table 7, entry 2). With a higher Ni-loading agglomeration of nickel occurred, while with a lower Ni²⁺/KIT-6 mass ratio catalyst activity was too low. The role of boron is to act as an anti-oxidation agent while the 3D pore structure of KIT-6 provides a suitable small steric hindrance to facilitate selective formation of *cis*-pinane.

Ni-B-alloys supported on carbon-silica hybrid material, called as Janus amphiphilic Ni-B-alloy catalyst, was also applied as a catalyst in α -pinene hydrogenation in aqueous medium [171]. In a water/oil mixture, the role of the catalyst was to act as a solid foaming agent which also promoted hydrogen dissolution and contact with α -pinene. This catalyst gave in water 98.5% selectivity to *cis*-pinane at 99% conversion (Table 7, entry 1) [171]. The support highly stable up to 500°C contains mesopores of the size of 5.6 nm and both graphitized sp³-C and disordered sp²-C as well as several types of N-species including graphitic-N, pyrrolic-N, and pyridinic-N. Metallic Ni particles were produced via chemical reduction with NaBH₄ during synthesis. The size of Ni-B alloy nanoparticles varies in the range of 1–8 nm and with the average of 4.5 nm inside the pores, while outside of the pore system they were 1.4 nm. Furthermore, metal particles were uniformly dispersed, and the small size of the alloy particles was stated to originate due to coordination of Ni with N atoms doped in the framework. This novel catalyst was reusable ca. eight cycles, however, after that some leaching or oxidation of Ni occurred. In addition, at high temperatures there is a risk of the crystallization of amorphous Ni-B alloy.

Ni supported on aluminophosphate catalyst exhibited also high conversion and selectivity to *cis*-pinane under solvent-free conditions (Table 7, entry 3) [164]. Alumino phosphate exhibits thermal and hydrothermal stability, being resistant toward oxidation [175]. This support has

mesopores in the range of 3–4 nm. Although recyclability of the catalyst was rather good and conversion was decreasing between the first and seventh runs from 98% to 95%, it was confirmed by TPR and TPO that hydrogen consumption decreased after recycling and Ni was partially leached from the catalyst. On the other hand, selectivity to *cis*-pinane remained constant. High selectivity was stated to originate from a minor small steric hindrance and a small pore size of the support [175]. It was concluded that Ni supported on alumino phosphate exhibits better performance in comparison to other supported Ni catalysts.

A novel circular economy approach is to hydrolyze rubbers to produce limonene, which will further be hydrogenated to cycloalkanes [162,172]. Polyisoprene rubbers were transformed into a tandem process in which hydrotreatment, and hydrogenation of biomass-based polyisoprene rubbers produced via β -scission was followed by intramolecular cyclization limonene and isoprene. In the forthcoming hydrogenation step, high yields of C10 cycloalkanes were formed both with Pt/C (Table 7, entry 4) and Ni/Al₂O₃-SiO₂ (Table 7, entry 5). Formation of C10 cycloalkanes was promoted by relatively low temperature of 200°C, while *p*-cymene was formed via limonene dehydrogenation at high temperature. The two main competitive reactions occurring are the Diels Alder reaction producing limonene as well as its scission to isoprene at low vs high temperature, respectively. A reaction mechanism was proposed based on the use of limonene as a model compound [172].

One-pot synthesis of menthols has been recently intensively studied over bifunctional catalysts [161,165,173] as well as selective hydrogenation of an unsaturated aldehyde to unsaturated alcohols, nerol and geraniol [155]. In one-pot synthesis of menthol, both citral [13, 14, 19, 161, 165, 167] and citronellal [161] were used as feedstock. In some cases, the catalytic properties were not suitable for menthol productions, e.g., Ru/HY (Table 7, entry 6) exhibited high hydrogen and dehydration ability. Both batch [161,165] and continuous operations have been recently applied in one-pot menthol synthesis and especially the properties of extrudates in continuous operation under mass transfer limitations have been investigated [167] and compared with the performance in a batch reactor.

Ni-supported on tungstophosphoric acid (TPA) mesoporous clay gave 56% selectivity to menthols at complete citral conversion at 80°C under 0.5 MPa (Table 7, entry 8), while the corresponding Pd supported catalyst was more active toward hydrogenated products [161]. The benefit of supporting tungstophosphoric acid on a clay is to enlarge the surface area of the catalyst. Furthermore, the support material, montmorillonite clay was dealuminated prior to loading the metal and tungstophosphoric acid to remove strong Brønsted acid sites. It was stated that especially Lewis acid sites in Ni-TPA-clay catalyst restricted the undesired

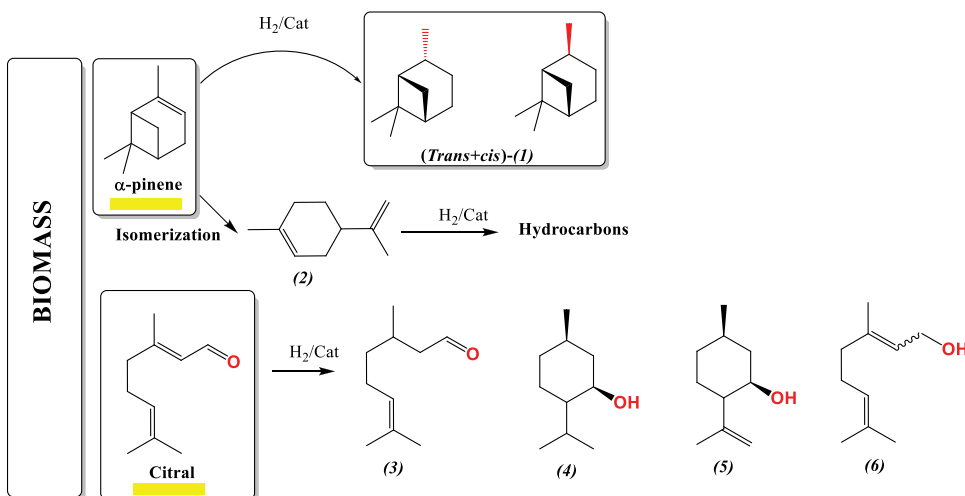


Figure 15. The main hydrogenated products are obtained from α -pinene, limonene and citral. 1=pinane, 2=limonene, 3=citronellal, 4=Menthol, 5=Isopulegol, 6=Geraniol/Nerol.

hydrogenation. From the mechanistic point of view, it was stated that strong Lewis acid sites together with weak Brønsted acid sites are preferred for cyclization of citronellal.

One-pot synthesis of menthol from citral was also investigated in a trickle bed reactor in the presence of mass transfer limitations [162,172]. Successful menthol synthesis was obtained over Ni/(H-Beta-38+ sepiolite) extrudates at 70°C under 20 bar total pressure giving maximally 56% selectivity to menthols [167]. The extrudates composed of 70 wt% H-Beta-38 and 30 wt% of sepiolite exhibited the Brønsted to Lewis acid ratio of 0.6 and the average nickel particle size of 25.5 nm. It was also stated that in this case conversion of citral decreased with increasing time on stream, when pressure was decreased as follows: during the first 180 min, the reaction was performed under 20 bar total pressure followed by 15 bar for next 170 min and finally 90 min under 10 bar. It was also observed that initially, when the catalyst acidity was high, the main products were defunctionalized ones, *i.e.* dehydrated menthols, while when the most acidic sites were poisoned, menthol yield rapidly increased. At the maximum menthol yield the ratio between menthols and acyclic hydrogenated products was still rather high, being 1.4 indicating that this catalyst was also active for hydrogenation instead of cyclization of the formed citronellal. Noteworthy is that stereoselectivity to the desired product L-menthol (77%) remained constant during the whole experiment despite pressure changes. As a comparison, a trial of using Ru-H-Y-80 (the number denotes SiO_2/Al_2O_3 ratio) in one pot synthesis of menthol from citral did not give any menthols due to the presence of Ru as a metal, while the acidity of this catalyst was mild (Table 7, entry 6) [173].

Table 7. Hydrogenation of terpenes by using supported heterogeneous materials.

Entry	Catalyst	Terpenoid	Reaction medium	Reaction conditions	X (%)	S (%)	Ref
1	Ni-B loaded on a carbon-silicon nanomaterial	α -Pinene	H ₂ O	1 g of substrate, 1 MPa H ₂ , 80°C, 3 h, 50 mg of catalyst, 4 mL of H ₂ O.	99	98.5 <i>cis</i> -pinane	[171]
2	Ni-B/KIT-6	α -Pinene	Ethanol	10 g turpentine oil, 4 MPa H ₂ , 10 mL solvent, 120°C, 3 h.	90.92	97.35 <i>cis</i> -pinane	[163]
3	Ni/APO-PT	α -Pinene	Solvent free	10 g substrate, 3.32 wt. % catalyst, 3 MPa H ₂ , 132°C, 1 h.	98.5	96.2 pinane	[164]
4	Pt/Carbon	Limonene	Vapor-phase	1.2 mg substrate, 1.2 mg catalyst, 110 mL min ⁻¹ H ₂ , 0.2 MPa H ₂ , 200°C.	100	100 cycloalkane C ₁₀	[172]
5	Ni/Al ₂ O ₃ -SiO ₂	Limonene	Vapor-phase	2.0 catalyst to feedstock mass ration, GHSV = 17s ⁻¹ , 0.2 MPa H ₂ , 2°C.	100	90.8 cycloalkane C ₁₀	[162]
6	Ru/H-Y-80	Citral	Cyclohexane	7.76 mmol substrate, 100 mg of catalyst, 70°C, 10 bar H ₂ .	26	78 acyclic hydrogenation products 22 cyclic products composed of: traces of menthols, 15 pulegols 7 defunctionalized products	[173]
7	Ni/(H-Beta-38 + sepiolite)	Citral	Cyclohexane	C ₀ = 0.086 M substrate, 20 bar H ₂ , contact time 4.2 min, residence time 16.7 min, time-on-stream 180 min (continuous mode).	88	56 (-)-menthol, 76 stereoselectivity to L-menthol	[167]
8	Ni-TPA-Mesoporous clay	Citral	Cyclohexane	4.5 mmol substrate, 0.2 g catalyst, 25 mL solvent, 80°C, 0.5 MPa H ₂ , 24 h.	100	56 menthols 2 isopulegols 12 3,7-dimethyl-1-octanol	[161]
9	Ni-HPA-Montmorillonite	Citral	Cyclohexane	C ₀ = 0.018 M substrate, 1 MPa H ₂ , 3.4% wt. substrate-catalyst, 80°C, 24 h.	100	63 menthols 5 citronellal 8 isopulegols 1 dihydrocitronellal 6 3,7-dimethyl-1-octanol	[165]

(Continued)

Table 7. (Continued).

Entry	Catalyst	Terpenoid	Reaction medium	Reaction conditions	X (%)	S (%)	Ref
10	Cu/Al ₂ O ₃ , coated with 10 wt% [C ₂ C ₁ Im][NTf ₂]	Citral	Cyclohexane	C ₀ = 0.1 M substrate, 400 mg catalyst, 0.3 MPa H ₂ , 100 mL solvent, 130°C, 6.67 h	95	42 citronellal 13 citronellol 31 geraniol 3 nerol	[174]
11	Meso-ZrO ₂	Citral	2-Propanol	2.50 mmol substrate, 130 mmol solvent, 0.3 g catalyst, 80°C, atmospheric pressure, 10 h	71	100 geraniol + nerol	[155]
12	Pd-TPA-Mesoporous clay	Citronellal	Cyclohexane	4.5 mmol substrate, 0.2 g catalyst, 25 mL solvent, 80°C, 0.5 MPa H ₂ , 3 h.	100	82 menthols 3 dihydrocitronellal 3 3,7-dimethyl- 1-octanol	[161]

GHSV: Gas hourly space velocity.

A very specific catalyst was prepared for selective hydrogenation of citral to unsaturated alcohols nerol and geraniol, namely Cu/Al₂O₃, which was coated with an ionic liquid containing 10 wt% of 1-ethyl-3-methylimidazolium *bis*(trifluoromethylsulfonyl)imide coating. It was stated that copper is prone to activate C-O bond instead of the C-C bond, although it is thermodynamically easier to hydrogenate ethylenic double bond than the carbonyl bond [174]. Metallic copper exhibits Lewis acidity [176]. As a comparison, the corresponding Cu/Al₂O₃ catalyst in the absence of an ionic liquid gave 30% selectivity to isopulegol.

As a comparison, transfer hydrogenation of citral using 2-propanol as a hydrogen donor for production of unsaturated alcohols was demonstrated over meso-ZrO₂ [155]. The catalyst calcined at an optimum temperature at 350°C gave 71% conversion and 100% selectivity to the desired unsaturated alcohols at 80°C. Only catalytic activity was changing with the calcination temperature, while selectivity to unsaturated alcohols was at all calcination temperatures 100%. High selectivity to unsaturated alcohols was related to a high surface area and Lewis acidity of the catalyst. In the temperature range for calcination of 350–600°C, citral conversion decreased with increasing calcination temperature and at the same time the surface area and acidity of the catalyst decreased explaining the catalytic results. Furthermore, mesoporous ZrO₂ could be easily regenerated via calcination and reuse [155].

8. Hydration

8.1. Exploring the importance of monoterpene hydration

The acid-catalyzed hydration of terpenes is one of the most favorable pathways to obtain different high-added value substances such as alcohols, aldehydes, and even epoxides. These are precursors for the perfume industry. Typical hydration of α -pinene yields different monocyclic and bicyclic compounds containing water molecules and products of terpenes isomerization of the terpenes because of the acid sites nature (Figure 16). As can be seen, the strong acid sites of the heterogeneous catalysts are responsible for the isomerization while the addition of water can tailor selectivity to the desired hydration products. Then, products such as terpineol and cineol can be considered as condensation products of the primary monoterpenes together with water.

Among a lot of derived hydration products, the main product which can be obtained in this way is α -terpineol. This material may be present in two enantiomeric forms, i.e.: S(-) and R(+); however, the S(-)-is the most abundant [177], being widely used in the fragrance and aroma industry. This colorless, crystalline solid, smelling of lilac, optically active monoterpeneoid can be found in flowers such as narcissus and freesia, in herbs, such as marjoram, oregano, and rosemary, and in lemon peel oil [178]. However, it can be synthesized in a relatively simple way by hydration of α -pinene using different heterogeneous catalysts (Table 8). α -Terpineol has various interesting biological effects such as cardiovascular and antihypertensive [187,188], antioxidant [189–191], anticancer [192,193], antinociceptive [194], antiulcer [195], anticonvulsant and sedative [196], antibronchitis [197], skin penetration enhancing [198], and finally insecticidal activity [199]. Four of the main companies which manufacture α -terpineol are as follows: Foreverest resource

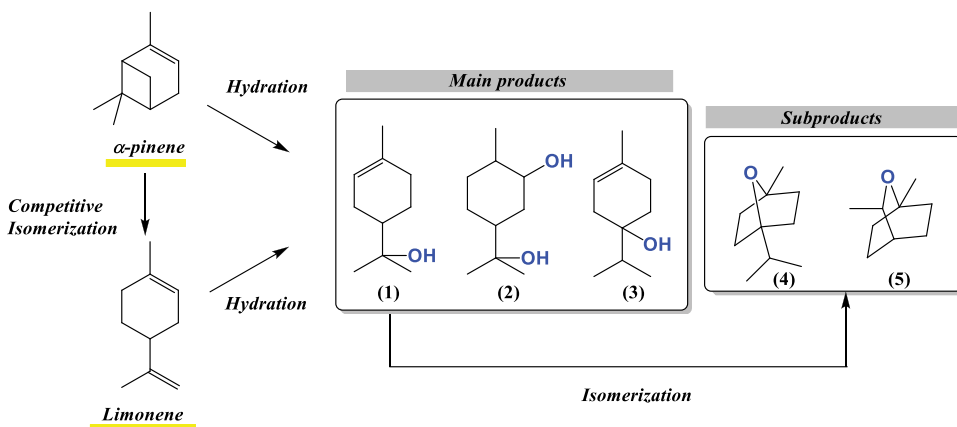


Figure 16. The most relevant hydration products of α -pinene and limonene: (1) α -terpineol, (2) 1,8-terpin (3) terpinen-4-ol (4) 1,4-cineol, (5) 1,8-cineol.

(Xiamen, china), EcoGreen International Group Limited (Wanchai, Hong Kong), Socer Brasil Indústria e Comércio Ltda (Sao Paulo, Brazil) and Workwell (Mohali, Punjab, India) [200].

8.2. Recent literature on hydration of monoterpenes

Synthesis of α -terpineol from α -pinene can be performed using heterogeneous catalysts and water. Acidic hydration is one of the main routes proposed for the selective synthesis of this molecule. Table 8 shows the main catalytic systems proposed for synthesis of this compound using heterogeneous catalysts. In the first case (Table 8, entry 1), an acidic beta zeolite (the number indicates the Si-to-Al ratio) was used as a catalyst for hydration of limonene. Relatively soft reaction conditions (50°C and 24 h) were applied to obtain directly α -terpineol as the major product. It was found that the reaction rate increased with temperature and with the amount of acetic acid. Selectivity to this target was observed to increase with the conversion when temperature was 50°C. Other byproducts such as eucalyptol, α -terpinene, terpinolene, *p*-cymene, and α -terpinyl acetate were detected. Similarly, to previous reactions, the amount and strength of the acid sites affect the product distribution. Strong acid sites can give isomerization rather than the condensation products [201]. Then, controlling the active acidic catalytic sites can drive the reaction to the desired hydration product. In this study, the addition of a weak organic acid to the reaction mixture had a positive effect on both the reaction rate and selectivity to α -terpineol.

Comparatively, an acid treated Montmorillonite K10 was used as the acid catalyst for the synthesis of α -terpineol starting from α -pinene (Table 8, entry 2). Montmorillonite is a natural material belonging to a very soft phyllosilicate group of minerals being also a member of the smectite group [202]. The acid treatment gives a material that can be used for several applications including acetylation of sugars [203], synthesis of heterocycle compounds [204], among others. For the present case, α -pinene hydration was carried out by using several solvents (acetone, n-butane, dibutyl ether, toluene, and 1,4-dioxane) at 80°C (in some of the cases at reflux) giving acceptable conversions but poor selectivity to α -terpineol. Maximum selectivity to the desired target (45%) was obtained at moderate conversion of pinene (up to 60%) using 1,4-dioxane as the solvent. Comparison of the acid-treated montmorillonite with the raw material reinforces the hypothesis that the acid treatment is necessary to achieve α -terpineol. In addition, acidity together with the specific surface area are important factors influencing the catalytic activity of the material.

A low-cost deep eutectic solvent (DES) was considered as a green and environmentally friendly solvent for various catalytic applications. Considering the acidic character of the reaction and formation of the carbocation intermediates of α -pinene generated under the reaction, isomerization

Table 8. Heterogeneous catalysts for hydration of terpenes.

Entry	Catalyst	Terpenoid	Reaction medium	Reaction conditions	X (%)	S (%)	Ref
1	Beta 25 zeolite	Limonene	-	50 wt. % of catalyst, 10% aqueous acetic acid (10 mL) (volume ratio limonene: H ₂ O = 1:4.5), 50°C, 24 h.	36	88 α-terpineol	[114]
2	Acid treated montmorillonite K10	α-Pinene	Acetone	250 mg substrate, 25 wt. % K10/HCl, 250 mg of H ₂ O, 3 g solvent, 80°C, 24 h.	74	3 α-terpineol	[179]
			n-Butanol		92	27 α-terpineol	
			Dibutyl ether		89	8 α-terpineol	
			Toluene		100	0 α-terpineol	
			1,4-Dioxane		60	45 α-terpineol	
3	Deep eutectic solvents (DES)	α-Pinene	Oxalic acid (OA)/ polyethylene glycol	0.03 mol DES (based on OA), 0.06 mol of substrate, 0.3 mol of H ₂ O, 75°C, 8 h	81.5	51.2 α-terpineol	[180]
4	Carbon-based solid acid catalyst with rice straw biomass	α-Pinene	Presence of solvent (not reported)	5 mL substrate, 5.25 mL of deionized water, 0.5 g catalyst, 20 mL solvent, 80°C, atmospheric pressure, 300 rpm, 24 h.	67.60	57.07 α-terpineol	[181]
5	Purolite CT175 (Ion exchange resin)	Turpentine oil	Isopropyl alcohol as solvent	1 g turpentine, 0.6 g H ₂ O, 2 mL solvent, 0.1 g catalyst, reflux temperature, 8 h.	97	57 α-terpineol	[182]
6	H ₂ SO ₄	α-Pinene	Ionic liquid as a green solvent	10.2 g substrate, 12 g H ₂ O, 24.1 g solvent, 3 g catalyst, 70°C, 4 h	93.2	26.8 α-terpineol	[183]
7	SO ₄ ²⁻ /Zr-MCM-41 HY HZSM-5 Si-MCM-41 Zr-MCM-41 SO ₄ ²⁻ /Si-MCM-41	α-Pinene	Supercritical carbon dioxide (scCO ₂)	1.36 g substrate, 0.54 g H ₂ O, 0.95 g chloroacetic acid, 9 MPa scCO ₂ , 60°C, 8 h	93.9	87.6 α-terpineol	[184]
					54.8	57.5 α-terpineol	
					56.1	58.1 α-terpineol	
					57.9	73.8 α-terpineol	
					37.6	55.8 α-terpineol	
					80.8	53.2 α-terpineol	
8	LC _x -SO ₃ H Amberlyst-15	α-Pinene	Isopropanol as solvent	4 g substrate, 4 g H ₂ O, 0.40 g catalyst, 20 mL solvent, 80°C, 300 rpm, 24 h.	95.3	58.1 α-terpineol	[185]
					97.4	34.4 α-terpineol	
9	p-Toluenesulfonic acid (PTSA) + oxalic acid (OA)	Turpentine oil	-	1 mol of substrate, excess of water, 0.2 mol PTSA, 1 mol of OA, 85°C, 6 h	99.1	21.7 cineole	[186]

would be preferred rather than hydration. DES was used for hydration of α-pinene at benign conditions (Table 8, entry 3). Interestingly, DES can act as both the solvent and catalyst in the reaction. A series of carboxylic acid-functionalized deep eutectic solvents was synthesized using a dicarboxylic oxalic acid as the hydrogen donor and the polyethylene glycol (PEG) with

different polymerization degrees. It was concluded that an increase in the molecular weight and dosage of PEG results in a decrease of acidity leading a notable effect in the catalytic activity. Under the optimal conditions (75°C, 8h), an acceptable conversion of the pinene (81.5%) was obtained, whereas selectivity to α -terpineol was 51.2%. Moreover, the catalyst can be refrigerated and reused in several cycles (up to seven including the fresh use) offering a clean catalytic route for the synthesis of α -terpineol.

On the other hand, searching of new catalytic systems for the green synthesis of α -terpineol is nowadays a hot topic reflecting a trend for rational exploitation of biomass. Interestingly, an acidic carbon based on rice straw biomass was prepared and used as an active catalyst for the synthesis of α -terpineol from α -pinene (Table 8, entry 4). Use of rice straw waste is based on the fact that almost 300 million tons are burned and the rest is left to rotting in the fields where it emits methane (greenhouse gas worse than CO₂) [205]. In the reported research, a carbon-based solid acid catalyst was prepared and fully characterized, with the focus on investigating both carbonization and sulfonation temperature. Conversion of pinene and selectivity to α -terpineol reached values of 67% and 57%, respectively, which were related with a density of the acid sites and porosity of this mesoporous materials having a surface area of 421 m²/g. Although the use of rice straw is environmentally friendly, details of the reuse were not reported.

An ionic exchange resin (purolite CT175: Polystyrenic microporous strong acid cation ion exchange resin in the hydrogen form) [182] was tested in both isomerization and hydration of biomass-derived turpentine using relatively mild conditions (Table 8, entry 5). The composition tested for the catalytic activity was 60:40 of α -pinene and β -pinene, respectively. Among many of ion exchange resins (CT175, Amberlyst15, Amberlyst 35 and Amberlyst 36) and solvents (water, THF, 1,4-dioxane, DMSO, n-hexane, ethanol, IPA, t-BuOH), the best ones were purolite CT175 and IPA as the benign solvent. At these conditions, the maximum conversion of pinene was 97% while the selectivity to α -terpineol reached 57%. Based on [182], the use of IPA in the reaction is beneficial vs other solvents because of better ionization of H⁺ from the resin and the solubility of the turpentine oil and water, which in fact can promote better miscibility and better catalytic activity. However, data in [182] indicate potential catalyst instability.

Within the context of green chemistry, an ionic liquid (IL) composed mainly of tripropylamine hydrogen sulfate was used as a solvent with sulfuric acid as the homogeneous catalyst (Table 8, entry 6). Although the transformation of α -pinene into α -terpineol was performed using homogeneous catalysis, the reuse of the inorganic phase (containing IL, water, and sulfuric acid) was carried out successfully. The low cost, highly stable ionic liquid and the use of sulfuric acid simplify this transformation being advantageous for the production of α -terpineol. However, selectivity of the reaction is as low as 27% at

almost total conversion of pinene (93%). Other by-products typical for isomerization were obtained e.g. 2-carene, limonene, and camphene.

In the context of heterogeneous catalysis, several materials including those related to MCM-41, HY, ZSM-5 [184] were tested for the efficient transformation of α -pinene into α -terpineol by using the supercritical carbon dioxide technology (Table 8, entry 7). The authors [184] have shown that high conversion of α -pinene and selectivity to α -terpineol (94% and 88%, respectively) in comparison with the previous reports can be obtained by using the system $\text{SO}_4^{2-}/\text{Zr-MCM-41}$. Modulating acidity of MCM-41 by incorporation of Zr and SO_4^{2-} can avoid the secondary reactions i.e. isomerization of pinene. Hydrothermal synthesis of Zr-MCM-41 following by impregnation of SO_4^{2-} suggests the presence of both Lewis and Brønsted acid sites in comparison with Zr-MCM-41 which exhibited only Lewis acidity. High selectivity to α -terpineol (73.8%) was achieved with only Si-MCM-41; however, conversion was only half in comparison with the main catalytic system. Reuses of the material (using different Zr precursors for the catalyst synthesis) were performed for three cycles concluding that formation of $\text{Zr}(\text{SO}_4)_2$ is the main reason requiring regeneration activity in $\text{SO}_4^{2-}/\text{Zr-MCM-41}$.

Following the green chemistry principles, an amphiphilic mesoporous carbon-based solid acid synthesized from Kraft lignin (KL) was tested and compared with Amberlyst-15 for hydration of α -pinene (Table 8, entry 8) [185]. Kraft lignin is the main source of energy in Kraft mills and is commercialized for liginosulfonate applications [206]. In recent years, its use and valorization have gained more attention. Kraft lignin was used as the starting material for the synthesis of the acidic catalyst. The authors suggested that the specific surface area, pore structure, and amphiphilic nature can be adjusted through the phosphoric acid dosage. Almost total conversion of α -pinene (95.3%) with a slightly exceeding 50% selectivity to α -terpineol was achieved. The use of isopropanol as a solvent is because of the solubility and better ionization as suggested previously for purolite CT175 (Table 8, entry 5). Both the architecture of the material together with the distribution and strength of the acid sites can control selectivity to the hydrated product. On the other hand, the catalyst was successfully reused up to five cycles with a slight decrease of both conversion and selectivity suggesting a high potential of the material for the mentioned application.

Previous studies were mainly focused mainly on the synthesis of α -terpineol because of its applications. However, another product which can be obtained from hydration of α -pinene is 1,8-cineole (Figure 16). 1,8-cineole (eucalyptol) is mainly obtained from essential oils of different plants (e.g.: *Pinus merkussi*) having a potential application as anti-inflammatory and antioxidant [207]. Cineole has been considered as the component with the highest market price exceeding even the one for α -terpineol. *P*-toluene sulfonic acid together with oxalic acid (OA) were tested for the synthesis of (1,8 and 1,4) cineol from

crude turpentine (Table 8, entry 9). The reaction was divided into two steps: hydration of turpentine to yield α -terpineol and then isomerization to 1,8-cineole. The highest conversion and selectivity to cineole (both 1,8 and 1,4) by using a strong acidic catalyst together with a weak organic catalyst was 99% and 22%, respectively. Catalyst stability was typically not considered [186].

9. Amination

9.1. Importance of terpene amines for fine chemistry

Terpene amines have potential to be used as drugs for neurological diseases and it is of high interest to produce them from renewable resources using easily reusable and relatively inexpensive heterogeneous catalysts [208–212]. Catalytic one-pot amination also has one benefit, the reaction can be carried out under an inert atmosphere without the presence of gaseous hydrogen. This reaction proceeds via the hydrogen borrowing mechanism, in which hydrogen is obtained from alcohol dehydrogenation to an aldehyde, which in turn reacts further with an amine to produce the corresponding imine. In the forthcoming step hydrogen transfer from the alcohol to the imine occurs via metal-hybrid intermediates forming the amine.

9.2. Recent reports for the synthesis of amines from monoterpenes

Several heterogeneous catalysts, such as Au and Pd as well as their combination supported on alumina, zirconia, different alkali metal oxides were used especially in the amination of myrtenol and its derivatives with aniline and other amines in [208–211]. As the main parameters, the types of the support [211], terpene alcohol [209] and catalyst redox-activation [208,210] were investigated with the main results summarized in Table 9. Scientifically, it is very demanding to produce an unsaturated amine 5 (Fig. 17) from one-pot amination of myrtenol with aniline, because it is easy to reduce the reactive C=C group in myrtenol and get myrtanol (6) instead of myrtenal (3). Furthermore, the produced myrtenal can also be easily reduced to myrtanal (7) promoting thus the formation of imine II (8) and amine II (9).

In one-pot amination of myrtenol, the highest selectivity to the desired amine 5 has been obtained with Au/ZrO₂ as a catalyst which exhibited both acidic and basic sites (Table 9, entry 41) [211]. The performance of this catalyst was also compared with alumina and alkali metal supported catalysts. Superiority of Au/ZrO₂ promoting high conversion and selectivity to the desired amine was related to its ability to catalyze hydrogen transfer which is an acid catalyzed reaction. Au/ZrO₂ exhibited also small average gold particle size in the range of 1.2–1.3 nm and zirconium oxide as in monoclinic phase

based on XRD. In addition, Au supported on basic supports gave much lower turnover frequencies in comparison to Au/ZrO₂.

The effect of the redox pretreatment of different Au, Pd, and Au-Pd catalysts supported on alumina was investigated in one pot amination of myrtenol (Table 9, entries 1-6) [208-210]. The results showed that the highest selectivity to the desired secondary amine I (5) and the corresponding imine I (4) was obtained over Au/Al₂O₃ pretreated with oxygen prior to the experiment (entry 5). This catalyst exhibited a small average particle size of gold, 2.4 nm and it contained only metallic gold. Furthermore, it was the most selective to amination routes, i.e., formation of products 4, 5, 8, and 9. On the other hand, a bimetallic Au-Pd/Al₂O₃ oxidized prior to the experiment gave the highest selectivity to the hydrogenation products (entry 1). Monometallic Pd-catalysts pretreated either with hydrogen or oxygen were selective to formation of hydrogenation products. The reason for lower selectivity of the pre-reduced Au/Al₂O₃ toward amination was stated to be a lack of aniline adsorption on the catalyst surface. Analogously to Au/Al₂O₃ [208] also preoxidized Au/ZrO₂ was more efficient for producing the target amine 5 than the corresponding hydrogen treated catalysts [210]. These results are explained as follows: oxygen treatment retains the basic sites required for alcohol activation, while hydrogen treatment decreases the amount of ionic gold known to promote the hydrogen transfer step. Furthermore, it was observed in [210] that both dehydrogenation/hydrogenation as well as hydrogen transfer were structure sensitive, i.e. the catalytic activity decreased with an increase in the metal particle size.

In addition to a study of the support nature and the catalyst pretreatment, the effect of substrate structure was investigated in monoterpene

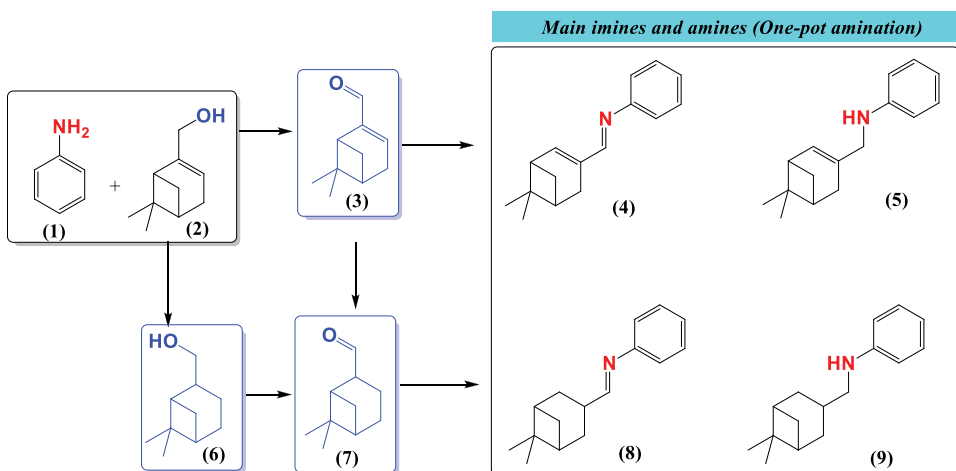


Figure 17. The scheme for one-pot amination of myrtenol (2) with aniline (1). Notation: 3. Myrtenal, 4. Imine I, 5. Amine I, 6. Myrtenol, 7. Myrtenal, 8. Imine II and 9. Amine II.

alcohol amination over Au/ZrO₂ catalyst (Table 9, *entries 7-28*) [209]. Au/ZrO₂ catalyst after oxidation at 350°C exhibited a relatively large amount of cationic gold species, which promote amination. Slow reaction rates were obtained with nopol. On the other hand, the highest selectivity to the desired secondary amine I was obtained with nopol. In the case of perillyl alcohol, a complicated product mixture was obtained as a result.

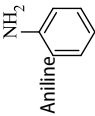
In comparison with the amine structure, the results showed that myrtenal conversion increased in the following order for three selected amines: 4-methylaniline < aniline < 4-bromoaniline (*entries 7, 10 and 12*) [209]. It was possible to correlate the corresponding rate constants with the Hammett equation showing that the highest rate was obtained with 4-bromoaniline due to its electron-withdrawing group, however, giving a high number of hydrogenated products due to polarization of C=C group. The amination rate of 3-aminopyridine was also ca. tenfold lower compared to aniline.

10. Photocatalytic transformations of some selected monoterpenes into high-added value chemicals

10.1. Synthesis of fine commodities from terpenes using photocatalytic processes

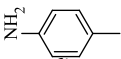
Heterogeneous photocatalysis involves the use of solar light, which is a sustainable source, milder reaction conditions in comparison to the traditional thermal catalysis affording faster reaction rates [213]. The photocatalytic activity in catalysis strongly depends upon capability of the catalyst to generate electron-hole pairs [214]. The material used in a reaction may be regarded as a “photocatalyst” only if the photon is considered as the reactant [215]. Different photocatalytic transformations have been observed for the synthesis of new chemicals from terpenes. Some of them include hydrogenation and epoxidation. Several factors can affect the performance of the materials, including the effectiveness potential of the light, the HOMO-LUMO bandgap in the material, the size of the reactor, the particle size and even the light source nature. Other factors include pH, size, and structure of the photocatalyst, surface area, temperature, irradiation time, etc. [216,217]. Then, strict selection of the conditions (light power and source, nature of the material, absorption capacity, etc.) should be critical for obtaining a better catalytic activity. Considering all these factors, we have included some relevant references in which photoinduced reactions for terpenes have been involved as discussed below, most of them with high selectivity and lower generation of subproducts.


Table 9. Heterogeneous catalysts for the amination of biomass-derived terpenes.

Entry	Catalyst	Terpenoid	Amination agent	Reaction conditions	TOF (s^{-1})	X (%)	S (%)	Ref
1	AuPd/Al ₂ O ₃ -TPO	Myrtenol	 Aniline	1 mmol substrate, 1 mmol amination agent, 10 mL toluene, 92 mg catalyst, 180°C, 14 h.	0.01	85	50 myrtenal, 3 25 myrtenol, 6 7 myrtenal, 7 8 Imine I, 4 4 Amine I, 5 3 Imine II, 8 4 Amine II, 9 6 myrtenal, 3 12 myrtenol, 6 6 myrtenal, 7 40 Imine I, 4 31 Amine I, 5 1 Imine II, 8 3 Amine II, 9 26 myrtenal, 3 31 myrtenol, 6 2 myrtenal, 7 32 Imine I, 4 2 Amine I, 5 3 Imine II, 8 2 Amine II, 9 8 myrtenal, 3 9 myrtenol, 6 20 myrtenal, 7 36 Imine I, 4 7 Amine I, 5 8 Imine II, 8 10 Amine II, 9 26 myrtenal, 3 12 myrtenol, 6 5 myrtenal, 7 35 Imine I, 4 19 Amine I, 5 1 Imine II, 8 1 Amine II, 9 21 myrtenal, 3 46 myrtenol, 6 1 myrtenal, 7 27 Imine I, 4 2 Amine I, 5 1 Imine II, 8 1 Amine II, 9	[208]
2	Au/Al ₂ O ₃ -TPO				0.02	92		
3	Pd/Al ₂ O ₃ -TPO				0.04	85		
4	AuPd/Al ₂ O ₃ -TPR				0.04	100		
5	Au/Al ₂ O ₃ -TPR				0.04	95		
6	Pd/Al ₂ O ₃ -TPR				0.08	90		

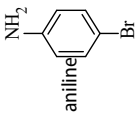
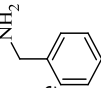
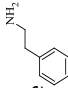
(Continued)

Table 9. (Continued).

Entry	Catalyst	Terpenoid	Amination agent	Reaction conditions	TOF (s^{-1})	X (%)	S (%)	Ref
7			Aniline	1 mmol substrate, 1 mmol amination agent, 10 mL toluene, 92 mg catalyst, 9 bar N_2 , 180°C.	n.d.	44 (2 h)	39 Amine I, 5 Amine II, 9 50 Imine 1, 4 3 Imine 2, 8	[209]
8					n.d.	87 (8 h)	52 Amine I, 5 6 Amine II, 9 34 Imine 1, 4 2 Imine II, 8	
9					n.d.	98 (16 h)	53 Amine I, 5 7 Amine II, 9 33 Imine 1, 4 2 Imine II, 8	
10		4-Methy	 laniline		n.d.	34 (2 h)	19 Amine I, 5 Amine II, 9 73 Imine 1, 4 4 myrtanal, 3 0.9 myrtanal, 7	
11					n.d.	89 (8 h)	37 sec amine 1 1 sec amine II 53 Imine 1 8 myrtanal, 3 2 myrtanal, 7	
12					n.d.	98 (16 h)	43 sec amine I 2 sec amine II 49 Imine 1 4 myrtanal, 6 Myrtanal, 7	

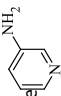
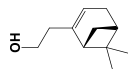
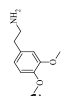
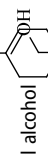
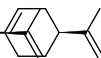
(Continued)

Table 9. (Continued).

Entry	Catalyst	Terpenoid	Amination agent	Reaction conditions	TOF (s ⁻¹)	X (%)	S (%)	Ref
13		Myrtenol	4-Bromo  aniline		n.d.	60 (2 h)	14 sec amine II 43 Imine II, 4 myrtenal, 7	
14					n.d.	99 (8 h)	13 myrtenal, 3 22 sec amine II 49 Imine II, 8	
15			Benzy  lamine		n.d.	48 (2 h)	36 sec amine 1 13 sec amine II 26 Imine 1 14 Imine II (1) myrtenal, 6	
16					n.d.	98 (8 h)	3 sec amine 1 35 sec amine II 49 Imine II	
17			Phen ethy		n.d.	40 (8 h)	63 sec amine 1 36 Imine 1	
18			lamine 		n.d.	53 (16 h)	51 sec amine 1 47 Imine 1	
19					n.d.	70 (24 h)	46 sec amine 1 1 sec amine II 52 Imine 1	

(Continued)

Table 9. (Continued).

Entry	Catalyst	Terpenoid	Amination agent	Reaction conditions	TOF (s ⁻¹)	X (%)	S (%)	Ref
20			 3-Aminopyridine		n.d.	19 (8 h)	21 sec amine I 74 Imine I 2 myrtanal, 6 1 myrtanal, 7	
21					n.d.	31 (16 h)	20 sec amine I 1 sec amine II 60 Imine I 11 myrtanal, 3 3 myrtanal, 7	
22					n.d.	44 (24 h)	23 sec amine I 2 sec amine II 58 Imine I 1 Imine II 12 myrtanal, 3 3 myrtanal, 7	
23		 Nopol	 3,4-Dimethoxyphenethylamine		n.d.	13 (16 h)	72 sec amine I 27 Imine I	
24			Aniline		n.d.	10 (8 h)	74 sec amine I 22 Imine I	
25					n.d.	40 (16 h)	76 sec amine I 10 Imine I	
26		 Perillyl alcohol	Aniline		n.d.	70 (2 h)	Complicated mixture of the products	
27					n.d.	99 (8 h)	1 sec amine I 19 sec amine II 0	
28		 Perillyl alcohol ^a	Aniline		n.d.	98 (8 h)	28 Imine I 11 Imine II 2 Aldehyde	

(Continued)

Table 9. (Continued).

Entry	Catalyst	Terpenoid	Amination agent	Reaction conditions	TOF (s^{-1})	X (%)	S (%)	Ref
29	Au/ZrO ₂ -TPO	Myrtenol	Aniline	1 mmol substrate, 1 mmol amination agent, 10 mL toluene, 92 mg catalyst (1.4 mol % Au), 9 bar N ₂ , 180°C, 16 h.	0.01	96	50 sec amine 1 36 Imine 1, 4 8 sec amine 2 5.6 myrtanol	[210]
30	Au/CeO ₂ -TPO				0.003	76	42 Imine 1, 4 32 Amine II, 9 16 myrtanal	
31	Au/La ₂ O ₃ -TPO				0.004	80	53 myrtanal 21 myrtanol 8 nol 8 myrtanal	
32	Au/ZrO ₂ -TPR				0.02	92	13 Imine 1, 4 48 Imine 1, 4 32 Amine 1, 5 10 myrtanal	
33	Au/CeO ₂ -TPR				0.01	86	43 myrtanal, 3 7 myrtanol, 6 33 Imine 1, 4 10 Amine II, 5 7 Imine II, 8	
34	Au/La ₂ O ₃ -TPR				0.003	84	65 myrtanal, 3 26 myrtanol, 6 10 myrtanal, 7	

(Continued)

Table 9. (Continued).

Entry	Catalyst	Terpenoid	Amination agent	Reaction conditions	TOF (s^{-1})	X (%)	S (%)	Ref
35	Au/Al ₂ O ₃	Myrtanol	Aniline	1 mmol substrate, 1 mmol amination agent, 10 mL toluene, 92 mg catalyst (1.4 mol % Au), 9 bar N ₂ , 180°C, 16 h.	0.01	90 (8 h)	37 Amine I, 5 5 Amine II, 9 42 Imine I, 4 2 Imine II, 8	[211]
36					n.d.	95 (16 h)	41 Amine I, 5 5 Amine II, 9 39 Imine I, 4 4 Imine II, 8	
37	Au/CeO ₂				0.004	76 (8 h)	7 Amine I, 5 21 Amine II, 9 35 Imine I, 4 7 Imine II, 8	
38	Au/La ₂ O ₃				0.004	80 (8 h)	3 Amine I, 5 2 Amine II, 9 16 Imine I, 4 1 Imine II, 8	
39	Au/MgO				0.007	73 (8 h)	17 Amine I, 5 6 Amine II, 9 35 Imine I, 4 3 Imine II, 8	
40	Au/ZrO ₂				0.01	96 (8 h)	50 Amine I, 5 4 Amine II, 9 36 Imine I, 4 4 Imine II, 8	
41	Au/ZrO ₂				n.d.	98 (16 h)	52 Amine I, 5 5 Amine II, 9 35 Imine I, 4 3 Imine II, 8	

TPO: catalyst pre-treated in oxygen. **TPR:** catalyst pre-treated in hydrogen. ^a Reaction temperature of 160°C. **n.d.:** not determined.

10.2. Recent literature on synthesis of biomass-derived terpenes using photocatalytic transformations

For example, Table 10 (*entry 1-6*) shows the catalytic activity of different TiO₂ nanoparticles-based materials for the hydrogenation of citral (see Figure 15, section hydrogenation). TiO₂ in different types and forms demonstrated a significant potential in photocatalysis because of their nontoxicity, reactivity, stability, and light absorption [225]. Photocatalytic hydrogenation has emerged as a new synthetic organic strategy for obtaining high-added value chemicals of interest in fine chemistry industry. Moreover, the transformations are highly regio- and stereoselective, which add additional advantages over other synthetic strategies. It seems that the calcination temperature plays a critical role in the synthesis of hydrogenated products from citral, e.g., nerol and geraniol. The optimum range for the calcination temperature giving the maximum yield of hydrogenated products (conversion >99%, selectivity to unsaturated alcohols of 99%) was 450°C–500°C. Apparently, an increase in the temperature of calcination decreased considerably conversion of citral, yielding, besides, other by-products such as nerol and citronellal. Comparison of these materials shows a dramatical change in the surface area of TiO₂ NP calcined at 500°C from those calcined at 750°C (50 m²/g vs 1.2 m²/g). A large surface together with hierarchical porous structures are beneficial for the synthesis of hydrogenated products from citral using light. The reuses revealed that the selected material can be reused only until two additional cycles with a notable decrease in the catalytic activity (conversion from 99% to 76% and selectivity from 99% to 93%).

On the other hand, a dioxo-molybdenum complex anchored to a large surface area MOF (in this case a COMOC: Gallium-based metal-organic framework) was tested for the green synthesis of epoxides starting from bicycle monoterpenes e.g.: α - and β -pinene, using oxygen as a green regenerated oxidizing agent (Table 10, *entry 7-13*). While MOF can enhance the dispersion of active catalytic units, the complex composed of dioxo dichloride molybdenum with dicarboxylic acid as the ligand is the oxygen transfer agent, which yields epoxide as the sole product. This process implies the oxygen transfer from the catalyst to the olefin and the reoxidation and generation of the catalytic unit using diatomic oxygen. Oxygen activation by using transition metals is a well-known process in which oxo-peroxo entities are formed [226]. Different immersion lamps, i.e. laser and halogen, with different excitation wavelengths were evaluated and the results showed drastic changes in conversion but not in selectivity (99% in all cases). While for α -pinene the change of the lamp produces a meaningful change in conversion (from 50% to 62%), the increase for β -pinene was only 5%. The results suggested that the use of laser is in fact more beneficial for epoxidation of the mentioned monoterpenes. Herein, the authors [219] obtained with this green strategy a maximum

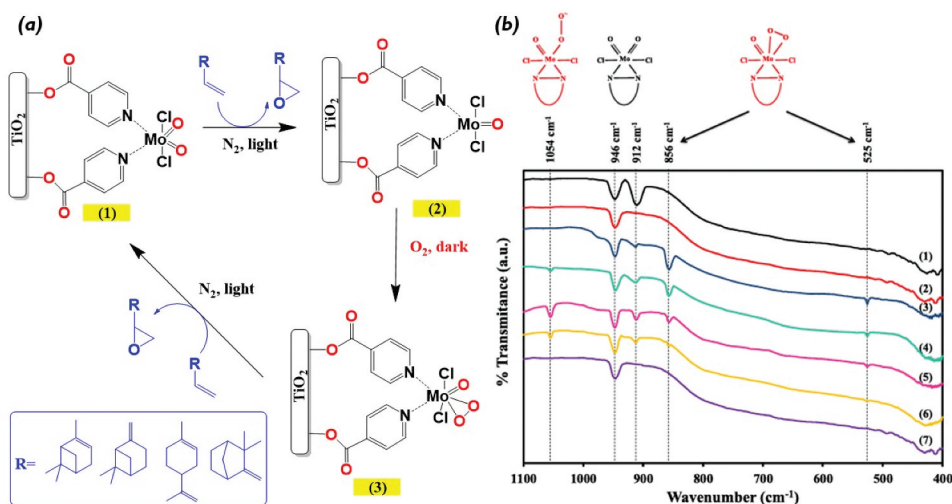


Figure 18. (a) Overall reaction pathways for the synthesis of epoxides from olefins using the dioxo-Mo (VI) anchored to TiO_2 , (b) Detection of the intermediates by using FTIR with ^{18}O labeling. Image b reproduced with permission from ref [227].

conversion of 62% with 99% selectivity to α -pinene epoxide but with longer times than previously reported. In addition, the proposed catalytic system was not robust due to the loss in the conversion decreasing from 62% in the fresh use to ca. 40% in the third cycle of use which made it not stable.

In the same way, the photo-assisted atom transfer to further synthesis of epoxides was performed (Table 10, *entry 14-17*) starting from renewable raw materials such as α -pinene, β -pinene, camphene and limonene. In this case, a mercury lamp with a smaller wavelength than reported in the previous research was used as the light source [220]. The same system, e.g.: dichloro-dioxo-bipy molybdenum (VI) complex (Bipy=2,2'-pyridine-4,4'-dicarboxylato) anchored on TiO_2 nanotubes was used as the catalytic material to achieve epoxidation. In this case, conversion of each monoterpene varied significantly due to i) reactivity of the olefin ii) the light source and power and iii) dispersion of the catalytically active units. The maximum conversion (87%) was achieved for α -pinene, whereas β -pinene was less active (conversion: 46%). Limonene and camphene were converted to similar values as α -pinene (75 and 65%, respectively). In some cases, the allylic oxidation products were obtained e.g.: verbenone, verbenol, myrtenal, and camphor, suggesting formation of oxygen radicals by interactions of molecular oxygen with the titanium dioxide support and also by the UV-Vis radiation as reported in [220] generating reactive oxygen species such as superoxide radical anions, hydroxyl radicals, etc.

Binary systems comprising TiO_2 and mesoporous silica nanoparticles and functionalized with hexadecyl chains or imidazolium groups were evaluated for the photo epoxidation of limonene using molecular oxygen as the

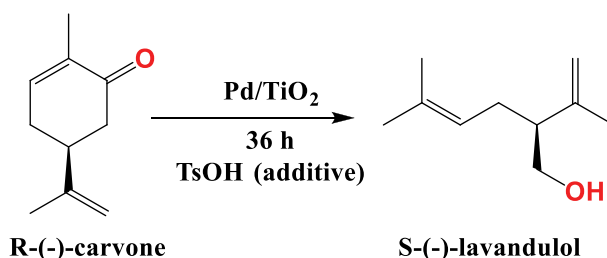


Figure 19. Schematic representation of the synthesis of S-(-)-lavandulol from R-(-)-carvone.

oxidizing agent (Table 10, entry 18-19). The use of Mn for the photocatalytic runs yields a very low conversion of limonene and selectivity to 1,2-limonene-epoxide, suggesting that Mn can act as a recombination center, and then decreasing the photo efficiency of the catalyst (not measured). The authors suggested that only the presence of composite TiO₂-SiO₂ in an optimum intermediate ratio can increase the selectivity of the desired epoxide. Higher exposure of TiO₂ gave lower catalytic activity in terms of epoxidation. As mentioned before, only TiO₂ can induce the hydroxyl radical-mediated oxidation therefore resulting in limonene overoxidation. The post modification with alkyl or imidazolyl groups can improve selectivity yielding up to almost 60% of selectivity at 120 min of the reaction. The highest selectivity at 180 min was achieved for both TSI and TSH composites having the same Ti-to-Si ratio, but with imidazolium groups (25 mol%) and C16 alkyl groups (25%), respectively. However, conversion of both of them reached poor values close to 60% and 30% (TSI and TSH, respectively). Although higher conversion values were not obtained with these materials, the surface functionalization can induce modification in the TiO₂-SiO₂ composite generating polarity changes and then favoring the surface-solvent-substrate interaction.

Similarly, that for titanium dioxide nanotubes and for Ga-containing MOFs (Table 10, entry 7-17), the Martinez-O's group designed, following the same concept, a dioxo-Mo complex over titanium dioxide analyzing the effect of different OH's groups on the surface of the support (Table 10, entry 20-25) and their catalytic activity in the oxygen atom transfer to further synthesis of α -pinene epoxide starting from renewable α -pinene. The amount of Mo anchored to different TiO₂ is directly related to the distribution, concentration, and different accessibility points of Ti-OH surface groups which, in fact, would depend on the preparation methodology of titania. In the same way, accessibility of such groups affects the epoxidation reaction of α -pinene giving significant differences in the conversion (ranging from 58 to 83%) but not in the selectivity to α -pinene epoxide (90–93%). The overall reaction mechanism proposed for these kinds of systems is illustrated in Figure 18. The first step (Figure 18a) is the coordination of the unsaturated terpene to the dioxo-molybdenum catalysts and then generating the intermediate (2). The latter

Table 10. Heterogeneous materials for the photocatalytic transformation of terpenes into high-added value chemicals.

Entry	Catalyst	Photocatalytic application	Reaction conditions	X (%)	S (%)	Ref
1	TiO ₂ NP* (450°C)	Selective hydrogenation of citral	40 mL anhydrous CH ₃ CN, 5 mL triethanolamine, 75 µL citral, 0.2 g catalyst, 20°C, 24 h, N ₂ atmosphere, 300 W Xe lamp light source.	99.0	62.3 Geraniol 37.7 Nerol	[218]
2	TiO ₂ NP* (500°C)			99.0	60.3 Geraniol 39.1 Nerol	
3	TiO ₂ NP* (250°C)			28.2	43.8 Geraniol 26.6 Nerol 29.6 Citronellal	
4	TiO ₂ NP* (600°C)			75.0	63.8 Geraniol 35.2 Nerol 1.0 Citronellal	
5	TiO ₂ NP* (700°C)			3.0	40.1 Geraniol 16.5 Nerol 43.4 Citronellal	
6	TiO ₂ NP* (800°C)			2.1	10.5 Geraniol 6.9 Nerol 82.6 Citronellal	
7	MoO ₂ Cl ₂ @COMOC-4	Epoxidation of α-pinene with molecular O ₂	Solution of the substrate in CH ₃ CN (1 × 10 ⁻² M) was deoxygenated by bubbling N ₂ for several hours, before the addition of the catalyst (30 mg), 19°C, 18 h, two immersion lamps (halogen lamp, λ = 467 nm; laser λ = 406 nm).	50 (467 nm)	99 Epoxide	[219]
8				62 (406 nm)	99 Epoxide	
9				35 (467 nm)	99 Epoxide	
10				40 (406 nm)	99 Epoxide	
11 ^a				33	99 Epoxide	
12 ^b	54	99 Epoxide				
13 ^c	60	83 Epoxide				
14	MoCl ₂ O ₂ Bipy/TiO ₂ -NT	Epoxidation of monoterpenes with molecular O ₂	10 mL of a substrate solution (1 × 10 ⁻² M), 15 mg of catalyst, CH ₃ CN as solvent, 19°C, atmospheric pressure, 18 h, mercury lamp (λ = 360 nm).	87 (α-Pinene)	90 Epoxide 8 Verbenone 2 Verbenol	[220]
15				46 (β-Pinene)	72 Epoxide 18 Myrtenal	
16				75 (R-Limonene)	85 1,2-Epoxides (cis and trans) 10 Diepoxide 5 Carvone	
17				65 (Camphene)	76 Epoxide 8 Camphor 16 Diol	
18	TiO ₂ /SiO ₂ -I**	Epoxidation of limonene with molecular O ₂	1 g/L of the catalyst was dispersed in an R-limonene solution (1.23 mM) in acetonitrile (10 mL). Oxygen was bubbled throughout for 10 min at room temperature. Then, the suspension under vigorous stirring, was irradiated using 6 fluorescent tubes (Philips, actinic lamps, 10 W each, at 365 nm), 3 h.	55	25 Epoxide	[221]
19	TiO ₂ /SiO ₂ -H**			35	35 Epoxide	

(Continued)

Table 10. (Continued).

20	MoCl ₂ O ₂ Bipy/TiO ₂ (P-25)	Epoxidation of α -pinene with molecular O ₂	Solution of the substrate in CH ₃ CN (1 x 10 ⁻² M) was deoxygenated by bubbling N ₂ for several hours, before the addition of the catalyst (15 mg), 19°C, 18 h, and UV-Vis light.	58	91 Epoxide 9 Ketone	[222]
21	MoCl ₂ O ₂ Bipy/TiO ₂ (HT-400)			63	93 Epoxide 7 Ketone	
22	MoCl ₂ O ₂ Bipy/TiO ₂ (SC-150)			67	91 Epoxide 9 Ketone	
23	MoCl ₂ O ₂ Bipy/TiO ₂ (NP)			72	93 Epoxide 7 Ketone	
24	MoCl ₂ O ₂ Bipy/TiO ₂ (NT from P-25)			77	92 Epoxide 8 Ketone	
25	MoCl ₂ O ₂ Bipy/TiO ₂ (NT from NP)			83	93 Epoxide 7 Ketone	
26	Pd/TiO ₂	Regio- and stereoselective hydrogenolysis of allylic alcohols to form unsaturated hydrocarbons	2 mmol intermediate diol, 15 mg Pd(5% wt.)/TiO ₂ , 2.5 mol % TsOH·H ₂ O, 5 mL CH ₃ OH, 36 h, Ar, 25°C, hv ($\lambda > 365$ nm)	88	56% (S)-(+)-lavandulol	[223]
27	HY-zeolite	Isomerization of α -pinene epoxide	0.5 g substrate, 10 mg catalyst, 2 mL dimethyl acetamide, 12 h, UV lamp (200-400 nm)	60	71 carveol 29 CA	[224]

NP: Nanoparticle * Value in parenthesis refers to the calcination temperature of the catalyst. **I:** refer to the functionalization of TiO₂/SiO₂ with 50 mol% of imidazolyl groups and **H** to the functionalization with 50 mol% of C16 alkyl groups. The solvent used in the photocatalytic reaction was dichloromethane, chloroform, and ethanol. **Bipy:** 2,2'-bipyridine-4,4'-dicarboxylic acid. **NT:** Nanotubes. **P-25:** Degussa P-25. **NP:** Sigma-Aldrich nanopowder. **HT:** Mesoporous TiO₂ support was prepared under hydrothermal conditions and CTAB-assisted. **SC:** Mesoporous TiO₂ support was prepared by sol-gel under supercritical CO₂.

in oxygen and dark can produce the oxo-peroxo adduct which was further confirmed using ¹⁸O labeling (Figure 18b). Finally, regeneration of the initial catalyst can be performed by donation of the intermediate (3) to another unsaturated terpene to yield a second epoxide molecule [227]. The green conditions applied for this strategy seem to be highly robust; however, the reaction time is longer than in other previous reports (>18 h), and especially when the catalyst is reused for several times. For this catalytic system, the reaction can take even 4 days to have the same conversion and selectivity as for the fresh one (96 h for the selected catalyst). The scope of the catalyst was also tested with other monoterpenes (β -pinene, limonene, and camphene), giving the corresponding epoxide as the major product. For limonene, the main product was 1,2-limonene epoxide rather than 8,9-limonene epoxide or even limonene di-epoxide.

Taking into advantage that light is a green renewable source for catalytic reactions, photocatalytic transfer hydrogenolysis of allylic

alcohol over Pd/TiO₂ was carried out at room temperature without stoichiometric generation of salt wastes. By this protocol, the synthesis of S-(-)-lavandulol from R-(-)-carvone can be performed avoiding additional steps. Lavandulol is an important intermediate and additive in perfumes and it can act as a defensive pheromone in the red-lined carrion beetle. Using light, the performance of the reaction starting from R-(-)-carvone achieved 88% conversion with 55% of selectivity to S-(-)-lavandulol (Figure 19). The very mild reaction conditions by using the selected Pd/TiO₂ and TsOH as the additive for 36 h can give selectively the desired product. Methanol can act as the hydrogen/electron donor, and the hole scavenger in photocatalysis, thereby showing together with the catalyst a direct route to useful synthesis of fine chemicals from renewable raw biomass.

Finally, HY zeolite together with light were employed for the selective synthesis of carveol and campholenic aldehyde from α -pinene epoxide. The results suggested that light plays a critical role in activating zeolite giving the acid proton and then isomerizing selectively to carveol. DMF as a polar basic solvent also favored synthesis of the respective alcohol over the aldehyde (Table 10, entry 27).

11. Coupling of monoterpenes with aldehydes: The Prins reaction

11.1. Acid transformation of terpenes with aldehydes: General considerations

Acid-catalyzed condensation of unsaturated hydrocarbons with carbonyl compounds was discovered in 1919 by the Dutch chemist Hendrik J. Prins [228] and is still a powerful tool in the synthesis of various functional compounds that, for example, are used in perfumery, as well as exhibiting various biological activities [228–230]. The Prins reaction is a versatile and convenient synthetic route for the preparation of oxygenated heterocyclic compounds, whose key step is the formation of an oxocarbenium ion that reacts with 1 equiv of the alkene in an intermolecular or intramolecular fashion [229]. Since the reaction often produces several products, their separation is carried out by distillation or column chromatography [230, 230].

The main source of renewable hydrocarbons is turpentine, which is produced annually in quantities of about 360,000 tons and contains α -pinene (40–85%), β -pinene (up to 35%), and 3-carene (up to 40%) [231]. Coupling of terpene hydrocarbons with formaldehyde (FA) allows one to obtain compounds containing a hydroxymethyl moiety, which are used in perfumery and as platform molecules for further synthesis [228,230,232].

11.2. Recent literature for the Prins-reaction of terpenes

Thus, during the catalytic condensation of β -pinene with FA (in the form of paraformaldehyde), nopol is formed (Figure 20a), which is produced on an industrial scale, has a woody aroma, and is used in perfume and cosmetic products [228,232]. The traditional catalyst for this reaction is ZnCl_2 , and in recent years, a number of studies have been published on the development of novel heterogeneous catalysts for the synthesis of nopol [233–244]. In the presence of Indian montmorillonite clay (MMT) impregnated with ZnCl_2 under optimized conditions, the selectivity for this product reached 97% with β -pinene conversion of 75%, which was comparable to the results on ZnCl_2 *per se*. (Table 11, entry 1-2). The original clay showed almost no catalytic activity [233].

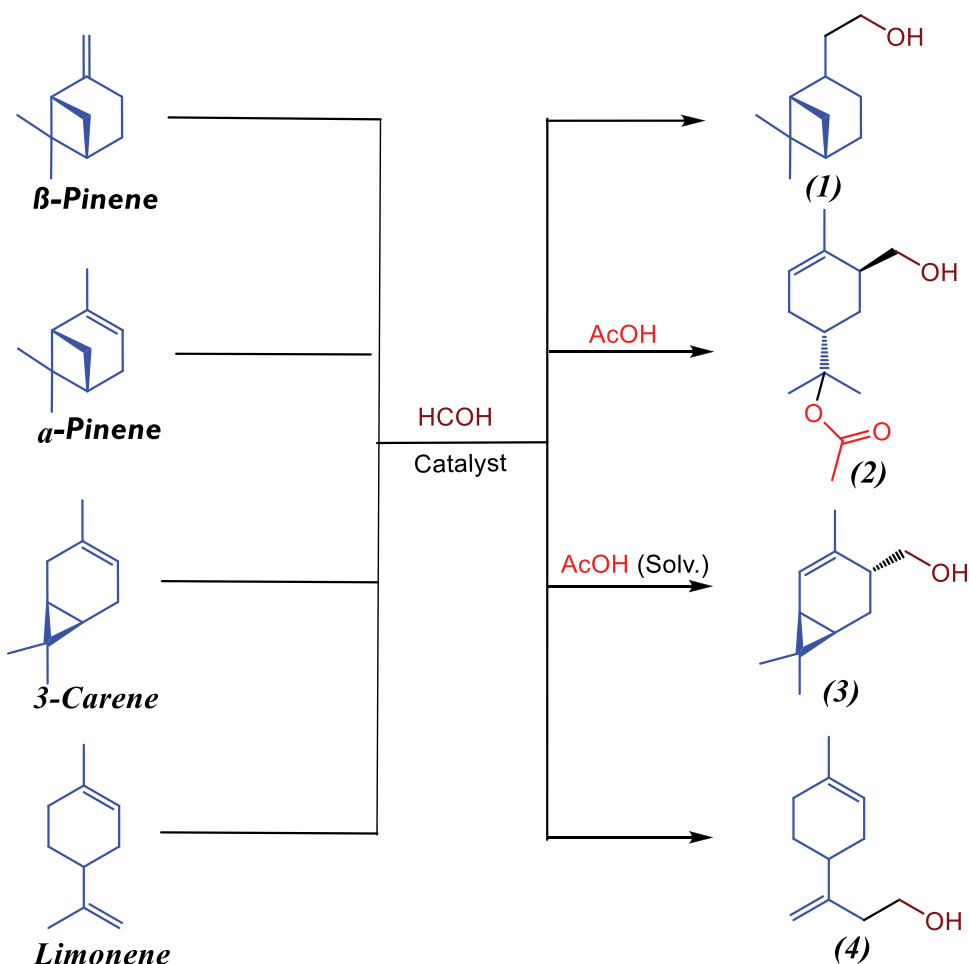


Figure 20. Examples of terpene hydrocarbons functionalization with hydroxymethyl groups. (1) Nopol, (2) 8-Acetoxy-6-hydroxymethyllimonene, (3) *Trans*-4-hydroxymethyl-2-carene, (4) Homolimonenol.

Table 11. Some relevant catalysts for the monoterpene compounds condensation with aldehydes.

Entry	Catalyst	Reactants	Reaction conditions	X (%)	S (%)	Ref.
1	ZnCl ₂ -MMT	β-pinene + FA (in form of para-formaldehyde)	5 mmol of substrate, 10 mmol of FA, 10 mL of acetonitrile, 0.1 g of catalyst, 80°C	75	97 Nopol	[233]
2	ZnCl ₂		5 mmol of substrate, 10 mmol of FA, 10 mL of acetonitrile, 0.136 g of catalyst, 80°C	95	93 Nopol	
3	SZ-1N		6 mmol of substrate, 18 mmol of FA, 0.15 g of catalyst (pretreated at 450°C), 80°C,	90	92 Nopol	[234]
4	SZ-1.5N		acetonitrile, substrate: solvent ratio 1:5, 9 h	92	95 Nopol	
5	SZ-2N			99	99 Nopol	
6	SZ-2N		6 mmol of substrate, 18 mmol of FA, 0.15 g of catalyst (pretreated at 450°C), 80°C, toluene, 9 h	40	88 Nopol 3 Nopyl acetate 9 Others	
7	SZ-2N		6 mmol of substrate, 18 mmol of FA, 0.15 g of catalyst (pretreated at 450°C), 80°C, 9 h, solvent-free	88	5 Nopol 95 Others	
8	Zn-Na-X		10 mmol of substrate, 20 mmol of FA, 20 wt. % catalyst, 90°C, 5 mL benzonitrile, 10 h	n.d.	66 Nopol	[237]
9	Zn-H-Y				84	
10	Zn-H-Beta				86	
11	Zn-H-ZSM-5				35	
12	Zn-H-MOR				18	
13	H-Beta				36	
14	Fe-Beta				35	
15	Mn-Beta				57	
16	K-Beta				43	
17	0.4 wt. % MoOx/γ-Al ₂ O ₃			60	83 Nopol 14 PIP	[238]
18	1 wt. % MoOx/γ-Al ₂ O ₃			70	87 Nopol 11 PIP	
19	9 wt. % MoOx/γ-Al ₂ O ₃			94	84 Nopol 12 PIP	
20	11 wt. % MoOx/γ-Al ₂ O ₃			96	86 Nopol 10 PIP	
21	20 wt. % MoOx/γ-Al ₂ O ₃			84	90 Nopol 7 PIP	
22	11 wt. % MoOx/γ-Al ₂ O ₃		5 ml cyclohexane as solvent	81	34	
23			Dichloromethane	100	40	
24			benzonitrile	82	89	
25			Acetonitrile	53	90	
26			DMSO	21	10	

(Continued)

Table 11. (Continued).

27	CuBTC		4 mmol of substrate, 8 mmol of FA, 0.2 g of catalyst, 80°C, acetonitrile, 6 h	n.d.	3 Nopol	[239]
28	FeBTC				27	
29	ZIF-8				9	
30	MIL-100(Fe)				82	
31	MIL-100(Cr)				64	
32	MIL-53(Al)				23	
33	USY				35	
34	BEA				28	
35	25wt%MoO ₃ -SiO ₂		10 mmol substrate, 20 mmol FA, 0.27 g catalyst, 80°C, benzonitrile, 24 h	77	99 Nopol	[240]
36	25wt%WO ₃ -SiO ₂			38	97	
37	25wt%ZnO-SiO ₂		Similar, 0.54 g of catalyst	78	96	
38	Sn-MCM-41-T		0.5 mmol of substrate, 1 mmol of FA, 1 mL ethyl acetate, 90°C, 2 h	65	98 Nopol	[241]
39	Sn-MCM-41-S			64	98 Nopol	
40	Sn/MCM-41	Turpentine oil (11% β-pinene) + FA	0.5 mmol of β-pinene, 1 mmol FA, 25 wt.% of catalyst, turpentine as solvent, 24 h.	69	96 Nopol	[235]
41	Sn/MCM-41	Turpentine oil (40% β-pinene) + FA	0.8 mmol of β-pinene, 1 mmol of FA, 12 mg of catalyst, 0.25 mL ethyl acetate, 90°C,	92	93 Nopol	[236]
42	HNT(halloysite nanotube)-HCl	α-Pinene + FA (in form of para-formaldehyde)	7.1 mmol of substrate, 14.2 mmol of FA, 1 g of catalyst, 12 mL of AcOH, 25°C	50	11 HML-Ac 33 TP-Ac 29 WMP	[245]
43	HNT-H ₃ PO ₄				12 HML-Ac 34 TP-Ac 28 WMP	
44	H-Beta-25				4 HML-Ac 21 TP-Ac 35 WMP	
45	H ₃ PO ₄		Similar, 2 eq of catalyst		20 HML-Ac 29 TP-Ac 14 WMP	
46	H ₃ PO ₄		Similar, 2 eq of catalyst, 8°C	46	24 HML-Ac 27 TP-Ac 15 WMP	
47	ZnCl ₂	3-Carene + FA (in form of para-formaldehyde)	7.1 mmol of substrate, 14.2 mmol of FA, 1 eq of catalyst, 6 mL of AcOH, 1 mL Ac ₂ O, 15°C, 120 min	50	8 HM2C 50 IBF 16 AcP	[246]
48	HNT-H ₃ PO ₄		Similar, 1 g of catalyst, 360 min	24	5 HM2C 26 IBF 45 AcP	
49	K-10			34	9 HM2C 30 IBF 40 AcP	
50	H ₃ PO ₄		Similar, 1 eq of catalyst, 105 min	50	50 HM2C 15 IBF 12 AcP	
51			Similar, 2 eq of catalyst, 45 min	50	60 HM2C 14 IBF 10 AcP	
52			Similar, 2 eq of catalyst, 21.3 mmol of FA, 35 min	50	66 HM2C 12 IBF 9 AcP	

(Continued)

Table 11. (Continued).

53	Sn-MCM-41	Limonene + FA (in form of para-formaldehyde)	FA: limonene molar ratio of 2:1, 0.75 mL of solution (0.62 M) in ethyl acetate, 18 mg of catalyst, 90°C, 24 h	19	89	homolimonelol [247]
54	Sn-KIT-6			21	88	
55	Sn-SBA-15	26	90			
56	20%HPW/SiO ₂	Limonene + crotonaldehyde	1 mmol of substrate, 3 mmol of aldehyde, 10 mg of catalyst, 1,2-dichlorethane, 50°C, 5 h	68	92	OBN [248]
57			Similar, 60°C	90	90	
58	CsPW		50°C	52	90	
59			70°C	83	86	
60	20%HPW/SiO ₂	α-Pinene + crotonaldehyde	1 mmol of substrate, 4.5 mmol of aldehyde, 25 mg of catalyst, 1,2-dichlorethane, 25°C, 1 h	96	82	
61		β-Pinene + crotonaldehyde		100	83	
62	HPW/SiO ₂	Limonene + cuminaldehyde	1 mmol of substrate, 3 mmol of aldehyde, 15 mg of catalyst, 1,2-dichlorethane, 40°C, 8 h	80	82	OBN 10 MD [249]
63	CsPW		Similar, 30 mg of catalyst, 60°C 3 h,	100	85	OBN 13 MD
64	HPW/SiO ₂		1 mmol of substrate, 3 mmol of aldehyde, 20 mg of catalyst, diethylcarbonate, 60°C, 8 h	91	82	OBN 16 MD
65	CsPW		Similar, 30 mg of catalyst, 9 h	70	85	OBN 12 MD
66	HPW/SiO ₂	α-Pinene + cuminaldehyde	Similar, 15 mg of catalyst, diethylcarbonate 50°C 2 h	100	75	OBN 22 MD
67	CsPW		Similar, 2 h	99	61	OBN 25 MD
68		α-Terpineol + cinnamaldehyde	Similar, 10 mg of catalyst, 70°C, 5 h	95	85	OBN 12 MD
68		Nerol + cinnamaldehyde	Similar, 30 mg of catalyst, 60°C, 3 h	100	62	OBN 19 MD
69	HPW	Limonene + benzaldehyde	1 mmol of substrate, 1 mmol of aldehyde, 50°C, 5 h	99	80	OBN [201]
70	HPW/SiO ₂			99	70	
71	HPW/P-25			92	72	
72	HPW/TiO ₂			40	50	
73	HPW/SBA-15			91	60	
74	HPW/Al ₂ O ₃			3	0	
75	K-10	2-Carene + 4-methoxybenzaldehyde	3.68 mmol of substrate, 3.38 mmol of aldehyde, 2.5 g of catalyst, solvent-free, RT, 1.5 h	78	31	IBF 5 OBN (isolated yield) [250]
76		2-Carene + vanillin aldehyde	2.94 mmol of substrate, 2.36 mmol of aldehyde, 2.5 g of catalyst, solvent-free, RT, 2 h	77	33	IBF 4 OBN (isolated yield)

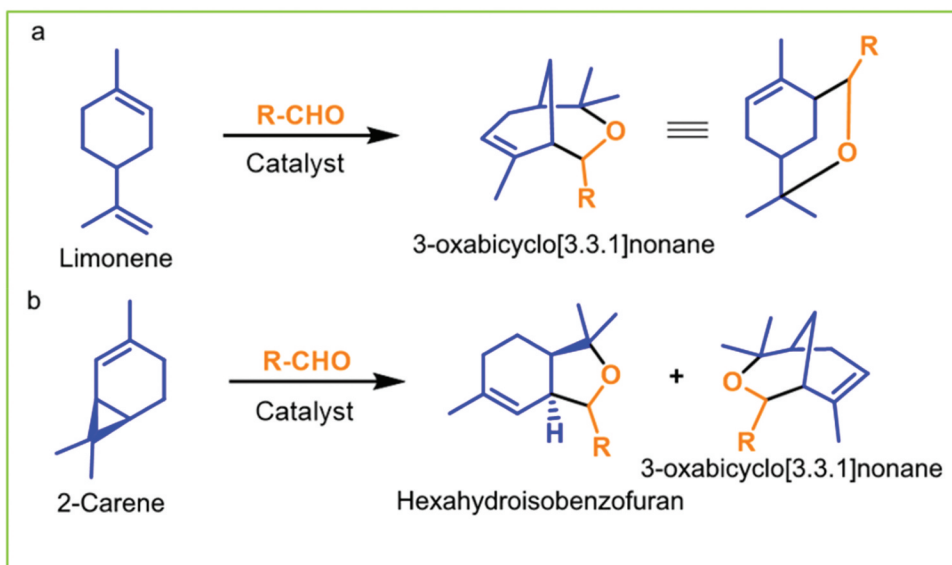
(Continued)

Table 11. (Continued).

77	HNT-HCl	2-Carene + 4-methoxybenzaldehyde	0.71 mmol of substrate, 0.71 mmol of aldehyde, 1 g of catalyst, cyclohexane, 50°C, 2 h	60	71 IBF 1 OBN	[251]
78	K-10		Similar, 3 h		52 IBF 2 OBN	
79	Amberlyst-15		2 h		3 IBF 13 OBN	
80	Scandium triflate		3 h	20	16 IBF 4 OBN	
81	K-10	2-carene containing reaction mixture	1 g of mixture (15% of 2-carene), 0.4 g of vanillin, 1.5 g of catalyst, RT, 20 h	89	60 IBF 7 OBN	[252]
82	K-30	obtained by 3-carene isomerization + vanillin		92	49 IBF 3 OBN	
83	Illite L-1			96	51 IBF 1 OBN	
84	HNT-HCl	Similar, 4-methoxybenzaldehyde	1 g of mixture (15% of 2-carene), 1 eq of aldehyde, 1 g of catalyst, cyclohexane, 50°C, 6 h	50	71 IBF 1 OBN	[250]

PIP: β -pinene isomerization products. **HML-Ac:** 8-acetoxy-6-hydroxymethylimonene. **TP-Ac:** terpinyl acetate; **WMP:** Wagner–Meerwein rearrangement products (borneol derivatives). **HM2C:** *trans*-4-hydroxymethyl-2-carene. **IBF:** isobenzofurans. **AcP:** acetylation products (*trans*-4-hydroxymethyl-2-carene acetate and its derivative). **OBN:** 3-oxabicyclo[3.3.1]nonene, MD: menthadienes

In [234], the catalysts based on sulfated zirconia (SZ) containing different amounts of sulfur were synthesized by two-stage precipitation and impregnation methods. The material obtained by impregnating $Zr(OH)_4$ with a 2N

**Figure 21.** Examples of limonene (a) and 2-carene (b) condensation with aldehydes.

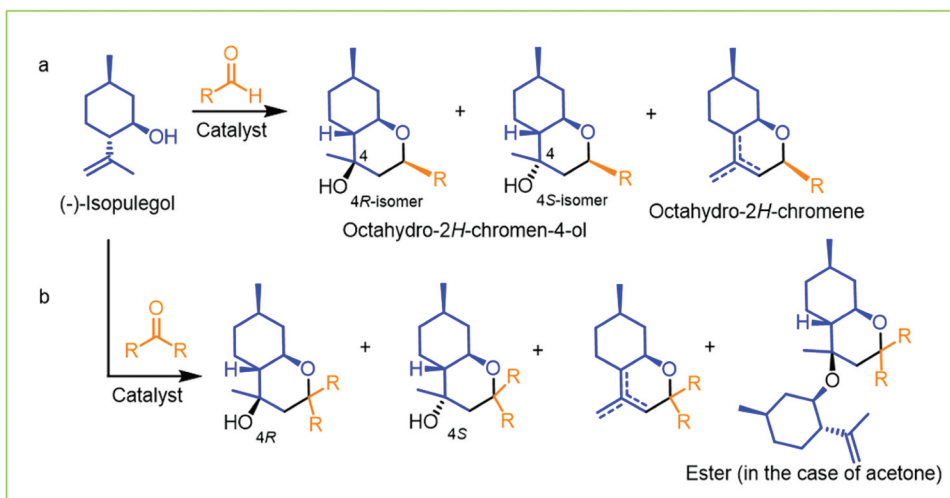


Figure 22. A scheme of (-)-isopulegol condensation with aldehydes (a) and ketones (b) carbonyl compounds to substituted octahydro-2*H*-chromenes.

solution of sulfuric acid was active (conversion >99%) with selectivity for nopol of *ca.* 99% in acetonitrile (Table 11, entry 5). The catalyst could be reused for up to five cycles with a negligible loss of activity and unchanged selectivity. A mechanism for nopol formation has been proposed, which involves the participation of both Lewis and Brønsted sites on the surface of SZ. Selectivity decreased when toluene was used, while practically no nopol was formed without the solvent (Table 11, entry 6-7).

Utilization of metal ion-exchanged zeolites as highly active and selective catalysts for the nopol synthesis was reported in [237]. The Zn-beta catalyst displayed the best performance among different types of solids with 86% of the desired product yield (Table 11). Acidity of the Zn-beta zeolite was correlated with the amount of zinc and activity of the reaction. For different metal ion-exchanged Beta catalysts, the yield of the desired product increased with a decrease in Brønsted to Lewis acidity (B/L) ratio. Thus, increasing the Zn loading into Beta zeolite from 0.14 to 0.57 mmol/g made it possible to increase selectivity to nopol to 94% due to decreasing of B/L from 0.45 to 0.07 [185]. At low amounts of Zn, selectivity was limited to formation of β -pinene isomerization products, apparently occurring at Brønsted acid sites.

An effective catalyst for the synthesis of nopol via the Prins reaction is also molybdenum oxide/ γ -alumina (MoOx/ γ -Al₂O₃) [238]. These solids with different Mo loading were synthesized by the impregnation method and carefully characterized. The total surface acid density of MoOx/ γ -Al₂O₃ increased with an increase in MoOx loading till to 11 wt %, which led to an increase in both β -pinene conversion and selectivity for the target product, while the amount of substrate isomerization products decreased (Table 11, entry 17 – 20). It has been shown that solvents with acceptor and donor number values from 10 to

20 (such as acetonitrile and benzonitrile) promote the desired condensation. The authors suggested that weak Brønsted and Lewis acidity in the catalyst contribute to the nopol formation, while on strong Brønsted acids the isomerization of β -pinene occurs [238].

The catalytic properties of a number of metal-organic frameworks (MOFs) such as CuBTC, FeBTC, MIL-100(Fe), MIL-100(Cr), ZIF-8, and MIL-53(Al) were studied in the condensation of β -pinene with formaldehyde (Table 11 entry 27 – 32 [239]). Activity of the investigated solids increased with the increasing concentration of accessible Lewis acid sites being the largest for MIL-100(Fe). In the presence of USY and BEA zeolites, the yield of nopol did not exceed 35% (Table 11, entry 33 – 34) due to isomerization of the substrate at strong Brønsted sites, which is similar to the conclusions made in [237,238]. The best catalyst, MIL-100(Fe), showed stability over three cycles without loss of activity.

Several metal (Mo, W and Zn) modified SiO_2 solids were prepared by the wetness impregnation method and tested in nopol synthesis [240]. Materials with 25 wt% of MoO_3 or ZnO loading on SiO_2 demonstrated both high activity and selectivity (up to 99%, Table 11, entry 35–37) toward nopol. Possibility of catalyst regeneration was also shown.

In [241], the reaction of β -pinene with FA was studied in the presence of Sn-modified MCM-41 obtained using traditional tetraethyl orthosilicate (TEOS) and cheaper Colombian sodium silicate as silicon sources. Materials with Na_2SiO_3 (Sn/MCM-41-S) showed crystalline, textural, and structural properties very similar to MCM-41 synthesized with TEOS (Sn/MCM-41-S). Solids obtained by both methods demonstrated high selectivity (up to 98%) at terpene conversion of *ca.* 65% after 2 h (Table 11, entry 38 – 39). It has also been shown that paraformaldehyde with a higher degree of polymerization is less active in the Prins reaction because of a lower rate of depolymerization.

Kinetics of β -pinene condensation with FA in ethyl acetate and toluene was studied with Sn/MCM-41 [242]. The largest adsorption constant for nopol with respect to the reactants allows to explain experimentally observed strong inhibition effect of this compound. Higher selectivity in ethyl acetate can be explained by better solubility of paraformaldehyde compared to that in toluene. The reaction proceeded with an apparent activation energy of 98 kJ/mol. The same research group recently demonstrated the feasibility of producing nopol over Sn/MCM-41 immobilized in a wall-coated microreactor using formaldehyde generated *ex-situ* [243]. The reaction rate equation is obtained from a reaction pathway based on the Langmuir-Hinshelwood formalism with dual sites and desorption of the product as a limiting step.

An assessment of the environmental impact of nopol synthesis showed that the impact of the solvent is most significant, and the use of ethyl acetate is beneficial. The carbon footprint for nopol catalytic synthesis from β -pinene was 13.0 and 37.4 kg CO_2 -eq for the system with solvent recirculation and

Table 12. Some relevant catalysts for the monoterpene condensation with carbonyl compounds.

Entry	Catalyst	Reactants	Reaction conditions	X (%)	S (%)	Ref.
1	H-K10	(-)-Isopulegol + different aldehydes	1 mmol of substrate, 1.2 mmol of aldehyde, 20 wt.% of catalyst, microwave radiation for 3 min, solvent-free	n.d.	50–84% OCh-ol (isolated yield) 4R/4S up to 20	[267]
2	H-Beta-25	(-)-Isopulegol + benzaldehyde	0.04 mol L ⁻¹ of isopulegol, benzaldehyde as solvent and reagent, 0.3 g of catalyst, 70°C, 120 min	100	74 OCh-ol 14 OCh	[268]
3	H-Beta-150			100	66 OCh-ol 20 OCh	
4	H-Beta-300			100	75 OCh-ol 7 OCh	
5	Fe-Beta-150			76	56 OCh-ol 25 OCh	
6	Au-Beta-25			90	67 OCh-ol 25 OCh	
7	Ce-Beta-150			100	18 OCh-ol 67 OCh	
8	Ce-MCM-41			100	5 OCh-ol 93 OCh	
9	M-HCl	(-)-Isopulegol + vanillin	0.65 mmol of substrate, 0.65 mmol of aldehyde, 100 mg of catalyst, 4 mL of toluene, 35°C, 2h	76	74 OCh-ol 4R/4S 5.7	[269]
10	K-HCl		Similar, 50°C	30	77 OCh-ol 4R/4S 6.2	
11	MK-HCl			26	90 OCh-ol 4R/4S 7.0	
12	K-10	(-)-Isopulegol + heteroaromatic aldehydes	0.3 – 0.4 g of substrate, 1 eq of aldehyde, 1 – 1.6 g of catalyst, solvent-free, RT	n.d.	50 – 86% (isolated yield) 4R/4S up to 10	[264]
13	Treated by HCl illite L-1	(-)-Isopulegol + thiophene-2-carbaldehyde	0.4 g of substrate, 1 eq (0.29 g) of aldehyde, 0.69 g of catalyst, solvent-free, 25°C, 1 h	99	82 OCh-ol 8 OCh 4R/4S 4.9	[270]
14	K-10			99	79 OCh-ol 8 OCh 4R/4S 4.3	
15	Treated by HCl glauconite		93	78	OCh-ol 9 OCh 4R/4S 4.4	
16	Treated by HCl illite L-1		Similar, in cyclohexane (0.26 mol/l), 20°C, 9 h	50	86 OCh-ol 9 OCh 4R/4S 5.7	
17			Similar, 40°C, 1 h		86 OCh-ol 9 OCh 4R/4S 5.7	
18		Similar, 60°C, 0.2 h	79 OCh-ol 14 OCh 4R/4S 5.8			

(Continued)

Table 12. (Continued).

19	HNT-HCl, air-dry	(-)-Isopulegol +thiophene- 2-carbaldehyde	0.4 g of substrate, 1 eq (0.29 g) of aldehyde, 0.69 g of catalyst, solvent-free, 25°C, 1 h	83	92 OCh-ol 4 OCh 4R/4S 6.5	[271]
20	HNT-HCl, dried at 105°C			98	85 OCh-ol 6 OCh 4R/4S 5.4	
21	HNT-HCl, dried at 200°C			99	78 OCh-ol 8 OCh 4R/4S 3.9	
22	HNT-HCl, dried at 350°C			95	76 OCh-ol 7 OCh 4R/4S 3.6	
23	HNT-HCl, air-dry	(-)-Isopulegol + different aldehydes	Similar, in cyclohexane (0.26 mol/l), 20°C	50	78 – 94 OCh-ol 3–8 OCh 4R/ 4S 7.6– 14.5	
24	HNT-HCl air-dry	(-)-Isopulegol +thiophene- 2-carbaldehyde	0.4 g of substrate in cyclohexane (0.5 mol/L), 1 eq (0.29 g) of aldehyde, 0.69 g of catalyst, 40°C, 6 h	99	91 OCh-ol 6 OCh 4R/4S 6.8	[272]
25	K-10 air-dry		Similar, 3 h		82 OCh-ol 11 OCh 4R/4S 4.3	
26	K-30 air-dry		Similar		82 OCh-ol 11 OCh 4R/4S 4.4	
27	Amberlyst- 15, dried at 110°C		Similar, 0.35 g of catalyst, substrate concentration of 0.09 mol/L, 1.5 h	60	31 OCh-ol 68 OCh 4R/4S 3.0	
28	Scandium triflate		Similar, in CH ₂ Cl ₂ (0.5 mol/L) 20°C, 5 mol. % of catalyst, 3 h		45 OCh-ol 39 OCh 4R/4S 3.4	
29	K10-CSA	(-)-Isopulegol + benzaldehyde	0.013 mol/L of substrate in benzaldehyde, 0.1 g of catalyst, 30°C, 1 min	90	70 OCh-ol 4R/4S 3.6	[273]
30	K10-CSP		Similar, 60 min		95 OCh-ol 4R/4S 5.5	
31	HNT-CSA		Similar, 70°C, 240 min		82 OCh-ol 4R/4S 4.0	
32	HNT-CSP		Similar		35 OCh-ol 4R/ 4S 11.5	
33	H-Beta-24 h-S-15		0.013 mol/L of substrate in benzaldehyde, 0.1 g of catalyst, 30°C	65	88 OCh-ol 12 OCh 4R/4S 7.6	[274]
34	H-Beta-12 h-R-150				90 OCh-ol 10 OCh 4R/4S 7.1	
35	H-Beta-17 h-R-150				91 OCh-ol 9 OCh 4R/4S 6.6	
36	H-Beta-24 h-R-150				83 OCh-ol 17 OCh 4R/4S 7.4	

(Continued)

Table 12. (Continued).

37	H-K-10	(-)-Isopulegol + different aldehydes	0.3 – 0.9 g of substrate, 1 eq of aldehyde, 0.5 – 1 g of catalyst, solvent-free, RT	n.d.	17 – 57 OCh-ol 31–59 OCh 4R/ 4S 3.0 – 17.0	[275]
38	HNT	(-)-Isopulegol +acetone	0.9 g of substrate, 2 eq of ketone, 0.9 g of catalyst, solvent-free 30°C, 30 min	50	77 OCh-ol 13 Och 10 Ether 4R/4S 8.2	[276]
39	K-10		Similar, 180 min		75 OCh-ol 15 Och 9 Ether 4R/4S 8.0	
40	Amberlyst-15		Similar, 3 min	50	67 OCh-ol 32 Och 1 Ether 4R/ 4S 13.6	
41	Scandium triflate		Similar, 5 mol. % of catalyst, in CH ₂ Cl ₂ , 180 min	70	16 OCh-ol 79 Och 1 Ether 4R/4S 22	
42	K10-CSA		Substrate in 25 mL of acetone (0.013 mol/L), 50 mg of catalyst, 30°C, 4 h	85	83 OCh-ol 17 Och 0 Ether 4R/4S 3.3	[277]
43			Similar, 0.052 mol/L	100	88 OCh-ol 12 Och 0 Ether 4R/4S 4.1	
44			Similar, 0.52 mol/L, 25°C	87	83 OCh-ol 11 Och 6 Ether 4R/4S 7.6	
45	K10-CSP		Similar, 0.013 mol/L	72	67 OCh-ol 33 Och 0 Ether 4R/4S 6.2	
46			Similar, 0.52 mol/L	30	78 OCh-ol 24 Och 6 Ether 4R/4S 6.7	
47	HB-1		Substrate in 50 mL of acetone (0.013 mol/L), 50 mg of catalyst, 30°C, 4 h	45	69 OCh-ol 33 Och 4R/ 4S 10.5	[278]
48	HB-2			47	66 OCh-ol 34 Och 4R/ 4S 11.1	
49	HB-3			35	61 OCh-ol 39 Och 4R/4S 8.5	
50	HB-4			52	65 OCh-ol 35 Och 4R/ 4S 10.8	
51	HB-5			38	65 OCh-ol 35 OCh 4R/ 4S 10.0	

(Continued)

Table 12. (Continued).

52	K-10	Diol + aromatic aldehydes	0.7 – 0.8 g of substrate, 1 eq of aldehyde, 3–3.5 g of catalyst, solvent-free, RT	n.d.	14–39 HCh-diol 7 HCh 4S/4R 1.3–3.0	[279]
53		Diol + aliphatic aldehydes	0.18 – 0.2 g of substrate, 1 eq of aldehyde, 0.15–0.6 g of catalyst, solvent-free, RT		34–80 HCh-diol n.d. HCh 4S/4R 1.0–3.0	[280]
54	H-Beta-25	Diol + benzaldehydes	0.04 mol L ⁻¹ of substrate, benzaldehyde (40 mL) as solvent and reagent, 10 mL of toluene, 0.3 g of catalyst, 70°C, 120 min (selectivity data at 90% conversion)	99	67 HCh-diol 4 HCh 7 BD	[268]
55	H-Beta-150			98	64 HCh-diol 4 HCh 8 BD	
56	H-Beta-300			81	64 HCh-diol 2 HCh 6 BD	
57	Fe-Beta-150			78	64 HCh-diol 7 HCh 7 BD	
58	Ce-MCM-41			92	67 HCh-diol 9 HCh 3 BD	
59	HNT-HCl	Diol + decanal	0.3 g (1.68 mmol) of substrate in toluene (0.34 mol/L), 1 eq of aldehyde, 0.56 g of catalyst, 40°C, 240 min	70	77 HCh-diol 23 HCh 4S/4R 1.6	[281]
60	Illite-HCl		Similar, 360 min		76 HCh-diol 24 HCh 4S/4R 1.0	
61	K-10		Similar, 180 min		78 HCh-diol 22 HCh 4S/4R 0.8	
62	Amberlyst-15		Similar, 5 min		10 HCh-diol 69 HCh 4S/4R 0.9	
63	Scandium triflate		Similar, in CH ₂ Cl ₂ , 20°C, 240 min	100	37 HCh-diol 60 HCh 4S/4R 2.3	
64	H-Beta-25	Verbenol epoxide + aldehydes	0.303 g of substrate, 2 eq of fluorobenzaldehyde, 150 mg of catalyst, 50 mL of ethyl acetate, 70°C, 120 min	100	1 BD 21 Diol	[282]
65			Similar, 5 eq of fluorobenzaldehyde, 300 mg of catalyst, 50 mL of toluene		13 BD 0 Diol	
66	Fe-Beta-150		Similar, 5 eq of benzaldehyde		9 BD 10 Diol	
67			Similar, 5 eq of fluorobenzaldehyde		10 BD 24 Diol	
68	H-Beta-150		Similar, 133 eq of benzaldehyde		40 BD 8 Diol	
69	Fe-H-Beta-150		Similar		46 BD 12 Dio	

OCh-ol: octahydro-2H-chromen-4-ol. **OCh:** octahydro-2H-chromenes. **HCh-diol:** hexahydro-2H-chromene-4,8-diols. **HCh:** hexahydro-2H-chromenes. **BD:** benzodioxin compounds.

without recirculation, respectively [244]. Nopol can also be obtained from turpentine containing β -pinene [235,236]. Thus, the Prins reaction was studied using turpentine with the substrate content of 11% on Sn/MCM-41 [235]. Performing multifactor optimization using response surface plots made it possible to establish optimal parameters that ensured selectivity for nopol of 96% (Table 11, entry 40). Note that other terpene hydrocarbons *per se* (α -pinene, 3-carene, and camphene) did not react with FA under the reaction conditions. When using raw materials with 40% β -pinene content on a similar catalyst, high selectivity to the target product was also observed (93%, Table 11, entry 41). Presence of turpentine also makes it possible to significantly reduce the amount of the solvent [236].

α -Pinene, unlike the β -isomer, contains an endocyclic double bond (Figure. 20b), which is obviously less active in the Prins reaction. Under conditions of acid catalysis, α -pinene undergoes direct protonation with ring opening, as well as the Wagner-Meerwein rearrangements with expansion of the bicyclic framework [231,232]. These structural features are obviously the reason for the lack of progress in the synthesis of hydroxymethyl derivatives of this terpene.

More recently, catalytic condensation of (-)- α -pinene with formaldehyde in acetic acid into a novel terpenoid 8-acetoxy-6-hydroxymethylimonene (Figure 20) has been studied [245]. Common Lewis and Brønsted acids catalyzed the desired condensation although selectivity did not exceed 24% in the case of phosphoric acid due to the side reactions. On acid-modified halloysite nanotubes with weak acidity (45 $\mu\text{mol/g}$), the products of a direct substrate protonation (such as terpinyl acetate) were predominantly formed (Table 11, entry 42 – 43). In the presence of strongly acidic H-Beta-25 (301 $\mu\text{mol/g}$) and phosphoric acid, selectivity to α -pinene addition products with formaldehyde and substrate direct protonation were comparable [245]. However, with H_3PO_4 the content of products formed via the Wagner-Meerwein rearrangement (borneol derivatives) was the smallest (14–15%) giving subsequently the largest selectivity to the desired 8-acetoxy-6-hydroxymethylimonene (up to 24%, Table 11, entry 46). According to DFT calculations in the presence of H_3PO_4 , there are no significant differences (83–85 kJ/mol) between the energies of the intermediates formed due to the addition of formaldehyde to α -pinene and its direct protonation correlating with activation energies for the formation of the target product and terpinyl acetate (78–82 kJ/mol). Synthesis was carried out on a scale up to 25 g. Obtained terpenoid can be considered as a new chiral platform for further synthesis.

The reaction of 3-carene with formaldehyde produces *trans*-4-hydroxymethyl-2-carene as one of the products (Figure 20c). The classic two-step synthesis of this terpenoid involves boiling the starting terpene with FA in acetic acid and subsequent saponification of the resulting acetate [253]. *Trans*-4-hydroxymethyl-2-carene has a flower odor with a fruit note and

has been commercialized by the perfume company Dragoco [254]. In addition, it is the precursor for the preparation of a number of chiral heterocyclic compounds [246,255,256], some of which have high cytotoxic activity [255].

A comprehensive study of the one-pot catalytic condensation of 3-carene with FA to *trans*-4-hydroxymethyl-2-carene was carried out in the recent study [257]. It has been shown that traditional Brønsted and Lewis acids, as well as aluminosilicates, are able to catalyze the reaction in AcOH, however, selectivity to the target product is limited due to side acetylation and addition of a second formaldehyde molecule.

Compounds of further condensation with FA (isobenzofurans) are mainly formed in the presence of Lewis acids (such as ZnCl_2), giving up to 50% yield (Table 11, entry 47), while weak to moderate acidic halloysite and K-10 (45–104 $\mu\text{mol/g}$) result in a low conversion of 3-carene with a prevalence of acetylation products (up to 45%) [257]. The largest selectivity toward *trans*-4-hydroxymethyl-2-carene at conversion of 50% was observed with phosphoric acid (50–66%). The yield of the desired terpenoid increased significantly with an excess of FA or catalyst loading (Table 11, entry 50–52), because the amount of the active form of formaldehyde is the key factor in the reaction. The DFT calculations show that further transformations of the desired terpenoid are energetically favorable in agreement with the experimental data [257]. The apparent activation energy is 76 kJ/mol, which is lower than in the case of α -pinene condensation with FA (84 kJ/mol [245]), as well as a similar reaction of β -pinene on Sn-MCM-41 (98 kJ/mol [242]) in ethyl acetate.

Limonene undergoes a Prins reaction with FA, resulting in the formation of the corresponding carbinol, also called homolimonelol (Figure 20d) [228,247]. This compound is used in perfumes and cosmetic products, and also finds application in organic synthesis [247]. Early works proposed a number of methods for its preparation, including thermal condensation at 180°C [258], or in the presence of SnCl_4 in methylene chloride [259].

A recent study [247] reported the utilization of Sn-modified mesoporous silicates MCM-41, SBA-15, and KIT-6 for the synthesis of homolimonelol at 90°C in ethyl acetate. The materials contained mainly Lewis acid sites due to the presence of Sn^{4+} on their surface, which determined the catalytic activity. Solid Sn-SBA-15 showed the highest activity (26% limonene conversion) with a homolimonelol selectivity of 90% (Table 11, entry 55). The reaction was scaled up to a 200 ml reactor, and the catalyst could be used five times without a loss of activity [247].

Limonene is also capable of reacting with aliphatic and aromatic aldehydes involving both double bonds, resulting in the formation of heterocyclic compounds with a 3-oxabicyclo[3.1.1]nonane structure [201,248,249,260]. The synthesis of this compound was first described in the presence of natural bentonite clay in work [260].

The condensation of limonene with crotonaldehyde using silica-supported tungstophosphoric heteropoly acid $\text{H}_3\text{PW}_{12}\text{O}_{40}$ (HPW) and its acidic salt $\text{Cs}_{2.5}\text{H}_{0.5}\text{PW}_{12}\text{O}_{40}$ (CsPW) as solid catalysts in dichloroethane resulted in the formation of 3-oxabicyclo[3.3.1]nonene products in a high selectivity (86–90%, [Table 11](#), [entry 56–59](#)). Utilization of α - and β -pinenes as substrates on HPW/ SiO_2 also yielded in similar products ([Table 11](#), [entry 60–61](#)), indicating that protonation of both pinenes and limonene produces a *p*-menthenyl cation as an intermediate, which further reacts with aldehyde.

In addition to limonene and pinenes, α -terpineol and nerol were used as substrates, and benzaldehyde, crotonaldehyde as well as cuminaldehyde and *trans*-cinnamaldehyde were used as aldehydes. Condensations were carried out on HPW/ SiO_2 and CsPW in green solvents particularly 2-methyltetrahydrofuran, dimethylcarbonate and diethylcarbonate, leading to 3-oxabicyclo[3.3.1]nonene products in good to excellent yields. Some quantitative results are given in [Table 11](#), [entry 62–68](#).

In [201], the limonene condensation with benzaldehyde in the presence of HPW supported on SiO_2 , TiO_2 , SBA-15, and P-25 oxides was studied ([Table 11](#), [entry 69–74](#)). Among these materials, the HPW/P-25 system, which has high activity, turned out to be the most selective to oxabicyclo[3.3.1]nonene (72%). By varying the reaction conditions, it was possible to improve the yield to 80%. The synthesis was carried out on a scale up to 10 g.

The terpene hydrocarbon 2-carene under heterogeneous catalysis conditions (montmorillonite K-10) reacts with aldehydes to form hexahydroisobenzofuran, as well as oxabicyclo[3.3.1]nonene compounds ([Fig. 21](#), [Table 11](#), [entry 75–76](#) [250]). In this case, the cyclopropane ring is involved in the isobenzofuran fragment formation, apparently due to its conjugation with the double bond, whereas in the case of condensation of 3-carene with FA, isobenzofuran moiety is formed due to the addition of a second FA molecule [257].

Later, the reaction of 2-carene with 4-methoxybenzaldehyde was studied as a model for the bioactive chiral hexahydroisobenzofurans production in over a number of acidic aluminosilicates [251]. It was shown that the selectivity for these products increased with decreasing a.s. concentration in the catalyst being the highest (71%) on modified by HCl halloysite nanotubes (HNT-HCl, [Table 11](#), [entry 77](#)) On strong Brønsted and Lewis acids (Amberlyst-15, scandium triflate), the yield of isobenzofurans did not exceed 16% with formation of mainly 2-carene isomerization products [251].

Note that 2-carene is an expensive compound [251]; however, it has been shown that it is formed in an amount of 10–15% during isomerization of 3-carene on illite and montmorillonite clays [252,261]. Based on this, the catalytic synthesis of isobenzofurans was developed by reacting a 2-carene containing reaction mixture with vanillin on clays with the isolated yields of

49–60% (Table 11, entry 81–83 [252]). Even higher selectivity for the target product was observed on HNT-HCl (71%) [251].

As a further progress of research [250–252,261], a number of novel iso-benzofurans and oxabicyclo[3.3.1]nonenes were synthesized by reacting 2-carbene containing a mixture with various aldehydes in the presence of commercial montmorillonite K-10 [262]. Biological studies have shown that some of the obtained compounds have a powerful ability to inhibit the TDP1 enzyme, which may be promising in the complex therapy of oncological diseases [262].

11.3. The Prins reaction of terpenoids: synthesis of heterocycles

The Prins reaction is a versatile and convenient synthetic route for the preparation of oxygenated heterocyclic compounds, whose key step is the formation of an oxocarbenium ion that reacts with 1 eq of the alkene in an intermolecular or intramolecular fashion [229]. Thus, reactions of terpenoid alcohols containing an unsaturated bond with aldehydes lead to the formation of substituted chromene (benzopyran) compounds [230]. Interest in the synthesis of chromenes is due, in particular, to their diverse and potent biological activity, and accordingly they have a high pharmaceutical potential [230,263–265]. This section discusses the synthesis of chromene and benzodioxin framework compounds in the context of heterogeneous catalysis, especially those with a high potential for pharmaceutical use.

A common naturally occurring and commercially available terpenoid is the unsaturated alcohol isopulegol [230]. It finds industrial application as an intermediate in the menthol synthesis and is also considered as a chiral platform for the production of bioactive agents [266].

A possibility of (-)-isopulegol condensation with aromatic and aliphatic aldehydes (Fig. 22a) in the presence of a heterogeneous catalyst (acid-treated montmorillonite K-10) under microwave conditions was first demonstrated in [267]. The reaction products were substituted octahydro-2*H*-chromen-4-ols, as 4*R*- and 4*S*-isomers, the total yields of which were 50–86% (Table 12, entry I). The reaction proceeded most selectively with 4-methyl- and 4-methoxy-substituted benzaldehydes.

Beta zeolites, as well as the mesoporous material MCM-41 including their metal-modified forms, were studied in the Prins reaction of isopulegol with benzaldehydes. The main reaction products on these catalysts were octahydro-2*H*-chromen-4-ols while octahydro-2*H*-chromenes were formed in much smaller quantities (Table 12, entry 2–8, [268]). The most selective system was Ce-MCM-41 with a comparably low Lewis and Brønsted acidity (147 $\mu\text{mol/g}$). It has been shown that formation of octahydro-2*H*-chromenes occurs by dehydration on catalysts characterized by high Brønsted acidity [268].

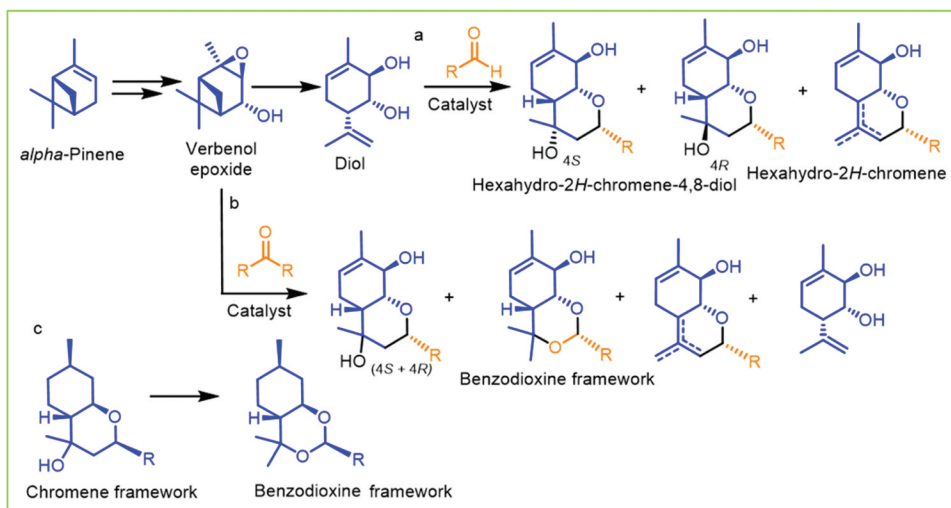


Figure 23. A scheme of diol (a) and verbenol oxide (b) condensation with aldehydes (a) as well as chromene transformation to benzodioxine compound (c).

Acid clays are effective catalysts for the synthesis of octahydro-2H-chromen-4-ols. Thus, montmorillonite clays from Russia and Kazakhstan were activated with hydrochloric acid, and the concentration of acid sites on their surface increased with increasing concentration of HCl used in the treatment [283]. In turn, this led to a decrease in (i) the ratio of the target to dehydration products, as well as (ii) the ratio of 4R/4S isomers.

In work [269], the catalytic properties were pretreated by HCl montmorillonite (M-HCl), kaolinite (K-HCl) and metakaolin (MK-HCl) of the Russian origin in the condensation of isopulegol and vanillin were studied. The substrate conversion in 2 h on M-HCl was significantly higher (76%) than on kaolin-based catalysts (26–30%) with selectivity toward octahydro-2H-chromen-4-ol in the range of 74–90% (Table 12, entry 9 – 11).

A large set of chiral compounds with the octahydro-2H-chromene scaffold was first synthesized by a reaction of (-)-isopulegol with furan-2-carbaldehyde, thiophene-2-carbaldehyde and their derivatives over montmorillonite K-10 with the yield of 50–86% (Table 12, entry 12) [264]. It was established that most of the obtained compounds exhibited significant analgesic activity. The product of the (-)-isopulegol reaction with thiophene-2-carbaldehyde is the most promising, since the 4R-isomer of the corresponding octahydro-2H-chromen-4-ol exhibits high and long-term (24 h) analgesic effect [264]. The yield of this compound was 78% with the 4R/4S ratio of 5.0. Based on the outstanding analgesic activity of the abovementioned 4R-isomer, a comprehensive study was carried out on (-)-isopulegol condensation with thiophene-2-carbaldehyde, focusing on stereoselective catalysis [270–272]. Thus, in this reaction on acid-modified illite clay (L-1, from Belarus), the

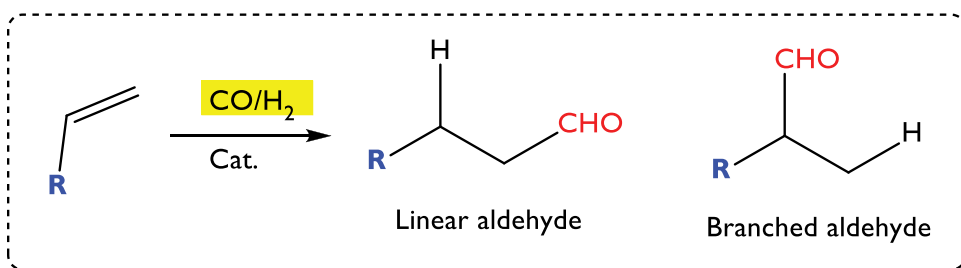


Figure 24. General scheme of the hydroformylation reaction.

yield of 4*R*-isomer of octahydro-2*H*-chromen-4-ol increased with decreasing catalyst acidity and the temperature, as well as by increasing the ratio of catalyst/reactants and the initial concentration of the reagents [270]. Kinetic modeling was used to explain the observed regularities. It was shown that formation of chromenes occurs both directly from the reagents and by dehydration of only 4*R*-diastereomer of chromenol. Some quantitative results are shown in Table 12, entry 13–18.

A significant advance in the field of stereoselective synthesis of chromenols was the utilization of halloysite nanotubes pretreated with HCl (HNT-HCl) in the Prins condensation of (-)-isopulegol with aliphatic and aromatic aldehydes. The reaction of these catalysts gave the desired products with very high 4*R*/4*S* isomer ratios (7.6–14.5). Unprecedented selectivity (79–83%) to 4*R*-isomer of thiophenyl-substituted chromenol exhibiting high analgesic activity was achieved. An increase in stereoselectivity with a decrease in the halloysite drying temperature and catalyst acidity clearly indicates formation of the target diastereomer on the weak Brønsted sites. Table 12 (entry 19–23) shows selected data reported in [271].

The mechanistic aspects as well as the effect of acid treatment of halloysite on its physico-chemical and catalytic properties in the reaction of (-)-isopulegol with thiophene-2-carbaldehyde was studied in detail [272]. At 99% of the substrate conversion in cyclohexane over HNT treated with 5% HCl selectivity to 4*R*-isomer of chromenol alone (ca. 80%) was achieved close to the sum of both diastereomers on a commercial montmorillonite K-10, whereas with scandium triflate it did not exceed 45% (Table 12, entry 24–28). A substantial difference in the order to the catalyst for the dried resin Amberlyst-15 (1.1 ± 0.12) and air-dry halloysite (1.95 ± 0.09) for the target 4*R*-isomer formation clearly indicates the key role of water in the reaction. A dual mechanism of the halloysite action was proposed implying formation of an intermediate with the reagents and transfer of the surface water to the intermediate giving chromenols. Stability and reusability of HNT were also demonstrated [272].

Acidic functionalization of the aluminosilicates surface can also be accomplished by grafting -SO₃H groups. Thus, montmorillonite K-10 and halloysite

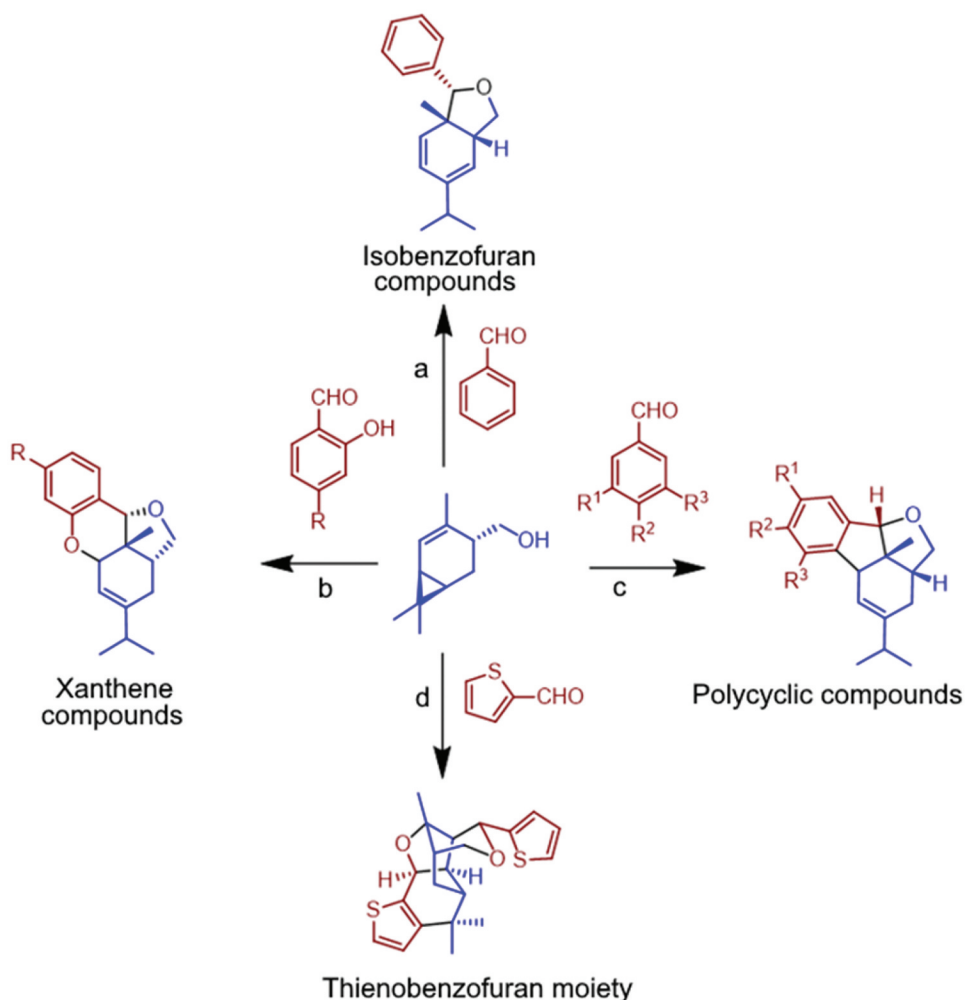


Figure 25. A scheme of heterocyclic compounds synthesis based on *trans*-4-hydroxymethyl-2-carene.

were pretreated with chlorosulfonic acid (CSA) or 2-(4-chlorosulphonylphenyl)ethyltrimetoxysilane (CSP) and tested in the Prins reaction of (-)-isopulegol with benzaldehyde as the reagent and the solvent (Table 12, entry 29-32) [273]. The highest selectivity toward octahydro-2*H*-chromenol (95% with 4*R*/4*S* of 5.5) was recorded in the presence of K10-CSP. Although halloysite treated with the same reagent afforded high stereoselectivity (4*R*/4*S* of 11.5), the total yield of chromenol was only 35%. The K10-CSP catalyst did not display any leaching [273].

In [274], a series of Beta zeolites with a systematic variation of synthesis parameters was prepared and tested in a similar reaction (Table 12, entry 33 – 36). The most efficient catalyst H-Beta-17(h-R-150) exhibited well-developed textural and structural properties as well as mild acidity (285 $\mu\text{mol/g}$) with the

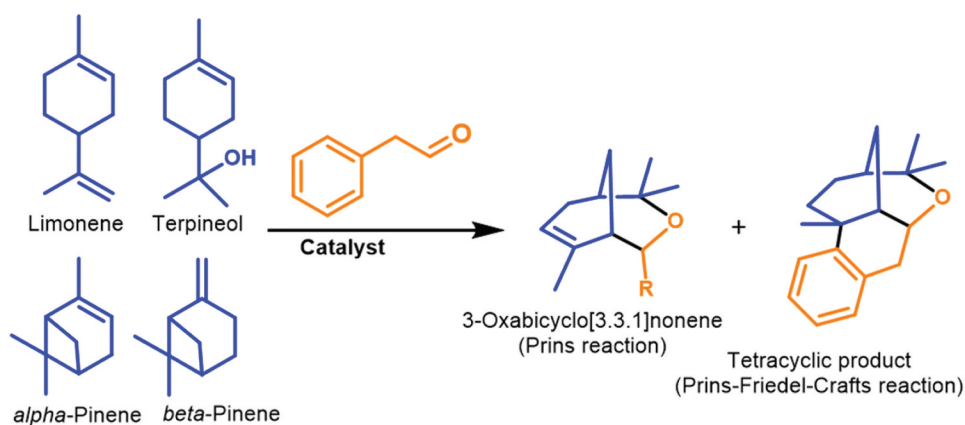


Figure 26. A scheme of monoterpene coupling with phenylacetaldehyde.

largest ratio of Brønsted to Lewis a.s. (10). This was accompanied by high selectivity to the desired product (4*R*-isomer, 79%) and the lowest amount of the side dehydration product (9%).

The condensation of (-)-isopulegol with ketones (*Fig. 22b*) occurs with much lower selectivity than in the case of aldehydes. Thus, a set of novel octahydro-2*H*-chromen-4-ols was synthesized using aliphatic and cyclic ketones in the presence of the H-K-10 catalyst with yields not exceeding 57% (*Table 12, entry 37*) [275]. 4*R*-isomer of chromenol produced via the substrate reaction with acetone was found to exhibit an outstanding activity against a number of H1N1 and H2N2 influenza viruses. Based on the high pharmaceutical potential of this product, further research was carried out to prepare selective catalysts for this reaction [276–278].

Thus, halloysite nanotubes treated with 5% HCl were applied as catalytic systems for the Prins reaction of (-)-isopulegol with acetone [276]. As a result, high selectivity (up to 77%, 4*R*/4*S* of 8.2) toward chromenols was achieved using HNT under solvent-free conditions (*Table 12, entry 38 – 41*) with the isolated yield of the 4*R*-isomer of 66%. The proposed reaction mechanism is more complex than in the case of aldehydes. Formation of the target chromenols occurs through water in addition to the cyclic intermediate. Interactions of this intermediate with isopulegol lead to stereoselective formation of an ester with the chromene structure (*Fig. 21b*), which after hydrolysis also gives chromenols.

Condensation of (-)-isopulegol with acetone was investigated over clays, including halloysite and montmorillonite functionalized with acid groups by treating them with chlorosulfonic acid (CSA) 2-(4-chlorosulfonylphenyl)-ethyltrimethoxysilane (CSP) [277]. The best catalyst was a highly acidic (294 $\mu\text{mol/g}$), large pore K10-CSA. By varying the temperature and the initial concentration of the reagents it was possible to achieve a high selectivity to

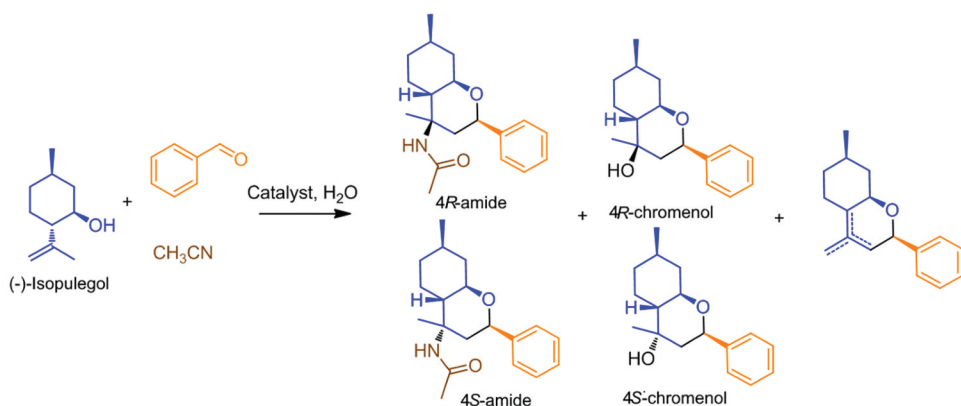


Figure 27. A scheme of (-)-isopulegol reaction with benzaldehyde and acetonitrile.

octahydro-2H-chromenol (up to 88%) with the 4R/4S ratio up to 7.6 (Table 12, entry 42–46).

A series of hierarchical beta zeolites (HB) obtained via the hydrothermal method was investigated in the same Prins reaction under mild (30°C) conditions [278]. The largest (-)-isopulegol conversion (52%) after 4 h was reached over HB-4 zeolite consisting of fused beta zeolite nanoparticles with a small (15 nm) size which resulted in the formation of the developed mesoporous structure (S_{meso} 230 m²/g, V_{meso} 0.81 cm³/g) with a high concentration of accessible to the reagents acid sites (202 μmol/g). Utilization of the prepared zeolite catalysts allowed to achieve selectivity to octahydro-2H-chromenol up to 69% with a high (up to 11.1) stereoisomers ratio (Table 12, entry 47–51).

High antiviral activity is also demonstrated by F- and OH-containing isopulegol-derived octahydro-2H-chromenes formed in the presence of the BF₃·Et₂O/H₂O catalytic system [284], which illustrates a high potential for further developments in this field. Another platform molecules for the synthesis of heterocyclic compounds promising for pharmaceutical applications are terpenoid p-menta-1,8-diene-5,6-diol (**diol**, Fig. 22a), which can be synthesized in several steps from α-pinene [230].

A platform molecule for the synthesis of chromene compounds promising for pharmaceutical applications is also the terpenoid p-menta-1,8-diene-5,6-diol (**diol**, Fig. 23) which can be synthesized in several steps from α-pinene, where the key stage is the epoxide verbenol isomerization [230]. The reaction of a diol with aromatic [279] and aliphatic [280] aldehydes leads to the formation of substituted hexahydro-2H-chromene-4,8-diols, some of which exhibit significant analgesic [279,280] or antiviral [230] activity. Initially, the synthesis of these heterocycles was carried out on montmorillonite K-10 clay without a solvent. As can be seen from Table 12 (entry 52–53), the yields of the target hexahydro-2H-chromene-4,8-diols and stereoselectivity

Table 13. Some catalysts for cascade reactions of monoterpenoids.

Entry	Catalyst	Reactants	Reaction conditions	X (%)	S (%)	Ref.
1	K-10	<i>trans</i> -4-hydroxymethyl-2-carene (HM2C) + benzaldehyde (4-methoxybenzaldehyde)	0.6 mmol of substrate, 0.8 mmol of aldehyde, 0.35 g of catalyst, 4 mL of CH ₂ Cl ₂ , 3 h, RT	n.d.	14 – 17 IBF (isolated yield)	[255]
2		HM2C + salicylaldehydes	Similar	65	29 – 62 Xanthene (isolated yield)	
3		HM2C + 3,4,5- trisubstituted benzaldehydes	Similar	n.d.	49 – 85 PC (isolated yield)	
4	HNT-HCl	HM2C + salicylaldehyde	0.35 g (1.85 mmol) of substrate, 1 eq of aldehyde, 0.37 mol/L (in CH ₂ Cl ₂), 1 g of catalyst (dried at 105°C), 25°C, 120 min	50	65 Xanthene 15 IBF	[256]
5	K-10		Similar, 10 min		66 Xanthene 11 IBF	
6	Amberlyst-15		Similar, 30 min		7 Xanthene 13 IBF	
7	HNT-HCl	HM2C + 3,4,5-trimethoxybenzaldehyde	Similar, 30 min		74 PC 11 IBF	
8	K-10		Similar, 15 min		78 PC 6 IBF	
9	Amberlyst-15		Similar, 10 min		7 PC	
10	K-10	HM2C + 3,4,5-trisubstituted benzaldehydes	Similar, substrate concentration of 0.06 mol/L in CH ₂ Cl ₂ , catalyst dried at 105°C 60-120 min	99	88 – 97 PC	
11	CsPW	Limonene+ phenylacetaldehyde	0.45 mmol of substrate, 4.45 mmol of aldehyde, anisole (3 mL total volume), 3 μmol of catalyst, 70°C, 1 h	100	60 TP 35 OBN	[314]
12			Similar, 90°C		45 TP 32 OBN	
13			Similar, 50°C, 5 h		54 TP 41 OBN	
14		α-terpineol+ phenylacetaldehyde	Similar, 70°C, 1 h		70 TP 28 OBN	
15			Similar, 2 h		78 TP 19 OBN	
16		α-pinene+ phenylacetaldehyde	Similar, 50°C, 1 h		60 TP 35 OBN	
17		β-pinene+ phenylacetaldehyde	Similar		47 TP 38 OBN	

(Continued)

Table 13. (Continued).

18	K10-CSA	(-)-isopulegol + benzaldehyde + acetonitrile	0.1 g (0.65 mmol) of substrate, 3.0 mmol of aldehyde, 20 mL of dry acetonitrile, 0.1 g of catalyst, 30°C, 0 mmol of water	50	42 Amides 4R/4S 1:4.3 14 OCh-ol 44 OCh	[315]
19			Similar, 2.2 mmol of water		62 Amides 4R/4S 1:2.9 17 OCh-ol 22 OCh	
20			Similar, 17.3 mmol of water		76 Amides 4R/4S 2.2:1 20 OCh-ol 5 OCh	
21	CNT-CSA		Similar		83 Amides 4R/4S 5.1:1 15 OCh-ol 2 OCh	
22	Amberlyst-15				47 Amides 4R/4S 2.8:1 35 OCh-ol 17 OCh	
23	<i>p</i> -TSA (0.53 mmol)			100	70 Amides 4R/4S 2.6:1 21 OCh-ol 9 OCh	
24	Biochar-CSA			50	84 Amides 4R/4S 5.7:1 13 OCh-ol 3 OCh	[316]
25	Biochar-CSP				67 Amides 4R/4S 2.4:1 24 OCh-ol 8 OCh	
26	CNT-CSP				69 Amides 4R/4S 3.5:1 22 OCh-ol 10 OCh	
27	HNT-CSP				57 Amides 4R/4S 2.5:1 31 OCh-ol 12 OCh	

IBF: isobenzofurans. **PC:** polycyclic compounds. **TP:** tetracyclic products. **OBN:** 3-oxabicyclo[3.3.1]nonene. **OCh-ol:** octahydro-2H-chromen-4-ol. **OCh:** octahydro-2H-chromenes

were lower than when using isopulegol as the substrate. When verbenol epoxide was used for the reaction with aldehydes, excluding the stage of its isomerization, in addition to chromenediols, formation of the products with the benzodioxine framework (*Fig. 23b*) in small quantities was observed [279]. Given the pharmaceutical potential for these compounds, additional mechanistic studies have been carried out [268].

Thus, the H- and Fe-forms of Beta zeolites, as well as mesoporous silicate Ce-MCM-41, were studied as catalysts for the Prins condensation of diol with benzaldehyde [268]. A high substrate conversion (up to 99%) was achieved after 2h with selectivity to hexahydro-2*H*-chromene-4,8-diols in the range of 64–67% (*Table 12, entry 54–58*). The reaction rate with diol was lower than in the case of isopulegol, apparently due to a decrease in the electron density in the reacting hydroxyl group by influencing the neighboring one. Selectivity to the desired products was decreased by subsequent transformations including dehydration and rearrangement into benzodioxin structures [268,281,282,285,286].

Condensation of diol with decanal was studied over acid-modified halloysite nanotubes and compared with clays and common catalysts [281]. Selectivity toward the target hexahydro-2*H*-chromene-4,8-diol with a high analgesic activity was 76–80% not depending practically on the aluminosilicate type (*Table 12, entry 59–63*), while the 4*S*/4*R* ratio decreased with increasing catalyst acidity. The largest selectivity to 4*S*-isomer (48.1%) on halloysite is a result of weak acidity of this nanocatalyst. Optimization of the key intermediate structure by DFT calculations shows that the nucleophile attack proceeds at the equatorial position with the 4*S*-diastereomer formation, which was preferred on HNT. On the contrary, with Brønsted (Amberlyst-15) and Lewis (scandium triflate) acids the target product yield did not exceed 37% because of dehydration [281]. Diol, similar to isopulegol, can also react with ketones. Moreover, the product of cyclohexanone interaction with this substrate on K-10 catalyst (yield 51%, 4*S*/4*R* of 2.0) demonstrated an analgesic effect significantly larger than that of sodium diclofenac [285]. The use of halloysite nanotubes in this reaction [281] makes it possible to significantly increase both the yield (67%) and stereoselectivity (4*S*/4*R* of 21.0), which makes further research in this area promising.

The verbenol epoxide reaction with aromatic aldehydes, including benzaldehyde over H- and Fe-Beta zeolites for the synthesis compounds with benzodioxin framework (*Fig. 23b*) was studied in [282]. Two parallel reactions occurred, namely epoxide isomerization giving diol and other products, as well as formation of the target product from the reagents. With an equivalent amount or a slight excess of aldehyde, isomerization products are formed. However, Fe-H-Beta-150 catalyst containing both Lewis and Brønsted acidity at a substrate-to-benzaldehyde ratio of 1:133 provided 46% selectivity with complete conversion of the epoxide. Based

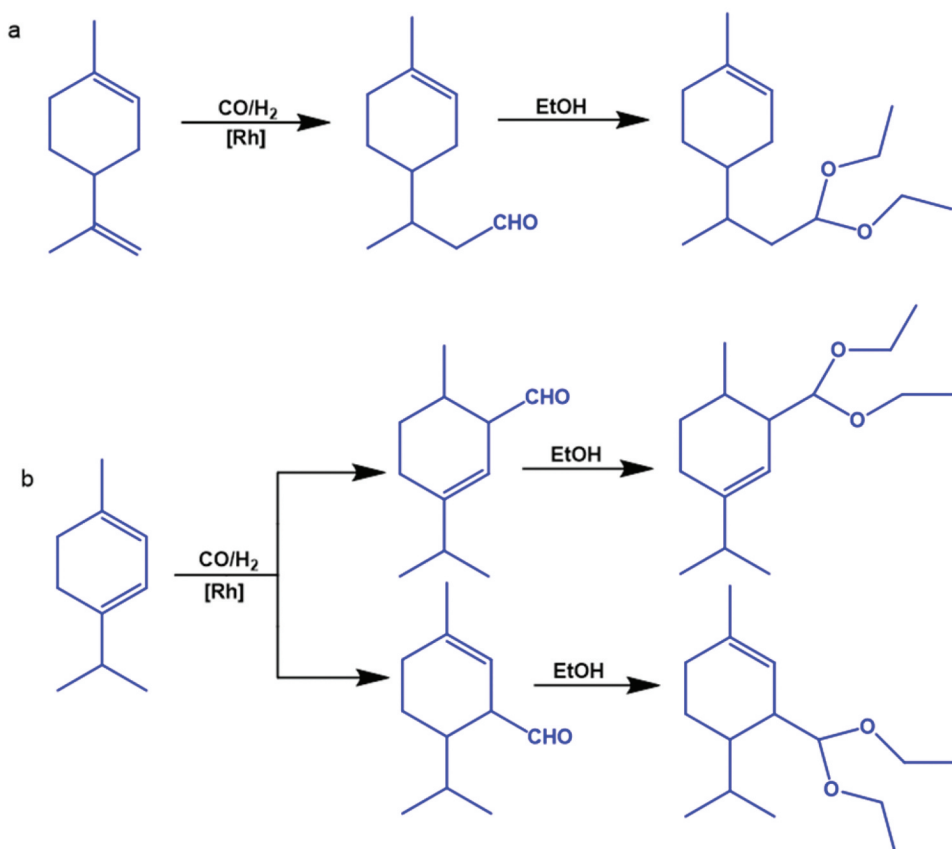


Figure 28. A scheme of limonene (a) and α -terpinene (b) tandem hydroformylation/acetalization.

on the kinetic analysis for Fe-H-Beta-150 a reaction network was proposed [282]. Some relevant experimental data are presented in Table 12, **entry 64–69**. Synthesis of benzodioxin compounds can be realized from isopulegol in two steps (Fig. 23c) [286]. At the first stage, its condensation with benzaldehyde on Ce-MCM-41 into octahydro-2H-chromen-4-ol took place with a selectivity of 93%. The second step involves rearrangement of the resulting product when the desired reaction of tetrahydropyran to dioxin moiety was observed in the presence of mesoporous Ce composite catalyst, which exhibited both, mild acidic and basic properties with selectivity of 36%.

Note that there are examples of the involvement of some terpenoids, in particular myrcene, verbenol, *trans*-sobrerol, terpineol, α - and β -pinene epoxides, in reactions with aldehydes, leading to formation of the heterocyclic compounds. These studies are performed in the context of organic chemistry and are summarized in the review [230]. A recent study also reports the synthesis of oxabicyclo[3.2.1]octenes from (-)-terpinen-4-ol using sulfamic acid with yields up to 97% [287]. The catalytic synthesis of menthol from

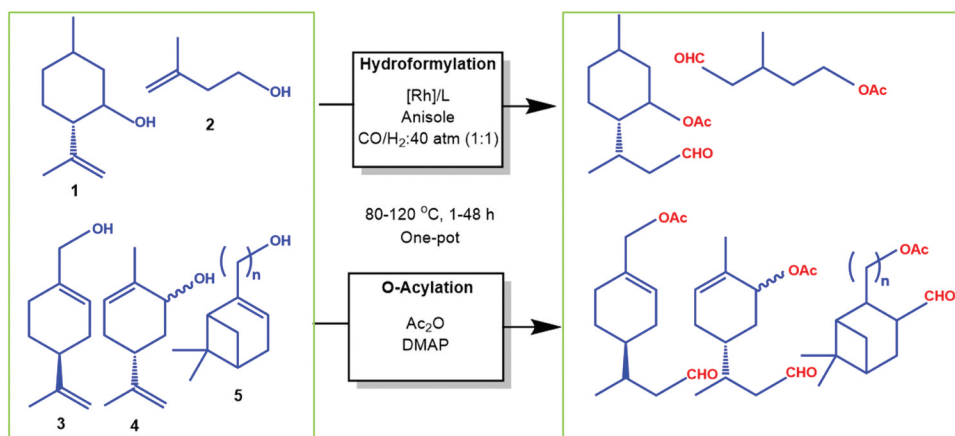


Figure 29. A scheme of (-)-isopulegol (1), isoprenol (2), perillyl alcohol (3), carveol (4) and nopol/myrtenol (5) one-pot hydroformylation/O-acylation (modified from [321]).

citral and citronellal in the presence of heterogeneous catalysts was recently reviewed in [288].

12. Hydroformylation of terpenes

Addition of carbon monoxide and hydrogen to olefins in the hydroformylation reactions can lead to both linear and branched aldehydes (Figure 24) [289–291]. The chemical reaction holds special significance due to the distinctive properties of aldehydes [292]. It was first discovered by Roelen in 1938 using cobalt catalyst systems [293]. Typically, terpenes undergo this reaction in the presence of transition metal catalysts, such as rhodium or cobalt complexes [294,295]. One of the initial catalysts reported for hydroformylation of terpenes, including α -pinene, dipentene, α -terpinene, and myrcene, is the crystalline dicobalt octacarbonyl, which was prepared from CoCO_3 [296]. Hydroformylation serves to modify terpenes by introducing functional groups capable of influencing specific properties or enabling further chemical transformations [297]. Hydroformylation of limonene, a major monoterpene found in citrus fruit oils, produces limonenal [298], a key ingredient in flavorings, soaps, and fragrances [299]. Modification of C=C bonds in different positions within the terpene structure through hydroformylation allows generation of various aldehyde products, each possessing distinct chemical functionalities.

Hydroformylation of endocyclic monoterpenes, including 2-carene, 3-carene, α -pinene, terpinolene, γ -terpinene, and α -terpinene, as substrates [300,301], has been investigated extensively in the past. Additionally, diterpenes such as kaurenoic and grandifloreneic acids have also been studied in this context [302]. These investigations employed the presence of PPh_3 or various diphosphines and phosphites under mild reaction conditions (80–100°C, 40–

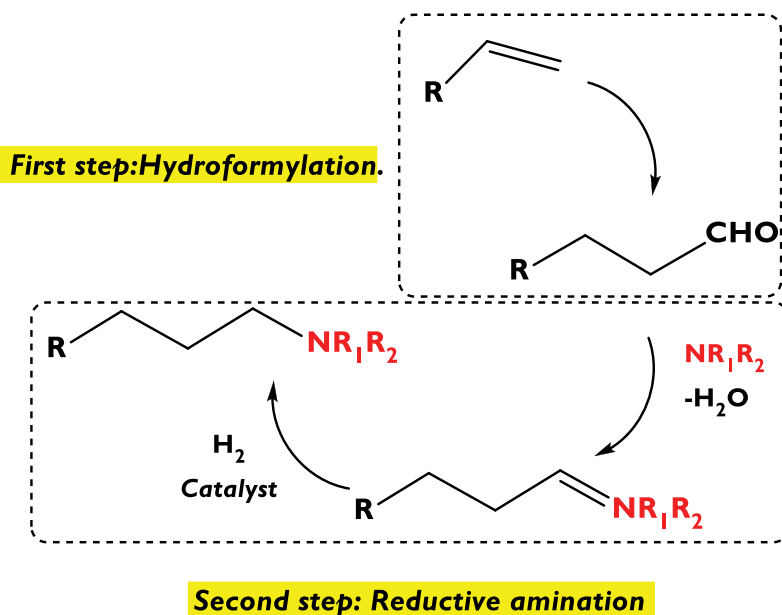


Figure 30. Schematic representation of the one-pot synthesis of amines from the tandem hydroformylation/reductive amination reaction.

80 atm total pressure, with a CO/H₂ molar ratio ranging from 2:1 to 1:2). The outcome demonstrated high conversion along with chemo- and regio-selectivity. For unmodified systems lacking phosphorous ligands, the rhodium catalyst could induce the isomerization of monoterpenes, which underwent hydroformylation at a relatively slow rate. However, the introduction of PPh₃, diphosphines, or triphenylphosphite, in a P/Rh ratio of at least 20, enhanced this process. A comprehensive review published by Gusevskaya et al. in 2013 covered hydroformylation of linear aliphatic and cyclic monoolefins as well as polyolefins [303], providing valuable insights up to that point.

More recently, hydroformylation of limonene using Rh-based catalytic systems, prepared in situ was explored, under relatively mild reaction conditions (40 atm of syngas and 80°C) [304]. Among homogeneous systems, those based on complexes of phosphine ligands like dicarbonyl(acetylacetonato) rhodium(I) with triphenylphosphine (PPh₃), exhibited exceptional activity. Specifically, limonene conversion of 96% and a 90% selectivity toward limonene were achieved after 4 h. Secondary products, terpinolene (6%) and menthene (<1%), were obtained through isomerization and hydrogenation routes, respectively. These findings suggested that the catalytically active species were hydrido-carbonyl complexes containing two phosphorus atoms coordinated to the Rh center.

A biphasic system consisting of water and toluene has been utilized for the hydroformylation of various acyclic terpenes, namely β-citronellene, linalool, and nerolidol, employing a rhodium-based catalyst [305]. The catalyst

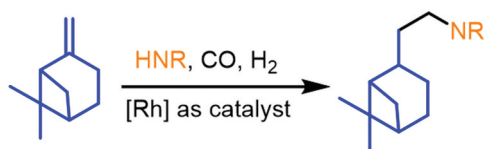


Figure 31. A scheme of terpenes hydroaminomethylation using β -pinene as an example.

precursor used was $[\text{Rh}(\text{COD})(\text{OMe})_2]$ (COD = 1,5-cyclooctadiene), and a water-soluble *tris*(3-sulfonatophenyl)phosphine trisodium salt (TPPTS) ligand was employed to maintain the catalyst solubility in the aqueous phase. For β -citronellene, a substrate with low solubility in water, no conversion was observed under the conditions of 20 atm total pressure, a CO/H₂ molar ratio of 1, 80°C, and 2 h. However, introduction of a small amount of cationic surfactants, such as cetyltrimethylammonium chloride (CTAC) at 2.5 mM (considering only the volume of the aqueous phase), facilitated a slow hydroformylation process, resulting in 10% conversion after 2 h. This rate could be substantially enhanced by progressively increasing the amount of surfactant. With 50 mM of CTAC 87% conversion was achieved, with overall selectivity 90% toward linear aldehydes and 10% to branched aldehydes. On the contrary, the hydroformylation of linalool in toluene solutions primarily yielded hemiacetals as the main products. These hemiacetals originated from the intramolecular cyclization of initially formed hydroxy aldehydes. Similarly, at 80°C, the presence of the surfactant (25 mM) in the biphasic system substantially enhanced the substrate conversion (98%), as compared to 10% conversion achieved using the free-surfactant system. The selectivity ratio between *cis* and *trans* hemiacetals was 97:3. Therefore, under identical reaction conditions, linalool exhibited significantly higher reactivity than β -citronellene. This discrepancy can be attributed to the larger hydrophilicity of linalool, allowing the reaction to take place not only at the water/organic medium interface but also within the aqueous phase. Additionally, linalool solubility was approximately 1000 times than that of β -citronellene.

In the case of nerolidol [305], hydroformylation resulted in the formation of a hemiacetal as the main product. This molecule existed in two natural isomeric forms: *cis* (Z-nerolidol) and *trans* (E-nerolidol), differing in the geometry of their central double bonds. Analogous to the linalool reaction, the target hemiacetal was formed through the intramolecular cyclization of initially produced hydroxy aldehydes, not previously reported in the literature. Different reaction conditions yielded selectivity ranging from 90% to 95%, with a minor non-functionalized sesquiterpenic acyclic triene identified as the remaining product. This minor product originated from dehydration and monohydrogenation of the nerolidol molecule [306]. Similar to the findings with linalool, the reactions employing CTAC concentrations ranging from 12.5 mM to 50.0 mM displayed nearly complete conversion within 2 h,

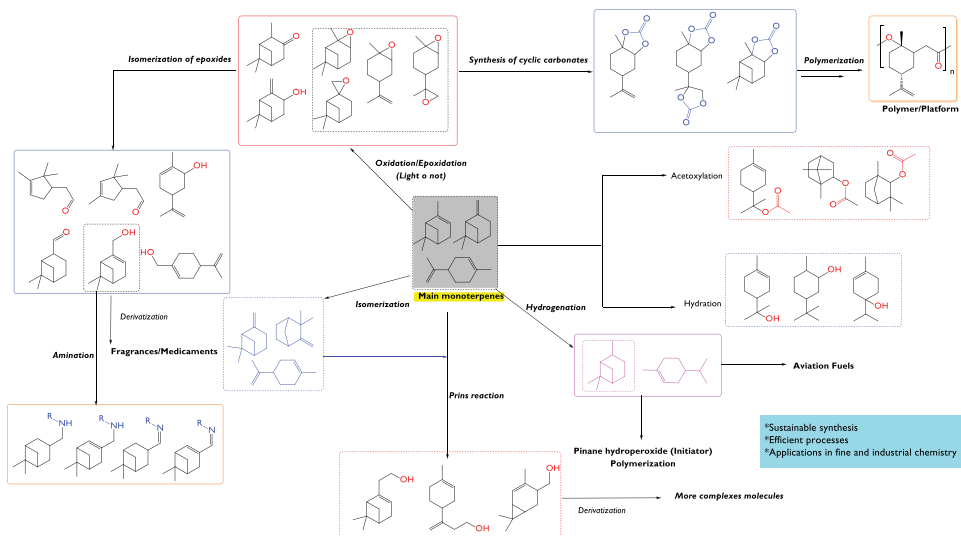


Figure 32. General scheme of the transformations of terpene by using heterogeneous catalysis.

accompanied by remarkable stereoselectivity of 96–98% for the *cis* isomers. In all three cases, a complete phase separation could be achieved by simply stopping the magnetic stirrer after the reaction and allowing the mixture to cool to room temperature. Furthermore, this system is deemed a promising green approach due to immobilization of the rhodium catalyst in water, an environmentally benign solvent. Moreover, facile separation of the catalyst from the products dissolved in the organic phase can be accomplished.

Homogeneous Rh, Co, and Pt complexes have been studied as catalysts for the hydroformylation of various terpenes [307]. A catalyst screening study using camphene as the substrate and toluene as the solvent revealed that, in all cases, the primary product was 3,3-dimethyl-2-norbornaneacetaldehyde (terminal aldehyde), present as a diastereomeric mixture of *exo* and *endo* isomers. Additionally, minor quantities of secondary products, such as tricyclene and isocamphene resulting from hydrogenation side reactions, were observed. A byproduct, fenchene, was formed due to an isomerization reaction. Among the tested catalysts, $\text{Rh}(\text{CO})_2(\text{acac})/\text{P}(\text{OPh})_3$ demonstrated the highest catalytic activity (TOF of 186 h^{-1}) when employing the following conditions: camphene concentration of 0.64 mol L^{-1} , catalyst concentration of $1.23 \times 10^{-3} \text{ mol L}^{-1}$, 7.4×10^{-3} moles of ligand, Rh: P molar ratio of 1:6, 100°C , and total pressure of 4.14 MPa. This catalyst gave the yield of 94% and selectivity of 99% toward the aldehyde. This outcome was attributed to facile dissociation of the phosphite ligand, which facilitated the rapid coordination of olefins to the metal center. Given its superior activity, the aforementioned catalyst was further evaluated in the hydroformylation of other terpenes, including (*R*)-limonene, β -pinene, γ -terpinene, 3-carene, *R*-(-)-carvone, α -pinene and myrcene.

Similar reaction conditions were employed, except for an initial terpene concentration of 0.37 mol L^{-1} . This catalyst exhibited remarkable activity in the hydroformylation of limonene and β -pinene, achieving conversions of 99% and 79%, respectively, along with corresponding aldehyde selectivity of 99% and 70%. Comparatively lower hydroformylation activities were observed for 3-carene and γ -terpinene, resulting in conversion of approximately 11% and 45.5%, respectively. In the cases of limonene and β -pinene hydroformylation, the main product obtained was 3-(4-methylcyclohex-3-enyl)butanal. Conversely, the products derived from 3-carene were 2-caranecarbaldehyde and 3-caranecarbaldehyde in equal amount.

Hydroformylation of hydroxyolefins, such as myrtenol and nopol, was investigated using a rhodium(I)/bulky phosphite catalytic system with toluene as the solvent. The experimental setup involved 0.20 M of substrate, 0.25 mM (5 μmol) of catalyst, 80 atm of gas phase ($\text{CO}/\text{H}_2 = 1:1$), and 20 mL of the solvent [308]. Both substrates exhibited considerable resistance to hydroformylation and displayed a notable tendency to form isomeric saturated aldehydes under the provided conditions. Despite these challenges, the catalytic systems enabled synthesis of the corresponding hydroxyaldehydes. After 48 h of the reaction, conversions of 90% and 68% were achieved for myrtenol and nopol substrates, respectively. Selectivity toward the primary aldehyde was 54% and 46% with myrtenol and nopol, respectively. The authors [308] attributed difficulties in hydroformylating these two olefins to the endocyclic, trisubstituted, and sterically hindered. Character of their double bonds. Additionally, the presence of the electron-withdrawing hydroxyl group in proximity with the olefinic bonds retarded their interactions with the Rh catalyst. Moreover, nopol exhibited lower reactivity, likely due to the homoallylic hydroxyl group's ability to form stable chelates with the Rh center. These chelates hindered the catalytic process from occurring at reasonable rates. As an alternative, diethyl carbonate can be used as an eco-friendly solvent for the hydroformylation of these olefins, replacing aromatic solvents derived from petrochemical sources.

13. Telescoping/One-pot multistep reactions

Cascade (tandem) reactions including Prins-initiated ones are an effective method for the synthesis of functional compounds, the main advantage being sequential formation of several chemical bonds in one reaction space, which eliminates a need for isolation and purification of intermediate products. Several recent reviews have been devoted to these reactions, being more focused on synthetic organic chemistry [230,309–311] rather than catalysis [312]. Moreover, very few publications consider solid catalysts for tandem terpenoid reactions.

13.1. Cascade Prins reactions

One of the platform molecules for the heterocyclic compounds preparation is *trans*-4-hydroxymethyl-2-carene (Fig. 25a-d) [246,255,256], which is obtained from 3-carene [253,257]. When it reacts with benzaldehyde (or *p*-methoxy derivative) on K-10 clay, isobenzofurans are formed (Fig. 25a, [255]), and in the presence of a hydroxyl group at the *o*-position of the aldehyde, a cascade Prins reaction occurs with formation of the xanthene framework (Fig. 25b, [255]). If there are three electron-donating substituents in the 3,4,5-position of the benzaldehyde ring, a cascade Prins-Friedel-Crafts reaction occurs (Fig. 25c, [255,313]), which gives tetracyclic compounds, some of which have cytotoxic activity [255]. The *trans*-4-hydroxymethyl-2-carene condensation with thiophene-2-carbaldehyde over K-10 leads to the formation of thienobenzofuran derivatives (Fig. 25d, [246]). The quantitative results are shown in Table 13, entry 1–3.

The reaction of *trans*-4-hydroxymethyl-2-carene with salicylic as well as 3,4,5-trisubstituted aldehydes has been studied in the presence of a number of clays, including montmorillonite K-10, illite and halloysite [256]. Both the reaction rate and selectivity to the target products (Fig. 25b,c) increased with an increase in acidity and clays drying temperature, demonstrating that relatively strong Brønsted and Lewis acid sites favored formation of these desired products. Under optimized reaction conditions, selectivity to tetracyclic products (Fig. 25c) reached 97% on montmorillonite K-10 with acidity of 104 $\mu\text{mol/g}$. It was shown that an electron-donor substituent at the *m*-position of benzaldehyde is critical for the Prins-Friedel-Crafts reaction [256]. The calculated thermodynamic

parameters for products are in complete agreement with the values of the initial rates of formation of target and by-products of the reaction. Some results reported in the literature are shown in Table 13, entry 4–10.

A one-pot tandem process has been developed which involves condensation of phenylacetaldehyde (formed by isomerization of styrene oxide) with common monoterpenes (Fig. 26, [314]), catalyzed by a cesium salt of tungstophosphoric heteropoly acid. In addition to the expected compound with an 3-oxabicyclo[3.3.1]nonene structure, formation of a Prins-Friedel-Crafts reaction product with a fused tetracyclic structure occurred in the yields of up to 78% (Table 13, entry 11–17). The reactions were performed under mild conditions in green solvents with a heterogeneous catalyst (CsPW) stable to leaching [314].

It is known that an (-)-isopulegol-derived octahydro-2*H*-chromene compounds containing the amide fragments are potent inhibitors of the TDP1 enzyme being promising in the complex anticancer therapy [317]. According to [318], synthesis of 4-amidotetrahydropyran compounds based on (-)-isopulegol can be carried out *via* the Prins-Ritter reaction in the presence of

2–3 eq of triflic acid at temperature from -50 to -25°C giving a complex product mixture.

A number of functionalized by chlorosulfonic acid (CSA) solids including carbon nanotubes (CNT) and montmorillonite K10 were studied in the Prins-Ritter reaction of (-)-isopulegol with benzaldehyde and acetonitrile (Fig. 27, [315]). An unusual strong effect of water addition on the overall selectivity to amides and its isomers ratio in the case of heterogeneous and homogeneous (*p*-toluenesulfonic acid) catalysis was found (Table 13, entry 18–24). DFT calculations showed that at 30°C formation of 4*S*-amide thermodynamically is more beneficial than that of chromenols and dehydration products. However, the addition of water results in a sharp increase in the reaction rate and 4*R*-amide selectivity due to a reaction transition to the kinetic control, leading eventually to both high yields and stereoselectivity. Thus, selectivity of the desired products (up to 83%) at 30°C after water addition exceeded the values reported in the literature previously.

A high selectivity to (-)-isopulegol-derived amides with the presence of H_2O was observed on catalysts modified with CSA reaching 84% (4*R*/4*S* of 5.7) in the case of biochar, while a relatively large amount of chromenols (up to 31%) was formed (Table 13, entry 25–27) on the solids functionalized by 2-(4-chlorosulfonylphenyl)ethyltrimethoxysilane (CSP) [316]. While the Prins condensation proceeds on weak acid sites [270–272], the Prins-Ritter reaction requires SO_3H -materials with strong (0.33–5.8 mmol/g) Brønsted acidity. Catalysts functionalized by CSP were stable, while for the solids modified with CSA, leaching of $-\text{SO}_3\text{H}$ groups was observed [316].

13.2. Cascade acetalization and hydroformylation reaction

Condensation of alcohols with aldehydes or ketones, namely acetalization/ketalization reactions, has been used as a strategy to protect carbonyl groups in synthetic chemistry and also as a way to produce ketals and acetals, important substances for pharmaceutical and fine chemical industry [319]. It has been reported that an effective catalyst for acetalization of β -citronellal with aliphatic alcohols is SO_3H -functionalized carbon obtained by pyrolysis of lignocellulosic waste followed by treatment with sulfuric acid. The resulting solids were highly acidic (up to 0.5 mmol/g) and provided both substrate conversion and acetal selectivity of more than 90%.

A promising method for the terpene compounds utilization is tandem hydroformylation/acetalization since it allows access to novel fragrances and flavors in one synthetic step (Figure 28) [320,321]. In [320] hydroformylation of limonene, α - and γ -terpinenes, and terpinolene in ethanol solutions was studied using $[\text{Rh}(\text{COD})(\text{OMe})_2]$ complex (COD = 1,5-cyclooctadiene) as a catalyst precursor with triphenylphosphine (PPh_3) or tris(*o*-^tbutylphenyl) phosphite ($\text{P}(\text{O}-\text{o}-^t\text{BuPh})_3$), as P-donor auxiliary ligands. Limonene

containing an endocyclic double bond gives a desired acetal (Figure 28a) in high yields (up to 90%) in both systems.

Hydroformylation of the conjugated diene, α -terpinene, using PPh_3 occurred with formation of the two corresponding aldehydes (Figure 28b, up to 78%), as well as acetals as minor products (no more than 51%). The use of $\text{P}(\text{O}-o\text{-}^t\text{BuPh})_3$ not only accelerated hydroformylation of the studied substrates but also significantly increased selectivity for acetalization products which in the case of α -terpinene reached 85%.

Hydroformylation of compounds containing hydroxyl groups is problematic, since the resulting aldehydes react with this moiety to give undesirable products [308,321]. To overcome these drawbacks, a protocol was developed that included one-pot hydroformylation and O-acylation by Ac_2O of a number of terpene alcohols in anisole preventing side reactions (Figure 29, [321]). Compounds previously described in [320] were used as a precursor to the catalyst $[\text{Rh}(\text{COD})(\text{OMe})_2]$ and ligands (PPh_3 , $\text{P}(\text{O}-o\text{-}^t\text{BuPh})_3$). In the case of myrtenol and nopol, the acylation step also avoids side isomerization and formation of chelates with rhodium particles.

Isopulegol and isoprenol under hydroformylation/acylation conditions tend to form compounds with the tetrahydropyran ring (up to 55%) due to intramolecular cyclization of the intermediate hydroxyaldehydes. To avoid cyclization, it is necessary that O-acylation occurs faster than hydroformylation, which is achieved by adding an additional catalyst, 4-dimethylaminopyridine (DMAP). This made it possible to completely avoid formation of tetrahydropyran products with high yields of desired acetoxyaldehydes. Overall, selectivity to acetoxyaldehydes (up to 99%) was much higher than to the analogous hydroxyaldehydes produced by hydroformylation only [321].

Another challenging transformation includes hydroaminomethylation of olefin bonds in terpenes. This transformation is a tandem reaction that involves hydroformylation followed by reductive amination (Figure 30) [322]. It is a one-pot process, where the same catalyst is responsible for both hydroformylation of the $\text{C}=\text{C}$ double bond, forming an aldehyde, and the subsequent amination and hydrogenation of the imine-enamine intermediate [323,324], giving finally a secondary or a tertiary amine [325]. Hydroformylation is extensively employed in the chemical industry, with an annual global production of over 10 million metric tons of the corresponding chemicals [326]. It finds applications primarily in the commodity sector but is also utilized in fine chemicals and pharmaceuticals [321]. Selectivity control is crucial, especially for more complex substrates, and it is commonly achieved by adding phosphorus (III) compounds as ligands to the metal complex catalysts [303].

As stated previously, tandem hydroaminomethylation of terpenes consists of the alkene hydroformylation step followed by reductive amination of the resulting aldehydes making it possible to obtain their amino derivatives in one

step [327], as illustrated in Fig. 31. The reaction has been studied using limonene, camphene and β -pinene, amines (di-*n*-butylamine, morpholine or *n*-butylamine) in toluene at 100°C and 60 bar an equimolar mixture of CO and H₂ in the presence of [Rh(cod)(μ -OMe)]₂ as a catalyst precursor with triphenylphosphine or tribenzylphosphine as additives. The yield of the corresponding amines was in the range of 75–94% [327].

In [328], hydroaminomethylation of biomass-derived alkenes (estragole, limonene, camphene, and β -pinene) has been studied using several amines, namely di-*n*-butylamine, morpholine, 4-methylpiperidine or 1,2,3,4-tetrahydroisoquinoline. The results obtained in the presence of *p*-cymene or anisole as solvents are like those for a more toxic toluene. The use of ethanol as a solvent made it possible not only to improve sustainability but also to obtain high yields of amines (up to 81–99%), especially for estragole and β -pinene [328].

Recently, a novel catalytic system based on Rh(I) and Co(0) in glycerol was proposed for the production of amines through the tandem hydroaminomethylation reaction of terpenes (limonene, β -pinene, and camphene) [329]. This system, under optimized conditions, is highly selective to the target amine and avoids hydrogenation of aldehyde-based substrates and intermediates, as well as aldol condensation. Mechanistically, the role of Rh is to promote the initial hydroformylation reaction and, in combination with Co, to promote rapid condensation of the aldehyde and amine, thereby preventing the aldol reaction. In turn, the role of Co and glycerol is to enhance the reduction of the transition enamine through hydrogenation and hydrogen transfer, respectively. It was suggested that only the metal-based molecular compounds are catalytically active, and their agglomeration to form nanoparticle systems leads to loss of activity in hydroaminomethylation [329].

14. Conclusions and perspectives

Terpenes and terpenoids are considered an important platform for synthesis of molecules of special complexity covering different fields not limited only to fragrances, intermediate chemicals, or pharmaceuticals. Because of their reactivity, monoterpenes can be transformed into valuable compounds using the reactions mentioned in this review. Furthermore, terpenes and their derivatives are naturally available representing an unlimited resource to replace current not sustainable industrial processes for the production of drugs, and specialty chemicals, etc. An interest in how terpenes can be transformed and how catalysts can be used has grown in recent years resulting in exploitation of alternative pathways to produce valuable chemicals (Figure 32). In this review, the most recent and relevant transformations of terpenes are discussed covering heterogeneous catalysis with the main emphasis on green chemistry and green chemical engineering.

Monoterpenes compounds, such as α -pinene, β -pinene, and limonene, have been widely recognized as the most investigated substrates for catalytic transformations due to significant abundance in essential oils derived from pine trees and citrus fruits. These compounds have been extensively studied for isomerization, oxidation, epoxidation, hydrogenation, and hydration, resulting in numerous scientific reports. Furthermore, there is a significant body of research on the isomerization of their corresponding epoxides, yielding important products like campholenic aldehyde, myrtanal, and dihydrocarvone from the epoxides of α -pinene, β -pinene, and limonene, respectively. These products find wide applications in various industries. In the case of amination, the literature highlighted the importance of investigating the transformation of myrtenol, a typical product of β -pinene epoxide isomerization, with aniline. This transformation leads to the production of imines and amines with significant industrial relevance. Another challenge in monoterpenes transformation is the valorization of CO_2 through its reaction with epoxides to generate renewable cyclic carbonates. This approach serves as an alternative to conventional (bio)polymers, providing a green alternative reducing intermediate purification steps, by minimizing energy consumption, resources utilization, and waste production.

This review explored alternative ways to oxidize and epoxidize monoterpenes, focusing on robust and stable catalytic systems. Allylic oxidation of compounds like α -pinene, β -pinene, and limonene can create valuable chemicals like verbenone, verbenol, pinocarveol, pinocamphone, etc. Controlling the reactivity of the olefin, oxidizing agent, catalyst structure, and temperature is key to achieving desired products. For epoxidation, more sustainable methods are still being developed, including catalysts with cheaper metals and milder reaction conditions. Developing new epoxide intermediates from terpenes is also valuable for further advancements in synthetic and organic chemistry.

Monoterpenes hold promise for sustainable fuel and chemical production. By hydrogenation routes, we can create jet fuel blends directly from monoterpenes using mild conditions and hydrogenation reactions. However, developing affordable catalysts with abundant metals is crucial for widespread adoption. On the other hand, by hydration pathways, just adding water to common monoterpenes like pinene or limonene using well-designed acidic materials can generate fragrant compounds and molecules with biological applications. The amount and type of acid, along with the water content, determine the specific products formed.

Developing one-pot catalytic pathways for monoterpenes such as α -pinene, β -pinene, and limonene, involving their epoxidation and subsequent isomerization, also represents a significant challenge. Achieving this goal requires establishing suitable reaction conditions, encompassing factors like temperature, solvent choice, oxidant selection, catalyst(s), the oxidant: substrate molar ratio, etc. Crucial consideration in these transformations is the presence of

water, often originating from typical oxidants like H₂O₂ or TBHP, as well as from the solvents. Water has a detrimental effect on high yields of the isomers of monoterpenes epoxides favoring secondary catalytic pathways such as hydration of epoxides and thereby resulting in the production of *trans*-sobrerol and limonene glycol from α -pinene and limonene, respectively. Furthermore, the right choices should be made regarding the acid strength of acidity, nature of the acid sites, and the solvent type. These parameters are highly relevant in the isomerization of these epoxides. Finally, involving terpenoids in cascade reactions makes it possible to produce complex compounds in one pot. On novel heterogeneous catalysts, they selectively proceed under mild conditions and some of the obtained products have approved biological activity.

ABREVIATIONS

Abreviation	Description
Amberlyst (15, 16 or 36)	Acidic Polymeric Resins
BET	Brunauer-Emmett-Teller
COMOC	Gallium-based Metal Organic Framework
COD	1,5-Cyclooctadiene
CSA	Chlorosulfonic Acid
CSP	2-(4-chlorosulfonylphenyl)-ethyltrimethoxysilane
CTAC	cetyltrimethylammonium chloride
DES	Deep Eutectic Solvent
DFT	Density Functional Theory
ee	Enantiomeric excess
E-Factor	Environmental factor
EOs	Essential oils
FA	Formaldehyde
Fe ₃ O ₄ .GO.Im	Magnetite imidazole-modified graphene oxide nanosheet
GHVS	Gas Hourly Space Velocity
HB	Hierarchical Zeolites
HF	Fluorhydric Acid
H2BIAN	bis(4- HOOC-phenyl)-acenaphthenequinonediimine)
HNT	Halloysite nanotubes
HOMO	Highest Occupied Molecular Orbital
HOAc	Acetic acid
HPA	Heteropolyacids
HPW	Heteropolytungstate acid
H ₂ O ₂	Hydrogen Peroxide
IL	Ionic liquid
INTRACEN	International Trade Center
IPA	Isopropanol
KIT-6	Ordered Mesoporous Silica with bicontinuous structure
KL	Kraft lignin
K-10	Montmorillonite K-10
LUMO	Lowest Occupied Molecular Orbital
MCM-41	Mobil Composition of Matter No. 41
MIL	Materials Institute of Lavoisier
MK	Metakaolin
MMF	Metal Macrocycle Framework
MMT	Indian Montmorillonite Clay
MnPor	Manganese based on Porphyrin
MOF	Metal Organic Framework
MPTMS	Mercaptopropyltrimethoxysilane

(Continued)

Abreviation	Description
MWW	Zeolite with structure type MWW-layered zeolite-
NBS	N-bromo Succinimide
NBSA.H ₂ O	Hydrated N-Bromo Succinimide
NTFPs	Non-Timber Forest Products
NT-TiO ₂	Nanotubes based on Titanium Dioxide.
OA	Oxalic Acid
PEG	Polyethyleneglycol
PMI	Process mass intensity
Purolite CT175	Polystyrenic microporous strong acid cation ion exchange resin in the hydrogen form
Q-10	Amorphous Commercial Silica
SAL ₂ Bz	(Z)-3-methyl-1-phenyl-4-(2,2,2-trifluoro-1-(2-hydroxyphenyl)imino)ethyl)-1H-pyrazol-5-ol)
SBA-15	Mesoporous Amorphous Silica coming from Santa Barbara University
SEM	Scanning Electronic Microscopy
SiO ₂	Silicon dioxide
ScCO ₂	Supercritical carbon dioxide
SE	Strain energy.
TBHP	Tert-butyl hydrogen peroxide
TDPI	O-[3-(trimethylammonio)phenyl]-1,3,2-dioxaphosphorinane 2-oxide iodide
TEM	Transmission Electronic Microscopy
TEOS	Tetraethylortosilicate
TiO ₂	Titanium Dioxide
TPA	Tungstophosphoric Acid
TPR	Temperature Programmed Reduction
TPO	Temperature Programmed Oxidation
TPPTS	tris(3-sulfonatphenyl)phosphine trisodium salt
TsOH	p-Toluenesulfonic acid
UHP	urea Hydrogen Peroxide
US	United States
USY	The ultrastable Y zeolite
UV-Vis	Ultraviolet and Visible Radiation
VOCs	Volatile Organic Compounds
WOx	Tungsten oxides
XRD	X-ray Diffraction
ZSM-5	Zeolite Socony Mobil-5

Acknowledgments

Luis A. Gallego-Villada is grateful to Universidad de Antioquia for their support during his research internship (Laboratory of Industrial Chemistry, Process Chemistry Centre, Åbo Akademi University) through the project 2022-53000 as part of the “Convocatoria Programática 2021-2022: Ingeniería y Tecnología” program, as well as the “Beca Doctoral Universidad de Antioquia” scholarship. Julián E. Sánchez-Velandia is grateful to Universidad Jaume I for the postdoctoral position during 2022-2023 (programa Propi UJI) and the project (PID2020-11962RB-C33),MCIN/AEI/10.13039/501100011033/European Union NextGeneration EU/PRTP. Alexander Sidorenko is grateful to National Academy of Sciences of Belarus (program “Wood Chemistry,” project 2.4.1) and State Committee for Science and Technology (X22KITG-026) for financial support.

Disclosure statement

No potential conflict of interest was reported by the author(s).

Funding

This work was supported by the Universidad Jaume I, European Union (project PID2020-11962RB-C33), (MCIN/AEI/10.13039/501100011033/European Union Next Generation EU/PRTP) Universidad de Antioquia (Project 2022-53000), National Academy of Science of Belarus (Program “Wood Chemistry”, project 2.4.1), State Committee for Science and Technology (X22KITG-026) and Abo Akademi University.

ORCID

Julián E. Sánchez-Velandia  <http://orcid.org/0000-0002-4914-6102>

Luis A. Gallego-Villada  <http://orcid.org/0000-0001-6415-3178>

Päivi Mäki-Arvela  <http://orcid.org/0000-0002-7055-9358>

Alexander Sidorenko  <http://orcid.org/0000-0003-1238-2184>

Dmitry Yu. Murzin  <http://orcid.org/0000-0003-0788-2643>

References

- [1] R.A. Sheldon. The E Factor: Fifteen Years on. *Green Chem.* 2007, 9, 1273–1283. DOI: 10.1039/b713736m.
- [2] C. Lucarelli, A. Vaccari. Examples of Heterogeneous Catalytic Processes for Fine Chemistry. *Green Chem.* 2011, 13, 1941. DOI: 10.1039/c0gc00760a.
- [3] H.-U. Blaser. Heterogeneous Catalysis for Fine Chemicals Production. *Catal. Today.* 2000, 60(3–4), 161–165. DOI: 10.1016/S0920-586100332-1.
- [4] V. Garcia. Cabassud, M., Le Lann, M.V., Pibouleau, L., Casamatta, G. Constrained Optimization for Fine Chemical Productions in Batch Reactors. *The Chemical Engineering Journal and the Biochemical Engineering Journal.* 1995, 59(3), 229–241. DOI: 10.1016/0923-0467(94)02949-0.
- [5] M. Le Lann. Modeling, Optimization and Control of Batch Chemical Reactors in Fine Chemical Production. *Annual Reviews in Control.* 1999, 23(1), 25–34. DOI: 10.1016/S1367-5788(99)00004-8.
- [6] S. Herman. Fragrance. In *Cosmetic Science and Technology: Theoretical Principles and Applications*; K. Sakamoto, R.Y. Lochhead, H.I. Maibach, Y. Yamashita, Eds.; United States, 2017; pp 1–835.
- [7] J.-L. Ríos. Essential Oils: What They are and How the Terms are Used and Defined. In *Essent. Oils Food Preserv*; Flavor Saf., Elsevier: 2016; pp 3–10. doi:10.1016/B978-0-12-416641-7.00001-8
- [8] M. Hyltdgaard, T. Mygind, R.L. Meyer. Essential Oils in Food Preservation: Mode of Action, Synergies, and Interactions with Food Matrix Components. *Front. Microbiol.* 2012, 3, 1–24. DOI: 10.3389/fmicb.2012.00012.
- [9] G. de J. Montoya-Cadavid, Aceites esenciales: Una alternativa de diversificación para el eje cafetero, 2010. <http://bdigital.unal.edu.co/50956/7/9588280264.pdf>.
- [10] E.E. Stashenko. *Aceites Esenciales*; Bucaramanga, Colombia, 2009.
- [11] T. Map, Trade Map, (n.d.) https://www.trademap.org/Country_SelProduct_TS.aspx?nvpm=1%7C%7C%7C%7C%7C3301%7C%7C%7C4%7C1%7C1%7C1%7C2%7C1%7C2%7C1%7C1%7C1 (accessed June 19, 2023).
- [12] Gross Domestic Product, Fourth Quarter and Year 2022 (Third Estimate), GDP by Industry, and Corporate Profits | U.S. Bureau of Economic Analysis (BEA), (2023).

- <https://www.bea.gov/news/2023/gross-domestic-product-fourth-quarter-and-year-2022-third-estimate-gdp-industry-and> (accessed June 19, 2023).
- [13] Noma, Y. Asakawa Y. Biotransformation of Monoterpenoids. *Compr. Nat. Prod.* 2010, *II*, 669–801. DOI: [10.1016/B978-008045382-8.00742-5](https://doi.org/10.1016/B978-008045382-8.00742-5).
- [14] R. Marmulla, J. Harder. Microbial Monoterpene transformations-a Review. *Front. Microbiol.* 2014, *5*, 1–14. DOI: [10.3389/fmicb.2014.00346](https://doi.org/10.3389/fmicb.2014.00346).
- [15] L.A. Baltina, N.G. Komissarova. Transformations of Pentacyclic Triterpenoids as a Route to the Future Medicines. *Stud. Nat. Prod. Chem.* 2023, 331–407. DOI: [10.1016/B978-0-323-91296-9.00001-0](https://doi.org/10.1016/B978-0-323-91296-9.00001-0).
- [16] A. Wawoczny, D. Gillner. The Most Potent Natural Pharmaceuticals, Cosmetics, and Food Ingredients Isolated from Plants with Deep Eutectic Solvents. *J. Agric. Food Chem.* 2023, *71*, 10877–10900. DOI: [10.1021/acs.jafc.3c01656](https://doi.org/10.1021/acs.jafc.3c01656).
- [17] T.M. Bennett, J. Portal, V. Jeanne-Rose, S. Taupin, A. Ilchev, D.J. Irvine, S.M. Howdle. Synthesis of Model terpene-derived Copolymers in Supercritical Carbon Dioxide for Cosmetic Applications. *Eur. Polym. J.* 2021, *157*, 110621. DOI: [10.1016/j.eurpolymj.2021.110621](https://doi.org/10.1016/j.eurpolymj.2021.110621).
- [18] Terpenes and Isoprenoids: A Wealth of Compounds for Global Use. *Planta* 2019, *249*, 1–8. DOI: [10.1007/s00425-018-3056-x](https://doi.org/10.1007/s00425-018-3056-x).
- [19] Y. Zhang, F. Seidi, M. Ahmad. Zheng, L. L.Cheng, Y. Huang, H. Xiao. Green and Sustainable Natural Derived Polysulfides for a Broad Range of Applications. *Green Chem.* 2023. DOI: [10.1039/D3GC02005C](https://doi.org/10.1039/D3GC02005C).
- [20] W. Cho, J. Hwang, S.Y. Lee, J. Park, N. Han, C.H. Lee, S. Kang, A. Urbas, J.O. Kim, Z. Ku, J.J. Wie. Highly Sensitive and Cost-Effective Polymeric-Sulfur-Based Mid-Wavelength Infrared Linear Polarizers with Tailored Fabry–Pérot Resonance. *Adv. Mater.* 2023, *35*, 2209377. DOI: [10.1002/adma.202209377](https://doi.org/10.1002/adma.202209377).
- [21] A. Manthiram, Y. Fu, S. Chung, C. Zu, Y. Su. *Rechar. Lithium–Sulfur Batt., Chem. Rev* 2014, *114*, 11751–11787. DOI: [10.1021/cr500062v](https://doi.org/10.1021/cr500062v).
- [22] Z.W. Seh, Y. Sun, Q. Zhang, Y. Cui. Designing high-energy lithium–sulfur Batteries. *Chem. Soc. Rev.* 2016, *45*, 5605–5634. DOI: [10.1039/C5CS00410A](https://doi.org/10.1039/C5CS00410A).
- [23] F.G. Müller, L.S. Lisboa, J.M. Chalker. Inverse Vulcanized Polymers for Sustainable Metal Remediation. *Adv. Sustain. Syst.* 2023, *7*. DOI: [10.1002/advsu.202300010](https://doi.org/10.1002/advsu.202300010).
- [24] N.A. Lundquist, Y. Yin, M. Mann, S.J. Tonkin, A.D. Slattery, G.G. Andersson, C. T. Gibson, J.M. Chalker. Magnetic Responsive Composites Made from a sulfur-rich Polymer. *Polym. Chem.* 2022, *13*, 5659–5665. DOI: [10.1039/D2PY00903J](https://doi.org/10.1039/D2PY00903J).
- [25] S.K. Bajpai, D. Dubey. Removal of Oil from Oil-in-Water Emulsion by Poly (Sulfur/Soya Bean Oil) Composite Adsorbent: An Equilibrium Study. *J. Polym. Environ.* 2021, *29*, 2385–2396. DOI: [10.1007/s10924-020-02032-y](https://doi.org/10.1007/s10924-020-02032-y).
- [26] M.J.H. Worthington, C.J. Shearer, L.J. Esdaile, J.A. Campbell, C.T. Gibson, S.K. Legg, Y. Yin, N.A. Lundquist, J.R. Gascooke, I.S. Albuquerque, J.G. Shapter, G.G. Andersson, D.A. Lewis, G.J.L. Bernardes, J.M. Chalker. Sustainable Polysulfides for Oil Spill Remediation: Repurposing Industrial Waste for Environmental Benefit. *Adv. Sustain. Syst.* 2018, *2*, 1800024. DOI: [10.1002/advsu.201800024](https://doi.org/10.1002/advsu.201800024).
- [27] M. Mann, J.E. Kruger, F. Andari, et al Sulfur Polymer Composites as controlled-release Fertilisers. *Org. Biomol. Chem* 2019, *17*, 1929–1936. DOI: [10.1039/C8OB02130A](https://doi.org/10.1039/C8OB02130A).
- [28] J.A. Smith, R. Mulhall, S. Goodman, G. Fleming, H. Allison, R. Raval, T. Hasell. Investigating the Antibacterial Properties of Inverse Vulcanized Sulfur Polymers. *ACS Omega.* 2020, *5*, 5229–5234. DOI: [10.1021/acsomega.9b04267](https://doi.org/10.1021/acsomega.9b04267).
- [29] R.A. Dop, D.R. Neill, T. Hasell. Antibacterial Activity of Inverse Vulcanized Polymers. *Biomacromolecules.* 2021, *22*, 5223–5233. DOI: [10.1021/acs.biomac.1c01138](https://doi.org/10.1021/acs.biomac.1c01138).

- [30] R. De Cássia Da Silveira E Sá, L.N. Andrade, D.P. De Sousa. A Review on anti-inflammatory Activity of Monoterpenes. *Molecules*. 2013, 18, 1227–1254. DOI: 10.3390/molecules18011227.
- [31] A.G. Guimarães, J.S.S. Quintans, L.J. Quintans-Júnior. Monoterpenes with Analgesic Activity-A Systematic Review. *Phyther. Res.* 2013, 27, 1–15. DOI: 10.1002/ptr.4686.
- [32] M.R. V. Santos, F. V. Moreira, B.P. Fraga, D.P. de Souza, L.R. Bonjardim, L.J. Quintans-Junior. Cardiovascular Effects of Monoterpenes: A Review. *Rev. Bras. Farmacogn.* 2011, 21, 764–771. DOI: 10.1590/S0102-695X2011005000119.
- [33] J.A. Gallo Corredor, R.A. Sarria Villa. Obtención de Colofonia y Trementina a Partir de Resina de Pino de la Especie patula y Posterior Evaluación de los Parámetros de Calidad. *Cienc. E Ing.* 2013, 5, 88–91.
- [34] J.L.G. Wong, K. Thornber, N. Baker. Evaluación de los recursos de productos forestales no madereros. 2001.
- [35] F.A. Neis, F. de Costa, A.T. de Araújo, J.P. Fett, A.G. Fett-Neto. Multiple Industrial Uses of non-wood Pine Products. *Ind. Crop Prod.* 2019, 130, 248–258. DOI: 10.1016/j.indcrop.2018.12.088 .
- [36] K.C. da Silva Rodrigues-Corrêa, J.C. de Lima, A.G. Fett-Neto. Oleoresins from Pine: Production and Industrial Uses. In *Nat. Prod*; Springer: Berlin Heidelberg, Berlin, Heidelberg, 2013; 4037–4060. DOI:10.1007/978-3-642-22144-6_175 .
- [37] L. Phun, D. Snead, P. Hurd, F. Jing. Industrial Applications of Pine-Chemical-Based Materials. In *Sustain. Polym. from Biomass*; Wiley-VCH Verlag GmbH & Co. KGaA: 2017; pp 151–179. doi:10.1002/9783527340200
- [38] A. Rodríguez-García, J.A. Martín, R. López, S. Mutke, F. Pinillos, L. Gil. Influence of climate Variables on Resin Yield and Secretory Structures in Tapped Pinus Pinaster Ait. in Central Spain. *Agric. For. Meteorol.* 2015, 202, 83–93. DOI: 10.1016/j.agrformet.2014.11.023.
- [39] R. Vallinayagam, S. Vedharaj, W.M. Yang, W.L. Roberts, R.W. Dibble. Feasibility of Using Less Viscous and Lower Cetane (LVLC) Fuels in A Diesel Engine: A Review. *Renew. Sustain. Energy Rev.* 2015, 51, 1166–1190. DOI: 10.1016/j.rser.2015.07.042 .
- [40] M. Yi, T. Jia, Dong, L. LZhang, C. Leng, S. Liu, M. Lai. Resin Yield in Pinus Elliottii Engelm. Is Related to the Resin Flow Rate, Resin Components and Resin Duct Characteristics at Three Locations in Southern China. *Ind. Crops Prod.* 2021, 160, 113141. DOI: 10.1016/j.indcrop.2020.113141.
- [41] Center for International Forestry Research, Pine Resin, 2004. <https://www.jstor.org/stable/resrep02039.28>.
- [42] D. Arias, Y. Guillén, C. M. López, F. J. Machado. Turpentine Oil Hydration Using Dealuminated Faujasite as Catalyst. *React.Kinet.Catal.Lett.* 2000, 69, 305–309. DOI: 10.1023/A:1005604017605.
- [43] L. Gallego-Villada, Estudio de pre-factibilidad técnica y económica de la producción de α -terpineol con el catalizador Amberlyst 15. Undergraduate Thesis, Universidad de Antioquia, Medellín, 2017.
- [44] H. Utami, A. Budiman, S. Sutijan, R. Roto, W.B. Sediawan. Synthesis of α -Terpineol from Turpentine by Hydration in a Batch Reactor, 17th ASEAN Reg. *Symp. Chem. Eng.* 2010, 1–5.
- [45] A. Budiman, T.I. Arifta, Diana, Sutijan. Continuous Production of α -Terpineol from α -Pinene Isolated from Indonesian Crude Turpentine. *Mod. Appl. Sci.* 2015, 9, 225–232. DOI: 10.5539/mas.v9n4p225.
- [46] N. Wijayati, H.D. Pranowo, J. Jumina, T. Triyono. Turpentine Oil Hydration Using Trichloroacetic Acid as Catalyst. *Am. J. Oil Chem. Technol.* 2013, 1, 21–26.

- [47] Severino, A., et al Effect of extra-lattice Aluminium Species on the Activity, Selectivity and Stability of Acid Zeolites in the Liquid Phase Isomerisation of α -pinene. *Appl. Catal. A Gen.* **1996**, *142*, 255–278. DOI: [10.1016/0926-860X\(96\)00091-9](https://doi.org/10.1016/0926-860X(96)00091-9) .
- [48] N.A. Comelli, E.N. Ponzi, et al α -Pinene Isomerization to camphene Effect of Thermal Treatment on Sulfated Zirconia. *Chem. Eng. J.* **2006**, *117*, 93–99. DOI: [10.1016/j.cej.2005.08.006](https://doi.org/10.1016/j.cej.2005.08.006).
- [49] V.M. Vaschetti, A.L. Cánepa, D. Barrera, K. Sapag, G.A. Eimer, S.G. Casuscelli. Limonene Oxyfunctionalization over Cu-modified Silicates Employing Hydrogen Peroxide and t-Butyl Hydroperoxide: Reaction Pathway Analysis. *Mol. Catal.* **2020**, *481*, 110234. DOI: [10.1016/j.mcat.2018.11.005](https://doi.org/10.1016/j.mcat.2018.11.005).
- [50] M.A. Ardagh, D.T. Bregante, D.W. Flaherty, J.M. Notestein. Controlled Deposition of Silica on Titania-Silica to Alter the Active Site Surroundings on Epoxidation Catalysts. *ACS Catal.* **2020**, *10*, 13008–13018. DOI: [10.1021/acscatal.0c02937](https://doi.org/10.1021/acscatal.0c02937).
- [51] E.B. Russo, J. Marcu. Cannabis Pharmacology: The Usual Suspects and a Few Promising Leads; *Adv. Pharmacol.* **2017**; 67–134. [10.1016/bs.apha.2017.03.004](https://doi.org/10.1016/bs.apha.2017.03.004).
- [52] S. V. Bhat, M.O. Gupta, K.R. Vaze. A Mild Synthetic Method for Selective Conversion of Camphene to Isoborneol Derivatives. *Org. Prep. Proced. Int.* **2023**, 1–6. DOI: [10.1080/00304948.2023.2219198](https://doi.org/10.1080/00304948.2023.2219198) .
- [53] D. Ponomarev, H. Mettee. Camphor and Its Industrial Synthesis. *Chem. Educ. J.* **2016**, *18*, 1–4.
- [54] A.S. Sokolova, O.I. Yarovaya, M.D. Semenova, A.A. Shtro, I.R. Orshanskaya, V. V. Zarubaev, N.F. Salakhutdinov. Synthesis and in Vitro Study of Novel Borneol Derivatives as Potent Inhibitors of the Influenza A Virus. *Medchemcomm.* **2017**, *8*, 960–963. DOI: [10.1039/C6MD00657D](https://doi.org/10.1039/C6MD00657D).
- [55] R.K. V. Nunes, U.N. Martins, T.B. Brito, A. Nepel, E. V. Costa, A. Barison, R.L.C. Santos, S.C.H. Cavalcanti. Evaluation of (–)-borneol Derivatives against the Zika Vector, *Aedes Aegypti* and a non-target Species. *Artemia Sp., Environ. Sci. Pollut. Res.* **2018**, *25*, 31165–31174. DOI: [10.1007/s11356-018-2809-1](https://doi.org/10.1007/s11356-018-2809-1) .
- [56] C. Su, X. Luo, J. Chen, D. Wu, L. Fan, J. Liu, H. Zheng. Effective Synthesis of Limonene over Mild alkali-modified 13X Catalysts in α -pinene Isomerization. *Microporous Mesoporous Mater.* **2023**, *348*, 112369. DOI: [10.1016/j.micromeso.2022.112369](https://doi.org/10.1016/j.micromeso.2022.112369).
- [57] P.S. Sinhmar, P.R. Gogate. Improved Activation of Titanium Dioxide Catalyst for Isomerization of Alpha Pinene and Understanding into Effect of Isomerization Parameters. *Arab. J. Sci. Eng.* **2022**, *47*, 5875–5893. DOI: [10.1007/s13369-021-05706-4](https://doi.org/10.1007/s13369-021-05706-4) .
- [58] A. Kamińska, P. Miądlicki, K. Kielbasa, M. Kujbida, J. Sreńscek-Nazzal, R.J. Wróbel, A. Wróblewska. Activated Carbons Obtained from Orange Peels, Coffee Grounds, and Sunflower Husks—Comparison of Physicochemical Properties and Activity in the Alpha-Pinene Isomerization Process. *Materials (Basel)*. **2021**, *14*, 7448. DOI: [10.3390/ma14237448](https://doi.org/10.3390/ma14237448).
- [59] Y. Liu, D. Zheng, B. Li, Y. Lyu, Wang, X. X.Liu, L. Li, S. Yu, X. Liu, Z. Yan. Isomerization of α -pinene with a Hierarchical Mordenite Molecular Sieve Prepared by the Microwave Assisted Alkaline Treatment. *Microporous Mesoporous Mater.* **2020**, *299*, 110117. DOI: [10.1016/j.micromeso.2020.110117](https://doi.org/10.1016/j.micromeso.2020.110117) .
- [60] X. Wang, L. Chen, D. Huang, J. Yue, Z. Luo, T. Zeng. The Modification, Characterization of H-Mordenite and Their Catalytic Activity in Isomerization of α -Pinene. *Catal. Letters.* **2018**, *148*, 3492–3501. DOI: [10.1007/s10562-018-2547-5](https://doi.org/10.1007/s10562-018-2547-5).
- [61] M. Gackowski, Ł. Kuterasiński, J. Podobiński, A. Korzeniowska, B. Sulikowski, J. Datka. Hierarchical Zeolite Mazzite: Physicochemical Properties and α -pinene Isomerization. *Appl. Catal. A Gen.* **2019**, *578*, 53–62. DOI: [10.1016/j.apcata.2019.03.016](https://doi.org/10.1016/j.apcata.2019.03.016).

- [62] J.E. Sánchez-Velandia, E. Pájaro, A.L. Villa, F. Martínez-O. Selective Synthesis of Camphene from Isomerization of α - and β -pinene over Heterogeneous Catalysts. *Microporous Mesoporous Mater.* **2021**, *324*, 111273. DOI: [10.1016/j.micromeso.2021.111273](https://doi.org/10.1016/j.micromeso.2021.111273).
- [63] W. He, S. Tashiro, M. Shionoya. Highly Selective acid-catalyzed Olefin Isomerization of Limonene to Terpinolene by Kinetic Suppression of Overreactions in a Confined Space of Porous metal-macrocycle Frameworks. *Chem. Sci.* **2022**, *13*, 8752–8758. DOI: [10.1039/D2SC01561G](https://doi.org/10.1039/D2SC01561G).
- [64] C.P. Tavera Ruiz, P. Gauthier-Maradei, M. Capron, C. Pirez, O. Gardoll, B. Katryniok, F. Dumeignil. Transformation of DL Limonene into Aromatic Compounds Using Supported Heteropolyacid Catalysts. *Catal. Letters.* **2019**, *149*, 328–337. DOI: [10.1007/s10562-018-2606-y](https://doi.org/10.1007/s10562-018-2606-y).
- [65] S.A. Sanchez-Vazquez, T.D. Sheppard, J.R.G. Evans, H.C. Hailes. The Selective Conversion of D-limonene to p, α -dimethylstyrene. *RSC Adv.* **2014**, *4*, 61652–61655. DOI: [10.1039/C4RA11558A](https://doi.org/10.1039/C4RA11558A).
- [66] B. Środa, A.G. Dymerska, P. Miądlicki, A. Wróblewska, B. Zielińska. Ti3C2 MXenes-based Catalysts for the Process of α -pinene Isomerization. *RSC Adv.* **2023**, *13*, 30281–30292. DOI: [10.1039/D3RA05055F](https://doi.org/10.1039/D3RA05055F).
- [67] J. Čejka, R. Millini, M. Opanasenko, D.P. Serrano, W.J. Roth. Advances and Challenges in Zeolite Synthesis and Catalysis. *Catal. Today.* **2020**, *345*, 2–13. DOI: [10.1016/j.cattod.2019.10.021](https://doi.org/10.1016/j.cattod.2019.10.021).
- [68] W. Schwieger, A.G. Machoke, T. Weissenberger, A. Inayat, T. Selvam, M. Klumpp. Hierarchy Concepts: Classification and Preparation Strategies for Zeolite Containing Materials with Hierarchical Porosity. *Chem. Soc. Rev.* **2016**, *45*, 3353–3376. DOI: [10.1039/C5CS00599J](https://doi.org/10.1039/C5CS00599J).
- [69] Hartmann, M. MThommes, W. Schwieger. Hierarchically-Ordered Zeolites: A Critical Assessment. *Adv. Mater. Interfaces.* **2021**, *8*, 2001841. DOI: [10.1002/admi.202001841](https://doi.org/10.1002/admi.202001841).
- [70] J.M. Escola, D.P. Serrano, Sanz, R.R.A. Garcia, A. Peral, I. Moreno, M. Linares. Synthesis of Hierarchical Beta Zeolite with Uniform Mesopores: Effect on Its Catalytic Activity for Veratrole Acylation. *Catal. Today.* **2018**, *304*, 89–96. DOI: [10.1016/j.cattod.2017.08.005](https://doi.org/10.1016/j.cattod.2017.08.005).
- [71] J. Zhu, Y. Zhu, L. Zhu, M. Rigutto, A. van der Made, C. Yang, S. Pan, L. Wang, et al. Highly Mesoporous Single-Crystalline Zeolite Beta Synthesized Using a Nonsurfactant Cationic Polymer as a Dual-Function Template. *J. Am. Chem. Soc.* **2014**, *136*, 2503–2510. DOI: [10.1021/ja411117y](https://doi.org/10.1021/ja411117y).
- [72] S. Soltanali, J.T. Darian. Synthesis of Mesoporous Beta Catalysts in the Presence of Carbon Nanostructures as Hard Templates in MTO Process. *Microporous Mesoporous Mater.* **2019**, *286*, 169–175. DOI: [10.1016/j.micromeso.2019.05.013](https://doi.org/10.1016/j.micromeso.2019.05.013).
- [73] Y. Zhou, Q. Deng, D. Deng, W. Liu, M. Zhai, Z. Wang, L. Han, K. Zhu. Multiscale Structural Control of MFI Zeolite Using poly-quaternary Ammonium Cation. *J. Mater. Chem. A.* **2023**, *11*, 15702–15716. DOI: [10.1039/D3TA02066E](https://doi.org/10.1039/D3TA02066E).
- [74] M.W. Giese, M.A. Lewis, L. Giese, K.M. Smith. Development and Validation of a Reliable and Robust Method for the Analysis of Cannabinoids and Terpenes in Cannabis. *J. AOAC Int.* **2015**, *98*, 1503–1522. DOI: [10.5740/jaoacint.15-116](https://doi.org/10.5740/jaoacint.15-116).
- [75] A. Hazekamp, K. Tejkalová, S. Papadimitriou. Cannabis: From Cultivar to Chemovar II —A Metabolomics Approach to Cannabis Classification. *Cannabis Cannabi. Res.* **2016**, *1*, 202–215. DOI: [10.1089/can.2016.0017](https://doi.org/10.1089/can.2016.0017).
- [76] J. Graßmann, S. Hippeli, R. Spitzenberger, E.F. Elstner. The Monoterpene Terpinolene from the Oil of Pinus Mugo L. in Concert with α -tocopherol and β -carotene Effectively Prevents Oxidation of LDL. *Phytomedicine.* **2005**, *12*, 416–423. DOI: [10.1016/j.phymed.2003.10.005](https://doi.org/10.1016/j.phymed.2003.10.005).

- [77] E. Aydin, H. Türkez, Ş. Taşdemir. Anticancer and Antioxidant Properties of Terpinolene in Rat Brain Cells. *Arch. Ind. Hyg. Toxicol.* **2013**, *64*, 415–424. DOI: [10.2478/10004-1254-64-2013-2365](https://doi.org/10.2478/10004-1254-64-2013-2365).
- [78] Y. Jeon, W.S. Chi, J. Hwang, et al Core-shell Nanostructured Heteropoly acid-functionalized metal-organic Frameworks: Bifunctional Heterogeneous Catalyst for Efficient Biodiesel Production. *Appl. Catal. B.* **2019**, *242*, 51–59. DOI: [10.1016/j.apcatb.2018.09.071](https://doi.org/10.1016/j.apcatb.2018.09.071).
- [79] L.A. Gallego-Villada, E.A. Alarcón, V. Palermo, P.G. Vázquez, G.P. Romanelli. Kinetics for the Biodiesel Production from Lauric Acid over Keggin Heteropolyacid Loaded in Silica Framework. *J. Ind. Eng. Chem.* **2020**, *92*, 109–119. DOI: [10.1016/j.jiec.2020.08.030](https://doi.org/10.1016/j.jiec.2020.08.030).
- [80] L.A. Gallego-Villada, E.A. Alarcón, D.M. Ruiz, G.P. Romanelli. Kinetic Study of the Esterification of t-cinnamic Acid over Preyssler Structure Acid. *Mol. Catal.* **2022**, *528*, 112507. DOI: [10.1016/j.mcat.2022.112507](https://doi.org/10.1016/j.mcat.2022.112507).
- [81] L.A. Gallego-Villada, E.A. Alarcón, C. Cerrutti, G. Blustein, Á.G. Sathicq, G. P. Romanelli. Levulinic Acid Esterification with N -butanol over A Preyssler Catalyst in A Microwave-Assisted Batch Reactor: A Kinetic Study. *Ind. Eng. Chem. Res.* **2023**, *62*, 10915–10929. DOI: [10.1021/acs.iecr.3c00893](https://doi.org/10.1021/acs.iecr.3c00893).
- [82] H. Kim, J.C. Jung, P. Kim, K.-Y. Lee, S.H. Yeom, I.K. Song, Preparation of heteropolyacid/carbon Catalyst and Its Application to Methacrolein Oxidation, *Stud. Surf. Sci. Catal.*, Elsevier Masson SAS, **2006**: pp. 801–808. [10.1016/S0167-2991\(06\)80983-3](https://doi.org/10.1016/S0167-2991(06)80983-3).
- [83] L.L. Name, S.H. Toma, H. Pereira Nogueira, L.H. Avanzi, R. Dos S. Pereira, L.F. Peffi Ferreira, K. Araki, R. Cella, M.M. Toyama. Phosphotungstic Acid Impregnated Niobium Coated Superparamagnetic Iron Oxide Nanoparticles as Recyclable Catalyst for Selective Isomerization of Terpenes. *RSC Adv.* **2021**, *11*, 14203–14212. DOI: [10.1039/D1RA00012H](https://doi.org/10.1039/D1RA00012H).
- [84] H. Cui, J. Zhang, Z. Luo, C. Zhao. Mechanisms into Dehydroaromatization of bio-derived Limonene to p-cymene over Pd/HZSM-5 in the Presence and Absence of H₂. *RSC Adv.* **2016**, *6*, 66695–66704. DOI: [10.1039/C6RA17159A](https://doi.org/10.1039/C6RA17159A).
- [85] The Good Scents Company, para-alpha-dimethyl Styrene, (2021). <https://www.thegoodscentscompany.com/data/rw1018551.html> (accessed October 23, 2023).
- [86] A.M. Api. Belsito, D. DBotelho, M. Bruze, G.A. Burton, M.A. Cancellieri, H. Chon, M. L. Dagli, M. Date, W. Dekant, C. Deodhar, A.D. Fryer, L. Jones, K. Joshi, M. Kumar, A. Lapczynski, M. Lavelle, I. Lee, D.C. Liebler, H. Moustakas, M. Na, T.M. Penning, G. Ritacco, J. Romine, N. Sadekar, T.W. Schultz, D. Selechnik, F. Siddiqi, I.G. Sipes. RIFM Fragrance Ingredient Safety Assessment, p,α-dimethylstyrene, CAS Registry Number 1195-32-0. *Food Chem. Toxicol.* **2022**, *169*, 113390. DOI: [10.1016/j.fct.2022.113390](https://doi.org/10.1016/j.fct.2022.113390).
- [87] M.A. Vannice. *Kinetics of Catalytic Reactions*, 1st ed.; Springer: New York, NY, **2005**.
- [88] H.S. Fogler. *Elements of Chemical Reaction Engineering*, 5th ed.; Prentice Hall, **2011**.
- [89] M.P. Stevens. *Polymer Chemistry: An Introduction*. **1999**.
- [90] E. Louisy, V. Khodyrieva, S. Olivero, V. Michelet, A. Mija. Use of Limonene Epoxides and Derivatives as Promising Monomers for Biobased Polymers. *Chempluschem.* **2022**, *87*, 1–9. DOI: [10.1002/cplu.202200190](https://doi.org/10.1002/cplu.202200190).
- [91] G. Majetich, J. Shimkus, Y. Li. Epoxidation of Olefins by β-bromoalkoxydimethylsulfonium Ylides. *Tetrahedron Lett.* **2010**, *51*, 6830–6834. DOI: [10.1016/j.tetlet.2010.10.068](https://doi.org/10.1016/j.tetlet.2010.10.068).
- [92] H. Guo, X. Lu, J. He. Zhang, H. HZhang, Y. Dong, D. Zhou, Q. Xia. Co-MOF Nanosheet Supported on ZSM-5 with an Improved Catalytic Activity for Air Epoxidation of Olefins. *Mater. Chem. Phys.* **2023**, *294*, 127001. DOI: [10.1016/j.matchemphys.2022.127001](https://doi.org/10.1016/j.matchemphys.2022.127001).

- [93] C. Wang, H. Zhan, X. Lu, R. Jing, H. Zhang, L. Yang, X. Li, F. Yue, D. Zhou, Q. Xia. A Recyclable Cobalt(III)-ammonia Complex Catalyst for Catalytic Epoxidation of Olefins with Air as the Oxidant. *New J. Chem.* **2021**, *45*, 2147–2156. DOI: [10.1039/d0nj05466f](https://doi.org/10.1039/d0nj05466f).
- [94] M.S. Nunes, D.M. Gomes, A.C. Gomes, P. Neves, R.F. Mendes, F.A.A. Paz, A.D. Lopes, A.A. Valente, I.S. Gonçalves, M. Pillinger. A 5-(2-Pyridyl)tetrazolate Complex of Molybdenum(VI), Its Structure, and Transformation to A Molybdenum Oxide-Based Hybrid Heterogeneous Catalyst for the Epoxidation of Olefins. *Catalysts*. **2021**, *11*, 1407. DOI: [10.3390/catal11111407](https://doi.org/10.3390/catal11111407).
- [95] R. Hajian, E. Bahrami. Mn(III)-Porphyrin Immobilized on the Graphene Oxide-Magnetite Nanocomposite as an Efficient Heterogeneous Catalyst for the Epoxidation of Alkenes. *Catal. Letters*. **2022**, *152*, 2445–2456. DOI: [10.1007/s10562-021-03827-x](https://doi.org/10.1007/s10562-021-03827-x).
- [96] M. Vasconcellos-Dias, C.D. Nunes, V. Félix, P. Brandão, M.J. Calhorda. New Heptacoordinate tungsten(II) Complexes with α -diimine Ligands in the Catalytic Oxidation of Multifunctional Olefins. *Inorganica Chim. Acta*. **2021**, *519*, 120263. DOI: [10.1016/j.ica.2021.120263](https://doi.org/10.1016/j.ica.2021.120263).
- [97] Y. Tao, O. De Luca, B. Singh, A.J. Kamphuis, J. Chen, Rudolf, P. Pescarmona, WO₃-SiO₂ Nanomaterials Synthesized Using a Novel template-free Method in Supercritical CO₂ as Heterogeneous Catalysts for Epoxidation with H₂O₂. *Mater. Today Chem*. **2020**, *18*, 100373. DOI: [10.1016/j.mtchem.2020.100373](https://doi.org/10.1016/j.mtchem.2020.100373).
- [98] D.K. Parmar, P.M. Butani, N.J. Thumar, P.M. Jasani, R. V. Padaliya, P.R. Sandhiya, H. D. Nakum, M.N. Khan, D. Makwana. Oxy-functionalization of Olefins with Neat and Heterogenized Binuclear V(IV)O and Fe(II) Complexes: Effect of Steric Hindrance on Product Selectivity and Output in Homogeneous and Heterogeneous Phase. *Mol. Catal.* **2019**, *474*, 110424. DOI: [10.1016/j.mcat.2019.110424](https://doi.org/10.1016/j.mcat.2019.110424).
- [99] J. Marreiros, Diaz-Couce, M.J. Ferreira, P.D. Vaz, M.J. Calhorda, C.D. Nunes. Synthesis and Catalytic Activity of Mo(II) Complexes of α -diimines Intercalated in Layered Double Hydroxides. *Inorganica Chim. Acta*. **2019**, *486*, 274–282. DOI: [10.1016/j.ica.2018.10.062](https://doi.org/10.1016/j.ica.2018.10.062).
- [100] S. Madadi, J.-Y. Bergeron, S. Kaliaguine. Kinetic Investigation of Aerobic Epoxidation of Limonene over Cobalt Substituted Mesoporous SBA-16. *Catal. Sci. Technol.* **2021**, *11*, 594–611. DOI: [10.1039/D0CY01700K](https://doi.org/10.1039/D0CY01700K).
- [101] C. Bisio, A. Gallo, R. Psaro, C. Tiozzo, M. Guidotti, F. Carniato. Tungstenocene-grafted Silica Catalysts for the Selective Epoxidation of Alkenes. *Appl. Catal. A Gen.* **2019**, *581*, 133–142. DOI: [10.1016/j.apcata.2019.05.027](https://doi.org/10.1016/j.apcata.2019.05.027).
- [102] C.K. Modi, R.S. Vithalani, D.S. Patel, N.N. Som, P.K. Jha. Zeolite-Y Entrapped metallo-pyrazolone Complexes as Heterogeneous Catalysts: Synthesis, Catalytic Aptitude and Computational Investigation. *Microporous Mesoporous Mater.* **2018**, *261*, 275–285. DOI: [10.1016/j.micromeso.2017.10.043](https://doi.org/10.1016/j.micromeso.2017.10.043).
- [103] H. Zhang, X. Lu, L. Yang, Y. Hu, M. Yuan, C. Wang, Q. Liu, F. Yue, D. Zhou, Q. Xia. Efficient Air Epoxidation of Cycloalkenes over bimetal-organic Framework ZnCo-MOF Materials. *Mol. Catal.* **2021**, *499*, 111300. DOI: [10.1016/j.mcat.2020.111300](https://doi.org/10.1016/j.mcat.2020.111300).
- [104] J.E. Sánchez-Velandia, L.M. Valdivieso, F. Martínez O, S.M. Mejía, A.L. Villa, J. Wärnä, D.Y. Murzin. Synthesis of trans-pinocarveol from Oxidation of β -pinene Using Multifunctional Heterogeneous Catalysts. *Mol. Catal.* **2023**, *541*, 113104. DOI: [10.1016/j.mcat.2023.113104](https://doi.org/10.1016/j.mcat.2023.113104).
- [105] V.I. Anikeev, I. V. Il'ina, S.Y. Kurbakova, A.A. Nefedov, K.P. Volcho, N. F. Salakhutdinov. Oxidation of α -pinene by Atmospheric Oxygen in the Supercritical

- CO₂—ethyl Acetate System in the Presence of Co(II) Complexes. *Russ. J. Phys. Chem. A.* **2012**, *86*, 190–195. DOI: [10.1134/S0036024412010049](https://doi.org/10.1134/S0036024412010049).
- [106] L.A. Gallego-Villada, E.A. Alarcón, A.L. Villa. Versatile Heterogeneous Catalytic System for the Selective Synthesis of Limonene Epoxide and Diepoxide. *Ind. Eng. Chem. Res.* **2023**, *62*, 20152–20169. DOI: [10.1021/acs.iecr.3c02633](https://doi.org/10.1021/acs.iecr.3c02633).
- [107] J.-A. Becerra, L.-M. González, A.-L. Villa. A bio-inspired Heterogeneous Catalyst for the Transformation of Limonene from Orange Peel Waste Biomass into value-added Products. *Catal. Today.* **2018**, *302*, 250–260. DOI: [10.1016/j.cattod.2017.07.012](https://doi.org/10.1016/j.cattod.2017.07.012).
- [108] S. Hajimirzaee, G.A. Leeke, J. Wood. Modified Zeolite Catalyst for Selective Dialkylation of Naphthalene. *Chem. Eng. J.* **2012**, *329–341*, 207–208. DOI: [10.1016/j.cej.2012.06.134](https://doi.org/10.1016/j.cej.2012.06.134).
- [109] M. Salavati-Niasari. Synthesis, Characterization and liquid-phase Hydroxylation of Phenol with Hydrogen Peroxide over Host (Nanopores of zeolite-Y)/guest (Oxovanadium(iv) Complexes of Tetraaza Macrocyclic Ligands) Nanocatalyst. *Inorganica Chim. Acta.* **2009**, *362*, 2159–2166. DOI: [10.1016/j.ica.2008.09.043](https://doi.org/10.1016/j.ica.2008.09.043).
- [110] A.S. Singh, D.R. Naikwadi, K. Ravi, A. V. Biradar. Chemoselective Isomerization of α -Pinene Oxide to trans-Carveol by Robust and Mild Brønsted Acidic Zirconium Phosphate Catalyst. *Mol. Catal.* **2022**, *521*, 112189. DOI: [10.1016/j.mcat.2022.112189](https://doi.org/10.1016/j.mcat.2022.112189).
- [111] J.E. Sánchez-Velandia, A. Luz Villa. Selective Synthesis of High-Added Value Chemicals from α -pinene Epoxide and Limonene Epoxide Isomerization over Mesostructured Catalysts: Effect of the Metal Loading and Solvent. *Catal. Today.* **2021**. DOI: [10.1016/j.cattod.2021.09.011](https://doi.org/10.1016/j.cattod.2021.09.011).
- [112] M. Chaves-Restrepo, A. Vilorio, J.E. Sánchez-Velandia, A.L. Villa. Effect of Reaction Conditions and Kinetics of the Isomerization of β -pinene Epoxide to Myrtanal in the Presence of Fe/MCM-41 and Fe/SBA-15. *React. Kinet. Mech. Catal.* **2022**, *135*, 2013–2029. DOI: [10.1007/s11144-022-02220-y](https://doi.org/10.1007/s11144-022-02220-y).
- [113] R. Barakov, N. Shcherban, et al Hierarchical Beta Zeolites as Catalysts in α -Pinene Oxide Isomerization. *ACS Sustain. Chem. Eng.* **2022**, *10*, 6642–6656. DOI: [10.1021/acssuschemeng.2c00441](https://doi.org/10.1021/acssuschemeng.2c00441).
- [114] K. Zitová, E. Vyskočilová, L. Červený. Preparation of α -terpineol and Perillyl Alcohol Using Zeolites Beta. *Res. Chem. Intermed.* **2021**, *47*, 4297–4310. DOI: [10.1007/s11164-021-04515-6](https://doi.org/10.1007/s11164-021-04515-6).
- [115] M.C. Cruz, J.E. Sánchez-Velandia, S. Causil, A.L. Villa. Selective Synthesis of Perillyl Alcohol from β -Pinene Epoxide over Ti and Mo Supported Catalysts. *Catal. Letters.* **2021**, *151*, 2279–2290. DOI: [10.1007/s10562-020-03489-1](https://doi.org/10.1007/s10562-020-03489-1).
- [116] Vrbková, E. EVyskočilová, M. Lhotka, L. Červený. Solvent Influence on Selectivity in α -Pinene Oxide Isomerization Using MoO₃-Modified Zeolite BETA. *Catalysts.* **2020**, *10*, 1244. DOI: [10.3390/catal10111244](https://doi.org/10.3390/catal10111244).
- [117] J.E. Sánchez-Velandia, S.M. Mejía, A.L. Villa. Reaction Mechanism of the Isomerization of Monoterpene Epoxides with Fe³⁺ as Active Catalytic Specie: A Computational Approach. *J. Phys. Chem. A.* **2020**, *124*, 3761–3769. DOI: [10.1021/acs.jpca.9b09622](https://doi.org/10.1021/acs.jpca.9b09622).
- [118] C.J.A. Ribeiro, M.M. Pereira, E.F. Kozhevnikova, I. V. Kozhevnikov, E. V. Gusevskaya, K.A. da Silva Rocha. Heteropoly Acid Catalysts in Upgrading of Biorenewables: Synthesis of para-menthonic Fragrance Compounds from α -pinene Oxide. *Catal. Today.* **2020**, *344*, 166–170. DOI: [10.1016/j.cattod.2018.12.023](https://doi.org/10.1016/j.cattod.2018.12.023).
- [119] V.N. Panchenko, V.L. Kirillov, E.Y. Gerasimov, O.N. Martyanov, M.N. Timofeeva. Isomerization of α -pinene Oxide to Campholenic Aldehyde in the Presence of Al-SiO₂ and Magnetic Al-SiO₂/Fe₃O₄ Catalysts. *React. Kinet. Mech. Catal.* **2020**, *130*, 919–934. DOI: [10.1007/s11144-020-01811-x](https://doi.org/10.1007/s11144-020-01811-x).
- [120] M. Pitínová-Štekrová, P. Eliášová, T. Weissenberger, M. Shamzhy, Z. Musilová, J. Čejka. Highly Selective Synthesis of Campholenic Aldehyde over Ti-MWW Catalysts by α -

- pinene Oxide Isomerization. *Catal. Sci. Technol.* **2018**, *8*, 4690–4701. DOI: [10.1039/C8CY01231H](https://doi.org/10.1039/C8CY01231H).
- [121] V. V. Costa, K.A. Da Silva Rocha, I. V. Kozhevnikov, E.F. Kozhevnikova, E. V. Gusevskaya. Heteropoly Acid Catalysts for the Synthesis of Fragrance Compounds from Biorenewables: Isomerization of Limonene Oxide. *Catal. Sci. Technol.* **2013**, *3*, 244–250. DOI: [10.1039/c2cy20526b](https://doi.org/10.1039/c2cy20526b).
- [122] R.F. Cotta, R.A. Martins, M.M. Pereira, K.A. da Silva Rocha, E.F. Kozhevnikova, I. V. Kozhevnikov, E. V. Gusevskaya. Heteropoly Acid Catalysis for the Isomerization of biomass-derived Limonene Oxide and Kinetic Separation of the trans-isomer in Green Solvents. *Appl. Catal. A Gen.* **2019**, *584*, 117173. DOI: [10.1016/j.apcata.2019.117173](https://doi.org/10.1016/j.apcata.2019.117173).
- [123] A.S. Singh, J.H. Advani, A. V. Biradar. Phosphonate Functionalized Carbon Spheres as Bronsted Acid Catalysts for the Valorization of bio-renewable α -pinene Oxide to Trans -carveol. *Dalt. Trans.* **2020**, *49*, 7210–7217. DOI: [10.1039/D0DT00921K](https://doi.org/10.1039/D0DT00921K).
- [124] S.M. Bruno, M. Pillinger, A.A. Valente, I.S. Gonçalves. Selective Isomerization of α -pinene Oxide to Campholenic Aldehyde by Ionic liquid-supported indenyl-molybdenum(II)-bipyridine Complexes. *J. Organomet. Chem.* **2022**, *122372*, 970–971. DOI: [10.1016/j.jorganchem.2022.122372](https://doi.org/10.1016/j.jorganchem.2022.122372).
- [125] D. Makarouni, C. Dimitriadi Evgenidi, C. Kordulis, V. Dourtoglou. Catalytic Conversion of biomass-derived Compounds to High Added Value Products Using an Acid Treated Natural Mordenite. *Sustain. Chem. Pharm.* **2023**, *33*, 101125. DOI: [10.1016/j.scp.2023.101125](https://doi.org/10.1016/j.scp.2023.101125).
- [126] Y. Lozon, A. Sultan, S.J. Lansdell, T. Prytkova, B. Sadek, K.-H.S. Yang, F.C. Howarth, N. S. Millar, M. Oz. Inhibition of Human $\alpha 7$ Nicotinic Acetylcholine Receptors by Cyclic Monoterpene Carveol. *Eur. J. Pharmacol.* **2016**, *776*, 44–51. DOI: [10.1016/j.ejphar.2016.02.004](https://doi.org/10.1016/j.ejphar.2016.02.004).
- [127] S. Mehra, D.R. Naikwadi, K. Singh, A. V Biradar, A. Kumar. Selective Isomerization of α -pinene Oxide to Trans -carveol by task-specific Ionic Liquids: Mechanistic Insights via Physicochemical Studies. *Green Chem.* **2023**. DOI: [10.1039/D3GC01757E](https://doi.org/10.1039/D3GC01757E).
- [128] J.E. Sánchez-Velandia, J.-A. Becerra, S.M. Mejía, A.L. Villa, F. Martínez O. Thermodynamics of the Isomerization of Monoterpene Epoxides. *ACS Omega.* **2021**, *6*, 34206–34218. DOI: [10.1021/acsomega.1c03049](https://doi.org/10.1021/acsomega.1c03049).
- [129] S.I. Erdagi, F.G. Boztas, C. Uyanik. The Formation of Sobrelol Ethers by the Alcoholysis of Pinene Epoxides. *J. Chem. Res.* **2016**, *40*, 318–319. DOI: [10.3184/174751916X14615863512197](https://doi.org/10.3184/174751916X14615863512197).
- [130] A. Rehman, F. Saleem F.Javed, A. Ikhlaq, S.W. Ahmad, A. Harvey. Recent Advances in the Synthesis of Cyclic Carbonates via CO₂ Cycloaddition to Epoxides. *J. Environ. Chem. Eng.* **2021**, *9*, 105113. DOI: [10.1016/j.jece.2021.105113](https://doi.org/10.1016/j.jece.2021.105113).
- [131] P.P. Pescarmona. Cyclic Carbonates Synthesised from CO₂: Applications, Challenges and Recent Research Trends. *Curr. Opin. Green Sustain. Chem.* **2021**, *29*, 100457. DOI: [10.1016/j.cogsc.2021.100457](https://doi.org/10.1016/j.cogsc.2021.100457).
- [132] T. Yan, H. Liu, Z.X. Zeng, W.G. Pan. Recent Progress of Catalysts for Synthesis of Cyclic Carbonates from CO₂ and Epoxides. *J. CO₂ Util.* **2023**, *68*, 102355. DOI: [10.1016/j.jcou.2022.102355](https://doi.org/10.1016/j.jcou.2022.102355).
- [133] F. Esteve, R. Porcar, M. Bolte, B. Altava, S. V. Luis, E. García-Verdugo. A Bioinspired Approach toward Efficient Supramolecular Catalysts for CO₂ Conversion. *Chem. Catal.* **2023**, *3*, 100482. DOI: [10.1016/J.CHECAT.2022.11.021](https://doi.org/10.1016/J.CHECAT.2022.11.021).
- [134] G. Fiorani, M. Stuck, C. Martín, M.M. Belmonte. Martín, E. Catalytic Coupling of Carbon Dioxide with Terpene Scaffolds: Access to Challenging Bio-Based Organic Carbonates. *ChemSusChem.* **2016**, *9*, 1304–1311. DOI: [10.1002/cssc.201600238](https://doi.org/10.1002/cssc.201600238).

- [135] A.B. Paninho, A.V.M. Nunes. Limonene Carbonate Synthesis from CO₂: Continuous high-pressure Flow Catalysis with Integrated Product Separation. *J. Supercrit. Fluids*. 2023, 193, 105827. DOI: [10.1016/j.supflu.2022.105827](https://doi.org/10.1016/j.supflu.2022.105827).
- [136] R. Mori. Replacing All petroleum-based Chemical Products with Natural biomass-based Chemical Products: A Tutorial Review. *RSC. Sustain.* 2023, 1, 179–212. DOI: [10.1039/D2SU00014H](https://doi.org/10.1039/D2SU00014H).
- [137] V.C. Eze, A. Rehman, M. Patel, S. Ahmad, A.P. Harvey. Synthesis of Cyclic α -pinane Carbonate – A Potential Monomer for bio-based Polymers. *RSC Adv.* 2022, 12, 17454–17465. DOI: [10.1039/D1RA07943C](https://doi.org/10.1039/D1RA07943C).
- [138] M. Bähr, A. Bitto, R. Mühlhaupt. Cyclic Limonene Dicarboxylate as a New Monomer for non-isocyanate Oligo- and Polyurethanes (NIPU) Based upon Terpenes. *Green Chem.* 2012, 14, 1447. DOI: [10.1039/c2gc35099h](https://doi.org/10.1039/c2gc35099h).
- [139] M. Bähr, R. Mühlhaupt, B.S. Ritter. Carbonate Group Comprising terpene-derived Monomers and isocyanate-free poly-urethanes, WO 2012/171659. 2012, A1.
- [140] P. Mikšovský, E.N. Horn, S. Naghdi, D. Eder, M. Schnürch, K. Bica-Schröder. Continuous Formation of Limonene Carbonates in Supercritical Carbon Dioxide. *Org. Process Res. Dev.* 2022, 26, 2799–2810. DOI: [10.1021/acs.oprd.2c00143](https://doi.org/10.1021/acs.oprd.2c00143).
- [141] M.C. Kroon, C.J. Peters. *Supercritical Fluids in Ionic Liquids*; Ion. Liq. Furth. UnCOILed, Wiley: in, 2014, pp 39–57. DOI: [10.1002/9781118839706.ch2](https://doi.org/10.1002/9781118839706.ch2).
- [142] M. Navarro, L.F. Sánchez-Barba, A. Garcés, J. Fernández-Baeza, I. Fernández. Bimetallic scorpionate-based Helical Organoaluminum Complexes for Efficient Carbon Dioxide Fixation into a Variety of Cyclic Carbonates. *Catal. Sci. Technol.* 2020, 10, 3265–3278. DOI: [10.1039/D0CY00593B](https://doi.org/10.1039/D0CY00593B).
- [143] Y. Hu, J. Steinbauer, V. Stefanow, A. Spannenberg, T. Werner. Polyethers as Complexing Agents in Calcium-Catalyzed Cyclic Carbonate Synthesis. *ACS Sustain. Chem. Eng.* 2019, 7, 13257–13269. DOI: [10.1021/acssuschemeng.9b02502](https://doi.org/10.1021/acssuschemeng.9b02502).
- [144] R. Calmanti, M. Selva, A. Perosa. Tungstate Ionic Liquids as Catalysts for CO₂ Fixation into Epoxides. *Mol. Catal.* 2020, 486, 110854. DOI: [10.1016/j.mcat.2020.110854](https://doi.org/10.1016/j.mcat.2020.110854).
- [145] Diana, Sutijan, Rochmadi, A. Budiman. Kinetics of Acetoxylation of Indonesian Crude Turpentine over Amberlyst 36 Wet: Pseudo-homogeneous Approach. *AIP Conf. Proc.* 2016, 050003. DOI: [10.1063/1.4958486](https://doi.org/10.1063/1.4958486).
- [146] Machado, J., et al SBA-15 with Sulfonic Acid Groups as a Green Catalyst for the Acetoxylation of α -pinene. *Microporous Mesoporous Mater.* 2012, 163, 237–242. DOI: [10.1016/j.micromeso.2012.07.028](https://doi.org/10.1016/j.micromeso.2012.07.028).
- [147] M. Golets, S. Ajaikumar, D. Blomberg, H. Grundberg, J. Wärnå, T. Salmi, J.-P. Mikkola. Liquid Phase Acetoxylation of α -pinene over Amberlyst-70 ion-exchange Resin. *Appl. Catal. A Gen.* 2012, 43–50, 435–436. DOI: [10.1016/j.apcata.2012.05.034](https://doi.org/10.1016/j.apcata.2012.05.034).
- [148] M. Golets, S. Ajaikumar, W. Larsson, D. Blomberg, H. Grundberg, J. Wärnå, T. Salmi, J.-P. Mikkola. A Kinetic Study of the Liquid Phase Acetoxylation of α -Pinene. *Top. Catal.* 2012, 55, 649–656. DOI: [10.1007/s11244-012-9844-9](https://doi.org/10.1007/s11244-012-9844-9).
- [149] M.K. Yadav, M. V. Patil, R. V. Jasra. Acetoxylation and Hydration of Limonene and α -pinene Using cation-exchanged Zeolite Beta. *J. Mol. Catal. A Chem.* 2009, 297, 101–109. DOI: [10.1016/j.molcata.2008.09.017](https://doi.org/10.1016/j.molcata.2008.09.017).
- [150] Dow-Lenntech, Product Data Sheet: Amberlyst 36Dry, n.d. www.lenntech.com (accessed August 24, 2023).
- [151] The Good Scents Company, terpinyl acetate, 2021. <http://www.thegoodscentscompany.com/data/rw1375491.html> (accessed August 24, 2023).
- [152] Lenntech, Amberlyst 70 - High Temperature Strongly Acidic Catalyst, 2006. <https://www.lenntech.com/Data-sheets/Dow-Amberlyst-70-L.pdf> (accessed August 24, 2023).

- [153] von Czapiewski, M. MA.R. Meier. Regioselective Catalytic Acetoxylation of Limonene. *Catal. Sci. Technol.* **2014**, *4*, 2318–2325. DOI: [10.1039/C4CY00231H](https://doi.org/10.1039/C4CY00231H).
- [154] G.P.P. Kamatou, I. Vermaak, A.M. Viljoen, B.M. Lawrence. Menthol: A Simple Monoterpene with Remarkable Biological Properties. *Phytochemistry*. **2013**, *96*, 15–25. DOI: [10.1016/j.phytochem.2013.08.005](https://doi.org/10.1016/j.phytochem.2013.08.005).
- [155] C.A. Akinnowo, N. Bingwa, R. Meijboom. Surface Properties Vs Activity of meso-ZrO₂ Catalyst in Chemoselective Meerwein-Ponndorf-Verley Reduction of Citral: Effect of Calcination Temperature. *Microporous Mesoporous Mater.* **2021**, *311*, 110693. DOI: [10.1016/j.micromeso.2020.110693](https://doi.org/10.1016/j.micromeso.2020.110693).
- [156] R. Tang, Q. Wen, M. Li, W. Zhang, Z. Wang, J. Yang. Recent Advances in the Biosynthesis of Farnesene Using Metabolic Engineering. *J. Agric. Food Chem.* **2021**, *69*, 15468–15483. DOI: [10.1021/acs.jafc.1c06022](https://doi.org/10.1021/acs.jafc.1c06022).
- [157] Efficient Myrcene Production Using Linalool Dehydratase Isomerase and Rational Biochemical Process in *Escherichia Coli*. *J. Biotechnol.* **2023**, *33–40*, 371–372. DOI: [10.1016/j.jbiotec.2023.05.008](https://doi.org/10.1016/j.jbiotec.2023.05.008).
- [158] I. Martinez-Botella, S. Littler, M. Kundra, C.H. Hornung. Valorisation of Terpenes by Continuous Flow Hydrogenation over 3D-printed Palladium Catalysts. *Tetrahedron Green Chem.* **2023**, *2*, 100014. DOI: [10.1016/j.tgchem.2023.100014](https://doi.org/10.1016/j.tgchem.2023.100014).
- [159] S.-K. Kim, F. Karadeniz. Biological Importance and Applications of Squalene and Squalane. In *Adv. Food Nutr. Res.*; 1st. Elsevier Inc, **2012**; 223–233. DOI: [10.1016/B978-0-12-416003-3.00014-7](https://doi.org/10.1016/B978-0-12-416003-3.00014-7)
- [160] García, S., et al Continuous Production of Squalane Using 3D Printed Catalytic Supports. *Johnson Matthey Technol. Rev* **2019**, *63*, 191–204. DOI: [10.1595/205651319X15535963555844](https://doi.org/10.1595/205651319X15535963555844).
- [161] A.K. Shah, M.A. Abro, S. Ahmed, A.A. Shah, A. Iqbal, M.A. Usto, S.N.S. Bukhari, G. Maitlo, A.S. Jatoi, M.S. Talpur. Catalytic Conversion of Liquid Phase Citral and Citronellal Hydrogenations to Menthols over Metal-12- Tungstophosphoric Acid Supported Mesoporous Clay Catalysts. *Biomass Convers. Biorefinery*. **2022**. DOI: [10.1007/s13399-022-02847-w](https://doi.org/10.1007/s13399-022-02847-w).
- [162] Wang, J., et al Catalytic Cascade Upcycling single-use Natural Rubber Glove Wastes into Fuels via a two-stage Pressurized fixed-bed Reactor. *Fuel Process. Technol* **2022**, *238*, 107490. DOI: [10.1016/j.fuproc.2022.107490](https://doi.org/10.1016/j.fuproc.2022.107490).
- [163] P. Huang, Q. Deng, L. Jiang, Y. Zhi, W. Yang, J. Huang, et al The Exploration of Sensitive Factors for the Selective Hydrogenation of α -Pinene over Recyclable Ni-B/KIT-6 Catalyst. *Catal. Letters* **2022**, *152*, 2352–2365. DOI: [10.1007/s10562-021-03811-5](https://doi.org/10.1007/s10562-021-03811-5).
- [164] C. Yang, B. Xiang, L. Jiang, F. Zhang, C. Liu, et al Selective Hydrogenation of α -pinene on a Nickel Supported Aluminophosphate Catalyst: Process Optimization and Reaction Kinetics. *Int. J. Chem. Kinet.* **2021**, *53*, 440–456. DOI: [10.1002/kin.21455](https://doi.org/10.1002/kin.21455).
- [165] A.K. Shah, G. Maitlo, A.A. Shah, I.A. Channa, G.A. Kandhro, H.A. Maitlo, U.H. Bhatti, et al One Pot Menthol Synthesis via Hydrogenations of Citral and Citronellal over montmorillonite-supported Pd/Ni-heteropoly Acid Bifunctional Catalysts. *React. Kinet. Mech. Catal* **2019**, *128*, 917–934. DOI: [10.1007/s11144-019-01679-6](https://doi.org/10.1007/s11144-019-01679-6).
- [166] I.I. Il'ina, I.L. Simakova, V.A. Semikolenov. Kinetics of Pinane Oxidation to Pinane Hydroperoxide by Dioxygen, *Kinet. Catal.* **2001**, *42*, 41–45. DOI: [10.1023/A:1004896512191](https://doi.org/10.1023/A:1004896512191).
- [167] I. Simakova, P. Mäki-Arvela, M. Martinez-Klimov, J. Muller, Z. Vajglova, M. Peurla, K. Eränen, D.Y. Murzin. Continuous Synthesis of Menthol from Citronellal and Citral over Ni-beta-zeolite-sepiolite Composite Catalyst. *Appl. Catal. A Gen.* **2022**, *636*, 118586. DOI: [10.1016/j.apcata.2022.118586](https://doi.org/10.1016/j.apcata.2022.118586).

- [168] R. Heijden, D. Jacobs, W. Snoeijer, D. Hallard, R. Verpoorte. The Catharanthus Alkaloids: Pharmacognosy and Biotechnology. *Curr. Med. Chem.* **2004**, *11*, 607–628. DOI: [10.2174/0929867043455846](https://doi.org/10.2174/0929867043455846).
- [169] S. Carnesecchi, R. Bras-Gonçalves, A. Bradaia, M. Zeisel, F. Gossé, M.-F. Poupon, F. Raul. Geraniol, a Component of Plant Essential Oils, Modulates DNA Synthesis and Potentiates 5-fluorouracil Efficacy on Human Colon Tumor Xenografts. *Cancer Lett.* **2004**, *215*, 53–59. DOI: [10.1016/j.canlet.2004.06.019](https://doi.org/10.1016/j.canlet.2004.06.019).
- [170] Y. Lei, P. Fu, X. Jun, P. Cheng. Pharmacological Properties of Geraniol – A Review. *Planta Med.* **2019**, *85*, 48–55. DOI: [10.1055/a-0750-6907](https://doi.org/10.1055/a-0750-6907).
- [171] F.-L. Yu, Y.-L. Shi, F.-Z. Wu, B. Yuan, C.-X. Xie, S.-T. Yu. Aqueous-phase Hydrogenation of α -pinene Catalyzed by Ni-B Alloys Loaded on a Janus Amphiphilic Carbon@silica Nanomaterial. *Ind. Crops Prod.* **2022**, *185*, 115140. DOI: [10.1016/j.indcrop.2022.115140](https://doi.org/10.1016/j.indcrop.2022.115140).
- [172] Wang, J., et al Converting Polyisoprene Rubbers into bio-jet Fuels via a Cascade Hydrolysis and vapor-phase Hydrogenation Process. *Energy Convers. Manag.* **2022**, *270*, 116250. DOI: [10.1016/j.enconman.2022.116250](https://doi.org/10.1016/j.enconman.2022.116250).
- [173] Z. Vajglová, M. Navas, P. Mäki-Arvela, K. Eränen, N. Kumar, M. Peurla, D.Y. Murzin. Transformations of Citral over Bifunctional Ru-H-Y-80 Extrudates in a Continuous Reactor. *Chem. Eng. J.* **2022**, *429*, 132190. DOI: [10.1016/j.cej.2021.132190](https://doi.org/10.1016/j.cej.2021.132190).
- [174] L. Naicker, M. Schörner, D. Kremitzl, H.B. Friedrich, M. Haumann, P. Wasserscheid. Influencing the Product Distribution in Citral Hydrogenation Using Ionic Liquid Modified Cu Catalysts. *ChemCatChem.* **2022**, *14*. DOI: [10.1002/cctc.202200388](https://doi.org/10.1002/cctc.202200388).
- [175] C. Yang, L. Jiang, et al Use of Pinene as a Solvent for the Synthesis of Aluminophosphate and Its Application in the Hydrogenation of Pinene. *Microporous Mesoporous Mater.* **2020**, *294*, 109856. DOI: [10.1016/j.micromeso.2019.109856](https://doi.org/10.1016/j.micromeso.2019.109856).
- [176] P. Hirunsit, C. Luadthong, K. Faungnawakij. Effect of Alumina Hydroxylation on Glycerol Hydrogenolysis to 1,2-propanediol over Cu/Al₂O₃: Combined Experiment and DFT Investigation. *RSC Adv.* **2015**, *5*, 11188–11197. DOI: [10.1039/C4RA14698K](https://doi.org/10.1039/C4RA14698K).
- [177] A. Sales, L. de O. Felipe, J.L. Bicas. Production, Properties, and Applications of α -Terpineol. *Food Bioprocess Technol.* **2020**, *13*, 1261–1279. DOI: [10.1007/s11947-020-02461-6](https://doi.org/10.1007/s11947-020-02461-6).
- [178] C. Khaleel, N. Tabanca, G. Buchbauer. α -Terpineol, A Natural Monoterpene: A Review of Its Biological Properties. *Open Chem.* **2018**, *16*, 349–361. DOI: [10.1515/chem-2018-0040](https://doi.org/10.1515/chem-2018-0040).
- [179] L. Sekerová, H. Černá, et al Preparation of α -Terpineol from Biomass Resource Catalysed by Acid Treated Montmorillonite K10. *Catal. Letters* **2021**, *151*, 2673–2683. DOI: [10.1007/s10562-020-03514-3](https://doi.org/10.1007/s10562-020-03514-3).
- [180] B. YUAN, D. ZHANG, C. XIE, F. YU, et al Hydration of α -pinene Catalyzed by Oxalic acid/polyethylene Glycol Deep Eutectic Solvents. *J. Fuel Chem. Technol.* **2021**, *49*, 330–338. DOI: [10.1016/S1872-5813\(21\)60017-8](https://doi.org/10.1016/S1872-5813(21)60017-8).
- [181] Z. Wei, D. Xiong, P. Duan, S. Ding, Y. Li, et al Preparation of Carbon-Based Solid Acid Catalysts Using Rice Straw Biomass and Their Application in Hydration of α -Pinene. *Catalysts* **2020**, *10*, 213. DOI: [10.3390/catal10020213](https://doi.org/10.3390/catal10020213).
- [182] V.T. Salvador, E.S. Silva, P.G.C. Gonçalves, R. Cella. Biomass Transformation: Hydration and Isomerization Reactions of Turpentine Oil Using Ion Exchange Resins as Catalyst. *Sustain. Chem. Pharm.* **2020**, *15*. DOI: [10.1016/j.scp.2020.100214](https://doi.org/10.1016/j.scp.2020.100214).
- [183] A. Aguilar-Elguezabal, et al Ionic Liquid as Green Solvent for the Synthesis of α -terpineol from α -pinene. *Sustain. Chem. Pharm.* **2020**, *15*, 100207. DOI: [10.1016/j.scp.2019.100207](https://doi.org/10.1016/j.scp.2019.100207).

- [184] H. Zhang, S. Yu. Hydration of α -Pinene over SO 4 2- /Zr-mcm-41 in Supercritical Carbon Dioxide. *ChemistrySelect*. 2019, 4, 3355–3359. DOI: 10.1002/slct.201900071.
- [185] J. Xie, Q. Han, B. Feng, Z. Liu. Preparation of Amphiphilic Mesoporous carbon-based Solid Acid from Kraft Lignin Activated by Phosphoric Acid and Its Catalytic Performance for Hydration of α -pinene. *BioResources*. 2019, 14, 4284–4303. DOI: 10.15376/biores.14.2.4284-4303.
- [186] I.A. Putra, M.M. Azis, T.H. Soerawidjaja, A. Indarto. Synthesis of Cineole from Raw Turpentine. *AIP Conf. Proc.* 2019, 020057. DOI: 10.1063/1.5095035.
- [187] E.T. Paulino, A.K.B.F. Rodrigues, M.L.D.P. Machado, K.R.V. de Oliveira, A. C. Bernardino, L.J. Quintans-Júnior, A.P. Oliveira, Ê.A.N. Ribeiro. Alpha-terpineol Prevents Myocardial Damage against isoproterenol-MI Induced in Wistar-Kyoto Rats: New Possible to Promote Cardiovascular Integrity. *Life Sci.* 2022, 290, 120087. DOI: 10.1016/j.lfs.2021.120087.
- [188] C.K.B. Sabino, E.S. Ferreira-Filho, M.B. Mendes, J.C. da Silva-Filho, M.P.T.R. Ponte, L. H.P. Moura, E.C.A. Oliveira, L.J. Quintans-Junior, M.R.V. Dos Santos, R. de Cássia Meneses Oliveira, et al Cardiovascular Effects Induced by α -terpineol in Hypertensive Rats. *Flavour Fragr. J.* 2013, 28, 333–339. DOI: 10.1002/ffj.3159.
- [189] J.L. Bicas, I.A. Neri-Numa, A.L.T.G. Ruiz, J.E. De Carvalho, G.M. Pastore. Evaluation of the Antioxidant and Antiproliferative Potential of Bioflavors. *Food Chem. Toxicol.* 2011, 49, 1610–1615. DOI: 10.1016/j.fct.2011.04.012.
- [190] H. Zengin, A. Baysal. Antibacterial and Antioxidant Activity of Essential Oil Terpenes against Pathogenic and Spoilage-Forming Bacteria and Cell Structure-Activity Relationships Evaluated by SEM Microscopy. *Molecules*. 2014, 19, 17773–17798. DOI: 10.3390/molecules191117773.
- [191] C.-Y. Wang, Y.-W. Chen, C.-Y. Hou. Antioxidant and Antibacterial Activity of Seven Predominant Terpenoids. *Int. J. Food Prop.* 2019, 22, 230–238. DOI: 10.1080/10942912.2019.1582541.
- [192] S.B. Hassan, Gali-Muhtasib, H. Göransson H, R. Larsson. Alpha Terpeneol: A Potential Anticancer Agent Which Acts through Suppressing NF-kappaB Signalling. *Anticancer Res.* 2010, 30, 1911–1919. <http://www.ncbi.nlm.nih.gov/pubmed/20651334>.
- [193] D.N. Gouveia, J.S. Costa, M.A. Oliveira, T.K. Rabelo, et al Guimarães, α -Terpineol Reduces Cancer Pain via Modulation of Oxidative Stress and Inhibition of iNOS. *Biomed. Pharmacother.* 2018, 105, 652–661. DOI: 10.1016/j.biopha.2018.06.027.
- [194] L.J. Quintans-Júnior, M.G.B. Oliveira, M.F. Santana, et al α -Terpineol Reduces Nociceptive Behavior in Mice. *Pharm. Biol.* 2011, 49, 583–586. DOI: 10.3109/13880209.2010.529616.
- [195] R. Souza, M. Cardoso, C. Menezes, J. Silva, D. De Sousa, J. Batista. Gastroprotective Activity of α -terpineol in Two Experimental Models of Gastric Ulcer in Rats. *Daru.* 2011, 19, 277–281. <http://www.ncbi.nlm.nih.gov/pubmed/22615669>.
- [196] F.F.F. Nóbrega, M.G.S.S. Salvadori, C.J. Masson, C.F. Mello, T.S. Nascimento, J.H. Leal-Cardoso, D.P. de Sousa, R.N. Almeida. Monoterpenoid Terpinen-4-ol Exhibits Anticonvulsant Activity in Behavioural and Electrophysiological Studies. *Oxid. Med. Cell. Longev.* 2014, 2014, 1–9. DOI: 10.1155/2014/703848.
- [197] Y.-A. Tsou, H.-J. Huang, W.W.-Y. Lin, C.Y.-C. Chen. Lead Screening for Chronic Obstructive Pulmonary Disease of IKK2 Inhibited by Traditional Chinese Medicine. *Evidence-based Complement. Altern. Med.* 2014, 2014, 1–16. DOI: 10.1155/2014/465025.
- [198] S.T.K. Narishetty, R. Panchagnula. Transdermal Delivery of Zidovudine: Effect of Terpenes and Their Mechanism of Action. *J. Control. Release.* 2004, 95, 367–379. DOI: 10.1016/j.jconrel.2003.11.022.

- [199] X. Liu, Y. Li, et al Identification of Repellent and Insecticidal Constituents of the Essential Oil of *Artemisia Rupestris* L. Aerial Parts against *Liposcelis Bostrychophila* Badonnel. *Molecules* **2013**, *18*, 10733–10746. DOI: [10.3390/molecules180910733](https://doi.org/10.3390/molecules180910733).
- [200] Expert Market Research, Top 4 Chemical Companies in the Global Terpeneol Market, 2022. <https://www.expertmarketresearch.com/articles/top-terpeneol-companies> (accessed July 12, 2023).
- [201] J.E. Sánchez-Velandia, H.G. Baldoví, A.Y. Sidorenko, J.A. Becerra, F. Martínez O. Synthesis of Heterocycles Compounds from Condensation of Limonene with Aldehydes Using Heteropolyacids Supported on Metal Oxides. *Mol. Catal.* **2022**, *528*, 112511. DOI: [10.1016/j.mcat.2022.112511](https://doi.org/10.1016/j.mcat.2022.112511).
- [202] N. Yaghmaeiyan, M. Mirzaei, R. Delghavi. Montmorillonite Clay: Introduction and Evaluation of Its Applications in Different Organic Syntheses as Catalyst: A Review. *Res. Chem.* **2022**, *4*, 100549. DOI: [10.1016/j.rechem.2022.100549](https://doi.org/10.1016/j.rechem.2022.100549).
- [203] P.M. Bhaskar, D. Loganathan. Per-O-acetylation of Sugars Catalysed by Montmorillonite K-10. *Tetrahedron Lett.* **1998**, *39*, 2215–2218. DOI: [10.1016/S0040-4039\(98\)00178-6](https://doi.org/10.1016/S0040-4039(98)00178-6).
- [204] J. Yadav, B.V. Reddy, K. Sadasiv, P.S. Reddy. Montmorillonite clay-catalyzed [4+2] Cycloaddition Reactions: A Facile Synthesis of Pyrano- and Furanquinolines. *Tetrahedron Lett.* **2002**, *43*, 3853–3856. DOI: [10.1016/S0040-4039\(02\)00679-2](https://doi.org/10.1016/S0040-4039(02)00679-2).
- [205] B.A. Goodman. Utilization of Waste Straw and Husks from Rice Production: A Review. *J. Bioresour. Bioprod.* **2020**, *5*, 143–162. DOI: [10.1016/j.jobab.2020.07.001](https://doi.org/10.1016/j.jobab.2020.07.001).
- [206] L. Dessbesell, et al Global Lignin Supply Overview and Kraft Lignin Potential as an Alternative for petroleum-based Polymers. *Renew. Sustain. Energy Rev.* **2020**, *123*, 109768. DOI: [10.1016/j.rser.2020.109768](https://doi.org/10.1016/j.rser.2020.109768).
- [207] Z.-M. Cai, J.-Q. Peng, Y. Chen, L. Tao, Y.-Y. Zhang, L.-Y. Fu, Q.-D. Long, X.-C. Shen. 1,8-Cineole: A Review of Source, Biological Activities, and Application. *J. Asian Nat. Prod. Res.* **2021**, *23*, 938–954. DOI: [10.1080/10286020.2020.1839432](https://doi.org/10.1080/10286020.2020.1839432).
- [208] Y.S. Demidova, I.L. Simakova, M. Estrada, S. Beloshapkin, E. V. Suslov, K.P. Volcho, N. F. Salakhutdinov, A. Simakov, D.Y. Murzin. One-Pot Myrtenol Amination over Au, Au-Pd and Pd Nanoparticles Supported on Alumina. *Catal. Letters.* **2019**, *149*, 3454–3464. DOI: [10.1007/s10562-019-02958-6](https://doi.org/10.1007/s10562-019-02958-6).
- [209] Y.S. Demidova, E. V. Suslov, I.L. Simakova, E.S. Mozhajcev, D. V. Korchagina, K. P. Volcho, N.F. Salakhutdinov, A. Simakov, D.Y. Murzin. One-pot Monoterpene Alcohol Amination over Au/ZrO₂ Catalyst: Effect of the Substrate Structure. *J. Catal.* **2018**, *360*, 127–134. DOI: [10.1016/j.jcat.2018.01.020](https://doi.org/10.1016/j.jcat.2018.01.020).
- [210] I.L. Simakova, Y.S. Demidova, M. Estrada, S. Beloshapkin, E.V. Suslov, K.P. Volcho, N. F. Salakhutdinov, D.Y. Murzin, A. Simakov. Gold Catalyzed one-pot Myrtenol Amination: Effect of Catalyst Redox Activation. *Catal. Today.* **2017**, *279*, 63–70. DOI: [10.1016/j.cattod.2016.01.044](https://doi.org/10.1016/j.cattod.2016.01.044).
- [211] Y.S. Demidova, I.L. Simakova, M. Estrada, S. Beloshapkin, E.V. Suslov, D.V. Korchagina, K.P. Volcho, N.F. Salakhutdinov, A.V. Simakov, D.Y. Murzin. One-pot Myrtenol Amination over Au Nanoparticles Supported on Different Metal Oxides. *Appl. Catal. A Gen.* **2013**, *348–356*, 464–465. DOI: [10.1016/j.apcata.2013.06.013](https://doi.org/10.1016/j.apcata.2013.06.013).
- [212] P. Mäki-Arvela, I.L. Simakova, D.Y. Murzin. One-pot Amination of Aldehydes and Ketones over Heterogeneous Catalysts for Production of Secondary Amines. *Catal. Rev.* **2023**, *65*, 501–568. DOI: [10.1080/01614940.2021.1942689](https://doi.org/10.1080/01614940.2021.1942689).
- [213] H. Wang, et al A Review on Heterogeneous Photocatalysis for Environmental Remediation: From Semiconductors to Modification Strategies. *Chin. J. Catal* **2022**, *43*, 178–214. DOI: [10.1016/S1872-2067\(21\)63910-4](https://doi.org/10.1016/S1872-2067(21)63910-4).

- [214] Ikram, M., et al A Review of Photocatalytic Characterization, and Environmental Cleaning, of Metal Oxide Nanostructured Materials. *Sustain. Mater. Technol.* **2021**, *30*, e00343. DOI: [10.1016/j.susmat.2021.e00343](https://doi.org/10.1016/j.susmat.2021.e00343).
- [215] X. Yang, D. Wang. Photocatalysis: From Fundamental Principles to Materials and Applications. *ACS Appl. Energy Mater.* **2018**, *1*, 6657–6693. DOI: [10.1021/acsaem.8b01345](https://doi.org/10.1021/acsaem.8b01345).
- [216] A. Kumar. A Review on the Factors Affecting the Photocatalytic Degradation of Hazardous Materials. *Mater. Sci. Eng. Int. J.* **2017**, *1*, 106–114. DOI: [10.15406/mseij.2017.01.00018](https://doi.org/10.15406/mseij.2017.01.00018).
- [217] R. Gusain, N. Kumar, S.S. Ray. Factors Influencing the Photocatalytic Activity of Photocatalysts in Wastewater Treatment, In: *Photocatal. Adv. Oxid. Process. Wastewater Treat.*, Wiley. **2020**, 229–270. DOI: [10.1002/9781119631422.ch8](https://doi.org/10.1002/9781119631422.ch8).
- [218] C. Luo, X. Liu, T. Lai, J. Li, G. Xia, W. Zou, H. Wang. Selective Photocatalytic Hydrogenation of Citral over Pure TiO₂ Nanoparticle. *Mater. Res. Express.* **2022**, *9*, 045012. DOI: [10.1088/2053-1591/ac6856](https://doi.org/10.1088/2053-1591/ac6856).
- [219] N.J. Castellanos, H. Martínez Q, F. Martínez O, K. Leus, P. Van Der Voort. Photo-epoxidation of (α , β)-pinene with Molecular O₂ Catalyzed by a dioxo-molybdenum (VI)-based Metal–Organic Framework. *Res. Chem. Intermed.* **2021**, *47*, 4227–4244. DOI: [10.1007/s11164-021-04518-3](https://doi.org/10.1007/s11164-021-04518-3).
- [220] H. Martínez Q, Á.A. Amaya, E.A. Paez-Mozo, F. Martínez O, S. Valange. Photo-assisted O-atom Transfer to Monoterpenes with Molecular Oxygen and a dioxoMo(VI) Complex Immobilized on TiO₂ Nanotubes. *Catal. Today.* **2021**, *375*, 441–457. DOI: [10.1016/j.cattod.2020.07.053](https://doi.org/10.1016/j.cattod.2020.07.053).
- [221] Gottuso, A., et al Catalytic and Photocatalytic Epoxidation of Limonene: Using Mesoporous Silica Nanoparticles as Functional Support for a Janus-like Approach. *J. Catal.* **2020**, *391*, 202–211. DOI: [10.1016/j.jcat.2020.08.025](https://doi.org/10.1016/j.jcat.2020.08.025).
- [222] H. Martínez, Á.A. Amaya, E.A. Páez-Mozo, F. Martínez O. Highly Efficient Epoxidation of α -pinene with O₂ Photocatalyzed by dioxoMo (VI) Complex Anchored on TiO₂ Nanotubes. *Microporous Mesoporous Mater.* **2018**, *265*, 202–210. DOI: [10.1016/j.micro-meso.2018.02.005](https://doi.org/10.1016/j.micro-meso.2018.02.005).
- [223] Y. Takada, J. Caner, S. Kaliyamoorthy, H. Naka, S. Saito. Photocatalytic Transfer Hydrogenolysis of Allylic Alcohols on Pd/TiO₂: A Shortcut to (S)-(+)-lavandulol. *Chem. – A Eur. J.* **2017**, *23*, 18025–18032. DOI: [10.1002/chem.201704099](https://doi.org/10.1002/chem.201704099).
- [224] D.R. Naikwadi, D. Muthukumar, R.J. Tayade, R.S. Pillai, A. V. Biradar. A Novel Route for Isomerization of α -pinene Oxide at Room Temperature under Irradiation of light-emitting Diodes. *Mater. Today Chem.* **2023**, *33*, 101682. DOI: [10.1016/j.mtchem.2023.101682](https://doi.org/10.1016/j.mtchem.2023.101682).
- [225] J. Schneider, et al Understanding TiO₂ Photocatalysis: Mechanisms and Materials. *Chem. Rev.* **2014**, *114*, 9919–9986. DOI: [10.1021/cr5001892](https://doi.org/10.1021/cr5001892).
- [226] I.W.C.E. Arends, R.A. Sheldon. Activities and Stabilities of Heterogeneous Catalysts in Selective Liquid Phase Oxidations: Recent Developments. *Appl. Catal. A Gen.* **2001**, *212*, 175–187. DOI: [10.1016/S0926-860X\(00\)00855-3](https://doi.org/10.1016/S0926-860X(00)00855-3).
- [227] H. Martínez, D.F. Valezi, et al Characterization of peroxo-Mo and superoxo-Mo Intermediate Adducts in Photo-Oxygen Atom Transfer with O₂, *Catal. Today* **2022**, *394–396*, 50–61. DOI: [10.1016/j.cattod.2022.02.016](https://doi.org/10.1016/j.cattod.2022.02.016).
- [228] F. Doro, N. Akeroyd, F. Schiet, A. Narula. The Prins Reaction in the Fragrance Industry: 100th Anniversary (1919–2019). *Angew. Chemie Int. Ed.* **2019**, *58*, 7174–7179. DOI: [10.1002/anie.201814470](https://doi.org/10.1002/anie.201814470).
- [229] E. Reyes, L. Prieto, U. Uria, L. Carrillo, J.L. Vicario. Recent Advances in the Prins Reaction. *ACS Omega.* **2022**, *7*, 31621–31627. DOI: [10.1021/acsomega.2c04765](https://doi.org/10.1021/acsomega.2c04765).

- [230] O.S. Patrusheva, K.P. Volcho, N.F. Salakhutdinov. Synthesis of oxygen-containing Heterocyclic Compounds Based on Monoterpenoids. *Russ. Chem. Rev.* **2018**, *87*, 771–796. DOI: [10.1070/RCR4810](https://doi.org/10.1070/RCR4810).
- [231] M. Golets, S. Ajaikumar, J.P. Mikkola. Catalytic Upgrading of Extractives to Chemicals: Monoterpenes to “EXICALS. *Chem. Rev.* **2015**, *115*, 3141–3169. DOI: [10.1021/cr500407m](https://doi.org/10.1021/cr500407m).
- [232] R.J. Nyamwihura, I.V. Ogungbe. The Pinene Scaffold: Its Occurrence, Chemistry, Synthetic Utility, and Pharmacological Importance. *RSC Adv.* **2022**, *12*, 11346–11375. DOI: [10.1039/D2RA00423B](https://doi.org/10.1039/D2RA00423B).
- [233] M.K. Yadav, R. V. Jasra. Synthesis of Nopol from β -pinene Using ZnCl₂ Impregnated Indian Montmorillonite. *Catal. Commun.* **2006**, *7*, 889–895. DOI: [10.1016/j.catcom.2006.04.002](https://doi.org/10.1016/j.catcom.2006.04.002).
- [234] S. V. Jadhav, K.M. Jinka, H.C. Bajaj. Synthesis of Nopol via Prins Condensation of β -pinene and Paraformaldehyde Catalyzed by Sulfated Zirconia, *Appl. Catal. A Gen.* **2010**, *390*, 158–165. DOI: [10.1016/j.apcata.2010.10.005](https://doi.org/10.1016/j.apcata.2010.10.005).
- [235] L.A. Gallego-Villada, E.A. Alarcón, A.L. Villa. Evaluation of Nopol Production Obtained from Turpentine Oil over Sn/MCM-41 Synthesized by Wetness Impregnation Using the Central Composite Design, *Mol. Catal.* **2020**, *498*, 111250. DOI: [10.1016/j.mcat.2020.111250](https://doi.org/10.1016/j.mcat.2020.111250).
- [236] I. Aguas, E. Alarcón, A.L. Villa. Turpentine Valorization by Its Oxyfunctionalization to Nopol through Heterogeneous Catalysis, *Heliyon.* **2020**, *6*. DOI: [10.1016/j.heliyon.2020.e03887](https://doi.org/10.1016/j.heliyon.2020.e03887).
- [237] V.S. Marakatti, A.B. Halgeri, G. V. Shanbhag. Metal ion-exchanged Zeolites as Solid Acid Catalysts for the Green Synthesis of Nopol from Prins Reaction, *Catal. Sci. Tech.* **2014**, *4*, 4065–4074. DOI: [10.1039/C4CY00596A](https://doi.org/10.1039/C4CY00596A).
- [238] V.S. Marakatti, D. Mumbaraddi, G. V. Shanbhag, A.B. Halgeri, S.P. Maradur. Molybdenum oxide/ γ -alumina: An Efficient Solid Acid Catalyst for the Synthesis of Nopol by Prins Reaction. *RSC Adv.* **2015**, *5*, 93452–93462. DOI: [10.1039/C5RA12106J](https://doi.org/10.1039/C5RA12106J).
- [239] M. Opanasenko, A. Dhakshinamoorthy, Y.K. Hwang, J. Chang, H. Garcia, J. Čejka. Superior Performance of Metal–Organic Frameworks over Zeolites as Solid Acid Catalysts in the Prins Reaction: Green Synthesis of Nopol. *ChemSusChem.* **2013**, *6*, 865–871. DOI: [10.1002/cssc.201300032](https://doi.org/10.1002/cssc.201300032).
- [240] E. Vrbková, B. Šteflová, E. Vyskočilová, L. Červený. Heterogeneous Mo/W/Zn–SiO₂ Based Catalysts in Nopol (2-(6,6-dimethyl-2-bicyclo[3.1.1]hept-2-enyl)ethanol) Synthesis. *React. Kinet. Mech. Catal.* **2020**, *131*, 213–232. DOI: [10.1007/s11144-020-01858-w](https://doi.org/10.1007/s11144-020-01858-w).
- [241] L.A. Gallego-Villada, E.A. Alarcón, A.L. Villa. Effect of Colombian Raw Materials on the Prins Condensation Reaction over Sn/MCM-41. *Catal. Today.* **2021**, *372*, 36–50. DOI: [10.1016/j.cattod.2020.10.040](https://doi.org/10.1016/j.cattod.2020.10.040).
- [242] D. Casas-Orozco, E. Alarcón, A. Villa. Kinetic Study of the Nopol Synthesis by the Prins Reaction over Tin Impregnated MCM-41 Catalyst with Ethyl Acetate as Solvent. *Fuel.* **2014**, *149*, 130–137. DOI: [10.1016/j.fuel.2014.08.067](https://doi.org/10.1016/j.fuel.2014.08.067).
- [243] D.C. García, J.H. Sánchez, J.D. Martínez, E.A. Alarcón, A.L. Villa. Nopol Production over Sn-MCM-41 Immobilized in a Wall-Coated Microreactor Using Formaldehyde Generated Ex-Situ. *ChemCatChem.* **2023**, *15*. DOI: [10.1002/cctc.202300209](https://doi.org/10.1002/cctc.202300209).
- [244] L.A. Gallego-Villada, C. Hasenstab, E.A. Alarcón, A.L. Villa. Identification by Life Cycle Assessment of the Critical Stage in the Catalytic Synthesis of Nopol Using Heterogeneous Catalysis. *Sustain. Prod. Consum.* **2021**, *27*, 23–34. DOI: [10.1016/j.spc.2020.10.017](https://doi.org/10.1016/j.spc.2020.10.017).

- [245] A.Y. Sidorenko, Y.M. Kurban, I.V. Il'ina, N. Li-Zhulanov, O. Patrusheva, V.V. Goltsova, M.P. Bei, A. Aho, J. Wärnå, I. Heinmaa, T.F. Kouznetsova, K.P. Volcho, N. F. Salakhutdinov, D.Y. Murzin, V.E. Agabekov. Catalytic Condensation of α -pinene with Formaldehyde. *J. Catal.* **2024**, *430*, 115306. DOI: [10.1016/j.jcat.2024.115306](https://doi.org/10.1016/j.jcat.2024.115306).
- [246] N.S. Li-Zhulanov, I. V. Il'ina, A. Yu. Sidorenko, D. V. Korchagina, K.P. Volcho, V. E. Agabekov, N.F. Salakhutdinov. Cascade Transformation of 4-hydroxymethyl-2-carene into Novel Cage Methanopyrano[4,3-b]thieno[3,2-g]benzofuran Derivative. *Mendeleev Commun.* **2022**, *32*, 443–445. DOI: [10.1016/j.mencom.2022.07.005](https://doi.org/10.1016/j.mencom.2022.07.005).
- [247] I. Aguas, M.J. Hidalgo, A.L. Villa, E.A. Alarcón. Homolimonenol Synthesis over Sn Supported Mesoporous Materials. *Catal. Today.* **2022**, *403–413*, 394–396. DOI: [10.1016/j.cattod.2021.07.025](https://doi.org/10.1016/j.cattod.2021.07.025).
- [248] V. V. Costa, K.A. da Silva Rocha, R.A. Mesquita, E.F. Kozhevnikova, I. V. Kozhevnikov, E. V. Gusevskaya. Heteropoly Acid Catalysts for the Synthesis of Fragrance Compounds from Biorenewables: Cycloaddition of Crotonaldehyde to Limonene, α -Pinene, and β -Pinene. *ChemCatChem.* **2013**, *5*, 3022–3026. DOI: [10.1002/cctc.201300208](https://doi.org/10.1002/cctc.201300208).
- [249] R.F. Cotta, K.A. da Silva Rocha, E.F. Kozhevnikova, I. V. Kozhevnikov, E. V. Gusevskaya. Heteropoly Acid Catalysts in Upgrading of Biorenewables: Cycloaddition of Aldehydes to Monoterpenes in Green Solvents. *Appl. Catal. B.* **2017**, *217*, 92–99. DOI: [10.1016/j.apcatb.2017.05.055](https://doi.org/10.1016/j.apcatb.2017.05.055).
- [250] I. V. Il'ina, K.P. Volcho, D. V. Korchagina, G.E. Salnikov, A.M. GenaeV, E. V. Karpova, N.F. Salakhutdinov. Unusual Reactions of (+)-car-2-ene and (+)-car-3-ene with Aldehydes on K10 Clay. *Helv. Chim. Acta.* **2010**, *93*, 2135–2150. DOI: [10.1002/hlca.201000145](https://doi.org/10.1002/hlca.201000145).
- [251] A.Y. Sidorenko, A.V. Kravtsova, P. Mäki-Arvela, A. Aho, T. Sandberg, I.V. Il'ina, N.S. Li-Zhulanov, D.V. Korchagina, K.P. Volcho, N.F. Salakhutdinov, D.Y. Murzin, V. E. Agabekov. Synthesis of Isobenzofuran Derivatives from Renewable 2-carene over Halloysite Nanotubes. *Mol. Catal.* **2020**, *490*, 110974. DOI: [10.1016/j.mcat.2020.110974](https://doi.org/10.1016/j.mcat.2020.110974).
- [252] A.Y. Sidorenko, I.V. Il'ina, A.V. Kravtsova, A. Aho, O.V. Ardashov, N.S. Li-Zhulanov, K. P. Volcho, N.F. Salakhutdinov, D.Y. Murzin, V.E. Agabekov. Preparation of Chiral Isobenzofurans from 3-carene in the Presence of Modified Clays. *Mol. Catal.* **2018**, *459*, 38–45. DOI: [10.1016/j.mcat.2018.07.025](https://doi.org/10.1016/j.mcat.2018.07.025).
- [253] G. Ohloff, H. Farnow, W. Philipp. Zur Kenntnis homologer Alkohole der Terpen- und Sesquiterpenreihe X. Synthese Des (+)-3-Hydroxymethyl- Δ^4 -Carens. *Justus Liebigs Ann. Chem.* **1958**, *613*, 43–55. DOI: [10.1002/jlac.19586130105](https://doi.org/10.1002/jlac.19586130105).
- [254] B.H. Sadowska, J. Gora. Synthesis and Odor Properties of Carene and Carane Derivatives. **1982**, *7*, 52–55. www.perfumerflavorist.com/fragrance/fine-fragrance/article/21861641/synthesis-and-odor-properties-of-carene-and-carane-derivatives.
- [255] S.Y. Kurbakova, I. V. Il'ina, O.S. Mikhailchenko, M.A. Pokrovsky, D. V. Korchagina, K. P. Volcho, A.G. Pokrovsky, N.F. Salakhutdinov. The Short Way to Chiral Compounds with Hexahydrofluoreno[9,1-bc]furan Framework: Synthesis and Cytotoxic Activity. *Bioorg. Med. Chem.* **2015**, *23*, 1472–1480. DOI: [10.1016/j.bmc.2015.02.013](https://doi.org/10.1016/j.bmc.2015.02.013).
- [256] A.Y. Sidorenko, Y.M. Kurban, A.V. Kravtsova, I.V. Il'ina, N.S. Li-Zhulanov, D. V. Korchagina, J.E. Sánchez-Velandia, A. Aho, K.P. Volcho, N.F. Salakhutdinov, D. Y. Murzin, V.E. Agabekov. Clays Catalyzed Cascade Prins and Prins-Friedel-Crafts Reactions for Synthesis of terpenoid-derived Polycyclic Compounds. *Appl. Catal. A Gen.* **2022**, *629*, 118395. DOI: [10.1016/j.apcata.2021.118395](https://doi.org/10.1016/j.apcata.2021.118395).
- [257] A.Y. Sidorenko, Y.M. Kurban, T.V. Khalimonyuk, I.V. Il'ina, N.S. Li-Zhulanov, O. S. Patrusheva, V.V. Goltsova, M.P. Bei, Z.V. Ihnatovich, J. Wärnå, K.P. Volcho, N. F. Salakhutdinov, D.Y. Murzin, V.E. Agabekov. Catalytic Condensation of 3-carene with Formaldehyde. *Mol. Catal.* **2024**, *552*, 113627. DOI: [10.1016/j.mcat.2023.113627](https://doi.org/10.1016/j.mcat.2023.113627).

- [258] A.T. Blomquist, J. Verdol, C.L. Adami, J. Wolinsky, D.D. Phillips. Thermal Condensation of Cyclic Olefins with Formaldehyde 1,2. *J. Am. Chem. Soc.* **1957**, *79*, 4976–4980. DOI: [10.1021/ja01575a040](https://doi.org/10.1021/ja01575a040).
- [259] A.T. Blomquist, R.J. Himics. Terpene-formaldehyde Reactions. II. d-Limonene. *J. Org. Chem.* **1968**, *33*, 1156–1159. DOI: [10.1021/jo01267a050](https://doi.org/10.1021/jo01267a050).
- [260] N.F. Salakhutdinov, K.P. Volcho, I. V. Il'ina, D. V. Korchagina, L.E. Tatarova, V. A. Barkhash. New Reactions of Isoprenoid Olefins with Aldehydes Promoted by Al₂O₃-SiO₂ Catalysts. *Tetrahedron.* **1998**, *54*, 15619–15642. DOI: [10.1016/S0040-4020\(98\)00977-6](https://doi.org/10.1016/S0040-4020(98)00977-6).
- [261] A.Y. Sidorenko, A. Aho, J. Ganbaatar, et al Catalytic Isomerization of α -pinene and 3-carene in the Presence of Modified Layered Aluminosilicates. *Mol. Catal* **2017**, *443*, 193–202. DOI: [10.1016/j.mcat.2017.10.014](https://doi.org/10.1016/j.mcat.2017.10.014).
- [262] I. V. Il'ina, N.S. Dyrkheeva, A.L. Zakharenko, A.Y. Sidorenko, N.S. Li-Zhulanov, D. V Korchagina, R. Chand, D.M. Ayine-Tora, A.A. Chepanova, O.D. Zakharova, E. S. Ilina, J. Reynisson, A.A. Malakhova, S.P. Medvedev, S.M. Zakian, K.P. Volcho, N. F. Salakhutdinov, O.I. Lavrik. Design, Synthesis, and Biological Investigation of Novel Classes of 3-Carene-Derived Potent Inhibitors of TDP1. *Molecules.* **2020**, *25*, 3496. DOI: [10.3390/molecules25153496](https://doi.org/10.3390/molecules25153496).
- [263] Majumdar, N., et al Catalytic Synthesis of 2H-Chromenes. *ACS Catal.* **2015**, *5*, 2329–2366. DOI: [10.1021/acscatal.5b00026](https://doi.org/10.1021/acscatal.5b00026).
- [264] E. Nazimova, A. Pavlova, O. Mikhailchenko, I. Il'ina, D. Korchagina, T. Tolstikova, K. Volcho, N. Salakhutdinov. Discovery of Highly Potent Analgesic Activity of isopulegol-derived (2R,4aR,7R,8aR)-4,7-dimethyl-2-(thiophen-2-yl)octahydro-2H-chromen-4-ol. *Med. Chem. Res.* **2016**, *25*, 1369–1383. DOI: [10.1007/s00044-016-1573-3](https://doi.org/10.1007/s00044-016-1573-3).
- [265] S. Slater, P.B. Lasonkar, S. Haider, M.J. Alqahtani, A.G. Chittiboyina, I.A. Khan. One-step, Stereoselective Synthesis of Octahydrochromanes via the Prins Reaction and Their Cannabinoid Activities. *Tetrahedron Lett.* **2018**, *59*, 807–810. DOI: [10.1016/j.tetlet.2018.01.040](https://doi.org/10.1016/j.tetlet.2018.01.040).
- [266] T. Minh Le, Z. Szakonyi. Enantiomeric Isopulegol as the Chiral Pool in the Total Synthesis of Bioactive Agents. *Chem. Rec.* **2022**, *22*. DOI: [10.1002/tcr.202100194](https://doi.org/10.1002/tcr.202100194).
- [267] G. Baishya, B. Sarmah, N. Hazarika. An Environmentally Benign Synthesis of Octahydro-2H-chromen-4-ols via Modified Montmorillonite K10 Catalyzed Prins Cyclization Reaction. *Synlett.* **2013**, *24*, 1137–1141. DOI: [10.1055/s-0032-1316915](https://doi.org/10.1055/s-0032-1316915).
- [268] M. Stekrova, P. Mäki-Arvela, N. Kumar, E. Behraves, A. Aho, Q. Balme, K.P. Volcho, N.F. Salakhutdinov, D.Y. Murzin. Prins Cyclization: Synthesis of Compounds with Tetrahydropyran Moiety over Heterogeneous Catalysts. *J. Mol. Catal. A Chem.* **2015**, *410*, 260–270. DOI: [10.1016/j.molcata.2015.09.021](https://doi.org/10.1016/j.molcata.2015.09.021).
- [269] M.N. Timofeeva, V.N. Panchenko, A. Gil, S. V. Zakusin, V. V. Krupskaya, K.P. Volcho, M.A. Vicente. Effect of Structure and Acidity of Acid Modified Clay Materials on Synthesis of octahydro-2H-chromen-4-ol from Vanillin and Isopulegol. *Catal. Commun.* **2015**, *69*, 234–238. DOI: [10.1016/j.catcom.2015.07.005](https://doi.org/10.1016/j.catcom.2015.07.005).
- [270] A.Y. Sidorenko, A.V. Kravtsova, J. Wärnå, et al Preparation of Octahydro-2 H -chromen-4-ol with Analgesic Activity from Isopulegol and Thiophene-2-carbaldehyde in the Presence of acid-modified Clays. *Mol. Catal* **2018**, *453*, 139–148. DOI: [10.1016/j.mcat.2018.05.007](https://doi.org/10.1016/j.mcat.2018.05.007).
- [271] A.Y. Sidorenko, A. V. Kravtsova, A. Aho, I. Heinmaa, K.P. Volcho, N.F. Salakhutdinov, V.E. Agabekov, D. Yu. Murzin, Acid-modified Halloysite Nanotubes as a Stereoselective Catalyst for Synthesis of 2 H -chromene Derivatives by the Reaction of Isopulegol with Aldehydes. *ChemCatChem.* **2018**, *10*, 3950–3954. DOI: [10.1002/cctc.201800974](https://doi.org/10.1002/cctc.201800974).

- [272] A.Y. Sidorenko, A.V. Kravtsova, A. Aho, I. Heinmaa, J. Wärnä, H. Pazniak, K.P. Volcho, N.F. Salakhutdinov, D.Y. Murzin, V.E. Agabekov. Highly Selective Prins Reaction over acid-modified Halloysite Nanotubes for Synthesis of isopulegol-derived 2H-chromene Compounds. *J. Catal.* **2019**, *374*, 360–377. DOI: [10.1016/j.jcat.2019.05.009](https://doi.org/10.1016/j.jcat.2019.05.009).
- [273] N. Li-Zhulanov, P. Mäki-Arvela, M. Laluc, A.F. Peixoto, E. Kholkina, T. Sandberg, A. Aho, K. Volcho, N. Salakhutdinov, C. Freire, A.Y. Sidorenko, D.Y. Murzin. Prins Cyclization of (-)-isopulegol with Benzaldehyde for Production of Chromenols over Organosulfonic Clays. *Mol. Catal.* **2019**, *478*, 110569. DOI: [10.1016/j.mcat.2019.110569](https://doi.org/10.1016/j.mcat.2019.110569).
- [274] A.O. Zaykovskaya, N. Kumar, E.A. Kholkina, N.S. Li-Zhulanov, P. Mäki-Arvela, A. Aho, J. Peltonen, M. Peurla, I. Heinmaa, B.T. Kusema, S. Streiff, D.Y. Murzin. Synthesis and physico-chemical Characterization of Beta Zeolite Catalysts: Evaluation of Catalytic Properties in Prins Cyclization of (-)-isopulegol. *Microporous Mesoporous Mater.* **2020**, *302*, 110236. DOI: [10.1016/j.micromeso.2020.110236](https://doi.org/10.1016/j.micromeso.2020.110236).
- [275] I. V. Ilyina, V. V. Zarubaev, I.N. Lavrentieva, A.A. Shtro, I.L. Esaulkova, D. V. Korchagina, S.S. Borisevich, K.P. Volcho, N.F. Salakhutdinov. Highly Potent Activity of isopulegol-derived Substituted Octahydro-2 H -chromen-4-ols against Influenza A and B Viruses. *Bioorg. Med. Chem. Lett.* **2018**, *28*, 2061–2067. DOI: [10.1016/j.bmcl.2018.04.057](https://doi.org/10.1016/j.bmcl.2018.04.057).
- [276] A.Y. Sidorenko, A.V. Kravtsova, I.V. Il'ina, J. Wärnä, D.V. Korchagina, Y.V. Gatilov, K. P. Volcho, N.F. Salakhutdinov, D.Y. Murzin, V.E. Agabekov. Clay Nanotubes Catalyzed solvent-free Synthesis of octahydro-2H-chromenols with Pharmaceutical Potential from (-)-isopulegol and Ketones. *J. Catal.* **2019**, *380*, 145–152. DOI: [10.1016/j.jcat.2019.10.015](https://doi.org/10.1016/j.jcat.2019.10.015).
- [277] M. Laluc, P. Mäki-Arvela, A.F. Peixoto, N. Li-Zhulanov, T. Sandberg, N. F. Salakhutdinov, K. Volcho, C. Freire, A.Y. Sidorenko, D.Y. Murzin. Catalytic Synthesis of Bioactive 2H-chromene Alcohols from (-)-isopulegol and Acetone on Sulfonated Clays. *React. Kinet. Mech. Catal.* **2020**, *129*, 627–644. DOI: [10.1007/s11144-020-01740-9](https://doi.org/10.1007/s11144-020-01740-9).
- [278] M. Laluc, R. Barakov, P. Mäki-Arvela, N. Shcherban, D.Y. Murzin. Catalytic Activity of Hierarchical Beta Zeolites in the Prins Cyclization of (-)-isopulegol with Acetone. *Appl. Catal. A Gen.* **2021**, *618*, 118131. DOI: [10.1016/j.apcata.2021.118131](https://doi.org/10.1016/j.apcata.2021.118131).
- [279] O. Mikhailchenko, I. Il'ina, A. Pavlova, E. Morozova, D. Korchagina, T. Tolstikova, E. Pokushalov, K. Volcho, N. Salakhutdinov. Synthesis and Analgesic Activity of New Heterocyclic Compounds Derived from Monoterpenoids. *Med. Chem. Res.* **2013**, *22*, 3026–3034. DOI: [10.1007/s00044-012-0310-9](https://doi.org/10.1007/s00044-012-0310-9).
- [280] I. Il'ina, A. Pavlova, D. Korchagina, O. Ardashov, T. Tolstikova, K. Volcho, N. Salakhutdinov. Synthesis and Analgesic Activity of monoterpenoid-derived alkyl-substituted Chiral hexahydro-2H-chromenes. *Med. Chem. Res.* **2017**, *26*, 1415–1426. DOI: [10.1007/s00044-017-1847-4](https://doi.org/10.1007/s00044-017-1847-4).
- [281] A.Y. Sidorenko, Y.M. Kurban, I.V. Il'ina, N.S. Li-Zhulanov, D.V. Korchagina, O. V. Ardashov, J. Wärnä, K.P. Volcho, N.F. Salakhutdinov, D.Y. Murzin, V.E. Agabekov. Catalytic Synthesis of terpenoid-derived hexahydro-2H-chromenes with Analgesic Activity over Halloysite Nanotubes. *Appl. Catal. A Gen.* **2021**, *618*, 118144. DOI: [10.1016/j.apcata.2021.118144](https://doi.org/10.1016/j.apcata.2021.118144).
- [282] A. Torozova, P. Mäki-Arvela, A. Aho, N. Kumar, A. Smeds, M. Peurla, R. Sjöholm, I. Heinmaa, D. V. Korchagina, K.P. Volcho, N.F. Salakhutdinov, D.Y. Murzin. Heterogeneous Catalysis for Transformation of Biomass Derived Compounds beyond Fuels: Synthesis of Monoterpenoid Dioxinols with Analgesic Activity. *J. Mol. Catal. A Chem.* **2015**, *397*, 48–55. DOI: [10.1016/j.molcata.2014.10.023](https://doi.org/10.1016/j.molcata.2014.10.023).
- [283] M.N. Timofeeva, K.P. Volcho, O.S. Mikhailchenko, V.N. Panchenko, V. V. Krupskaya, S. V. Tsybulya, A. Gil, M.A. Vicente, N.F. Salakhutdinov. Synthesis of octahydro-2H-

- chromen-4-ol from Vanillin and Isopulegol over Acid Modified Montmorillonite Clays: Effect of Acidity on the Prins Cyclization. *J. Mol. Catal. A Chem.* **2015**, *398*, 26–34. DOI: [10.1016/j.molcata.2014.11.016](https://doi.org/10.1016/j.molcata.2014.11.016).
- [284] I. V. Ilyina, O.S. Patrusheva, V. V. Zarubaev, M.A. Misiurina, A. V. Slita, I.L. Esaulkova, D. V. Korchagina, Y. V. Gatilov, S.S. Borisevich, K.P. Volcho, N.F. Salakhutdinov. Influenza Antiviral Activity of F- and OH-containing isopulegol-derived octahydro-2H-chromenes. *Bioorg. Med. Chem. Lett.* **2021**, *31*, 127677. DOI: [10.1016/j.bmcl.2020.127677](https://doi.org/10.1016/j.bmcl.2020.127677).
- [285] I. Il'ina, E. Morozova, A. Pavlova, D. Korchagina, T. Tolstikova, K. Volcho, N. Salakhutdinov. Synthesis and Analgesic Activity of Aliphatic ketones-derived Chiral hexahydro-2H-chromenes. *Med. Chem. Res.* **2020**, *29*, 738–747. DOI: [10.1007/s00044-020-02518-3](https://doi.org/10.1007/s00044-020-02518-3).
- [286] M. Stekrova, P. Mäki-Arvela, E. Leino, K.M. Valkaj, K. Eränen, et al Two-step Synthesis of Monoterpenoid Dioxinols Exhibiting Analgesic Activity from Isopulegol and Benzaldehyde over Heterogeneous Catalysts. *Catal. Today* **2017**, *279*, 56–62. DOI: [10.1016/j.cattod.2016.03.046](https://doi.org/10.1016/j.cattod.2016.03.046).
- [287] T.L. Lambat, S.H. Mahmood, D. Taher, S. Banerjee. Sulfamic Acid Catalyzed oxonium-ene Reactions under Ball Milling Conditions: Straightforward Access to Highly Functionalized Oxabicyclo[3.2.1]octenes. *Curr. Res. Green Sustain. Chem.* **2021**, *4*, 100118. DOI: [10.1016/j.crgsc.2021.100118](https://doi.org/10.1016/j.crgsc.2021.100118).
- [288] P. Mäki-Arvela, I. Simakova, Z. Vajglová, D.Y. Murzin. One-Pot Synthesis of Menthol from Citral and Citronellal over Heterogeneous Catalysts. *Catal. Surv. from Asia.* **2023**, *27*, 2–19. DOI: [10.1007/s10563-022-09376-6](https://doi.org/10.1007/s10563-022-09376-6).
- [289] Behr, A., et al Towards Resource Efficient Chemistry: Tandem Reactions with Renewables. *Green Chem.* **2014**, *16*, 982–1006. DOI: [10.1039/C3GC41960F](https://doi.org/10.1039/C3GC41960F).
- [290] E. V. Gusevskaya, E.N. Dos Santos, R. Augusti, A.D.O. Dias, C.M. Foca. Platinum/tin Catalyzed Hydroformylation of Naturally Occurring Monoterpenes. *J. Mol. Catal. A Chem.* **2000**, *152*, 15–24. DOI: [10.1016/S1381-1169\(99\)00264-2](https://doi.org/10.1016/S1381-1169(99)00264-2).
- [291] P.J. Baricelli, M. Rodríguez, L.G. Melean, M. Borusiak, I. Crespo, J.C. Pereira, M. Rosales. Hydroformylation of Natural Olefins with the [Rh(COD)(μ-OMe)]₂/TPPTS Complex in BMI-BF₄/toluene Biphasic Medium: Observations on the Interfacial Role of CTAB in Reactive Systems. *Mol. Catal.* **2020**, *497*, 111189. DOI: [10.1016/j.mcat.2020.111189](https://doi.org/10.1016/j.mcat.2020.111189).
- [292] M. Yamashita, K. Nozaki. Hydroformylation, Other Hydrocarbonylations, and Oxidative Alkoxy carbonylation. In *Compr. Organomet. Chemistry III*, 3rd ed.; D. M. Mingos, R.H. Crabtree, Eds.; Elsevier Ltd, **2007**; pp 435–471.
- [293] B. Cornils, W.A. Herrmann, M. Rasch, Otto Roelen. Pioneer in Industrial Homogeneous Catalysis. *Angew. Chemie Int. Ed. English.* **1994**, *33*, 2144–2163. DOI: [10.1002/anie.199421441](https://doi.org/10.1002/anie.199421441).
- [294] A. Armstrong, N.J. Convine. One or More CC Bonds Formed by Addition: Addition of Carbon Electrophiles and Nucleophiles to CC Multiple Bonds, In: *Compr. In Org. Funct. Gr. Transform.*; Elsevier, **2005**, Vol. II, pp 287–311. DOI: [10.1016/B0-08-044655-8/00007-6](https://doi.org/10.1016/B0-08-044655-8/00007-6).
- [295] J.L.F. Monteiro, C.O. Veloso. Catalytic Conversion of Terpenes into Fine Chemicals. *Top. Catal.* **2004**, *27*, 169–180. DOI: [10.1023/B:TOCA.0000013551.99872.8d](https://doi.org/10.1023/B:TOCA.0000013551.99872.8d).
- [296] W.H. Clement, M. Orchin. Hydroformylation of Terpenes. *I&EC Prod. Res. Dev.* **1965**, *4*, 283–286. DOI: [10.1021/i360016a018](https://doi.org/10.1021/i360016a018).
- [297] Kjonaas, R. Croteau, Demonstration that Limonene Is the First Cyclic Intermediate in the Biosynthesis of Oxygenated p-menthane Monoterpenes in *Mentha Piperita* and Other *Mentha* Species. *Arch. Biochem. Biophys.* **1983**, *220*, 79–89. DOI: [10.1016/0003-9861\(83\)90389-2](https://doi.org/10.1016/0003-9861(83)90389-2).

- [298] G. Rubulotta, E.A. Quadrelli. Terpenes: A Valuable Family of Compounds for the Production of Fine Chemicals. In *Stud. Surf. Sci. Catal*; 1st. Elsevier B.V, 2019; 215–229. DOI: [10.1016/B978-0-444-64127-4.00011-2](https://doi.org/10.1016/B978-0-444-64127-4.00011-2)
- [299] G.T. Whiteker, C.J. Cobley, *Applications of Rhodium-Catalyzed Hydroformylation in the Pharmaceutical, Agrochemical, and Fragrance Industries*; in: 2012. pp 35–46. [10.1007/3418_2011_28](https://doi.org/10.1007/3418_2011_28).
- [300] J.G. da Silva, H.J.V. Barros, et al Rhodium Catalyzed Hydroformylation of Monoterpenes Containing a Sterically Encumbered Trisubstituted Endocyclic Double Bond under Mild Conditions. *Appl. Catal. A Gen.* 2007, 326, 219–226. DOI: [10.1016/j.apcata.2007.04.014](https://doi.org/10.1016/j.apcata.2007.04.014).
- [301] J.G. da Silva, C.G. Vieira, E.N. Dos Santos, E. V. Gusevskaya. Hydroformylation of Endocyclic Double Bonds in para-menthenic Terpenes under Mild Conditions. *Appl. Catal. A Gen.* 2009, 365, 231–236. DOI: [10.1016/j.apcata.2009.06.019](https://doi.org/10.1016/j.apcata.2009.06.019).
- [302] A.F. Peixoto, D.S. de Melo, T.F. Fernandes, Y. Fonseca, E. V. Gusevskaya, A.M.S. Silva, R.R. Contreras, M. Reyes, A. Usubillaga, E.N. Dos Santos, M.M. Pereira, J.C. Bayón. Rhodium Catalyzed Hydroformylation of Kaurane Derivatives: A Route to New Diterpenes with Potential Bioactivity. *Appl. Catal. A Gen.* 2008, 340, 212–219. DOI: [10.1016/j.apcata.2008.02.015](https://doi.org/10.1016/j.apcata.2008.02.015).
- [303] E. V. Gusevskaya, J. Jiménez-Pinto, A. Börner. Hydroformylation in the Realm of Scents. *ChemCatChem.* 2014, 6, 382–411. DOI: [10.1002/cctc.201300474](https://doi.org/10.1002/cctc.201300474).
- [304] M. Rosales, O. Soto, B. González, I. Pacheco, P.J. Baricelli. Kinetics and Mechanisms of Homogeneous Catalytic Reactions: Part 15. Regio-specific Hydroformylation of Limonene Catalysed by Rhodium Complexes of Phosphine Ligands. *Transit. Met. Chem.* 2018, 43, 451–461. DOI: [10.1007/s11243-018-0232-6](https://doi.org/10.1007/s11243-018-0232-6).
- [305] C.G. Vieira, M.C. de Freitas, K.C.B. de Oliveira, A. de Camargo Faria, E.N. Dos Santos, E. V. Gusevskaya. Synthesis of Fragrance Compounds from Renewable Resources: The Aqueous Biphasic Hydroformylation of Acyclic Terpenes. *Catal. Sci. Technol.* 2015, 5, 960–966. DOI: [10.1039/C4CY01020E](https://doi.org/10.1039/C4CY01020E).
- [306] M.C. de Freitas, K.C.B. de Oliveira, A. de Camargo Faria, E.N. Dos Santos, E. V. Gusevskaya. Rhodium Catalyzed Hydroformylation of Nerolidol. *Catal. Sci. Technol.* 2014, 4, 1954–1959. DOI: [10.1039/C3CY01104F](https://doi.org/10.1039/C3CY01104F).
- [307] N.S. Pagar, R.M. Deshpande. Highly Efficient Rhodium-Phosphite Catalyzed Hydroformylation of Camphene and Other Terpenes. *Asian J. Chem.* 2019, 31, 213–219. DOI: [10.14233/ajchem.2019.21656](https://doi.org/10.14233/ajchem.2019.21656).
- [308] F.G. Delolo, K.C.B. Oliveira, E.N. Dos Santos, E. V Gusevskaya. Hydroformylation of biomass-based Hydroxyolefins in eco-friendly Solvents: New Fragrances from Myrtenol and Nopol. *Mol. Catal.* 2019, 462, 1–9. DOI: [10.1016/j.mcat.2018.10.011](https://doi.org/10.1016/j.mcat.2018.10.011).
- [309] C. Liu, W. Huang, J. Zhang, Z. Rao, Y. Gu, F. Jérôme. Formaldehyde in Multicomponent Reactions. *Green Chem.* 2021, 23, 1447–1465. DOI: [10.1039/D0GC04124F](https://doi.org/10.1039/D0GC04124F).
- [310] Padmaja, P. Tandem Prins Cyclizations for the Construction of Oxygen Containing Heterocycles. *Org. Biomol. Chem.* 2020, 18, 7514–7532. DOI: [10.1039/D0OB00960A](https://doi.org/10.1039/D0OB00960A).
- [311] M.-E. Chen, et al Recent Advances of Ritter Reaction and Its Synthetic Applications. *Org. Chem. Front* 2021, 8, 4623–4664. DOI: [10.1039/D1QO00496D](https://doi.org/10.1039/D1QO00496D).
- [312] M.J. Climent, A. Corma, S. Iborra, M.J. Sabater. Heterogeneous Catalysis for Tandem Reactions. *ACS Catal.* 2014, 4, 870–891. DOI: [10.1021/cs401052k](https://doi.org/10.1021/cs401052k).
- [313] I. V Ilyina, N.S. Li-Zhulanov, Y. V Gatilov, K.P. Volcho, A.Y. Sidorenko, V.E. Agabekov, N.F. Salakhutdinov. (2aR,2a1S,5aR,9bR)-4-Isopropyl-7,8-dimethoxy-2a1-methyl

- 2,2a,2a1,3,5a,9b-hexahydrofluoreno[9,1-bc]furan. *Molbank*. **2023**, *2023*, M1734. DOI: [10.3390/M1734](https://doi.org/10.3390/M1734).
- [314] R.F. Cotta, R.A. Martins, K.A. da Silva Rocha, E.F. Kozhevnikova, I. V. Kozhevnikov, E. V. Gusevskaya. Coupling of Phenylacetaldehyde and Styrene Oxide with Biorenewable Alkenes in eco-friendly Solvents. *Catal. Today*. **2021**, *381*, 254–260. DOI: [10.1016/j.cattod.2020.05.068](https://doi.org/10.1016/j.cattod.2020.05.068).
- [315] A.Y. Sidorenko, N.S. Li-Zhulanov, P. Mäki-Arvela, T. Sandberg, A. V. Kravtsova, A. F. Peixoto, C. Freire, K.P. Volcho, N.F. Salakhutdinov, V.E. Agabekov, D.Y. Murzin. Stereoselectivity Inversion by Water Addition in the –SO₃H-catalyzed Tandem Prins-Ritter Reaction for Synthesis of 4-amidotetrahydropyran Derivatives. *ChemCatChem*. **2020**, *12*, 2605–2609. DOI: [10.1002/cctc.202000070](https://doi.org/10.1002/cctc.202000070).
- [316] A.Y. Sidorenko, Y.M. Kurban, A.F. Peixoto, N.S. Li-Zhulanov, J.E. Sánchez-Velandia, A. Aho, J. Wärnå, Y. Gu, K.P. Volcho, N.F. Salakhutdinov, D.Y. Murzin, V.E. Agabekov. Brønsted Acid Catalyzed Prins-Ritter Reaction for Selective Synthesis of terpenoid-derived 4-amidotetrahydropyran Compounds. *Appl. Catal. A Gen.* **2023**, *649*, 118967. DOI: [10.1016/j.apcata.2022.118967](https://doi.org/10.1016/j.apcata.2022.118967).
- [317] N. Li-Zhulanov, et al A Novel Class of Tyrosyl-DNA Phosphodiesterase 1 Inhibitors that Contains the Octahydro-2H-chromen-4-ol Scaffold. *Molecules* **2018**, *23*, 2468. DOI: [10.3390/molecules23102468](https://doi.org/10.3390/molecules23102468).
- [318] B. Sarmah, G. Baishya, R.K. Baruah. First Example of a Prins–Ritter Reaction on Terpenoids: A Diastereoselective Route to Novel 4-amido-octahydro-2H-chromenes. *RSC Adv.* **2014**, *4*, 22387. DOI: [10.1039/c4ra02124j](https://doi.org/10.1039/c4ra02124j).
- [319] N.P.G. Lopes, F.C. Ballotin, A.P. de Carvalho Teixeira, R.M. Lago. Acetalization of β -citronellal over A Renewable Carbon Catalyst Obtained from Bio-Oil Sulfonation: A Green Route to Obtain Valuable Feedstocks. *Waste Biomass Valorization*. **2023**. DOI: [10.1007/s12649-023-02216-2](https://doi.org/10.1007/s12649-023-02216-2).
- [320] C.G. Vieira, J.G. da Silva, C.A.A. Penna, E.N. Dos Santos, E. V. Gusevskaya. Tandem hydroformylation-acetalization of para-menthenic Terpenes under non-acidic Conditions. *Appl. Catal. A Gen.* **2010**, *380*, 125–132. DOI: [10.1016/j.apcata.2010.03.045](https://doi.org/10.1016/j.apcata.2010.03.045).
- [321] F.G. Delolo, G.M. Vieira, J.A. Avendaño-Villarreal, A. de Oliveira Dias, E.N. Dos Santos, E. V. Gusevskaya. Working Together to Avoid Unwanted Reactions: Hydroformylation/O-acylation of terpene-based Hydroxyolefins. *J. Catal.* **2023**, *421*, 20–29. DOI: [10.1016/j.jcat.2023.03.003](https://doi.org/10.1016/j.jcat.2023.03.003).
- [322] P. Kalck, M. Urrutigoity. Tandem Hydroaminomethylation Reaction to Synthesize Amines from Alkenes. *Chem. Rev.* **2018**, *118*, 3833–3861. DOI: [10.1021/acs.chemrev.7b00667](https://doi.org/10.1021/acs.chemrev.7b00667).
- [323] M. Ahmed, A.M. Seayad, R. Jackstell, M. Beller. Amines Made Easily: A Highly Selective Hydroaminomethylation of Olefins. *J. Am. Chem. Soc.* **2003**, *125*, 10311–10318. DOI: [10.1021/ja030143w](https://doi.org/10.1021/ja030143w).
- [324] P. Eilbracht, L. Bärffacker, et al Tandem Reaction Sequences under Hydroformylation Conditions: New Synthetic Applications of Transition Metal Catalysis. *Chem. Rev.* **1999**, *99*, 3329–3365. DOI: [10.1021/cr970413r](https://doi.org/10.1021/cr970413r).
- [325] I. L. Simakova, A. V. Simakov, D. Yu. Murzin. Valorization of Biomass Derived Terpene Compounds by Catalytic Amination. *Catalysts*. **2018**, *8*, 365. DOI: [10.3390/catal8090365](https://doi.org/10.3390/catal8090365).
- [326] B. Zhang, D. Peña Fuentes, A. Börner. Hydroformylation. *ChemTexts*. **2022**, *8*, 2. DOI: [10.1007/s40828-021-00154-x](https://doi.org/10.1007/s40828-021-00154-x).
- [327] D.S. Melo, S.S. Pereira-Júnior, E.N. Dos Santos. An Efficient Method for the Transformation of Naturally Occurring Monoterpenes into Amines through

- rhodium-catalyzed Hydroaminomethylation. *Appl. Catal. A Gen.* **2012**, 70–76, 411–412. DOI: [10.1016/j.apcata.2011.10.021](https://doi.org/10.1016/j.apcata.2011.10.021).
- [328] A. de Oliveira Dias, M.G.P. Gutiérrez, J.A.A. Villarreal, R.L.L. Carmo, K.C.B. Oliveira, A. G. Santos, et al Sustainable Route to biomass-based Amines: Rhodium Catalyzed Hydroaminomethylation in Green Solvents. *Appl. Catal. A Gen.* **2019**, 574, 97–104. DOI: [10.1016/j.apcata.2019.02.003](https://doi.org/10.1016/j.apcata.2019.02.003).
- [329] A. Pérez Alonso, D. Pham Minh, D. Pla, M. Gómez. A Cooperative Rh/Co-Catalyzed Hydroaminomethylation Reaction for the Synthesis of Terpene Amines. *ChemCatChem.* **2023**, 15. DOI: [10.1002/cctc.202300501](https://doi.org/10.1002/cctc.202300501).